ISSN 0280-5731 LMV-rapport 1999:12

PROCEEDINGS OF THE 13th GENERAL MEETING OF THE NORDIC GEODETIC COMMISSION

PART 2

GÄVLE, SWEDEN
25 - 29 MAY 1998

edited by BO JONSSON

Gävle, Sweden
1999

LANTMÄTERIET

The 13th NKG General Meeting
Gävle, Sweden

Contents

GALOS: Geodetic Aspects of the Law of the Sea.

Bjørn Geirr Harsson
Statens kartverk – Geodetic Institute
Kartverksveien 21
N-3500 Hønefoss
Norway

What is GALOS?

History of GALOS (Geodetic Aspects of the Law Of the Sea)

1988 - The idea of forming a group of geodesists with special interests in geodetic aspects of the law of the sea was conceived in Las Cruces, New Mexico, USA.

1989 - Formal establishment as a "Special Study Group" of the International Association of Geodesy (IAG) in Edinburgh, IAG Scientific Assembly. Petr Vanicek, Canada, was the first chairman of the Special Study Group called GALOS

1990 - Meeting with the International Hydrographic Organization's (IHO's) TALOS group in Monaco. (TALOS = Technical Aspects of the UN Convention on the Law of the Sea)
- 1st. technical meeting with INSMAP '90 in Miami, Florida, USA.

1991 - The 2nd. technical meeting with IUGG General Assembly in Vienna; GALOS becomes a Subcomission of ISCOMAP of IAG.

1992 - Bali I, 1st International Conference in Bali Beach Hotel. About 75 participants from 4 continents. Lawyers, geodesists, hydrographers and oceanographers presented 24 technical papers.

1993 - Meeting with IAG Scientific Assembly in Beijing.

1994 - The 3rd technical meeting with INSMAP '94 in Hannover; ABLOS established.

1995 - The 4th technical meeting with IUGG General Assembly in Boulder, Colorado, USA; GALOS becomes a Committee of IAG, with the mandate of looking into Geodetic Aspects of the Law Of the Sea (GALOS). These aspects consist of positioning, datum considerations, uncertainties and time variations in position, i.e., they are encountered in maritime boundary delimitations and enforcement. Close cooperation with the International Hydrographic Organization (IHO) has been sought right from the beginning and put in place already in 1990.

1996 - Bali II. 2nd International Conference, Putri Bali Hotel. Nearly 100 participants from 20 countries. Lawyers, geodesists, hydrographers and oceanographers presented 34 papers.

1997 - The 5th technical meeting with IAG Scientific Assembly in Rio. Bjørn Geirr Harsson, Norway, succeeded Petr Vanicek as chairman.

1998 - The 6th technical meeting in Fredericton, Canada.

ABLOS (The IHO/IAG Advisory Board on Hydrographic and Geodetic Aspects of the Law Of the Sea) was established in September 1994, during the technical meeting with INSMAP '94 in Hannover, Germany.
The objectives of ABLOS is

-to provide advice and guidance and, where applicable, offer expert interpretation of the hydrographic, geodetic and other technical aspects of the Law of the Sea to the parent organizations, their member states or to other organizations on request.
-to (monitor and) review state practice and jurisprudence on Law of the Sea matters with respect to their relevance to the work of the Board in order that it may be in a position to provide expert advice when needed.
-to study, promote and encourage the development of appropriate techniques in the application of the technical provisions contained within the UN Convention on the Law of the Sea.

The Advisory Board was in 1994 composed of nine full members, preferably chosen with wide geographic distribution. Each of the parent organizations (IHO and the IAG) appointed four members. One member was appointed by the UN Division for Ocean Affairs and the Law of the Sea Office of Legal Affairs in an ex-officio capacity. There may be any number of corresponding members appointed by the parent organizations. These corresponding members may attend meetings as observers with voice but no vote.

The Advisory Board reports to both the International Hydrographic Organization and the International Association of Geodesy at least once each year and at Conferences/General Assemblies of each Organization.

Activities for ABLOS are
-to maintain close contact with the UN Office of the Law of the Sea.
-to review and update, as necessary, the International Hydrographic Bureau's Special Publication S 51 – A Manual of technical Aspects of the United Nations' Convention on the Law of the Sea –1982.
-to convene meetings and technical conferences related to the Law of the Sea.
-to publish the proceedings of seminars and technical conferences and selected reports of Board meetings where desirable.

When ABLOS was formed, GALOS appeared to serve as a useful technical arm of ABLOS, certainly on matters pertaining to geodesy.

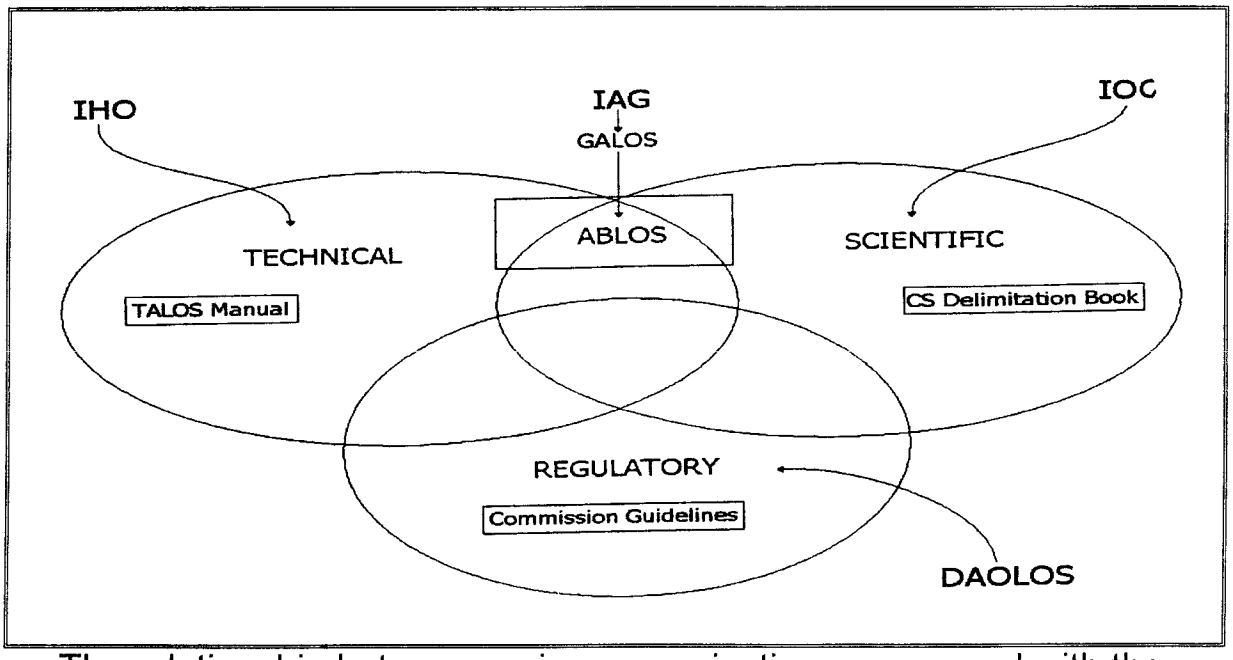

The relationship between various organisations concerned with the technical aspects of the law of the sea.

LAW OF THE SEA CONFERENCE: A CHRONOLOGY AS GIVEN IN THE UN PUBLICATION "The Law of the Sea, United Nations Convention on the Law of the Sea", 1983.

1958 - First United Nations Conference on the Law of the Sea: 96 States meet in Geneva and adopt four international conventions covering the territorial sea, the high seas, the continental shelf and fishing and conservation of living resources.

1960 - Second United Nations Conference on the Law of the Sea fails to produce and substantive agreement on the limits of the territorial zone and fishing rights.

1967 - The United Nations General Assembly decides that technological and other changes in the world require the international community to address the matter of laws governing the seas beyond national jurisdiction. A 35-member ad hoc committee is set up by the Assembly to study the matter.

1968 - The *ad hoc* committee grows to 41 members and is *renamed Committee on the Peaceful Uses of the Sea-Bed and the Ocean Floor beyond the Limits of National Jurisdiction.*

1970 - As a result of the Sea Bed Committee's work the General Assembly adopts a *Declaration of Principles Governing the Sea-Bed and Ocean Floor, and the Subsoil Thereof, beyond the Limits of National Jurisdiction.* These areas are declared the "common heritage of mankind". The Assembly also decides to convene the Third United Nations Conference of the Law of the Sea and the Sea-Bed Committee, enlarged to 91 members, is given the job of preparing for the Conference. By 1973 it puts out a 6-volume report.

1973 - First session of the Conference (organizational, New York) elects officers, begins work on rules of procedure. Hamilton Shirley Amerasinghe of Sri Lanka is chosen as President of the Conference.

1974 - Second session, Caracas. Adopts rules of procedure; 115 countries speak in general debate. First attempt to deal with alternate texts submitted by Sea-Bed Committee.

1975 - Third session, Geneva. A "single negotiating text" produced by Committee Chairmen, sets out in treaty language the provisions to be included.

1976 - Fourth session, New York. The results of negotiations set out in a "revised single negotiating text".

1976 - Fifth session, New York. Further progress in some areas, impasse on how deep-sea mining should be organized and regulated.

1977 - Sixth session, New York. An "informal composite negotiating text" marks continuing deliberations.

1978 - Seventh session, first Geneva, then New York. Seven negotiating groups created to tackle "hard core" differences.

1979 - Eighth session, first Geneva, then New York. First revision of the 1977 negotiating text emerges. Decision taken to complete work on Convention by 1980.

1980 - Ninth session, first New York, then Geneva. "Informal text" of Draft Convention produced. Plans to hold final session in 1981.

1981 - Tenth session, first New York, then Geneva. First official text of Draft Convention issued. Jamaica and Federal Republic of Germany chosen as seats for the international Sea-Bed Authority and the International Tribunal for the Law of the Sea respectively. United States cites difficulties in sea-bed provisions. "Final decision-making session" set for 1982.

1982 - Eleventh session (Part I, 8 March - 30 April), New York. All efforts at reaching general agreement having been exhausted, the Conference votes on a number of amendments to the Draft Convention. At the end, at the request of the United States, there is a recorded vote. The Convention is adopted on 30 April by 130 votes to 4 against, with 17 abstentions.

Eleventh session (Part II, 22 - 24 September), New York. Approves Drafting Committee changes in the Convention, adopts draft Final Act, selects Jamaica as site of signing session.

1982 (6 - 10 December) - Convention and Final Act are signed at Montego Bay, Jamaica, by 119 delegations.

1983 - Preparatory Commission meets in Kingston, Jamaica, to begin work on the creation of International Sea-Bed Authority and International Tribunal for the Law of the Sea.

The UN Convention on the Law of the Sea was open for signature from 10 December 1982 to 9 December 1984. In that period 159 states and other entities signed the Convention. Up to that time this was the highest number of signatories of any multilateral treaty. By the 16th November 1993 the required number of states (60) had ratified the Convention. Having reached that number of ratifications, the Convention entered into force on the 16th November 1994.

The Law of the Sea

The definition of baseline points, including their coordinates and corresponding geodetic datum, is a fundamental parts of the Law of the Sea. Baseline points along the coast form the framework from which the seaward boundaries of territorial sea, contiguous zone, fishery zone and exclusive economic zone can be computed and defined within the law. A geodetic understanding of these parts of the law is therefore of greatest importance. Many of the articles in the law are related to geodesy, and we will look at some of them.

TERRITORIAL SEA AND CONTIGUOUS ZONE

SECTION 1. GENERAL PROVISIONS

Article 2

Legal status of the territorial sea, of the air space over the territorial sea and of its bed and subsoil

1. The sovereignty of a coastal State extends, beyond its land territory and internal waters and, in the case of an archipelagic State, its archipelagic waters, to an adjacent belt of sea, described as the territorial sea.
2. This sovereignty extends to the air space over the territorial sea as well as to its bed and subsoil.
3. The sovereignty over the territorial sea is exercised subject to this Convention and to other rules of international law.

SECTION 2. LIMITS OF THE TERRITORIAL SEA

Article 3

Breadth of the territorial sea

Every State has the right to establish the breadth of its territorial sea up to a limit not exceeding 12 nautical miles, measured from baselines determined in accordance with this Convention.

Article 4

Outer limit of the territorial sea

The outer limit of the territorial sea is the line every point of which is at a distance from the nearest point of the baseline equal to the breadth of the territorial sea.

Article 5

Normal baseline

Except where otherwise provided in this Convention, the normal baseline for measuring the breadth of the territorial sea is the low-water line along the coast as marked on large-scale charts officially recognized by the coastal State.

Article 6
Reefs

In the case of islands situated on atolls or of islands having fringing reefs, the baseline for measuring the breadth of the territorial sea is the seaward low-water line of the reef, as shown by the appropriate symbol on charts officially recognized by the coastal State.

Article 7
Straight baselines

1. In localities where the coastline is deeply indented and cut into, or if there is a fringe of islands along the coast in its immediate vicinity, the method of straight baselines joining appropriate points may be employed in drawing the baseline from which the breadth of the territorial sea is measured.
2. Where because of the presence of a delta and other natural conditions the coastline is highly unstable, the appropriate points may be selected along the furthest seaward extent of the low-water line and, notwithstanding subsequent regression of the low-water line. the straight baselines shall remain effective until changed by the coastal State in accordance with this Convention.
3. The drawing of straight baselines must not depart to any appreciable extent from the general direction of the coast, and the sea areas lying within the lines must be sufficiently closely linked to the land domain to be subject to the regime of internal waters.
4. Straight baselines shall not be drawn to and from low-tide elevations, unless lighthouses or similar installations which are permanently above sea level have been built on them or except in instances where the drawing of baselines to and from such elevations has received general international recognition.
5. Where the method of straight baselines is applicable under paragraph 1, account may be taken, in determining particular baselines, of economic interests peculiar to the region concerned, the reality and the importance of which are clearly evidenced by long usage.
6. The system of straight baselines may not be applied by a State in such a manner as to cut off the territorial sea of another State from the high seas or an exclusive economic zone.

Article 8
Internal waters

1. Except as provided in Part IV, waters on the landward side of the baseline of the territorial sea form part of the internal waters of the State.
2. Where the establishment of a straight baseline in accordance with the method set forth in article 7 has the effect of enclosing as internal waters areas which had not previously been considered as such, a right of innocent passage as provided in this Convention shall exist in those waters.

Article 9
Mouths of rivers

If a river flows directly into the sea, the baseline shall be a straight line across the mouth of the river between points on the low-water line of its banks.

Article 10
Bays

1. This article relates only to bays the coasts of which belong to a single State.
2. For the purposes of this Convention, a bay is a well-marked indentation whose penetration is in such proportion to the width of its mouth as to contain land-locked waters and constitute more than a mere curvature of the coast. An indentation shall not, however, be regarded as a bay unless its area is as large as, or larger than, that of the semi-circle whose diameter is a line drawn across the mouth of that indentation.
3. For the purpose of measurement, the area of an indentation is that lying between the low-water mark around the shore of the indentation and a line joining the low-water mark of its natural entrance points. Where, because of the presence of islands an indentation has more than one

mouth, the semi-circle shall be drawn on a line as long as the sum total of the lengths of the lines across the different mouths. Islands within an indentation shall be included as if they were part of the water area of the indentation.

4. If the distance between the low-water marks of the natural entrance points of a bay does not exceed 24 nautical miles, a closing line may be drawn between these two low-water marks, and the waters enclosed thereby shall be considered as internal waters.
5. Where the distance between the low-water marks of the natural entrance points of a bay exceeds 24 nautical miles, a straight baseline of 24 nautical miles shall be drawn within the bay in such a manner as to enclose the maximum area of water that is possible with a line of that length.
6. The foregoing provisions do not apply to so-called "historic" bays, or in any case where the system of straight baselines provided for in article 7 is applied.

Article 11

Ports

For the purpose of delimiting the territorial sea, the outermost permanent harbour works which form an integral part of the harbour system are regarded as forming part of the coast. Off-shore installations and artificial islands shall not be considered as permanent harbour works.

Article 12

Roadsteads

Roadsteads which are normally used for the loading, unloading and anchoring of ships, and which would otherwise be situated wholly or partly outside the outer limit of the territorial sea, are included in the territorial sea.

Article 13

Low-tide elevations

1. A low-tide elevation is a naturally formed area of land which is surrounded by and above water at low tide but submerged at high tide. Where a low-tide elevation is situated wholly or partly at a distance not exceeding the breadth of the territorial sea from the mainland or an island, the low-water line on that elevation may be used as the baseline for measuring the breadth of the territorial sea.
2. Where a low-tide elevation is wholly situated at a distance exceeding the breadth of the territorial sea from the mainland or an island, it has no territorial sea of its own.

Article 14

Combination of methods for determining baselines

The coastal State may determine baselines in turn by any of the methods provided for in the foregoing articles to suit different conditions.

Article 15

Delimitation of the territorial sea between States with opposite or adjacent coasts

Where the coasts of two States are opposite or adjacent to each other, neither of the two States is entitled, failing agreement between them to the contrary, to extend its territorial sea beyond the median line every point of which is equidistant from the nearest points on the baselines from which the breadth of the territorial seas of each of the two States is measured. The above provision does not apply, however, where it is necessary by reason of historic title or other special circumstances to delimit the territorial seas of the two States in a way which is at variance therewith.

Article 16

Charts and lists of geographical coordinates

1. The baselines for measuring the breadth of the territorial sea determined in accordance with articles 7, 9 and 10, or the limits derived therefrom, and the lines of delimitation drawn in accordance with articles 12 and 15 shall be shown on charts of a scale or scales adequate for ascertaining their position. Alternatively, a list of geographical coordinates of points, specifying the geodetic datum, may be substituted.
2. The coastal State shall give due publicity to such charts or lists of geographical coordinates and shall deposit a copy of each such chart or list with the Secretary-General of the United Nations.

The Article 47, Article 75 and Article 84 contain similar requirements for charts and lists of geographical coordinates related to archipelagic states, exclusive economic zone and continental shelf.

Article 57
Breadth of the exclusive economic zone

The exclusive economic zone shall not extend beyond 200 nautical miles from the baselines from which the breadth of the territorial sea is measured.

Article 76
Definition of the continental shelf

1. The continental shelf of a coastal State comprises the sea-bed and subsoil of the submarine areas that extend beyond its territorial sea throughout the natural prolongation of its land territory to the outer edge of the continental margin, or to a distance of 200 nautical miles from the baselines from which the breadth of the territorial sea is measured where the outer edge of the continental margin does not extend up to that distance.

2. The continental shelf of a coastal State shall not extend beyond the limits provided for in paragraphs 4 to 6.

3. The continental margin comprises the submerged prolongation of the land mass of the coastal State, and consists of the sea-bed and subsoil of the shelf, the slope and the rise. It does not include the deep ocean floor with its oceanic ridges or the subsoil thereof.

4. (a) For the purposes of this Convention, the coastal State shall establish the outer edge of the continental margin wherever the margin extends beyond 200 nautical miles from the baselines from which the breadth of the territorial sea is measured, by either:
   (i) a line delineated in accordance with paragraph 7 by reference to the outermost fixed points at each of which the thickness of sedimentary rocks is at least 1 per cent of the shortest distance from such point to the foot of the continental slope; or
   (ii) a line delineated in accordance with paragraph 7 by reference to fixed points not more than 60 nautical miles from the foot of the continental slope.

   (b) In the absence of evidence to the contrary, the foot of the continental slope shall be determined as the point of maximum change in the gradient at its base.

5. The fixed points comprising the line of the outer limits of the continental shelf on the sea-bed, drawn in accordance with paragraph 4 (a)(i) and (ii), either shall not exceed 350 nautical miles from the baselines from which the breadth of the territorial sea is measured or shall not exceed 100 nautical miles from the 2,500 metre isobath, which is a line connecting the depth of 2,5000 metres.

6. Notwithstanding the provisions of paragraph 5, on submarine ridges, the outer limit of the continental shelf shall not exceed 350 nautical miles from the baselines from which the breadth of the territorial sea is measured. This paragraph does not apply to submarine elevations that are natural components of the continental margin, such as its plateaux, rises, caps, banks and spurs.

7. The coastal State shall delineate the outer limits of its continental shelf, where that shelf extends beyond 200 nautical miles from the baselines from which the breadth of the territorial sea is

measured, by straight lines not exceeding 60 nautical miles in length, connecting fixed points, defined by coordinates of latitude and longitude.

8. Information on the limits of the continental shelf beyond 200 nautical miles from the baselines from which the breadth of the territorial sea is measured shall be submitted by the coastal State to the Commission on the Limits of the Continental Shelf set up under Annex II on the basis of equitable geographical representation. The Commission shall make recommendations to coastal States on matters related to the establishment of the outer limits of their continental shelf. The limits of the shelf established by a coastal State on the basis of these recommendations shall be final and binding.

9. The coastal State shall deposit with the Secretary-General of the United Nations charts and relevant information, including geodetic data, permanently describing the outer limits of its continental shelf. The Secretary-General shall give due publicity thereto.

10. The provisions of this article are without prejudice to the question of delimitation of the continental shelf between States with opposite or adjacent coasts.

References

IHO, 1993. 3rd Edition. "A Manual on Technical Aspects of the United Nations Convention on the Law of the Sea - 1982". Special Publication No 51, International Hydrographic Bureau, Monaco.

UN, The Law of the Sea, 1983. "United Nations Convention on the Law of the Sea". UN, New York.

UN, The Law of the Sea, 1989. "Baselines: An Examination of the relevant Provisions of the United Nations Convention on the Law of the Sea ". ISBN 92-1-133308-2. UN, New York.

UN, The Law of the Sea, 1989. "Baselines: National Legislation". ISBN 92-1-133325-3. UN, New York.

UN, The Law of the Sea, 1994. "Practice of States at the time of entry into force of the United Nations Convention on the Law of the Sea". ISBN 92-1-133474-8. UN, New York.

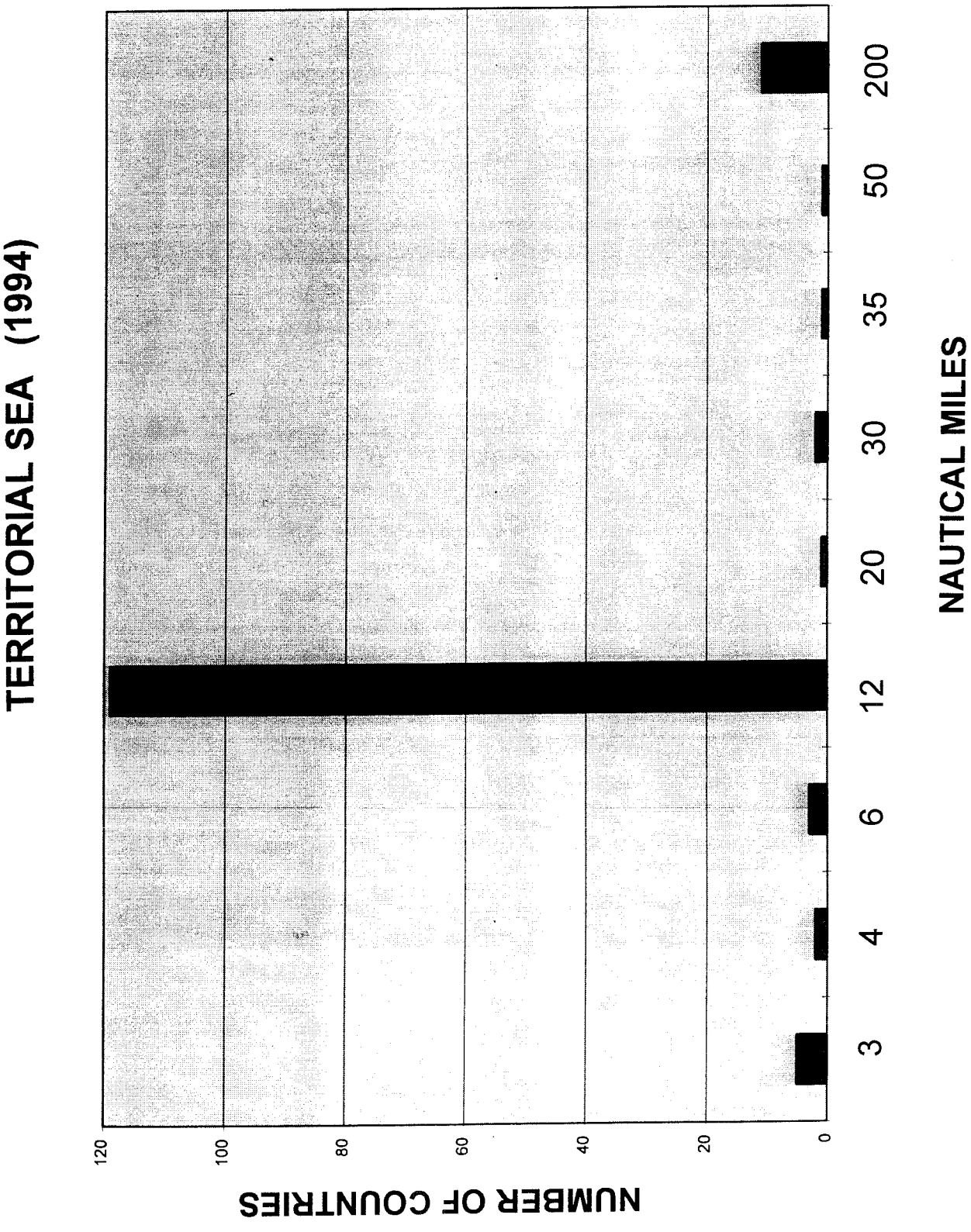
TERRITORIAL SEA (1994)
NUMBER OF COUNTRIES
0
20
40
60
80
100
120
3
4
6
12
20
30
35
50
200
NAUTICAL MILES

STRAIGHT BASELINE

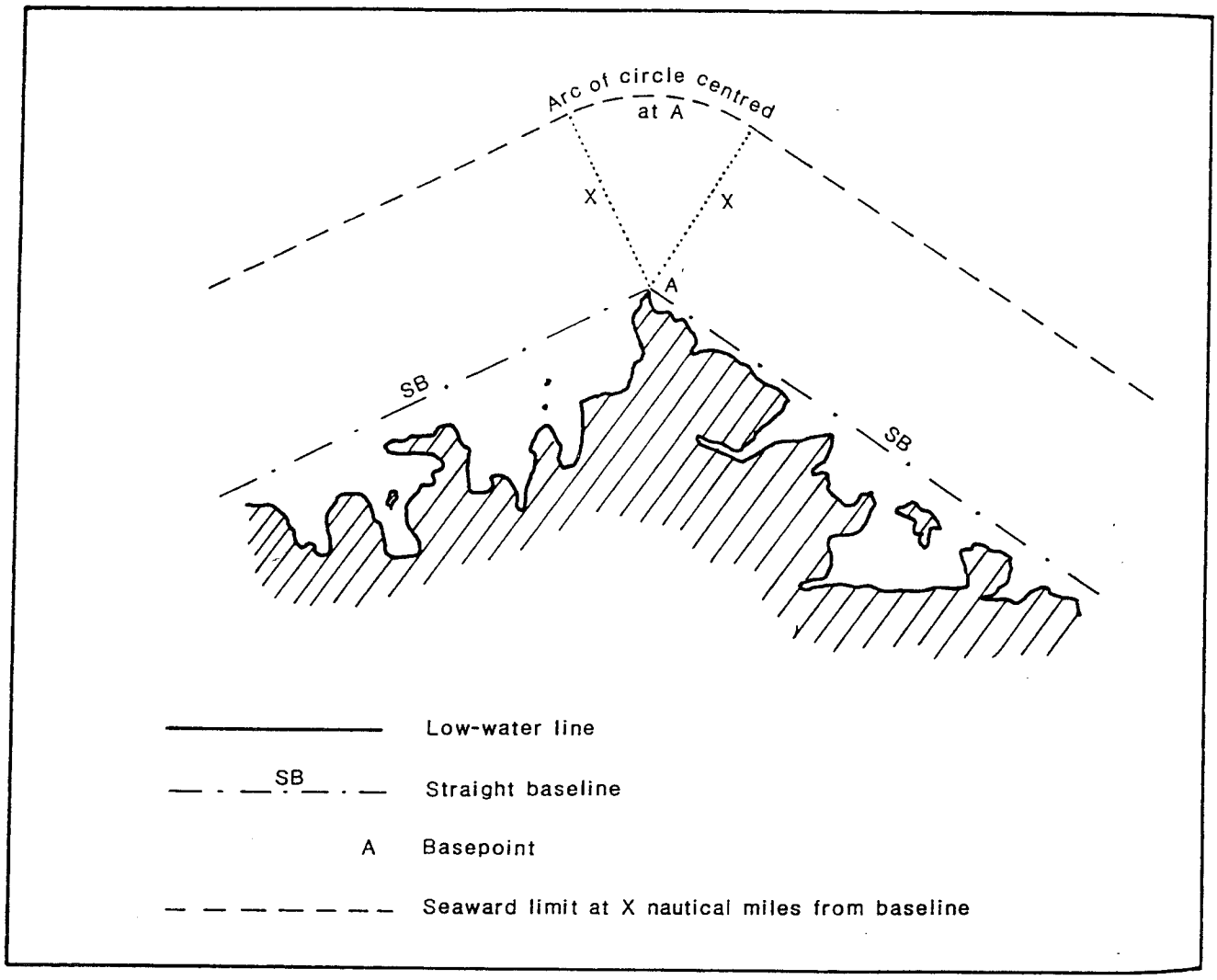

CONTINENTAL SHELF
LOS CONVENTION, ARTICLE 76

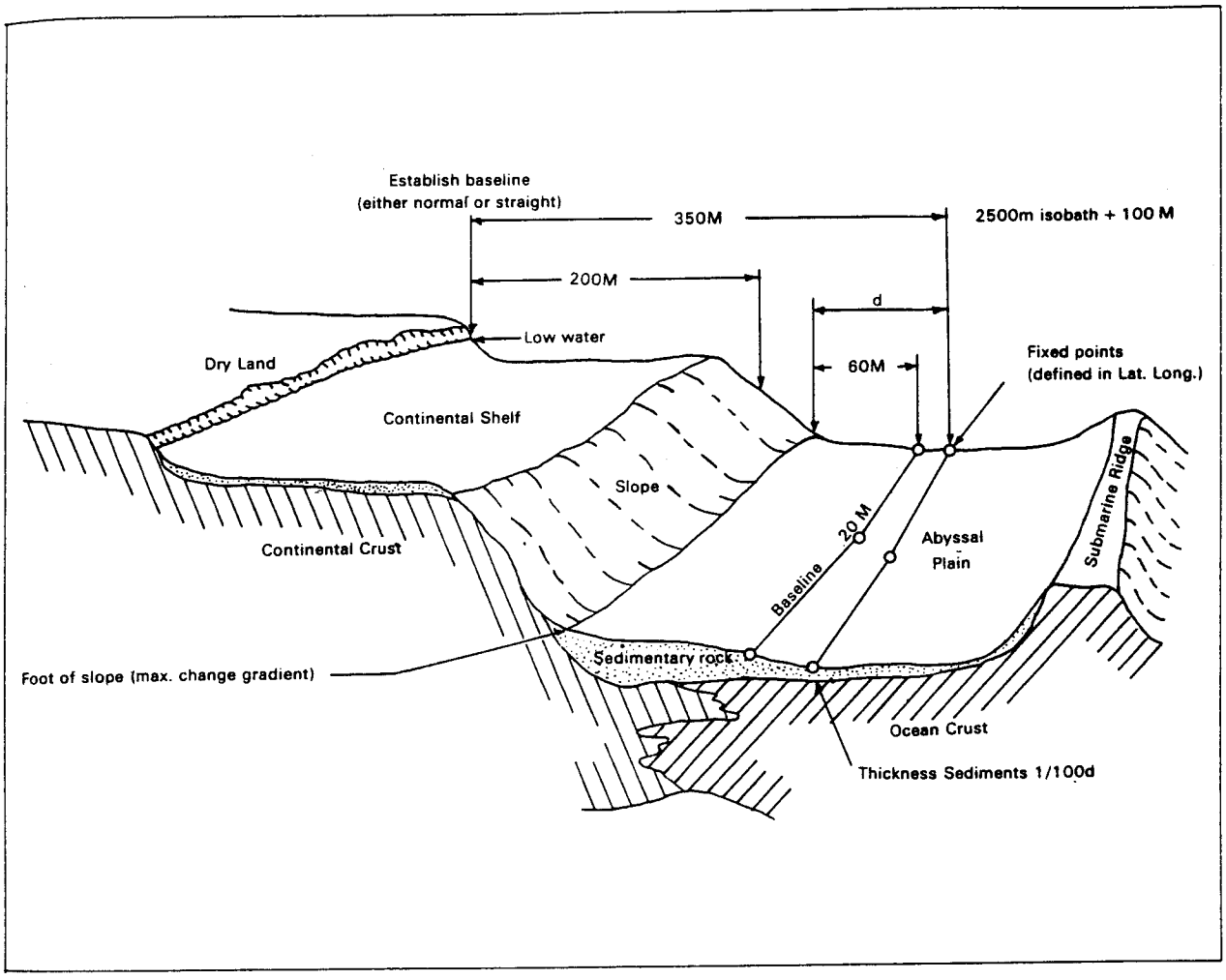

VERTICAL DATUMS

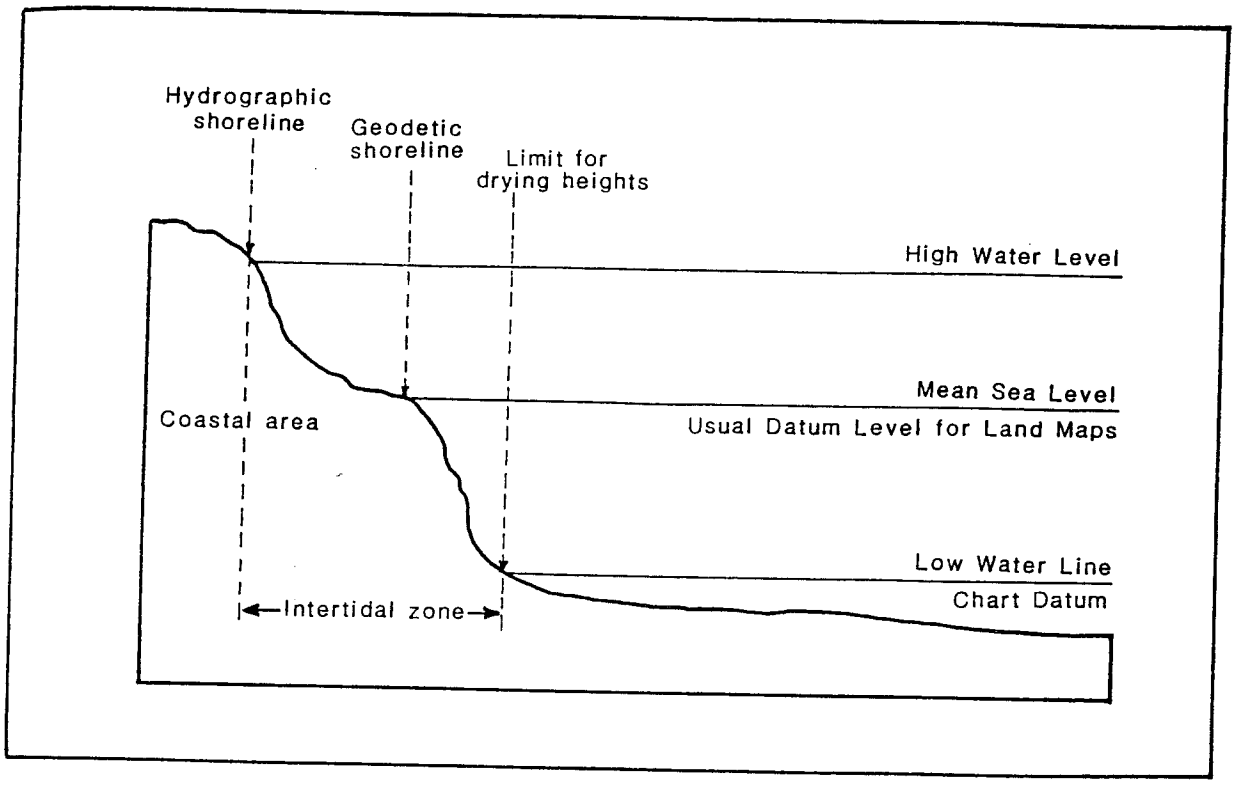

THE NKG-96 GEOID

Rene Forsberg
KMS, Rentemestervej 8, DK-2400 Copenhagen NV, Denmark
J. Kaminskis
State Land Survey of Latvia, 11. Novembra Krastmala 31, LV-1484 Riga, Latvia
Dag Solheim
Statens Kartverk, N-3500 Hönefoss, Norway

Abstract:
The NKG-96 geoid model is an updated high-resolution geoid model for the Scandinavian and Baltic region, done by spherical FFT approaches, taking topography into account by a hybrid RTM/Helmert condensation approach. Significant new data sources have entered the geoid solution: a new spherical harmonic reference model, new gravity data over many regions, including the Baltic republics and the Russian border regions, and new high-resolution topographic sources. ERS-1 geodetic mission satellite altimetry has been included in the Baltic, using Fourier-based draping techniques, and taking sea surface topography from tide gauge levellings into account. Compared to more than 300 GPS-levelling points across the region the geoid shows a fit at the 10 cm level, thus being a major improvement over earlier models. In local regions with good gravity coverage, such as Denmark, the geoid fitted to the national GPS net yields accuracies at the 1 cm-level, thus allowing accurate operational levelling by GPS.

INTRODUCTION

The geoid determination project in the Nordic region (recently expanded with the Baltic countries) has been a continuing process for more than a decade. The work has been carried out within the framework of a working group under the Nordic Geodetic Commission (NKG), with the currently adopted standard model termed NKG-89 (Forsberg, 1990). This paper represents an updated version of this model, with significant new data, and the most recent EGM-96 reference model (Lemoine et. al, 1996). The computed model covers the central part of the Nordic and Baltic area in a single FFT solution, with additional equivalent FFT solutions for Iceland and Svalbard.

The by far most time-consuming work relating to the gravimetric geoid determination has been the collection and validation of available gravity data, and inclusion of data into the joint data base at KMS, holding more than 900.000 gravity observations covering Scandinavia and surrounding areas from Greenland to the Urals. In recent years significant new data have been entered into the data base from Norway and Sweden (geological survey data and offshore data), from the Baltic republics (point data from digitized maps and station sheets) as well as data from Eastern Germany, Poland and Russia. The data coverage is shown in Fig. 1. The most recent data addition used for was a joint Nordic marine gravity survey in the Baltic and Bothnian seas, carried out October 1996 to obtain additional data for geoid determination.

To obtain the necessary resolution and quality of the geoid model, detailed digital elevation models (DEM's) are indispensable. All areas of the region are now - opposed to earlier solutions - covered by high-resolution DEM's, provided by the national survey agencies, or from the recently released NGDC CD-ROM of global topography ("GLOBE"), derived from averages of dense (3") heights of the classified DTED height data base of Defense Mapping Agency. Table 1 shows the resolution of the available height data. Detailed terrain corrections were computed from the most detailed height data, and merged combined height grids at various resolutions (0.01°, 0.025°, ..) were constructed and validated for other purposes such as geoid terrain corrections.

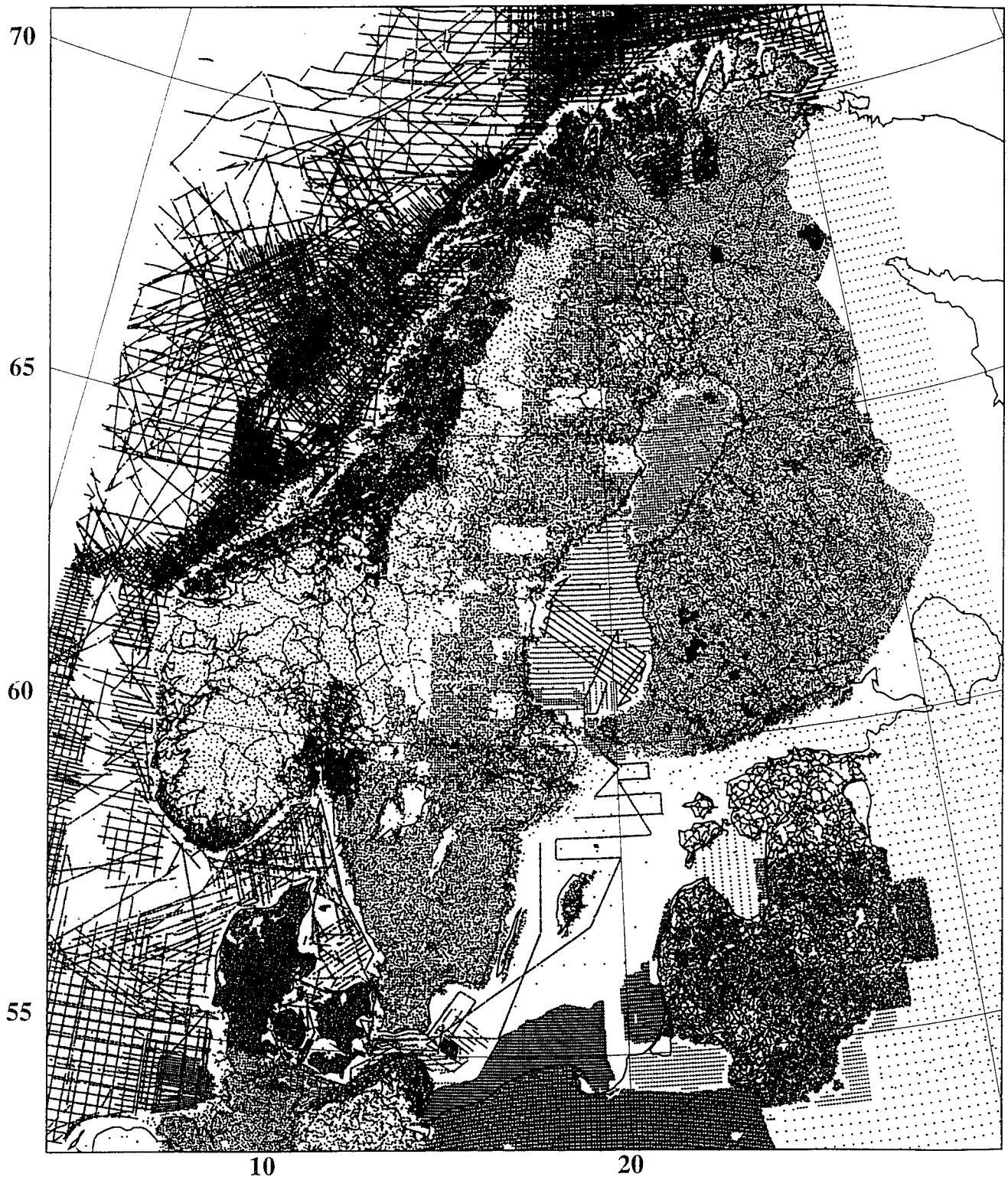

Fig. 1. Gravity data coverage of the Nordic and Baltic area.

Table 1. Resolution of most detailed height models used

Country	*DEM resolution*	*Source*	*Country*	*DEM resolution*	*Source*
Norway	100 x 100 m	Statens Kartverk	Lithuania	approx. 1 km	Lithuania Tech. Univ.
Denmark	200 x 200 m	KMS	Germany	approx. 1 km	IfAG
Sweden	500 x 500 m	LMV	Other areas	30"	"GLOBE"

GRAVIMETRIC GEOID DETERMINATION

The present geoids have been computed by the remove-restore technique, yielding in principle quasigeoid heights ζ. In this method the geoid signal is constructed by subdividing it into three parts

$$\zeta = \zeta_1 + \zeta_2 + \zeta_3 \tag{1}$$

where the first part is the global field, coming from a spherical harmonic expansion

$$\zeta_1 = \frac{GM}{R\gamma}\sum_{n=0}^{N}\left(\frac{R}{r}\right)^n\sum_{m=0}^{n}(C_{nm}cosm\lambda + S_{nm}sinm\lambda)P_{nm}(\sin\phi) \tag{2}$$

the second part from the topography, and the third part from the contributions of "residual" gravity (i.e., gravity anomalies minus the global field contribution and gravimetric terrain effects).

The EGM-96 geopotential model has been used as a reference model, using a full three-dimensional grid interpolation scheme ("sandwich" grid interpolation) to take into account the height variations, as well as the height-dependent atmospheric correction.

Terrain effects have been removed in a consistent RTM terrain data reduction, taking into account the topographic irregularities relative to a mean height surface with a resolution of approx. 100 km, for details see Forsberg (1984). The mean height surface, to which the residual topography refers, has been obtained by a gaussian low-pass filter applied on the composite DEM of the region. Table 2 shows the effect of removing the reference field and terrain effects on the selected subset of gravity data of the region (1.5' x 3' pixel select). As can be seen from the table the standard deviation of the residual is quite small, illustrating the usefullness of the remove-restore technique (1).

Table 2. Statistics of gravity data reductions in Nordic area 53-73°N, 1-33° E (unit: mgal)

Points: 182239	mean	std.dev.	min	max
Original data	-0.78	25.05	-141.24	193.18
Δg - EGM96 ref.	-1.54	15.47	-167.85	132.00
Δg - ref. - RTM	0.47	9.84	-68.76	89.06

Residual gravity anomalies are in principle converted into residual height anomalies by spherical FFT evaluation (Strang van Hees, 1990), using an improved multiband-formulation of the

original method. The spherical FFT method in principle evaluates Molodensky's integral

$$\zeta_3 = \frac{R}{4\pi\gamma} \iint_{\sigma} (\Delta g_3 + g_1^c)\ S(\psi)\ d\sigma \tag{3}$$

where g_1^c is the first term of the Molodensky series for the *reduced* field, which for most practical purposes may be neglected. The expression (3) may be written as a spherical convolution in latitude and longitude (ϕ,λ) for a given reference parallel ϕ_{ref}, and by utilization of a number of bands a virtually exact convolution expression may be obtained by a suitable linear combination of the bands. For each such band the convolution expressions may be evalutated by FFT using

$$\zeta_3 = S_{ref}(\Delta\phi,\Delta\lambda) * \Delta g_3(\phi,\lambda)\sin\phi = \mathcal{F}^{-1}[\mathcal{F}(S_{\phi_{ref}}).\mathcal{F}(\Delta g \sin\phi) \tag{4}$$

where S_{ref} is a (modified) Stokes' kernel function, and * and $\mathcal{F}$ the two-dimensional convolution and Fourier transform, respectively, for details see Forsberg and Sideris (1993).

In the actual application of the method, the data are gridded by least-squares collocation, and a 100% zero padding is used to limit the periodicity errors of FFT. This yields an FFT transform of 1600 x 1280 points for the region. The topographic restore signal (ζ_2) is evaluated simultanously with (4) using the first-order mass-layer approximation to the RTM geoid effect given in Forsberg (1985). By merging these computations, the data for FFT will actually turn into a modified Faye anomaly

$$\Delta g_{FFT} = \Delta g_3 + 2\pi G\rho(h - h_{ref}) \tag{5}$$

and thus be similar to "Helmert" methods based on Faye anomalies, but still in principle the method gives height anomalies ζ, and the outcome of the computations is the quasigeoid.

USE OF SATELLITE ALTIMETRY IN THE BALTIC SEA

To improve the sparse gravity coverage in the southern Baltic Sea, gravity data was predicted from geodetic mission ERS-1 satellite altimetry. The ERS-1 altimetry was reduced for sea-slope effects using the sea surface topography model of Ekman and Mäkinen (1994), and the altimetry data subsequently edited, cross-over adjusted and gridded to yield an estimate of the geoid surface. Fig. 2 shows the good coverage of altimetry available.

The gridded sea-surface heights were subsequently inverted to gravity using Wiener filtering inverse Stokes FFT (Forsberg and Solheim, 1988), and this gravity grid has subsequently been "draped" upon the existing gravity data using collocation techniques, producing a smooth, merged gravity data set across the southern Baltic. In the draping technique the residual gravity error

$$\epsilon = \Delta g_{observed} - \Delta g_{ERS-1} \tag{6}$$

is gridded into a gravity "correction" grid by least-squares collocation (using a "long" correlation length typical of sea-surface topography), and subsequently applied to the altimetry-derived gravity to obtain "bias-free" gravity anomalies. The "draping" method will diminish errors due to sea-surface topography, as well as errors due to lack of altimeter data on land. The method works well with the sparse gravity data (ship and ocean bottom gravimetry) available in the Baltic, and an independent check was obtained with the recent (October 1996) joint Nordic

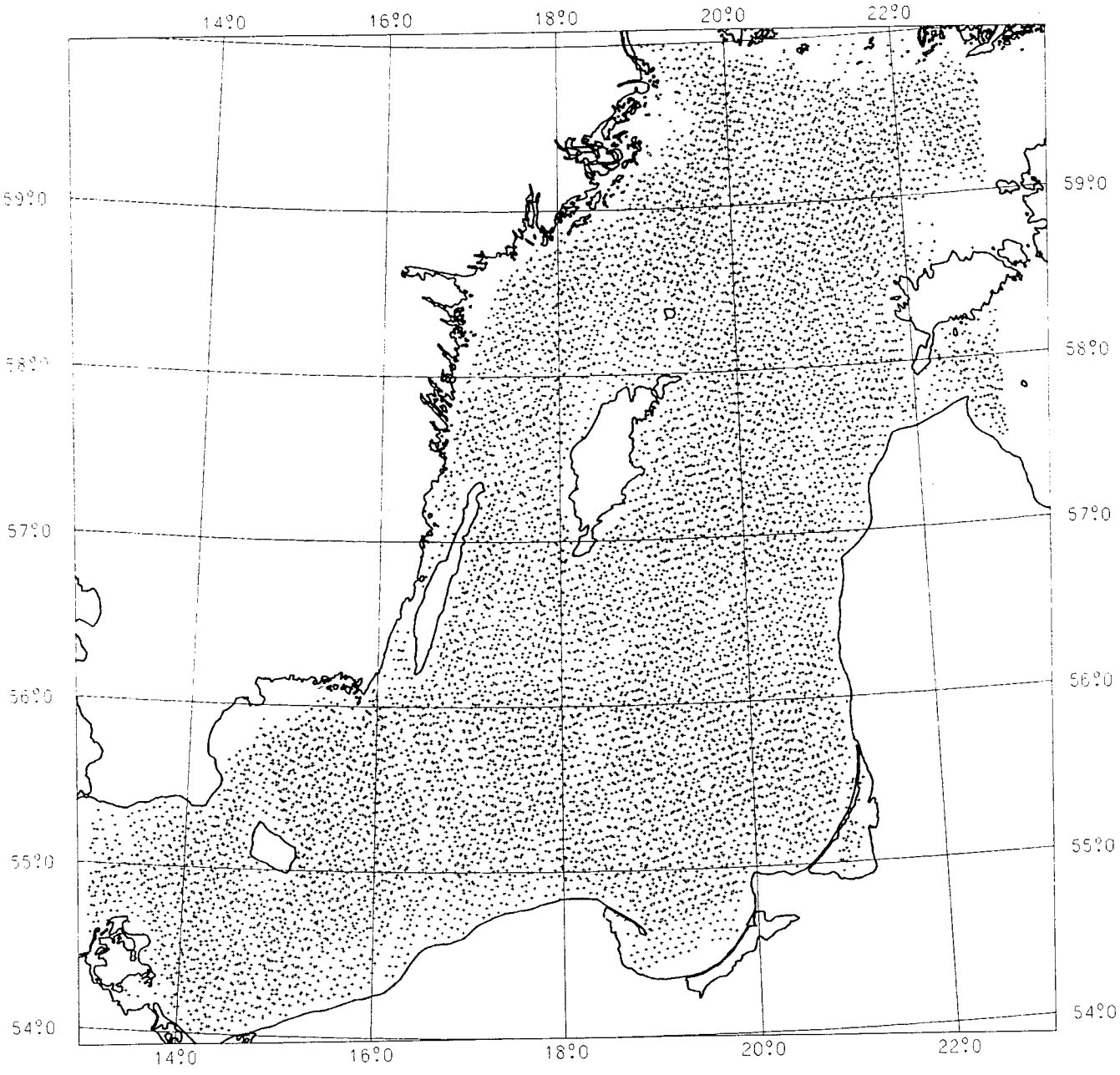

Fig. 2. ERS-1 satellite altimetry data in the southern Baltic Sea

marine gravity survey, which indeed showed an earlier draped altimetry solution to be good to 5 mgal without significant bias. In the final computation of the NKG-96 geoid the altimetry data was thus used with a 5 mgal standard deviation, selected only in areas void of marine gravimetry, and merged with rest of the data.

FINAL GEOID AND COMPARISONS TO GPS

The final geoid was computed on the EGM96 ellipsoid (a = 6378136.3 m). To transfer the geoid into the (approximate) local Nordic sea level, a correction of -1.06 m was applied to transfer to the WGS ellipsoid, as well as taking into account global geoid errors and sea-surface topography.

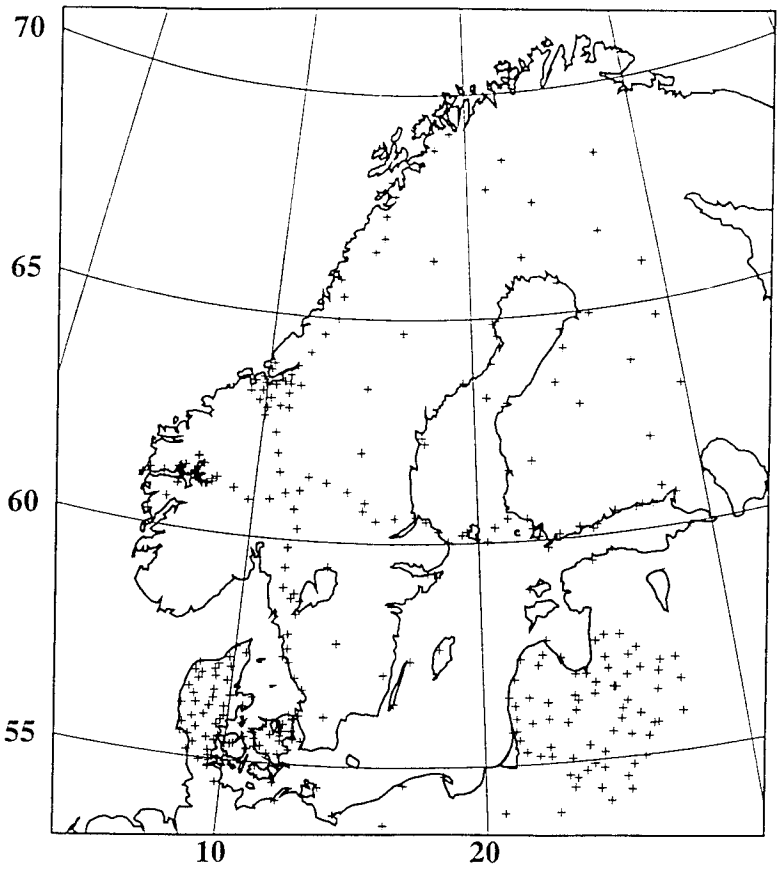

Fig. 3. Location of GPS/levelling points

The transformation constant was determined from a set of approx. 300 GPS/levelling stations of the region (Fig. 3). The GPS points have been approximately transformed into the ITRF93/UELN datum using the E-W Scandinavian GPS/levelling line data as reference (SWET line, cf. Poutanen et al, 1994), transforming the other GPS/levelling networks into the SWET system through common points and known differences between national levelling datums. The final NKG-96 geoid is shown in Fig. 4.

The statistics of the GPS geoid fits for different GPS surveys are given in Table 3, both before and after applying a 4-parameter trend function of form

$$\epsilon = \zeta_{grav} - \zeta_{GPS} = \cos\phi\cos\lambda a_1 + \cos\phi\sin\lambda a_2 + \sin\phi a_3 + R a_4 + \epsilon' \qquad (7)$$

which corresponds to a Helmert transformation for geoid undulations. From Table 3 it appears that a surprisingly good geoid fit is obtained over many areas, reflecting not only a good fit of the geoid, but also very accurate GPS and levelling results.

For an improved local fit, the residual geoid error ϵ' of (7) may be modelled by least-squares collocation, similar to the draping technique applied for altimetry. In this way the geoid may be completely taylored to GPS, but in this way errors of GPS/levelling will enter the geoid model as well. To give an example of such local geoid fitting, the danish GPS network REFDK (B. Madsen, pers.comm.) has been used, assuming an error of the GPS/levelling data of 5 mm, and a correlation length of ϵ' of 50 km. The errors of the geoid fit of the taylored geoid is shown in Table 4. The first row shows the fit to the 67 constrained GPS points, being small as expected, and the second row is the comparison to an independent GPS set of 70 GPS stations extending in a belt along the west coast of Jutland (J.Nielsen, pers.comm.). The comparison of the independent GPS net shows that in an r.m.s. sense the tayloring of the NKG-96 geoid has yielded

a geoid accurate to 1 cm for Denmark.

Table 3. Fit of GPS/levelling data sets to NKG-96 geoid (unit: m).

GPS data set / *source*	Mean diff.	Std.dev.	Stdev. 4-par fit
IfE profile (*Torge*, Germany-Tromsø, 46 pts.)	0.016	0.097	0.045
SWET profile (*Poutanen*, 34 pts., used as ref.)	-0.001	0.118	0.065
Sweden (SWEPOS, 21 points, *B.G. Reit*)	0.059	0.078	0.054
Finland (42 points, *from M. Poutanen*)	-0.072	0.148	0.087
Baltic Sea Level Project (30 points, *Poutanen*)	0.101	0.094	0.068
Lithuania (36 points, *from E. Parseliunas*)	0.001	0.080	0.078
Latvia (26 points, *from J. Kaminskis*)	-0.006	0.090	0.077
Denmark (67 points, *from B. Madsen*)	-0.148	0.023	0.020
Trondheim area (20 points, *from G. Simensen*)	0.121	0.065	0.061
Sognefjord area (42 pts. in local system, *SK*)	(-0.348)	0.112	0.048
All data	0.004	0.123	0.096

Table 4. Comparison of taylored geoid for Denmark to GPS nets (unit: m)

Fit to:	Mean	Std.dev.	Min	Max
REFDK constrained GPS data	0	0.008	-0.023	0.018
Independent GPS data	-0.001	0.011	-0.020	0.026

CONCLUSIONS AND ACKNOWLEDGEMENTS

A new geoid model of the Nordic region has achieved 10 cm accuracy over 1000 km+ baselines, and a local example (Denmark) has shown that 1 cm geoid fitting is possible. The model will be useful for geodetic height determination by GPS.

We thank the Nordic and Baltic geodetic agencies and many individuals for providing the necessary gravity and GPS data. The gravity data represent results of vast field works over many decades. We also thank DMA for providing the EGM96 reference model.

REFERENCES

Ekman, M., J. Mäkinen: Mean sea surface topography in a unified height system for the Baltic Sea area. Proc. 12th General meeting of the NKG, Ullensvang, Norway, pp. 244-258, 1994.

Forsberg, R.: A Study of Terrain Reductions, Density Anomalies and Geophysical Inversion Methods in Gravity Field Modelling. Reports of the Department of Geodetic Science and Surveying, No. 355, The Ohio State University, Columbus, Ohio, 1984.

Forsberg, R.: Gravity field terrain effect computations by FFT. Bull. Geod., 59, pp. 342-360, 1985.

Forsberg, R. and D. Solheim: Performance of FFT methods in local gravity field modelling. Proc.

Chapman Conf. on Earth's gravity field, Ft. Lauderdale, Florida, pp. 100-103, 1988.
Forsberg, R.: A new high-resolution geoid of the Nordic area. In: Determination of the geoid. IAG symposium 106, Milano, Proc. published by Springer Verlag, 1990.
Forsberg, R., M. G. Sideris: Geoid computations by the multi-band spherical FFT approach. Manuscripta Geodaetica, 18, pp. 82-90, 1993.
Lemoine, F.G., et. al.: The development of the NASA GSFC and DMA joint geopotential model. Proc. Symposium on Gravity, Geoid and Marine Geodesy, Tokyo, 1996.
Poutanen, M, K. Gjerde, L. Jivall, F. Madsen: Final results of the SWET-92 GPS campaign. Proc. 12th General meeting of the Nordic Geodetic Commission, Ullensvang, Norway, 1994, pp.294-303.
Strang van Hees, G.: Stokes formula using fast Fourier techniques. Manuscripta Geodaetica, vol. 15, pp. 235-239, 1990.

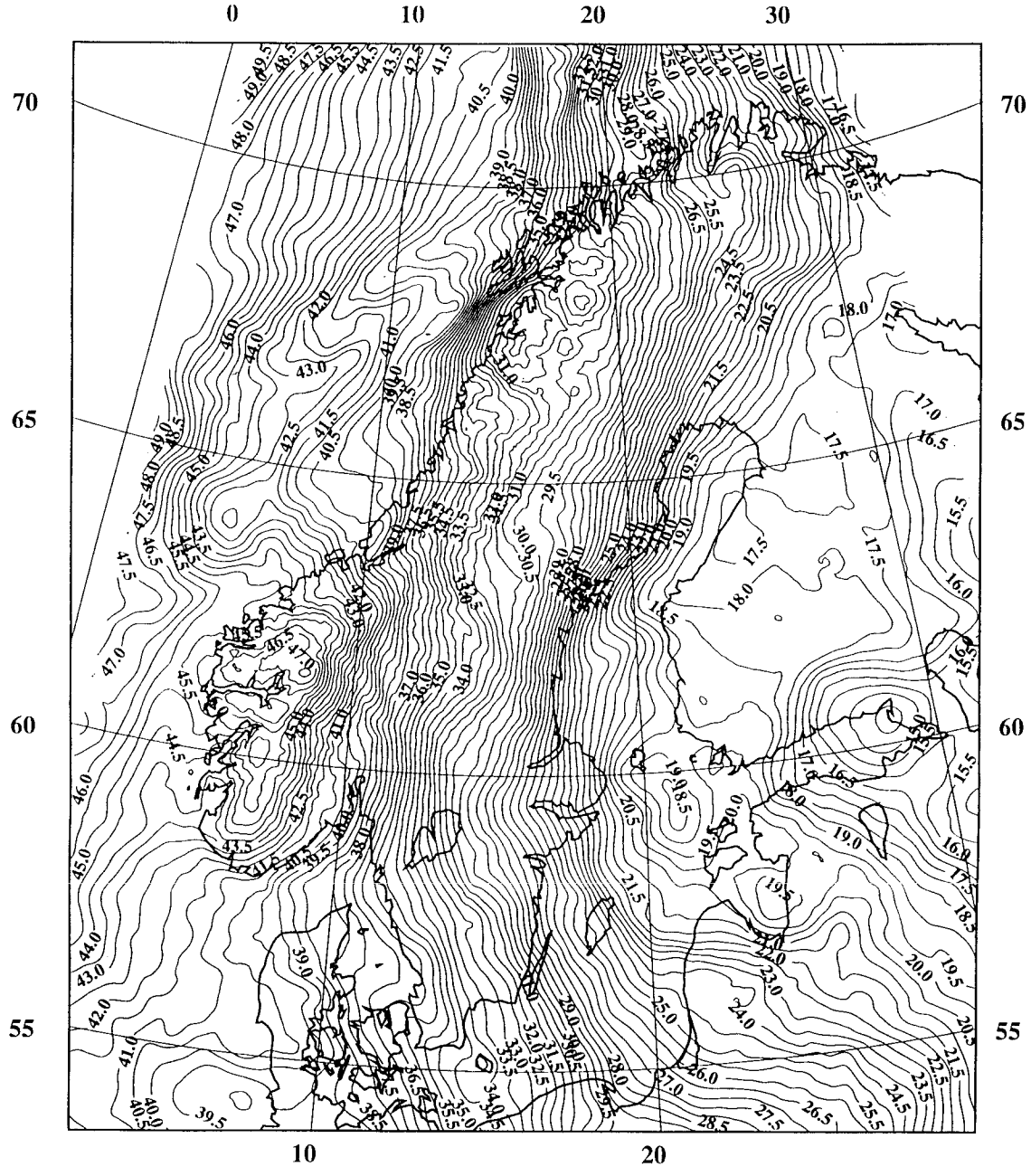

Fig. 4. NKG-96 geoid, contour interval 0.5 m

New gravimetric calibration line of the Finnish Geodetic Institute

Hannu Ruotsalainen, Jaakko Mäkinen and Jussi Kääriäinen
Finnish Geodetic Institute
P.O.Box 15
FIN-02431 Masala ,Finland
tel +358 9 255550
fax +358 9 29555200
e-mail Jaakko.Makinen@fgi.fi

Abstract

We have established a calibration line for relative gravimeters, to replace Helsinki–Olkkala used since 1959. The new line is called Masala–Vihti, and it has 6 stations spaced at 10...11 mgal. The total range is 53 mgal with a driving distance of 40 km on good roads. The starting point is in the new headquarters of the Finnish Geodetic Institute, with an excenter outside the building. The end point is in a lightweight shed where either indoor or outdoor conditions can be arranged. The 4 intermediate points are outdoors. The gravity values at the end points were measured with the JILAg-5 absolute gravimeter in 1997. The line will be used to determine the linear calibration factors of gravimeters employed in regional gravity surveys and geophysical prospecting, and to monitor the performance of gravimeters for geodetic work.

Introduction

In 1959 the Finnish Geodetic Institute (FGI) established a calibration line between the reference station Helsinki (no. 240001) and the station Olkkala (no. 590652) in the municipality of Vihti northwest from Helsinki (Kiviniemi 1963, 1964). The line exploited the gravity high in Vihti to achieve a 64 mgal range with 50 km driving distance, with no help from elevation differences. The gravity range resulted both from practical considerations and from the limited range (80 mgal) of the Worden Master 227, the mainstay of FGI gravity work in those days. The gravity difference of the line (63.94 mgal) was derived from the gravity difference between Helsinki and Hammerfest through the First Order Gravity Net (FOGN) of Finland (Kiviniemi 1964).

The starting point (low gravity end) in downtown Helsinki soon proved problematic. In 1968–1969 its gravity decreased by 46 μgal (measured), when a tunnel was excavated in the rock beneath. Anticipating that, the point had in 1968 been transferred to the FOGN station Helsinki 2 (no. 680001) on the steps of Kallio Church. This gave a range of 66.04 mgal (Kiviniemi, 1980).

The second starting location was not stable either. First, in 1972 the tunnel for the underground railway in Helsinki decreased its gravity by 4 μgal (modelled). Then in 1986 local excavation work caused a further decrease of 15 μgal (modelled).

The end point in Olkkala has had its problems, too. It is situated on a boulder in a stream, near the outlet from a small lake. The boulder probably rests on bedrock as its elevation has been quite stable, but the varying water level in the stream causes gravity variation of several microgals.

Over the years the line has been called Helsinki/Kallio Church–Vihti/Olkkala, in all combinations, at least colloquially. It has been used by several institutes to calibrate Worden gravity meters and other meters employed in regional gravity surveys and geophysical prospecting, i.e., for measuring gravity differences which are maximally of the same order as the line itself. The calibration of quartz spring gravimeters may change more than 1×10^{-4} per year, necessitating frequent checking.

For LaCoste & Romberg model G-meters (LCR-G) the range is insufficient. The LCR-G periodic calibration errors can cause biases of the order of 20 μgal (see for instance Kiviniemi, 1974). With the small range this translates to an error of 3×10^{-4} in the linear calibration factor, intolerable in view of the instrument's high precision. Regular LCR measurements on the calibration line are performed, but they serve to monitor the line itself, and gravimeter performance in general. Instead, the calibration of the LCR-G meters is done between absolute stations over a range of 500...900 mgal (Mäkinen and Haller, 1983).

This will not change with the new line, which will fill the same purposes as the old Helsinki–Olkkala, but hopefully without its stability problems. The new line Masala–Vihti was also designed from the beginning to have absolute measurements at the end points, which would have been quite difficult to arrange for Helsinki–Olkkala.

Site selection and construction

The FGI building in Masala (where the institute is located since 1995) is situated in a gravity low. The building encompasses a laboratory for gravimetric work with 4 piers on bedrock. Thus it was natural to establish the low-gravity end of the new line there. For the other end we use to advantage the same gravity high as for the old line. The new site (no. 971012) in Vihti is 1 km southwest from the old site, in the same valley but on bedrock and 100 m away from the stream. Water level in the stream is not an issue anymore. Subsurface water and snow cover will be, maximally at the 5 μgal level. Compared with the old line, 13 mgal has been lost in the gravity difference, mostly at the low end. The distance is 40 km and the driving time 35 min on open roads outside the city. The locations are shown in Figure 1.

The station in Vihti is on a small highly convex outcrop of bedrock. A platform of size 2×3 m^2 was constructed on it in reinforced concrete, 0.5...0.1 m thick. That is just the minimum to make a flat surface and to contain the steel reinforcement, which also anchors the pier into the rock (very important). Stainless steel was used to avoid magnetic effects in relative meters. (Absolute meters are immune enough anyway.) The platform serves both as a pier and a floor. Absolute measurements with the JILAg meter, the most stringent test available, have proved it very stable.

A lightweight shed consisting of a roof over an semi-open frame was erected on the platform. During the absolute measurements plywood boards were fitted to the frame to make the

building thermally isolated (Figure 2). Normally the frame is open and the station is at outdoor temperature but protected from rain and snow and partly from wind.

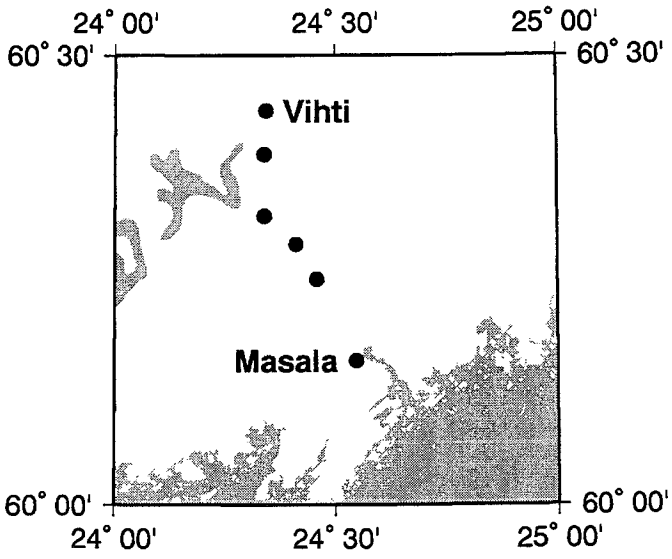

Figure 1. Location of the calibration line.

Figure 2. Two outside views of the Vihti station, in normal condition (left), and fitted with plywood boards for the absolute measurement (right).

The gravity laboratory in the FGI building in Masala has four 1×1 m^2 piers which go down to bedrock at 3 m depth. The piers are not monolithic, the top 5 cm was poured afterwards to bring the surface to floor level. Such a layer does not attach solidly and this initially caused difficulties with the JILAg-5. Drop recoil, transferred to the pier through the dropping chamber tripod, causes a tilt of this top layer, which is then transmitted to the interferometer through its legs. Interferometer tilts which are coherent with the drop event cause errors in the

distance measurement in the JILAg meter (and all other absolute meters up to the FG5; see for instance Niebauer et al., 1995).

The problem was solved by planting brass supports for the interferometer through the top layer into the body of the pier, resistant enough against the shaking. The alternative would have been to hack off the top layer altogether, aesthetically perhaps less pleasing. Even after improvement the pier is not as good as the one in Vihti (Figure 3).

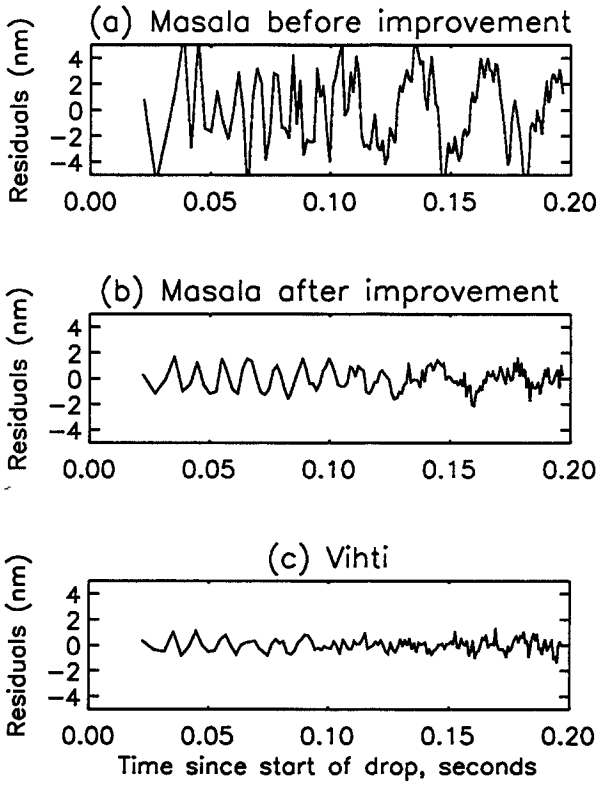

Figure 3. Drop residuals in Masala (a) before and (b) after improving the pier (see text), and (c) in Vihti. The JILAg-5 determines the acceleration of free fall by fitting a second degree polynomial to 150 observed pairs of time and distance which take some 0.2 s to collect. Systematic features in the residuals from this fit depend mainly on pier stability. Here the residuals have been averaged over 25 drops to emphasize the systematics.

In practice, the starting point for the calibration line is not the absolute station in Masala (no. 961002) but its outdoor excenter (no. 971007) , such that the meters to be calibrated need not be subjected to temperature shocks. Moreover, users do not need to make arrangements to enter the building.

In addition to the end points, there are 4 intermediate stations (nos. 971008...971011), spaced at 10...11 mgal (Figure 1). They are outdoors on bedrock, in the immediate vicinity of the route between the end points. They are marked with stainless steel bolts but without other constructions. If we are able to accumulate enough measurements with different instruments, then the ensemble of the stations can be used to determine periodic calibration errors of LCR gravimeters.

First measurements

Absolute measurements with the JILAg-5 (Faller et al., 1983) were performed in Vihti and Masala in September 1997 by the second author, occupying both stations once. Figure 4 shows the observation series in Vihti. Vertical gradients were measured by the first author with the LCR G600, a single set on both stations. Table 1 summarizes the results. The uncertainty in gravity difference at pier level is now 7 μgal or 1.3×10^{-4} (one-sigma) which we do not find satisfactory. The absolute meter will soon be upgraded and more measurements performed. We expect to get down to about 4 μgal uncertainty.

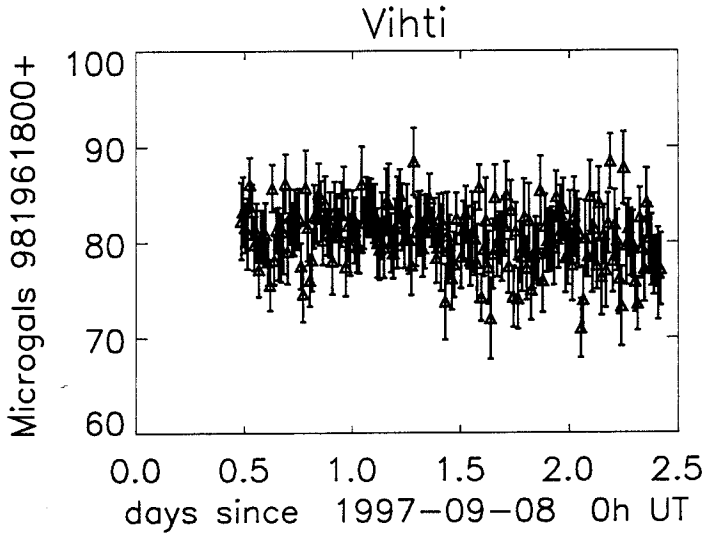

Figure 4. Absolute observations at the Vihti station with the JILAg-5. Each point is the mean of a set of 25 drops, about 6 minutes of data. There are 186 such sets, starting every quarter of an hour. Error bars are standard deviations of the mean.

Table 1. Determination of the gravity difference on the calibration line Masala–Vihti. The uncertainties given are one-sigma. The uncertainty estimates are based on the repeatability of measurements in long time series (10 years) on reference sites, and as such are rather pessimistic. Formal standard errors (statistical scatter only) are below 0.5 μgal for the absolute measurements and around 1 μgal for the gradient measurements.

Station	Absolute result at h_{ref} above pier μgal	h_{ref} metres	Vertical gradient, μgal/m	Reduction to pier level μgal	Result at pier level μgal
Vihti 971012	981 961 881 ± 5	0.836	–384 ± 3	321 ± 2	981 962 202 ± 5
Masala 961002	981 908 753 ± 5	0.836	-320 ± 3	268 ± 2	981 909 021 ± 5
gravity difference at pier level					53 181 ± 7

Note on the vertical gradient of gravity

The large difference in vertical gradients in Vihti and Masala (Table 1) must be taken into account by the users of the line. Moreover, rough modelling predicts that in Vihti the gravity change as a function of height is in fact strongly non-linear, on account of the massive pier and of the pointed rock outcrop the pier stands on. But this is a second order effect and is unlikely to exceed 10 μgal even in the middle of the range used in the gradient measurement (see next paragraph). Anyway, we are going to measure it.

Before further discussion, let us point out that while modern methods of processing absolute observations do require that the gradient be known over the drop distance (typically 0.2 m), the error due to using an approximate value is relatively small and can be completely eliminated by quoting gravity at a suitable point within this 0.2 m. Thus the "measurement of the vertical gradient" in absolute gravity work is usually not designed to determine the gradient in detail, neither over the drop distance nor down to the pier. It should rather be interpreted as a transfer of gravity to pier level: A relative measurement between two levels is performed, the upper level is close to the height at which absolute gravity is observed, and the lower level means simply mounting the gravimeter on the pier.

Thus in our "gradient" or "transfer" measurements the levels of the gravity sensitive point within the LCR G-600 were 51 mm and 791 mm in Olkkala, and 52 mm and 796 mm in Masala. The calculation of the transfer using a vertical gradient of gravity is just a way to reduce the relative measurement to 0 mm and 836 mm, respectively (cf. Table 1). Only the errors made over these few centimetres count, not how the gradient between the observation level and the pier level varies in detail.

In order to make the levels on top coincide exactly, we would just need to modify our tripod. But on the bottom there is not much we can do—no instrument in the near future will be able to put its gravity sensor on the pier surface. Some authors have expressed concern about the reduction to the pier for these inaccessible lowest 50-odd millimetres, as on them simple linear calculations are usually erroneous due to the strong attraction of the pier. However, approximation error over 50 mm cannot amount to much. Moreover, from a practical point of view this is in fact the most worry-free part of the reduction path, precisely because it is inaccessible and no instrument will be measuring within it. We only need to require that everybody uses the same gradient over it, and it does not matter whether this number is right, wrong, or purely conventional.

If one dislikes this approach, one might resort to a combination of detailed measuring and modelling to extend the gradient reliably to the inaccessible part. This extension is largely a wasted effort. More sensibly, one might decide to transfer and quote the gravity, not at pier level, but at some accessible level above it, accessibility being dictated by the instruments which need to be accommodated. For the LCR meters the minimum would be about 50 mm, for the increasingly popular Scintrex CG-3 as much as 260 mm, if one insists on using the original tripod.

In some ways the ideal solution would be to persuade the users to measure near the height of the absolute observations. In order to achieve this, we should first make them conscious of the sensor heights of their instruments but that we have to do anyway. (The only way to avoid it would have been to find stations with similar gradients.) Then we would probably have to

provide them with special tripods for the purpose, as the calibration line is the only place where they would need them. To abandon the users to fend for themselves in this respect would hardly be compatible with idea of the calibration line as a public metrological service the FGI is offering.

The most user-friendly approach then would be to provide them with correct gravity differences at all (accessible) heights, in practice with gravity values at some reference height and detailed-enough gradient information. The reference height then does not matter in substance but pier level has the advantage of user familiarity.

Summary

We have established a calibration line with a gravity difference of 53.18 mgal, subdivided in five parts of 10...11 mgal. The uncertainty of 1.3×10^{-4} from first measurements shall be improved. More detailed vertical gradients at the end points are needed for easy use with different instruments.

References

Faller, J.E., Y.G. Guo, J. Gschwind, T.M. Niebauer, R.L. Rinker and J. Xue (1983): The JILA portable absolute gravity apparatus. BGI Bull. Inf. 53, 87–97.

Kiviniemi, A. (1963): Om kalibreringslinjer vid de finska tyngkraftmätningarna. Protokoll, Nordiska Kommissionen för Geodesi, Det Fjerde Nordiske Geodetmøte, 14–18 mai 1962, pp. 177–180. Norges Geografiske Oppmåling, Oslo.

Kiviniemi, A. (1964): The first order gravity net of Finland. Publ. Finn. Geod. Inst 59.

Kiviniemi, A. (1974): High precision measurements for studying the secular variation in gravity in Finland. Publ. Finn. Geod. Inst. 78.

Kiviniemi, A. (1980): Gravity measurements in 1961-1978 and the results of the gravity survey of Finland in 1945-1978. Publ. Finn. Geod. Inst 91.

Mäkinen, J. and L.-Å. Haller (1982): Calibration of LaCoste-Romberg gravimeters on the northern part of the European absolute calibration line. Proceedings of the General Meeting of the IAG, Tokyo, May 7–15, 1982, pp. 402–405. Special issue of the Journal of the Geodetic Society of Japan, Kyoto.

Niebauer, T.M., G.S. Sasagawa, J.E. Faller, R. Hilt and F. Klopping (1995): A new generation of absolute gravimeters. Metrologia 32, 159-180.

Gravity and GPS measurements in Greenland

Frans Rubek & René Forsberg
National Survey and Cadastre (KMS)
Geodynamic Office
Rentemestervej 8
DK-2400 Copenhagen NV
Denmark
e-mail: fr@kms.dk / rf@kms.dk

Abstract

Until recently Greenland was one of last major gravity data voids in the world. The remote island with its fairly inaccessible topography and long distance between habitated make gravity measurements difficult and expensive. In the period 1991-1997 KMS has undertaken extensive surveys around the entire coast, and thereby covered all ice-free areas with a reasonably dense gravity and GPS network. In combination with airborne and marine gravimetry, satellite and airborne altimetry, ice cap and sea ice surveys, and new digital elevation models from different sources, this has improved the geodetic coverage of Greenland dramatically. With the succesful completion of the surface gravity surveys in the summer of 1997, this presentation aims at giving an outline of these programs and an overview of the results, with emphasis on the period 1991-1997.

Introduction

In Greenland, land gravity has been measured in a small scale since the fifties as part of more traditional geodetic surveys, but dedicated gravity surveys with helicopters was not initiated until the late seventies in connection with satellite Doppler surveys. In 1986-1988 the KMS (at that time Geodetic Institute) undertook three larger surveys in sparsely populated eastern and south-eastern Greenland, partly to collect gravity data from this unsurveyed area, and partly to collect position data by Doppler and GPS in order to improve the fairly imprecise maps of the region.

Starting in 1991, KMS has undertaken month-long gravity surveys each summer in the framework of the *Greenland Gravity Project*, a US-Danish cooperation sponsored by NIMA (National Image and Mapping Authority, formerly Defense Mapping Agency), with the aim of covering all ice-free areas of Greenland with a reasonably dense gravity network. The resulting local and regional GPS networks were a natural spin-off from these surveys, and are being combined with new, high-precision first order GPS networks including a small but increasing number of permanent stations.

The field projects continue over Greenland marine areas 1998-99 as airborne gravity, cf. Forsberg et al., this volume. The interior of Greenland was covered in 1991-92 (Brozena, 1991).

Field operations

The coastal gravity surveys of Greenland often covered logistically difficult regions, with large distances between habitated places, available airstrips and supply bases, necessitating expensive fuel lay-outs by helicopter sling operations or flights with Twin-Otter aircraft. Occasionally it was possible for the survey crew to live in towns or settlements, but more often it was necessary to

be based at remote airfields, weather stations or even temporary field camps. Typically, the KMS crew would consist of two to four geodesists/surveyors and helicopter crew would be one pilot and one mechanic.
Gravity measurements (made with LaCoste&Romberg relative gravimeters) were made in standard survey loops connected to reference points, which again are connected in a network to the (few) absolute gravity stations in Greenland and neighbouring countries. During each survey, new gravity and GPS reference points were established, documented and connected to the existing networks.

Geographical positions and heights

Until 1993 navigation and positioning was made using aerial photographs and heights were obtained by barometric levelling - constrained by a few static GPS or doppler measurements at older triangulation points and at sea level. Since 1993 however, navigation, positioning and height determination has been done primarily with helicopter-mounted GPS in kinematic mode, using aerial photographs and barometers only as backup. Typically, 12-15 epochs of 15 seconds length were sufficient to give the necessary precision (10-15 m r.m.s.) and also short enough to match the time used by the surveyor(s) to note barometric pressure, instant GPS position, mark landing point on photograph, optionally measure/judge height above sea level - and read the gravimeter. The kinematic solutions were made relative to one or two reference GPS stations. At long survey loops an additional GPS reference station was used when possible, placed at fuel caches or older fixpoints closer to the survey area.

Gravity reading at old triangulation point

Twin-Otter unloading fuel drums at frozen lake

During each survey, a local GPS net would be established and connected to the existing networks. A preliminary processing and adjustment were made in the field, but final adjustment and coordinates were made afterwards using precise orbits. Great care was taken in the field on a daily basis to document, check and save all data to computers and/or logbooks.
GPS-derived ellipsoidal heights were converted to orthometric heights by

$$H_{ORTHOMETRIC} = h_{ELLIPSOIDAL} - N + \Delta N$$

where N is geoid height and ΔN is a correction term to absorb the discrepancy between orthometric heights from GPS and locally observed sea level heights (where available). For the conversion of the GPS heights, a geoid model of Greenland was used, which was based on all

available gravity (and other) data from previous years. In 1997, the ΔN-values were reasonably small, typically at the 0.5 m level. This reflects both average geoid errors and local sea surface topography. Comparisons for gravity points at sea level showed that r.m.s. accuracies down to below 2 m in elevation were obtained by the used GPS positioning method.
In a few cases no reliable GPS solution could be found and positions were instead (until 1993) judged from aerotriangulation using the marked landing spot on a photograph or (after 1993) read from the conventional navigation GPS unit in the helicopter (r.m.s. 30-50 m). Heights are in this case found by barometric levelling, where observed pressure is converted into apparent pressure heights using a standard atmosphere model, modified to fit all the other GPS data in the measurement loop, with adoption of trends in the sea-level pressure, and estimation of empirical gradients. Heights determined by barometric levelling normally had an accuracy of around 5 m.

Adjustment of gravity observations

Gravity observations were always done with LaCoste & Romberg model G relative gravimeters. The readings were calibrated, reduced for earth tides, scale factor corrected, and subsequently computed in a least-squares adjustment, solving for station gravity values, instrument biases, tares and drift. The reference ties and survey loops are processed together in this scheme. The (few) absolute gravity stations in Greenland and neighbouring countries were held fixed during the processing.
In 1997 the adjustment of all observations gave an estimated standard deviation of 0.045 mGal for a single reading, which must be considered as very good, given the inevitably rough handling of the gravimeter.
The model G gravimeters generally perform well, with good loop closure and few tares. Large tares are rare but have occured, and because the exact time of these tares normally are impossible to resolve, they will affect all gravity values in the given loop by a similar error.

Gravity reading at mountain top

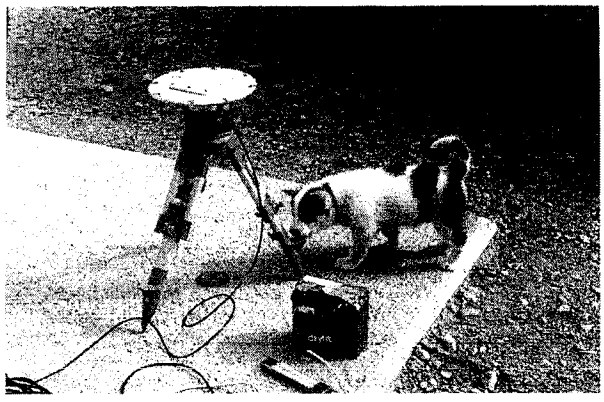

Error source by static GPS measurements

Terrain corrections and final gravity anomalies

Terrain corrections have been computed for most gravity stations in Greenland, using the most precise digital elevation model(s) available in the given area. The computations are done with the spline-densified prism method out to a distance of 50 km from the computation points, neglecting ice sheet and sea depth effects, which are largely unknown. Terrain corrections may be very large for some stations (up to 40 mGal), especially at the edge of cliffs at fjords and glaciers.
The final gravity anomalies are computed in the GRS80 normal gravity system, with Bouguer

density 2.67.
The resulting Bouguer anomaly maps confirm the overall isostatic trend of the Greenland Bouguer anomalies (negative at the inland ice margin, and positive at the outer coast), but occasionally also show major geological anomalies from e.g. sedimentary basins.
An overview of the location of all Greenalnd surface gravity points in KMS' database can be found in figure 1.

Geoid computations

As a requirement for the GPS operations, a sequence of geoid models have been computed for Greenland, updated as the surveys progressed. The models have been based on spherical FFT methods, using airborne and surface gravity data, and utilizing a continously improving Greenland DEM, including ice heights and thicknesses. For details of the geoid modelling techniques see Forsberg and Sideris (1993). As part of the geoid project gravity data has been compiled into a 5' data grid, including downward continued airborne data (Forsberg and Kenyon, 1996). This data grid has entered the recently released NIMA/NASA earth gravity field model EGM96, filling up a formerly significant data void.

Conclusions

A succesful gravity survey of a large region has been done, combining a helicopter-borne gravity survey of the ice-free regions with an airborne survey of the interior.

References

Brozena, J.: *The Greenland Aerogeophysics Project: Airborne gravity, topography and magnetic mapping of an entire continent.* Proc. IAG symposium 110: From Mars to Greenland: Charting gravity with space and airborne instruments, Springer Verlag, pp. 203-214, 1991.

Forsberg, R. and M. G. Sideris: *Geoid computations by the multi-band spherical FFT approach.* Manuscripta Geodaetica, no. 18, 1993, pp. 82-90.

Forsberg, R. and S. Kenyon: *Evaluation and downward continuation of airborne gravity data - the Greenland example.* proc. Int. Symp. on Kinematic systems in Geodesy, Geomatics and Navigation, Banff, Canada, pp. 531-538, 1994.

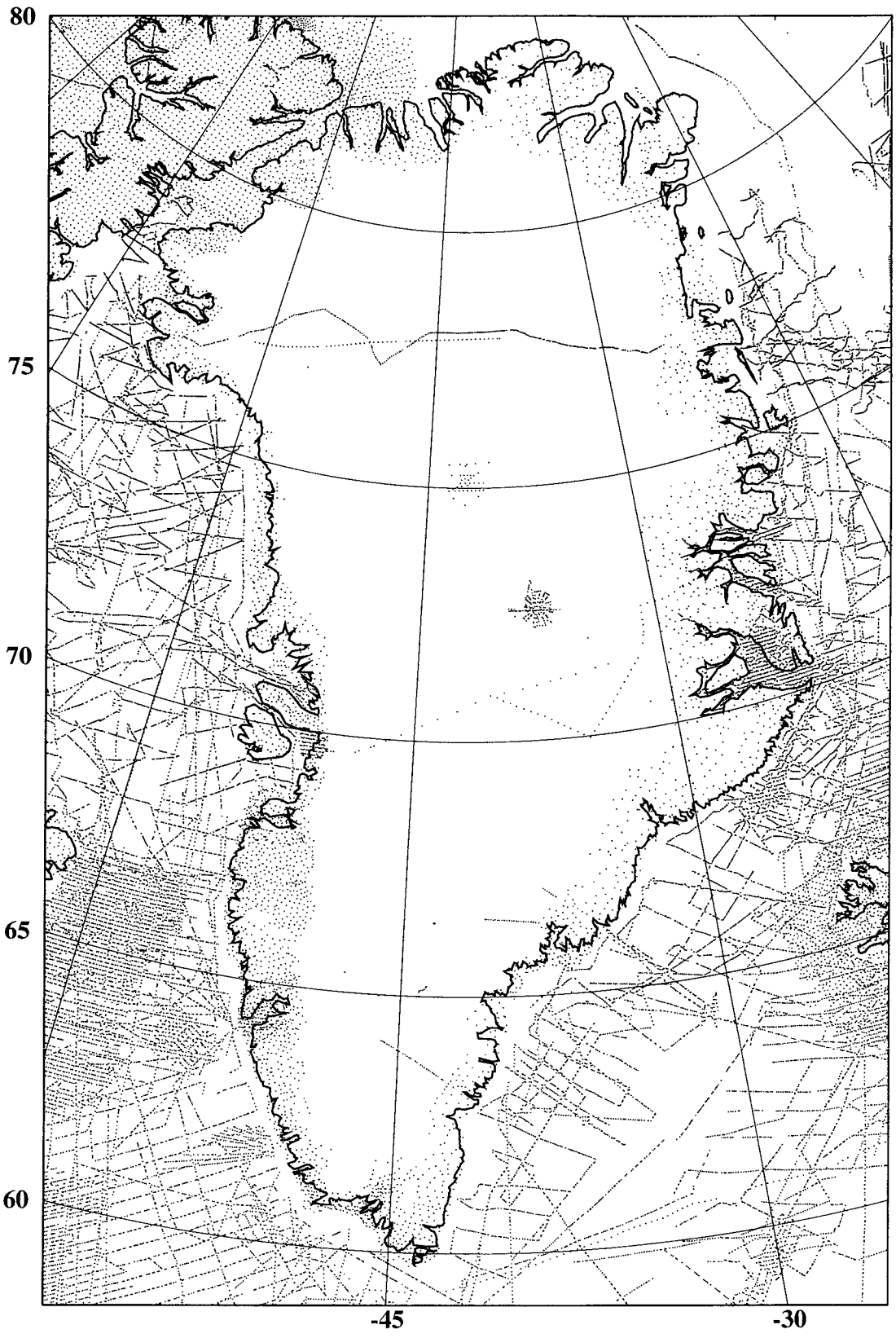

Figure 1. Overview of all Greenland surface gravity points in KMS' database

AIRBORNE GRAVITY IN SKAGERRAK AND ELSEWHERE: THE AGMASCO PROJECT AND A NORDIC OUTLOOK

R. Forsberg and A. V. Olesen, KMS, Rentemestervej 8, DK-2400 Copenhagen NV, Denmark
L. Timmen, M. Nesemann, G. Xu, GeoForschungsZentrum Potsdam, Germany
L. Bastos and S. Cunhas, University of Porto, Portugal
A. Gidskehaug, University of Bergen, Norway
U. Meyer and T. Boebel, Alfred Wegener Institute, Bremerhaven, Germany
K. Hehl, Technische Fachhochschule, Berlin
Dag Solheim, Statens Kartverk, Norway

Abstract: *Airborne gravity projects in Skagerrak, Fram Strait and the Azores have been carried out succesfully within the EU -supported AGMASCO project, in order to determine the marine geoid. In the paper airborne gravity results are presented from Skagerrak, showing that accuracies of 2 mgal are obtainable. Airborne gravity may in the future be an obvious area for Nordic cooperation, especially in Arctic and Antarctic areas. Joint Danish-Norwegian projects in Greenland and Svalbard have thus succesfully been carried out in the summer of 1998, as a spin-off of the AGMASCO project.*

INTRODUCTION

AGMASCO (Airborne Geoid Mapping System for Coastal Oceanography) is a project funded by the European Commission within the frame of the MAST-III program. The basic idea is to determine geoid heights (N) from an airborne gravity system, and at the same time measure the height above the sea-surface (H) by airborne altimetry. This allows the determination of the sea-surface topography (z) through the equation

$$z = h - H - N$$

where h is the ellipsoidal height of the airplane, determined by kinematic GPS techniques relative to one or more reference receivers on the coast. The determination of the oceanographic sea-surface may in turn be converted ocean currents under the geostrophic assumption. Thus - in principle, at least - it is possible to detect ocean currents from a combination of airborne gravity and altimetry.

It is the purpose of the AGMASCO project to demonstrate the feasibility and accuracy of the airborne geoid determination method, which directly will be a consequence of the accuracy and bias stability of airborne gravimetry, as the geoid is to be determined from the gravimetry by standard methods of physical geodesy such as collocation and spherical FFT approaches.

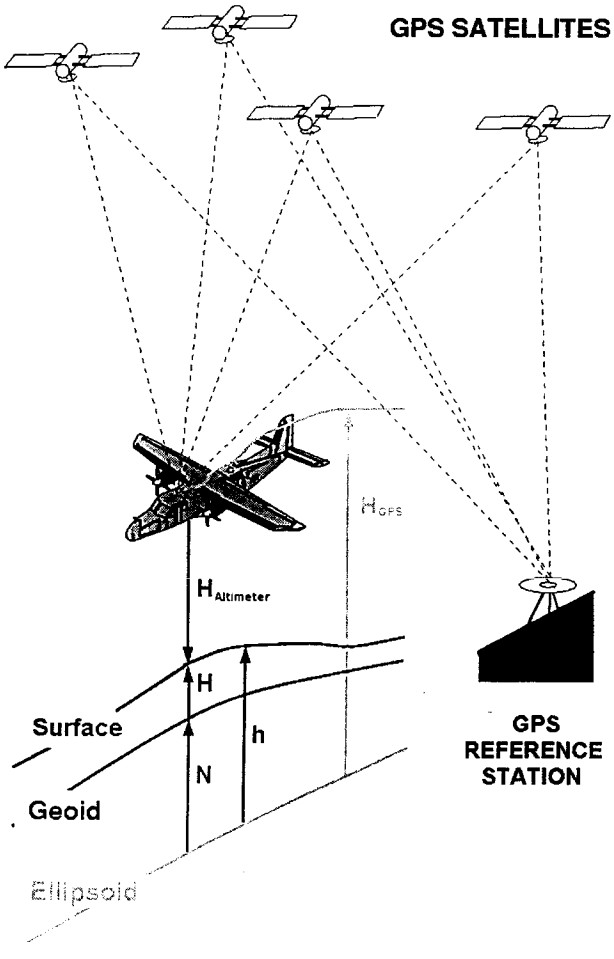

Fig. 1.

The use of airborne gravity and altimetry for geoid determination was demonstrated by Brozena et al. (1993), and for an extensive review of the potential of airborne gravity for geoid determination see Schwarz (1996). For early results of the AGMASCO project see Forsberg et al. (1996).

The field work campaigns of the AGMASCO project has now been completed, with an airborne survey of the Skagerrak done in 9 days of September 1996, using a Do-228 airplane belonging to AWI ("Polar-4"), and a large-scale application experiment around the Azores in October 1997, flown with a Casa-212 of the Portuguese Air Force. In addition a number of lines were flown across the Fram Strait between Greenland and Svalbard in August 1997, as a special AGMASCO project carried out in addition to AWI own airborne gravity measurements in the region ("NORDGRAV" project).

Fig. 2 shows the coverage of the primary projects in Skagerrak. In both Skagerrak and the Azores ground thruth measurements were carried out by the University of Bergen vessel (R/V Haakon Mossby), to evaluate the performance of the airborne measurements. The ground thruth measurements include marine gravimetry (sailing under selected airborne tracks) as well as independent oceanographic measurements (CTD and ADCP) allowing determination of instantanous sea-surface topography. Several airborne tracks were selected to coincide with Topex/Poseidon or ERS-2 satellite altimetry tracks, allowing independent evaluation of the airborne altimetry.

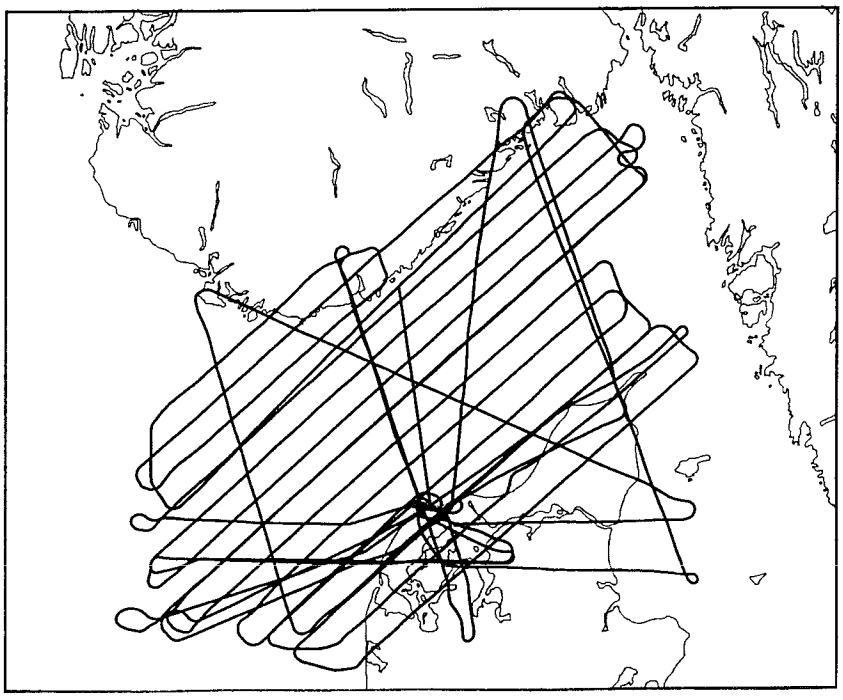

Fig. 2. Airborne gravity survey in Skagerrak

THE MEASUREMENT SYSTEM

In the AGMASCO hardware setup a LaCoste & Romberg marine gravimeter, modified by ZLS corporation, is used as the primary gravity sensor. The gravimeter S-99, owned by the University of Bergen, was used in the Skagerrak flights. A triad of QA-3000 high accuracy accelerometers

is being developed on an experimental basis to augment the gravity sensor by a high-resolution scalar total acceleration measurement, but the early prototype have up to now not yet yielded useful results, and research is ongoing.

Vertical accelerations of the airplane are separated from gravitational accelerations by kinematic GPS. Two Trimble 4000 SSI receivers are used in the airplane for GPS positioning, with reference GPS receivers located at reference sites throughout the survey area.

Airborne altimetry is done both by an Optech laser altimeter, and a high-precision radar altimeter, developed at University of Stuttgart. Both of these units are capable of measurement accuracy of a few cm. The altimetry allows an independent estimate of the vertical airplane accelerations over sea areas, as well as allow a direct measurement of sea-surface topography, a primary purpose of the project. The altimetry data is calibrated by runway overflights, with a detailed map of runway heights provided by local kinematic GPS surveys by car.

To allow vertical pointing of the laser, and the correct lever arm transfer of GPS coordinates to gravimeter sensor, attitudes are determined by INS. On the Do-228 a Honeywell Lasernav system was used, whereas a new Litton system was used in the Azores flights.

Data from all sensors was logged on a central data logger, developed at GFZ Potsdam, from which data was downloaded on PC cards.

For most tracks the comparison of filtered GPS and altimeter accelerations agreed at an accuracy level of 1 mGal or better, even for preliminary GPS solutions based on one reference station only. An example is shown in Fig. 3. In this track the r.m.s. deviation is 0.81 mGal between the filtered GPS and laseraltimetry-derived acceleration (the deviation between GPS and laser derived vertical accelerations around 1400 s is coincident with a dominant gravity anomaly). On longer tracks, however, GPS errors may be much more significant and there is need for additional research into detecting spurious GPS outliers, e.g. occurring with some software systems when the satellite constellation changes. The INS data are expected to be most useful for this purpose.

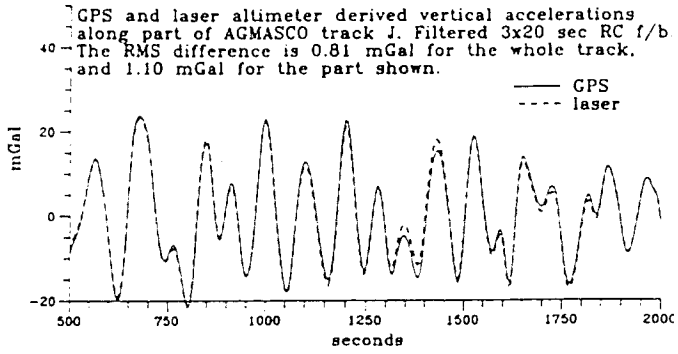

Fig. 3. Comparison of GPS-derived and laser altimetry-derived vertical accelerations (track J).

GRAVITY DATA PROCESSING AND FILTERING

Whereas GPS appears to work well in determining vertical disturbing accelerations, the gravimeter processing system must be optimized in order to get most out of the data. The Lacoste and Romberg gravimeter used for the airborne measurements is basically a quite complex system, where both spring tension and beam velocity are used for measuring gravity changes, with the

system mounted on gyro-stabilized platform, slaved to be horizontal relative to filtered horizontal accelerometer measurements (a 4 minute damping period used in most AGMASCO flights). In addition online corrections are computed for several instrumental effects including cross-coupling. For an in-depth description of the LC&R marine gravimeter see Valliant (1989).

The determination of the scale factor relating gravimeter beam velocity and the spring tension (the "K"-factor) is typically done in the laboratory, but we have found that it may with advantage be done from the airborne data themself, by cross-correlating the vertical phugoid accelerations measured by GPS, and the similar vertical accelerations measured by the gravimeter (cf. Fig. 4), for more details see (Olesen et al., 1997). The cross-correlation process at the same time allows for estimating possible time offsets between the data streams with an accuracy of a fraction of a second (1 Hz data used in the present processing).

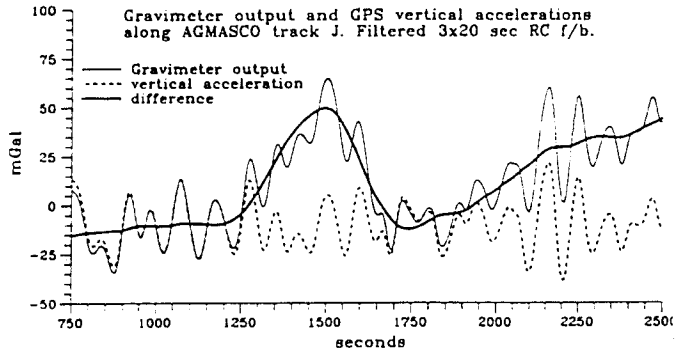

Fig. 4. An example of vertical accelerations in flight as measured by the gravimeter and GPS.

A major error source in airborne gravity measurement is platform off-levelling errors. The correction due to platform tilt may to first order be estimated from a combination of measured horizontal accelerations (from GPS, "a") combined with platform horizonal accelerometer measurements ("A") by

$$C_{tilt} \approx \frac{A^2 - a^2}{2g}$$

As seen from this formula the accelerations enter unlinearly, and it is therefore critical to apply filtering and tilt corrections in the right way. We have found that only short filtering (time constant of a few sec) should be applied to "A" and "a" prior to estimating the tilt correction, and have used a cross-correlation technique similar to the "K"-factor to estimate scale factors of the horizontal accelerometers as well. Finally a least-squares adjustment has been done for selected unlinear and cross-coupling parameters on a complete survey basis, for details see ibid. (1997).

The filtering applied is based on zero-phase forward/backward multiple RC filters, or staged forward/backward Butterworth filters. The latter has a more steep frequency cut-off, but with a slight tendency for "ringing" close to major, well-defined gravity anomalies. Filtering parameters used have been determined based on the smoothness of the flights, but have typically been with a resolution around 70-100 sec, corresponding to 5-7 km at an airspeed of 130 knots.

From gravity measured at air, free-air anomalies are readily determined by

$$\Delta g = g_{meas} - \frac{d^2 h_{GPS}}{dt^2} + C_{eot} - \gamma_0 + 0.3086[\frac{mgal}{m}](h_{GPS} - N)$$

where C_{eot} is the Eotvos correction (including centrifugal and ellipsoidal terms, cf. Harlan, 1968), and N a preliminary geoid model (NKG96 in Skagerrak, cf. Forsberg et al., this volume). The linear gradient term in the above expression is justified by the low flight elevation (nominally 1200 ft) used in the AGMASCO projects. The comparison of airborne gravity at cross-over points is done by free-air anomalies rather than actual gravity, since anomalies to first order will be independent of the actual flight elevation (but of course it would be equivalent just to apply a normal gravity gradient on measured gravity).

THE SKAGERRAK RESULTS

The Skagerrak airborne field experiment was carried out in the days September 13-21, 1996, and immediately followed by a 1-week ship cruise by the R/V Haakon Mossby collecting ground truth gravity and oceanographic data. Flight conditions were generally good over the ocean, with some turbulence experienced over land. The survey was flown at a nominal altitude of 1200 ft and a speed of 130 knots.

The Skagerrak region was selected as a demonstration test area for several reasons: There is a very large, localized 50 mgal gravity anomaly (traditionally interpreted as a buried Tertiary volcano) just south of the Norwegian coast, which makes an excellent target for aerogravity. At the same time minor, well-defined gravity anomalies associated with salt domes occur on the Danish side of Skagerrak, and generally the gravity anomaly field is fairly well known from earlier 1960's-vintage marine and land gravimetry, cf. fig. 5.

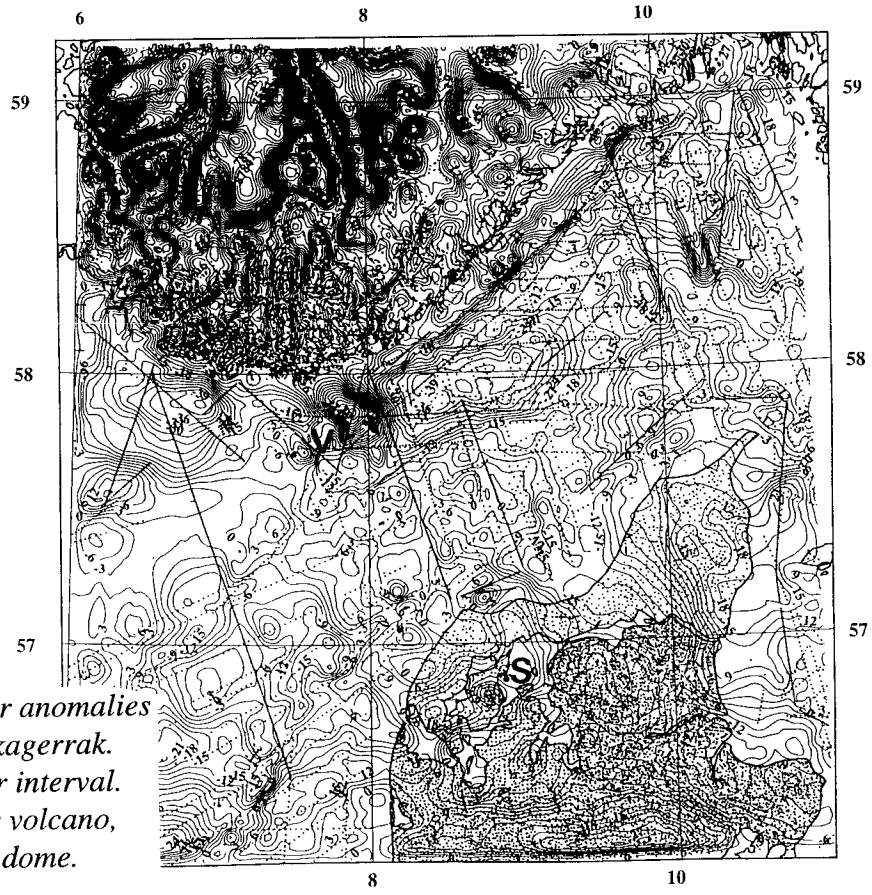

Fig. 5. Free-air anomalies at 1200 ft in Skagerrak. 3 mgal contour interval. "V" is tertiary volcano, "S" Mors salt dome.

Another major reason for selecting Skagerrak is the varying oceanography, with fairly strong currents, and an oceanographic "front" created from mixing of the more brackish Baltic waters with the saltier North Sea waters. A numerical oceanographic model including tides, wind forcing and river runoff was run by the Norwegian Meteorological Institute, and yields grids of expected sea-surface topography on an hourly basis. An example is shown in fig. 6, showing the quite large amplitudes of the sea-surface topography.

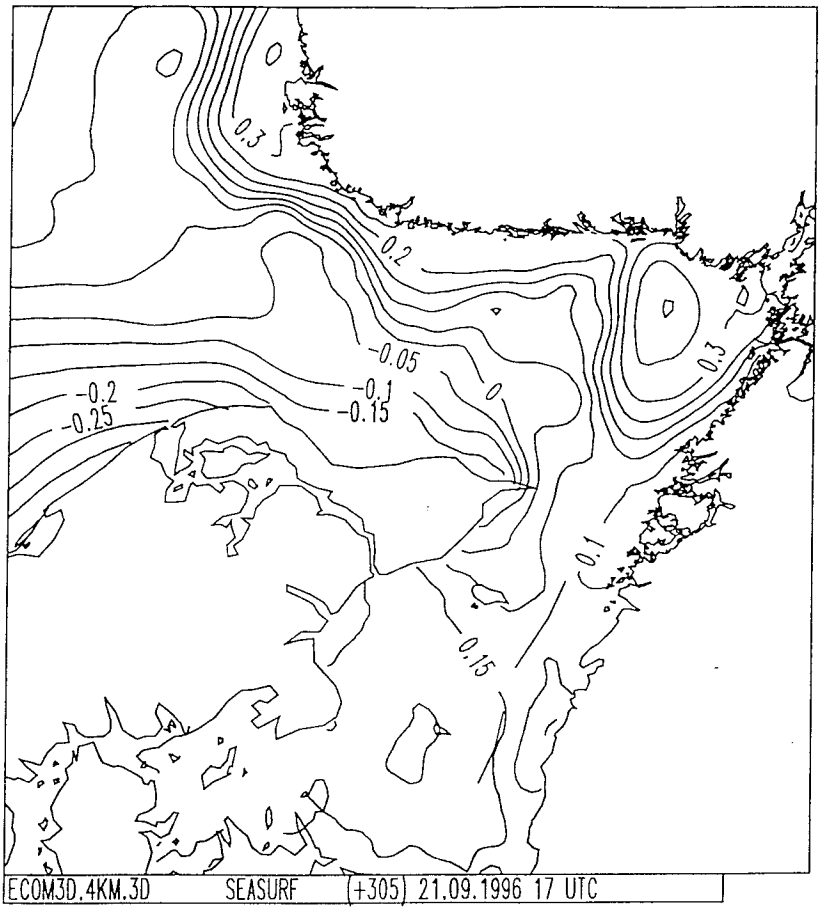

Fig 6. Sea-surface topography in Skagerrak on Sep. 21 at 17 UTC. Contour interval 5 cm.

GPS solutions for the Skagerrak campaign have not been finally computed, so final airborne altimetry results are not yet available. Three reference GPS sites were used, located in Denmark (Hanstholm), Norway (Kristianssand) and Sweden (Vänersborg SWEPOS site). At present GPS results are based on the Hanstholm site only, but work is ongoing on producing final solutions utilizing all available data, using a dedicated program developed by Xu at GFZ. Fig. 7 shows an example of the measured sea-surface topography along the central SW-NE trending TOPEX track, along with Topex measurements along the same track. It is seen that the overall trends of the sea-surface topography is well resolved in the airborne altimetry.

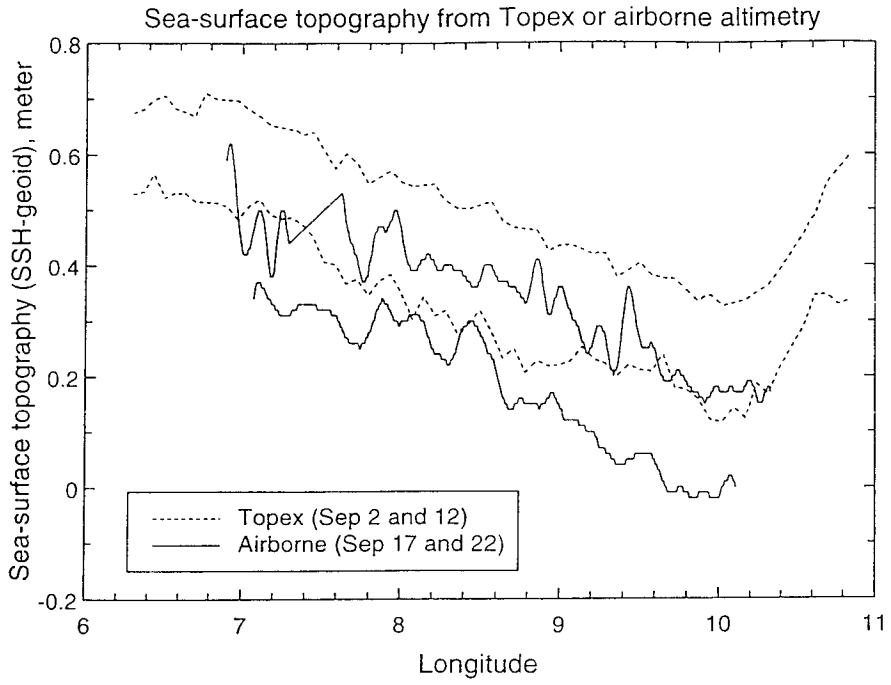

Fig. 7. Sea-surface topography from Topex and airborne altimetry on four different days for central Skagerrak SW-NE track.

The gravity in Skagerrak was processed along the lines outlined in the previous section, basing the gravity on a reference station is the Danish fundamental gravity reference network close to Hanstholm. Due to loss of data following airplane turns, and a few instrumental problems, about 20% of the survey line data could not be processed, but the remaining could be processed without problems, including some data from some quite turbulent flights. Fig. 8 and 9 shows some comparisons of ship/land data (upward continued to 1200 ft by FFT methods), and the airborne data. It is seen that both the large "volcano" gravity anomaly of Fig. 8, and the smaller anomaly associated with a salt dome in Fig. 9 is resolved quite nicely, with little apparent bias errors, most important for geoid determination.

Table 1 shows the results of a cross-over analysis of all the processed gravity data, using a processing scheme both with and without estimating new cross-coupling and unlinear instrumental parameters. The table shows for both methods the r.m.s. cross-over errors before and after applying a bias correction to each track. It therefore appears that the r.m.s. accuracy of the airborne data is around 2 mgal (r.m.s. cross-over errors are larger by the square root of 2). Another test of data accuracy involve upward continued ground thruth data (including the ground thruth marine data collected by R/V Haakon Mossby), Table 2 shows the statistics of comparison to ground thruth data along lines with reliable ground thruth. These number again support an r.m.s. accuracy of the airborne data of 2 mgal, considering the uncertainty of the upward continuation process and the ground data.

Table 1. R.m.s. cross-over errors (mgal) for AGMASCO Skagerrak aerogravity survey

	Standard processing	Using improved error model
Before adjustment	3.0	2.9
After bias-only adjustment	2.4	2.3

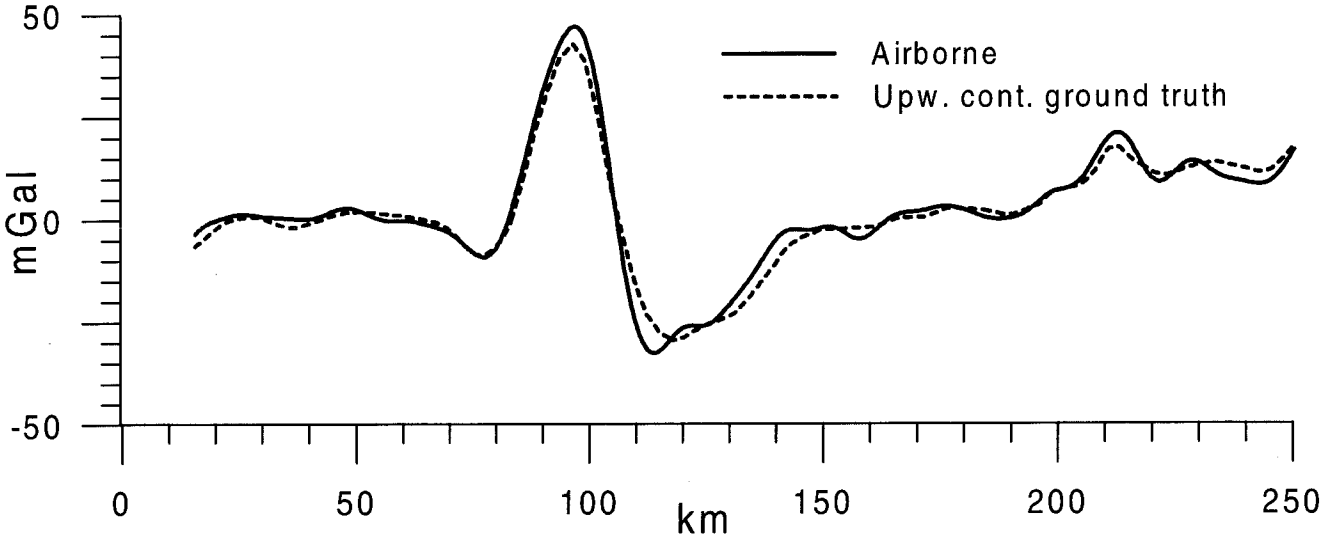

Fig. 8. Airborne and surface gravity anomalies along track crossing "volcano" anomaly.

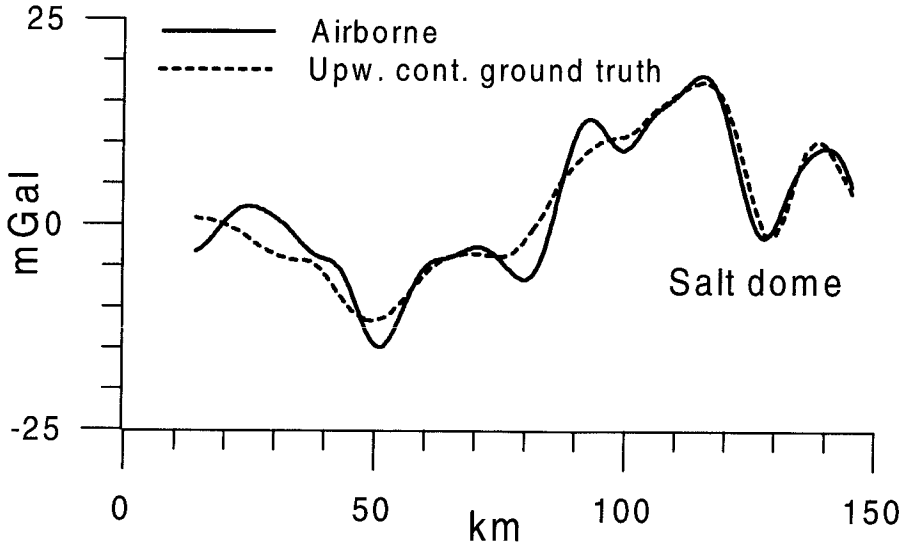

Fig. 9. Airborne and surface gravity data on west-east track crossing Mors dome, Jutland. The poor fit to the west (left) of the salt dome is due to lack of surface gravity data in the North Sea.

Table 2.R.m.s. comparison (mgal) of airborne data to upward continued ground thruth

	Standard processing	Using improved error model
Ground thruth comparison	2.7	2.5

The geoid of Skagerrak was determined using the airborne data by computing a new version of the Nordic standard geoid NKG-96 (Forsberg et al., this volume). Computations were exactly corresponding to NKG-96 (utilizing gravity and digital terrain data for the entire Scandinavian area in an FFT remove/restore process), except that the new airborne data was added. The computed new geoid model showed nearly identical results to NKG96, except for two areas with changes up to 15 cm. This is not surprising, given the fact that Skagerrak is covered with quite dense, albeit older, marine gravity data, which has entered the NKG96 solution. One can therefore say that the geoid computed from airborne and marine gravity data agrees very well, justifying the use of airborne data in other regions with insufficient marine gravity data coverage.

To judge the quality of the geoid results from airborne versus surface data, a special comparison was done on 47 high-precision GPS-levelling points in northern Jutland (fig*10*). These data points are all levelled GPS stations, yielding geoid estimates accurate to approx. 1 cm. The comparisons of the GPS points to two geoids - one incorporating only surface data, and one incorporating *only* airborne data in Skagerrak (surface data used outside Skagerrak) - are shown in Table 3. It is seen that the r.m.s. fit of both geoids are identical, and only a minor offset in mean difference could indicate slight difference in bias between the airborne data and the older marine gravity data.

Table 3. Comparion of GPS-levelling points in Northern Jutland to airborne geoid model

Unit: meter	Mean	Std.dev.
Geoid from surface data only	0.047	0.027
Geoid from airborne data	0.039	0.027

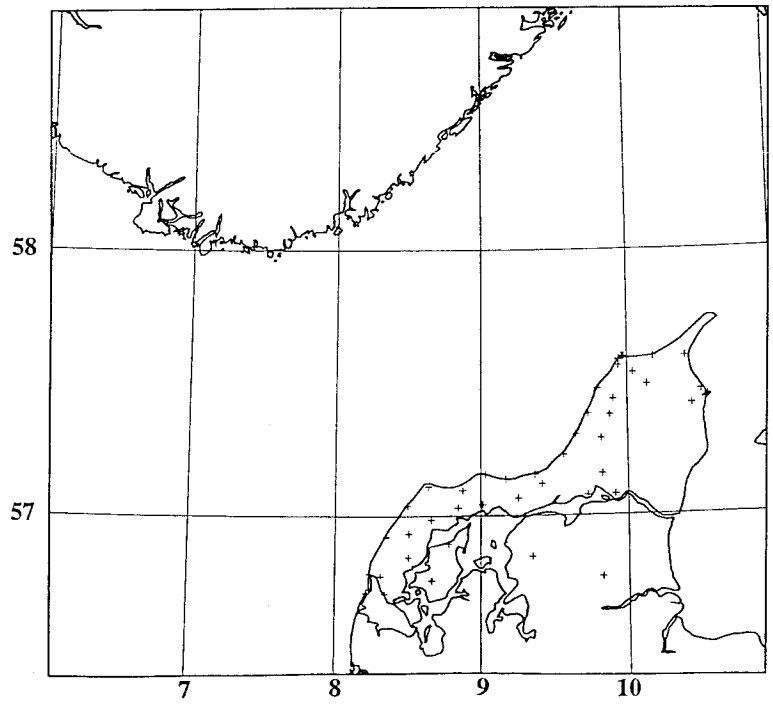

Fig. 10. Location of GPS-levelling

CONCLUSIONS AND A NORDIC OUTLOOK

The airborne gravity survey of the Skagerrak region appears to be succesful, with an apparent accuracy of 2 mgal r.m.s. and a resolution around 6 km or so. This means that airborne gravity is performing at a level close to marine gravimetry. Additionally it has been seen that geoids computed from airborne gravity matches surface data solutions well.

Given the economy of airborne gravimetry over ship-based gravimetry, it is therefore clear that the use of airborne gravimetry is an attractive alternative, and also an area of future potential Nordic cooperation projects, following the footsteps of the succesful AGMASCO cooperation, and earlier cooperations on gravity data base and geoid computations.

Currently AGMASCO spin-off projects are ongoing in Greenland and Svalbard in a Danish-Norwegian cooperation (fig. 11 shows succesful flight tracks done in June 1998 under very good conditions, with a new compact system mount in a Greenlandair Twin-Otter), but the future should also see more areas being covered this way, especially e.g. filling the data voids of the southern Baltic Sea, more areas in the Arctic, and adding airborne gravity to ongoing Nordic activities in Antarctica.

ACKNOWLEDGEMENT

Support for the AGMASCO project was provided by the EU under contract MAS3-CT95-0014.

REFERENCES

Brozena, J. M., M. Peters and R. Forsberg: Direct measurement of absolute sea-surface height from an aircraft. Geophysical Research Letters, vol. 20., no. 9, pp. 875-878, 1993.

Forsberg, R. K. Hehl, L. Bastos, A. Gidskehaug, U. Meyer: Development of an Airborne Geoid Mapping System for Coastal Oceanography (AGMASCO). Proc. Int. Symp. of Gravity, Geoid and Marine Geodesy (GraGeoMar96), pp. 163-170, Tokyo, 1996.

Harlan, R. B.: Eotvos corrections for airborne gravimetry. J. Geophys. Res., 73, pp. 4675-4679, 1968.

Olesen, A. V., R. Forsberg and A. Giskehaug: Airborne gravimetry using the Lacoste and Romberg gravimeter - an error analysis. Proc. Int. Symp. on kinematic systems in geodesy, geomatics and navigation (KIS-97), University of Calgary, pp. 613-618, 1997.

Schwarz, K. P.: Airborne gravimetry and the boundary value problem. Lecture Notes, International Summer School on Mathematical Geodesy, Como, Italy, 1996.

Valliant, H.: The Lacoste and Romberg gravity sensor. In: CRC Handbook of Geophysical Exploration at Sea, Boca Raton Press, 1989.

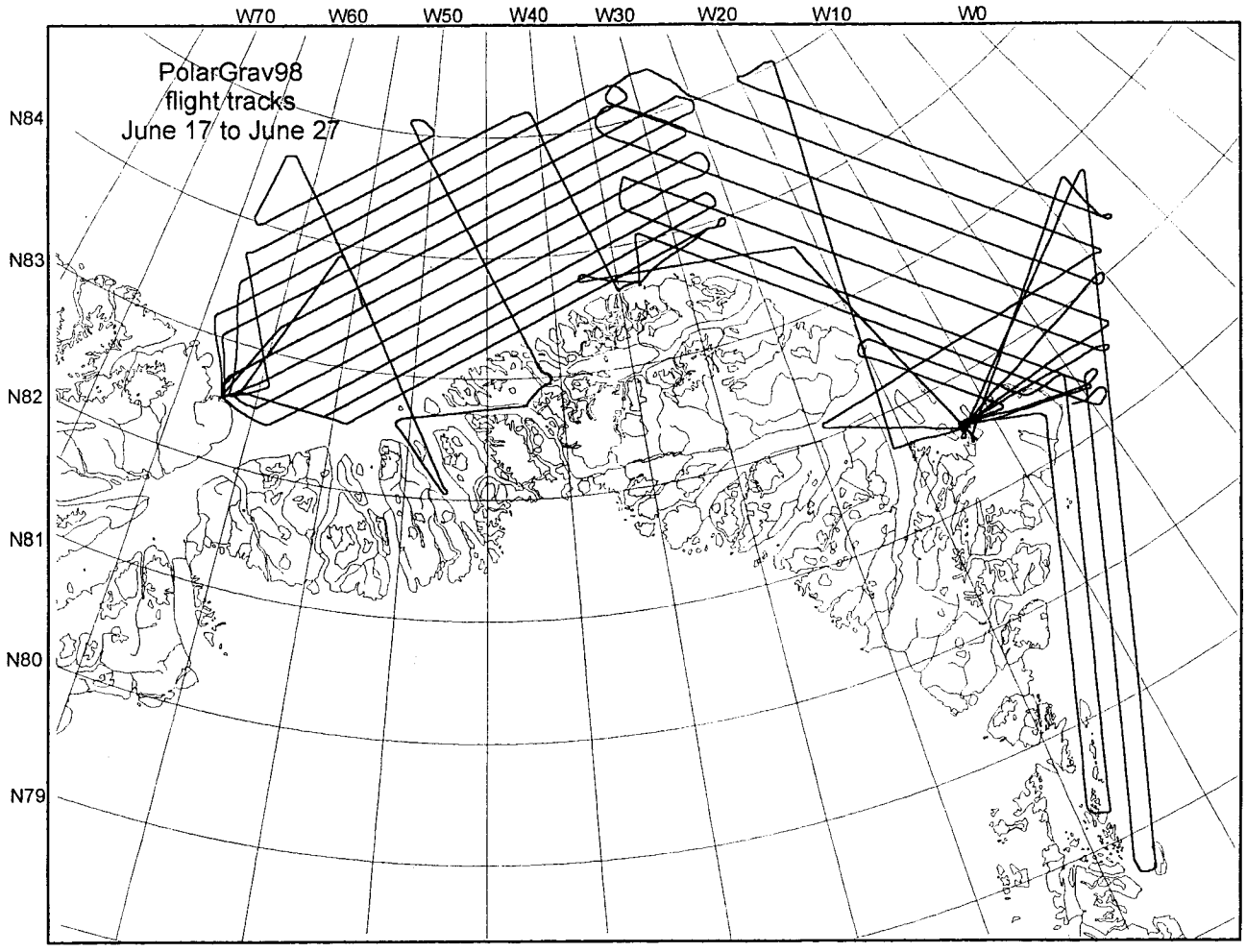

Fig. 11. Polargrav-98 flights north of Greenland, completed June 1998

The gravity spectrum observed by superconducting gravimeter at the Metsähovi station, Finland

by
Heikki Virtanen and Jussi Kääriäinen

Finnish Geodetic Institute
Geodeetinrinne 2, FIN-02431 Masala
heikki.virtanen@fgi.fi, jussi.kaariainen@fgi.fi

Abstract

The superconducting gravimeter, GWR T020, participating the Global Geodynamic Project, has been recorded almost continuously since August 1994. In addition to the tides, we present main results of the gravity observations beginning from microseimic band, including free oscillations of the Earth, up to Chandler wobble period. In addition, results of environmental effects on gravity, due to the variations in groundwater level and airpressure are given.

Introduction

The installation of superconducting gravimeter in 1994 at Metsähovi station has opened new era to observe temporal gravity variations in Finland on nanogal level (1 ngal = 10^{-12} g). The new gravity laboratory, the installation of the gravimeter and the instrumentation has been reported earlier, see eg. (VIRTANEN 1994, VIRTANEN and KÄÄRIÄINEN 1995, 1997). The gravimeter has been working almost continuously, we have had only two short datagaps due to the technical problems of peripherial devices.

The data aquisition system has the sampling rates 1 s for gravity signal, 10 seconds for outer pressure and 1 min for diagnostic purposes. Timing is based on GPS.

The level of groundwater level in a nearby well has been measured manually up to March 1998, when a pressure sensor was immersed into the water to record the level variations. At the Metsähovi station there is also weather station for humidity, air pressure and temperature. To study the relation between precipitation and gravity the rainfall measurements will be necessary in the future.

The aim of the run of superconducting gravimeter is to observe and record the temporal gravity variations with periods from 1 s up to years. In this paper we present the obtained results in this range. We have, however, not yet observed any cyclic phenomenon in subtidal band from 1 hour to 6 hours, which include Earth's core modes. This subnanogal band needs worldwide stacking of data. In July 1997 project GGP, (Global Geodynamic Project) was launched for six years in order to study the influence of global phenomena on the gravity. Seventeen similar cryogenic gravimeters participate this project and for the uniformity of the instrumentation the low-pass filter for the gravity data was changed in September 1997. The corner frequency of the filter is now 16 sec which allows the quantitative record of microseismicity. The data bank of GGP-project is in International Centre of Earth Tides (ICET) in Brussels.

Gravity spectrum

Local surface gravity varies in both time and magnitude with periods from one second up to years. The associated amplitudes start from subnanogals and reach hundreds of microcals (ratio of 10^6) in case of tides. In Fig.1 the periods of different geophysical phenomena and their influece on the gravity are given. Oceanic noise generated by storms in North Atlantic causes gravity variations with periods from some seconds to 15 seconds having the influence of 100 μgal (1 μgal = 10^{-9} g). Seismic normal modes begin at 10 second (500

μgal) and surface waves have their maximum influence at the period of 20 seconds (10 μgal). Free oscillation modes excitated by big earthquakes have periods up 54 minutes. The spectral range from one hour to 6 hours includes different Earth's core modes. One type of these modes is Slichter triplet, which is due to the translation movement of Earth's innermost core with periods close to 5 hours. Amplitudes of these modes are expected to be less than one nanogal.

Amplitudes in tidal band vary from 10 ngals (quarterdiurnal waves) to 100 μgals (diurnal and semidiurnal waves). Close to the annual tidal waves there is the polar motion consisting of two components annual and Chandlerian periods (430 days) with similar amplitudes of 4μgal.

Variations in the groundwater level are of seasonal feature with an influence of 2 - 3 μgal on the gravity.

Realizing that the present noise level of SG is about one ngal, instrument thus is capable to observe a great variety of geophysical phenomena.

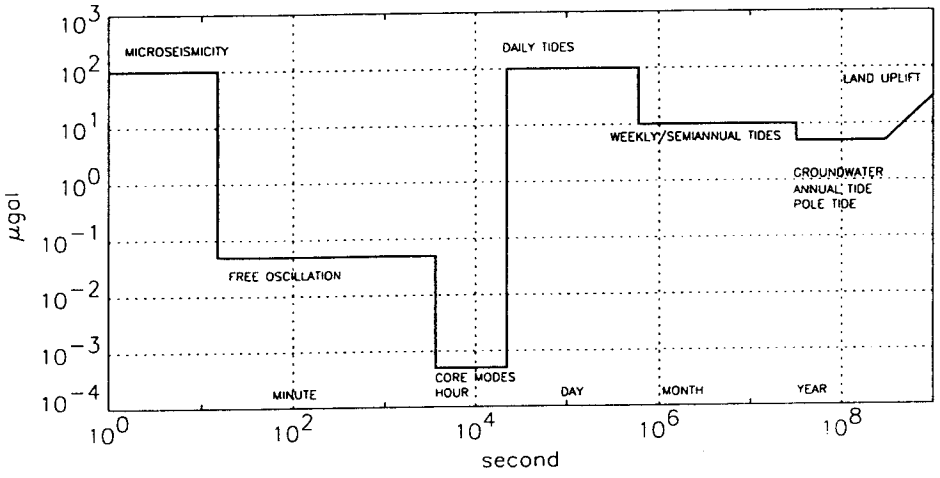

Figure 1. Effect of some geophysical phenomena on the gravity.

Microseismicity

Microseismicity has seasonal variations, the phenomenon being strongest at the winter. Microseismic storms are well correlated with weather conditions at the North Atlantic (Fig. 3). The installed lowpass filter has allowed quantitative observations since September 1997. With this filter the attenuation is 7 dB at the period of 6 seconds. The typical twinpeak spectrum of microseismicity is presented in Fig. 2a when a strong storm appeared in Norwegian coast (28. Feb. 1998). Fig. 2c shows the corresponding gravity spectrum from one silent day (22. Mar. 1998). The period of the primary peak is near 12 seconds and generated by the impact of the waves against the coast, especially of the Norwegian one. The secondary peak is due pumping effect against sea bottom when two wavefronts meet each other (LONGUET-HIGGINS, 1950). This will happen if surfs reflect from the coast or two different syclons meet at the sea. The type of spectrum 2a is called Norwegian type. The other type is called oceanic spectrum, presented in figure 2b (1. Jan. 1998). The source is the sea near to Bretagne, France. The maximum intensity of the peaks in this case is shifted towards longer wavelengths. Fig.3 presents, time, spectral distribution and intensity of microseismicity. The data window is shifted one hour (3600 samples) in the successive spectra and the power spectral density is calculated using FFT techniques. The whole figure includes 2400 spectra.

Thin vertical lines over whole spectral region are due to earthquakes. The qualitative studies for years 1994 - 1998 show clear annual distribution of microseismicity, in the summertime there is much less microseismic noise in Finland. The pass of the cold weather front may also be a source for microseismicity.

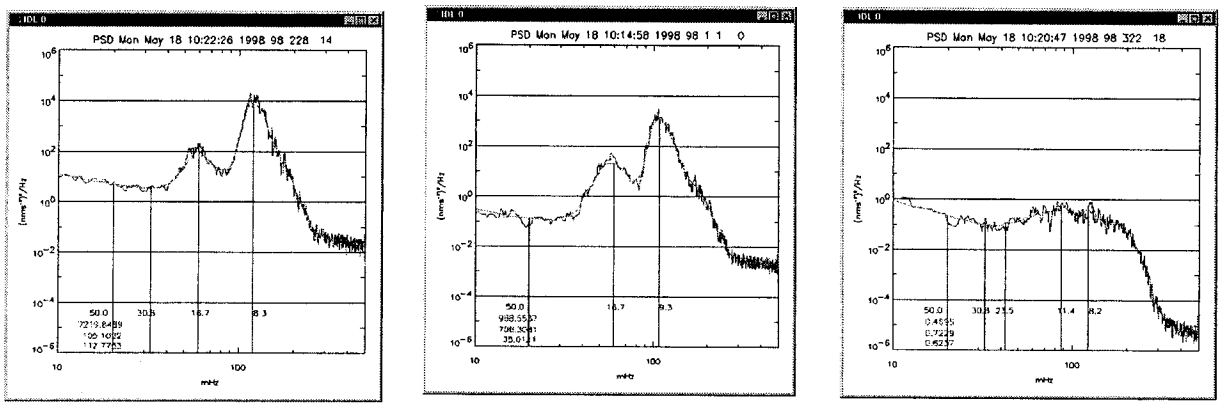

a) b) c)

Figure 2. Typical gravity power spectral density at microseismic region (10 - 500 mHz). **a)** Norwegian type spectrum, **b)** Oceanic type spectrum and **c)** Silent day spectrum.

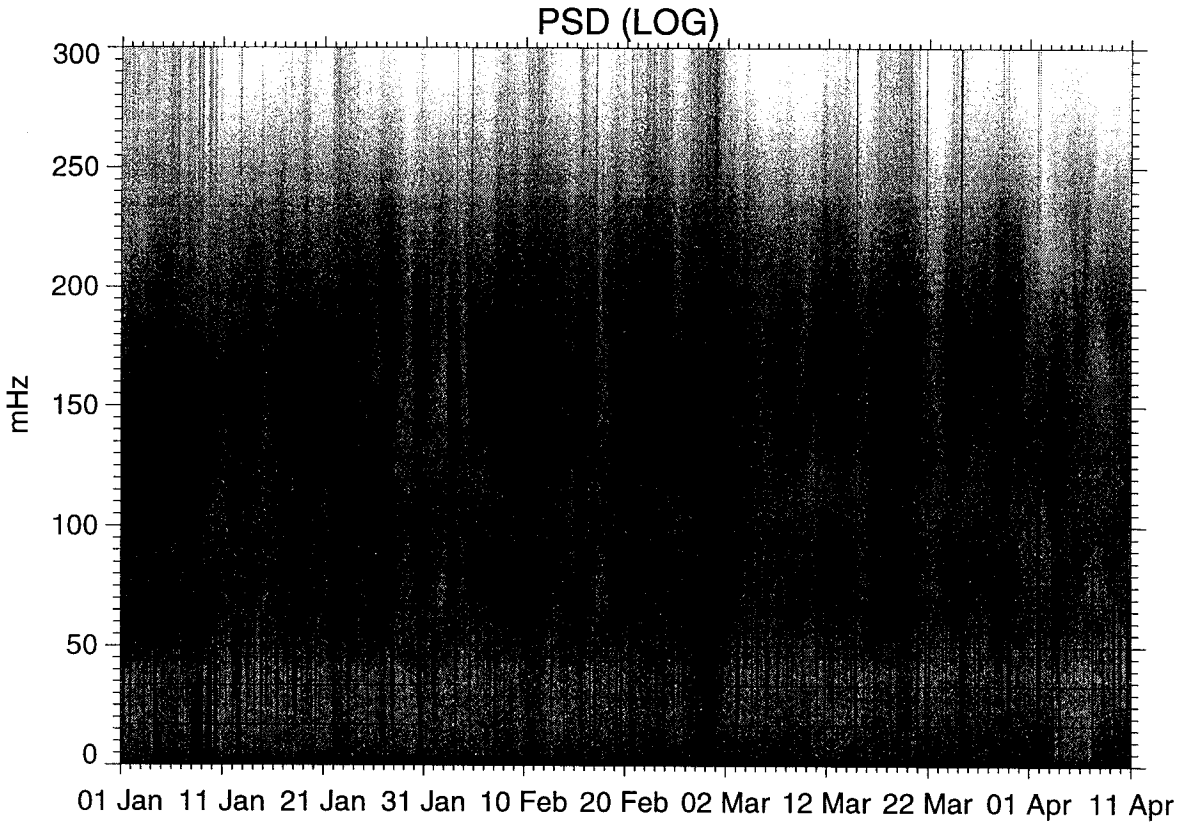

Figure 3. Power spectral density of microseismicity in logarithmic scale from 1. Jan. 1998 to 11. Apr. 1998. The horizontal axis represents the day and the vertical axis frequencies in mHz. Black color indicates high intensity.

Free oscillation of the Earth

Free oscillation of the Earth consists of radial, spheroidal and toroidal modes (MASTERS and WIDMER, 1995). Two first deform the earth in radial direction and are directly observable by a gravimeter. Lowest spheroidal mode ($_0S_2$) has a period of 53.6 minutes (0.311mHz) and is the upper the limit for the seismic band. The radial mode $_0S_0$ has period of 20.3 minutes (0.821mHz). Big earthquakes excitate free oscillation modes of the Earth. There are about ten events in every year, which magnitudes bigger than 7Mw, enough to cause strong oscillations for detailed geophysical studies.
The following example were calculated after a strong Earthquake in Kuril island, 4th Oct. 1994 (13:23 UT), magnitude 8.2Mw. In the result of spectral analyses presented in Figs. 4 - 7 we have used tide-free, air pressure corrected gravity data decimated to 1 minute. To remove drift and tidal residuals high pass filter (1 hour) was applied. The spectral analyses was carried out using Lomb-Scargle periogram method (HOCKE, 1998) with Hanning window. The different modes are clearly visible. In Fig. 4 also the lowest spheroidal and radial modes ($_0S_2$ and $_0S_0$) can be seen. In the shorter part of the spectrum in Fig. 5, maximum amplitudes are close to 50 ngal. The coupled toroidal modes (eg. $_0S_{11}/_0T_{12}$) also appear. The spheroidal modes decay in 2 - 3 days (Fig. 6) while the $_0S_0$ attenuates very slowly (Fig. 7) and is observable in 25% of all observational time (VIRTANEN and KÄÄRIÄINEN, 1997). In general, a spectral behaviour depend on magnitudes, depth and triggering mechanism of an earthquake.

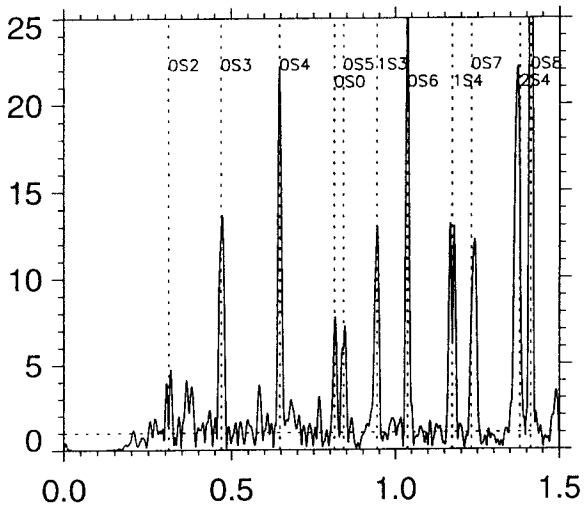

Figure 4. Free oscillation spectrum 5. - 6. Oct. 1994 (long periodic seismic band). Frequencies are in mHz and amplitudes in nanogals. The length of data for spectra is 48 hours.

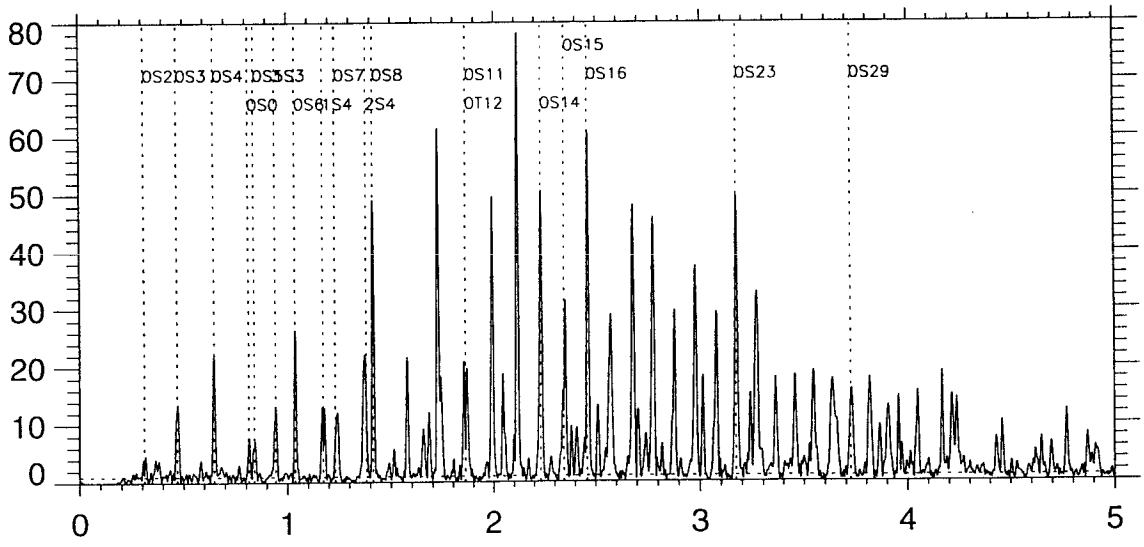

Figure 5. Free oscillation spectrum 5. - 6. Oct. 1994. Frequencies are in mHz and amplitudes in nanogals. The length of data for spectra is 48 hours.

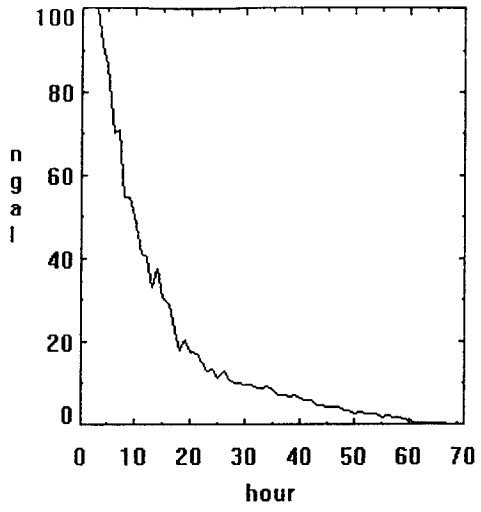

Figure 6. The amplitude attenuation of spheroidal mode $_0S_{15}$ (2.35 mHz) after the earthquake in the Kuril Islands on Oct. 1994 (from VIRTANEN, 1996).

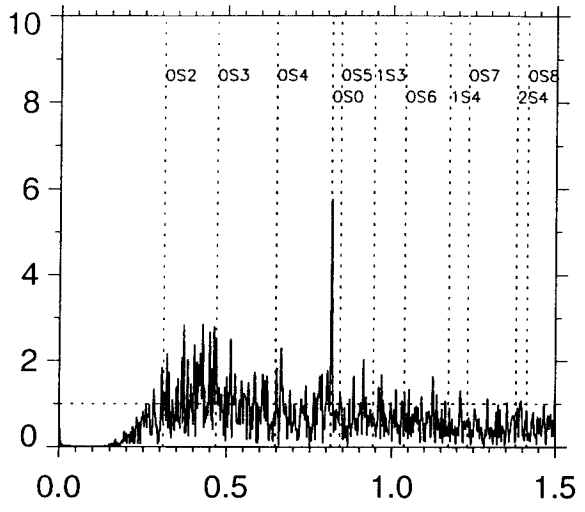

Figure 7. The radial mode $_0S_0$ on 10. - 15 Oct. 1994. The length of time serie is 144 hours.

Tides and the influence of the airpressure

The highpass filtered tidal parameters for 39 waves will be soon published (VIRTANEN and KÄÄRIÄINEN, 1998). The wavegroups are the same as in earlier study with spring gravimeter ET-18 (JENTZSCH and KÄÄRIÄINEN, 1994). The result of main waves are well consistent both in phase and amplitude with earlier studies, showing proper calibration of both instruments. The standard deviation is 0.859nms^{-2}. In the tidal analyses we have used the programme package ETERNA 3.20 (WENZEL 1996). The tidal potential used is that of HARTMANN and WENZEL (HARTMANN and WENZEL, 1995). The resonance effect of liquid core clearly appears between K1 and PSI1 wavegroups.

In concordance with several others authors we have found that the admittance coefficient for air pressure is frequency dependend. Using tidal analyses for long periodic waves (from MTM - to SA) we have obtained the value -3.03 nms^{-2}/hPa for the admittance. The same result was obtained by using cross-spectral analyse program ADMITT (NEUMEYER and PFLUG, 1997). For higher frequencies the admittance is of order -3.8 nms^{-2}/hPa.

The frequency dependency is presented in Fig. 8. Higher admittance at lower frequencies means the regional atmospheric loading effect of around 4 mm/10hPa.

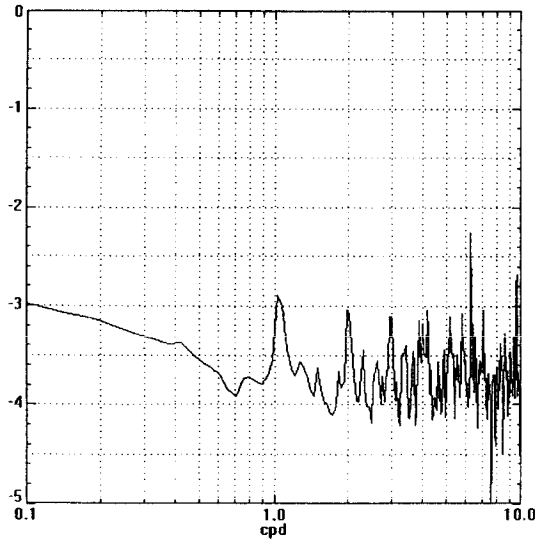

Figure 8. The complex air pressure admittance (nms^{-2}/hPa) observed at Metsähovi from 0.1 to 10 cpd (from VIRTANEN and KÄÄRIÄINEN, 1997).

Long periodic gravity variations

There are several annual and near annual phenomena which cause gravity variations e.g. annual tide, polar tide, including annual and Chandlerian component and variation of groundwater level. The correct separation of these phenomena needs several years of observations. In analysing long periodic phenomena, the proper drift model is essential. We have used 3rd degree polynomial fit for the drift. The land uplift effect is not taken into account but appears as a linear drift. The linear drift during last year has been about 3μgal/ year.

In Fig. 9 the observed effect of polar motion is depicted. In this the model tide with the tidal parameters at the site, airpressure effect, drift (3rd polynomial) and the effect of groundwater level have been removed.

In Fig 10 we show the influence of the groundwater level variations. The correlation of 1.8μgal/metre for groundwater admittance and δ-factor 1.165 for pole tide were found using fixed value 1.16 for annual tide. The amplitude of pole tide is about 4 μgal. The range of groundwater level variations is 1.8 metres (depth 5.1 - 6.9 metres), causing an annual gravity variation of 3 - 4 μgals. The level of the groundwater is the highest in springtimes and the lowest in autumns. The admittance for groundwater level leads to the porosity value of 5% of the bedrock.

Conclusion

The superconducting gravimeter T020 at the Metsähovi station has shown to be a proper instrument to study temporal gravity variations in wide range. In addition to tides SG is able to monitor the microseismicity and retrieve seismic eigenmodes up to 0.1 Hz of the same quality as an ordinary broadband seismometer. (HINDERER, 1996). Generally, the environmental noise leve at the Metsähovi site is low. Due to the small and smooth drift of the instrument, it is also possible to study long periodic effect such as pole tide and annual variations of ground water level. As a member in GGP project, we will also be able to participate the research of global geophysical phenomena such as core modes, silent and slow earthquakes and atmospheric effects.

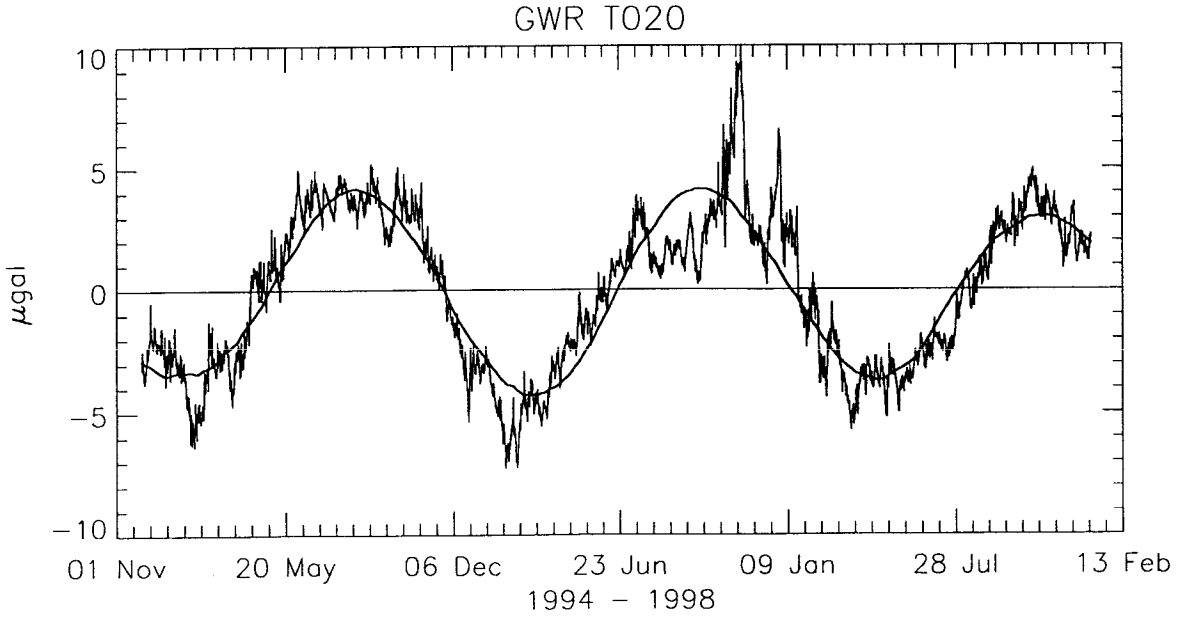

Figure 9. The observed pole tide (broken line) and the calculated one (solid line).

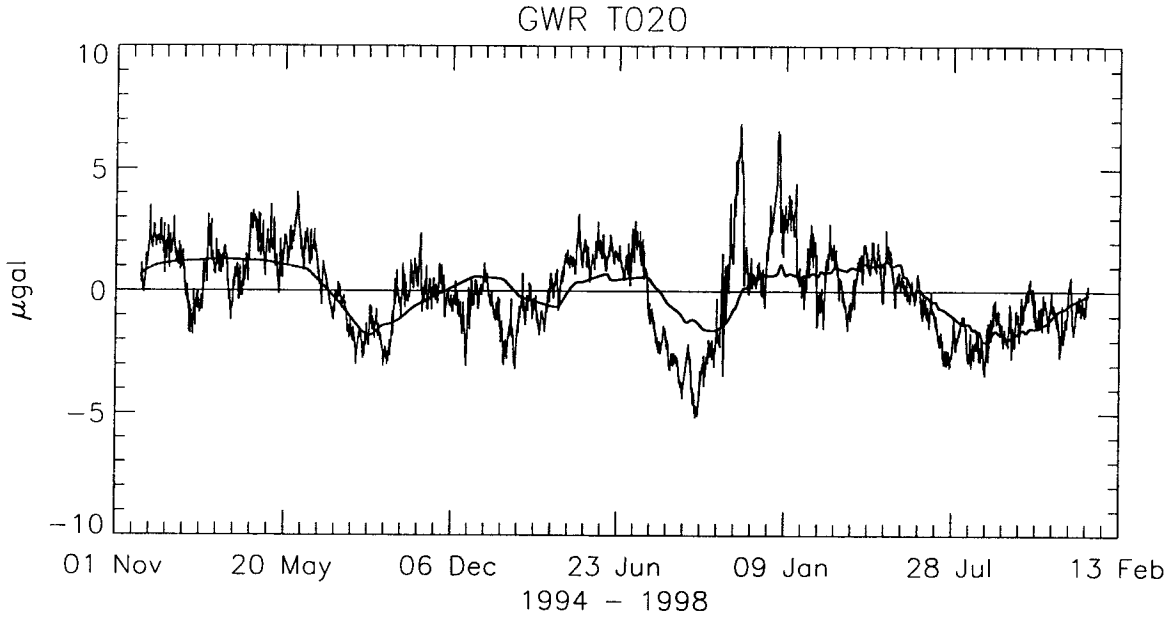

Figure 10. Gravity residuals (broken line) and observed groundwater level (solid line).

References

Hartmann, T., Wenzel, H.-G., 1995: Catalogue HW95 of the tide generating potential, *Bulletin d'information Marees Terrestres*, Vol. 123., p. 9278

Hinderer, J., 1996: Gravity and Earth's Global Structure and Dynamics. *Acta Geod. Geoph. Mont. Hung,* Vol 31, p. 305-327.

Hocke, K., 1998: Phase estimation with the Lomb Scargle periogram method, *Ann. Geophysicae* 16, p.356 - 358.

Jentzsch, G., Kääriäinen, J., 1994: Tidal gravity and tilt measurements at Metsähovi/ Finland: Final Report, *Procedings of the 12th General Meeting of The Nordic Geodetic Commission Ullengsvang, Norway, 30. may - 3. june 1994*, pp. 155 - 163, Hønefoss.

Longuet-Higgins, M., 1950: A theory of the origin of microseism, *Phil, trans. Roy. Soc,* London, A243, p. 1-35.

Masters, G., Widmer, R., 1995: Free oscillation: Frequencies and attenuations, In: *Global Earth Physics, A Handbook of physical Constants, Am geophys. Union, Washington DC,* p. 104 - 125.

Virtanen, H., 1994: The new gravity laboratory and superconducting gravimeter of Finnish Geodetic Institute, *Procedings of the 12th General Meeting of The Nordic Geodetic Commission Ullengsvang, Norway, 30. May - 3. June 1994*, 191 - 197, Hønefoss.

Virtanen, H., Kääriäinen, J., 1995: The installations of and first results from the superconducting gravimeter GWR 20 at the Metsähovi station, Finland, *Rep. Finn. Geod. Inst.* 95:1. Helsinki.

Virtanen, H., Kääriäinen, J., 1997: The GWR T020 superconducting gravimeter 1994 - 1996 at the Metsähovi station, Finland. *Rep. Finn. Geod. Inst.* 97:4. Kirkkonummi.

Virtanen, H., Kääriäinen, J., 1998: One thousand days of superconducting gravimetry on Finland, Proceedings of the thirteenth International Symposium on Earth Tides, Brussels (in press).

Wenzel, H.-G., 1996: Earth Tide Data Processing Package ETERNA 3.20, Black Forest observatory, Schiltach, Karlsruhe.

Summary of the session The Future of NKG.

Some of the covered issues during the general discussion in the session The future of NKG are listed below:

- NKG is a very unique organisation with the close relations to the Mapping Authorities and Universities in the Nordic countries, don't change this concept.
- The decreasing number of Professors in Geodesy in the Nordic countries is an indication that we should increase the information to the politicians about the benefits of Geodesy.
- Geodesy has a very promising future if we take into consideration the requirements from the modern society, including both geophysics and remote sensing. The Working groups of NKG work very good and the role of the Nordic Mapping Authorities is also working well.
- The scientific activity in NKG is very important, but there is a danger that Geodesy is replaced by geomatics and geoinformatics.
- The Nordic countries are strong together. The collaboration should be increased in the activities reference systems and data analysis. Some of these issues are handled in the sub-commission EUREF of IAG, but it could be worthwhile to have also a NKG Working group.
- How can Science and Technology be combined?
- The collaboration between the Nordic and Baltic countries is working well, but it is desirable that it is increased
- The collaboration between NKG and IAG/FIG was discussed

The Finnish Permanent GPS Network - FinnRef

Hannu Koivula, Matti Ollikainen and Markku Poutanen
Finnish Geodetic Institute
Geodeetinrinne 2, FIN-02430, Masala, Finland
email: FinnRef@fgi.fi

The Finnish Geodetic Institute has established a network of 12 permanent GPS stations in Finland (FinnRef - earlier known as FinnNet). The planning of the network started during the winter 92/93. The first stations were installed in 1994 and the last one was built in 1996. The stations are equipped with Geodetic Ashtech Z-12 receivers using Dorne Margolin type Choke Ring antennas, which are located on steel grid masts or on concrete pillars. All the stations are working fully automatically. The network is used as a 1st order reference frame in Finland for GPS users, for the crustal dynamics studies and for providing RTCM corrections in real time applications. FinnRef has been used as a reference frame or as a source of data for numerous national and international GPS campaigns. We will introduce FinnRef and its function in Finland and give an overview of the projects FinnRef has taken part in.

1. Introduction

The Finnish permanent GPS network FinnRef (the name was changed in 1998, May 19 from FinnNet to FinnRef due to Trademark conflict with a consortium of the telephone companies called Finnet*) is a part of the Fennoscandian Regional Permanent GPS Network, which was established by the Nordic Geodetic Commission in response to the initiative of the directors of the Nordic Mapping agencies (KAKKURI *et al.*, 1995). The continuous GPS observations were started in Metsähovi Geodetic Observatory in May 1991 and its present tower was erected in 1992. Satellite laser observations has been made in Metsähovi since 1978 and there has been a mobile VLBI measurement in Sjökulla, some 3 km NE of the Observatory. Next to the VLBI point there is also a DORIS beacon that became operational in 1990. Metsähovi is an important base point of the Finnish Permanent GPS Network due to its international ties e.g. to ITRF, EUREF, IGS, and CIGNET.

* Finnet is a trademark of the Finnet group (Finland)

2. Planning of the network

The planning of the network started at the end of the 1992 when it was decided that the network of 12 stations will be established. Possible site candidates were chosen according to the following rules. The stations should cover the country so that the maximum land uplift differences can be detected. The stations should be built on the bedrock and there should be an open sky at least above 15 degrees. The absolute gravity is or can be measured on the spot. Stations should easily be connected to the precise levelling network and to the telephone and electricity networks (CHEN and KAKKURI, 1994). The first reconnaissance trips were made during the spring 1993 and later that year the first stations were built.

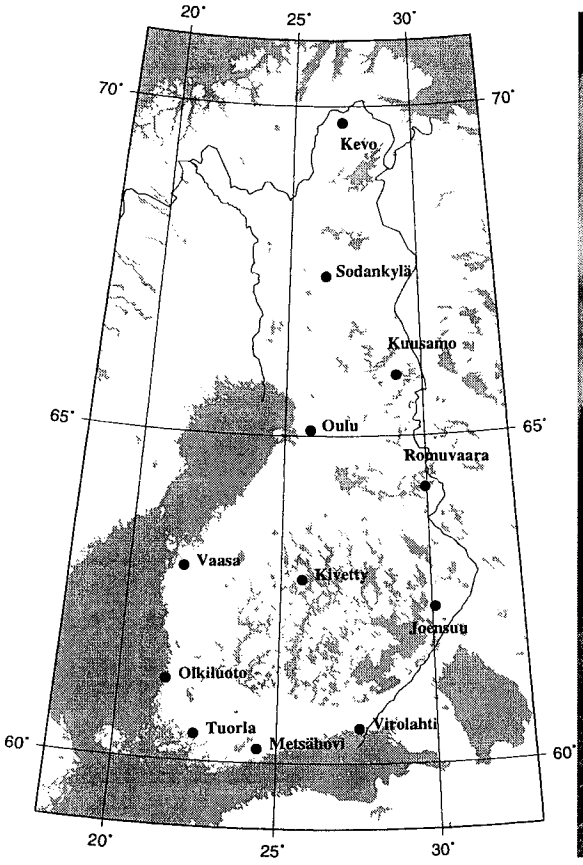

Fig. 1. The Finnish permanent GPS network - FinnRef.

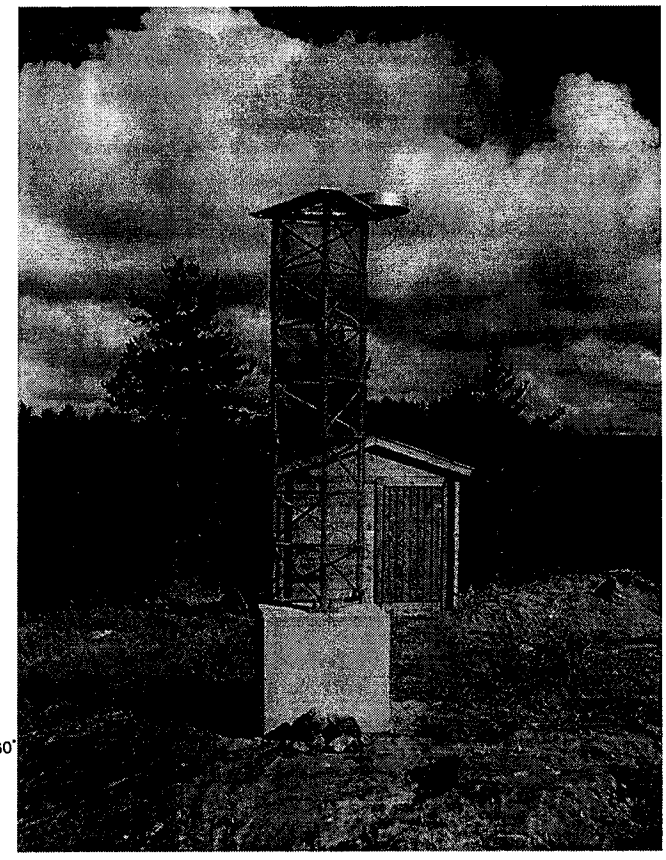

Fig. 2. Joensuu permanent GPS station Lat 62°23 Lon 30°06'. In the background is a small warmed cabin for the receiver.

3. The Equipments of the stations

Antenna platforms

We use three different types of antenna platforms (Fig. 3a-c). The standard configuration is a 2.5 m high steel grid mast (Fig. 3a), which is used at JOENsuu, KUUSamo, SODAnkylä, TUORla, VAASa and VIROlahti. A similar mast, but 5 m high is used at KEVO. 2.5 m mast was chosen because we wanted to minimise the effect of the thermal expansion. In the case of 2.5 m mast the thermal expansion effects to the height less than ±1 mm during the yearly cycle. This amount was considered to be acceptable. Three stations (OLKIluoto, KIVEtty and ROMUvaara) are built in co-operation with Posiva Oy. Posiva Oy is responsible of finding a suitable place for nuclear power waste disposal. Around these sites are local networks which are remeasured semi annually in order to locate possible deformations. For this reason a more stable platform than a steel grid mast was needed. On these places concrete pillars were chosen (Fig. 3b). The last two stations have higher masts. In Metsähovi is an anchored 25 m height steel grid mast and in OULU station a cylindrical 8 m medal mast. In both cases the height of the GPS antenna is invar stabilised (Fig. 3c). The invar stabilisation means that the antenna is isolated from the mast with an attachment piece and a spring system, which is anchored to the bedrock with invar bar or wire. A more detailed explanations of the invar stabilisation in Metsähovi can be found in (PAUNONEN, 1993). The system for Oulu was adopted from Metsähovi.

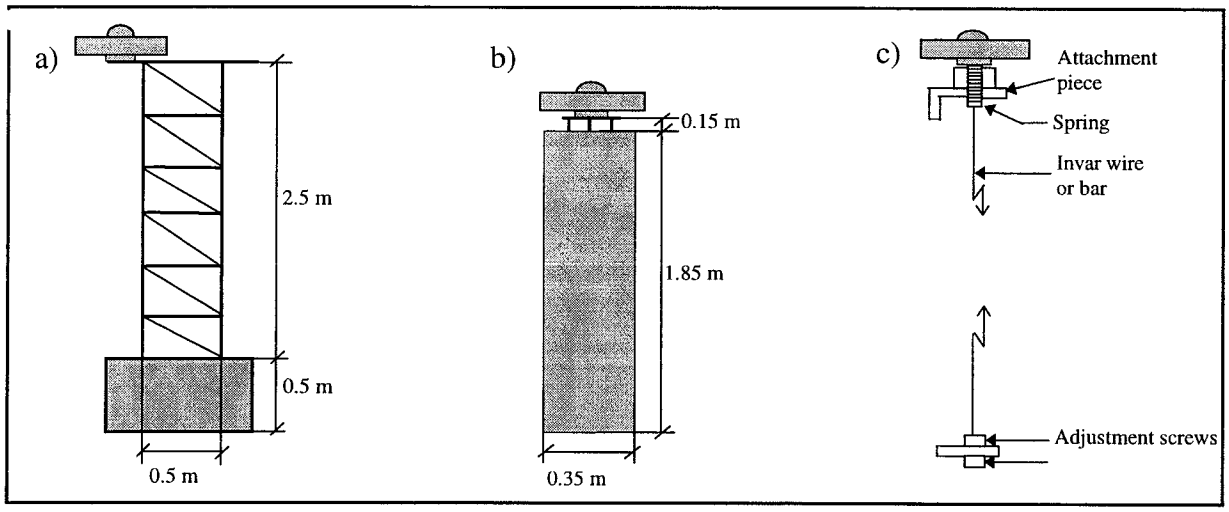

Fig 3a-c. *The three different antenna platforms of FinnRef. a) the standard 2.5 m high steel grid mast, b) a 2 m high concrete pillar to be used at the high accuracy local deformation network and c) an invar stabilisation system for higher masts.*

Hardware and software

All the stations are equipped with Ashtech Z-12 GPS receiver, D+M choke ring antennas (Ash or T), modem and power supply. Exception for this is Metsähovi where we have Turbo Rogue SNR-8100 receiver and D+M B antenna. At Metsähovi we use also an external H-maser; at all other station receiver's internal oscillator is used. The data is collected with a sampling interval of 30 s and the cut off angle is 5°. In addition the remote cabins are warmed so that the temperature will never be below zero. The basic configuration can be seen in Figure 4. In 1995 we started with 8 channel Turbo Rogue SNR-8100 receivers, which provided code and phase measurements on both frequencies. Later the receivers were changed to 12 channel Ashtech Z-12 receivers which also provides us with Dopplers on L1 and L2. At the moment a wide range of different software versions are used on receivers, but later this year (1998) we will install 1F60 software together with Vaisala PTU 220 meteosensors to all stations.

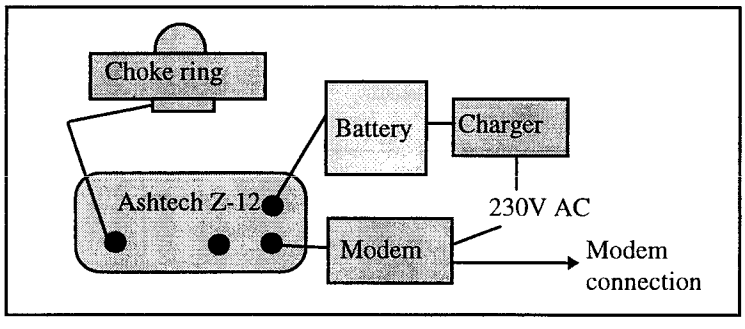

Fig. 4. *The equipments of the FinnRef stations.*

Station sites

Because some of the stations are located on remote places or at the great distances from the FGI we tried to find places close other Institutes, Observatories etc. where we can reach somebody in case of minor problems. KEVO station is at the premises the Subarctic research centre of the University of Turku. OULU station is at the Aarne Karjalainen Observatory of the University of

Oulu. People from the University visits the station weekly. SODAnkylä station is at Pittiövaara some 10 km west from Sodankylä. The station is not permanently occupied, but it is visited weekly by local staff of the Sodankylä Geophysical Observatory. TUORla station is at the Astronomical Observatory of the University of Turku located some 10 km south-east from Turku. There is about 30 people working at the Observatory. At KIVEtty, OLKIluoto and ROMUvaara stations we have contact persons who can check the stations. METSähovi is in FGI's Geodetic Observatory. JOENsuu, KUUSamo, VAASa and VIROlahti have a heated 2x3 m wooden cabins, and these are also places where we have no contact persons to look after the receiver. At OLKI, KIVE and ROMU there are 1,5x2 m heated element cabins. At all other places we used an existing building for the equipment.

Station	IERS Domex	Installed	Receiver	Antenna	Radome	Platform	Lat. N	Lon. E
METS	10503S011	01-Jan-92	Rogue SNR-C	DM B	-------	25 m SG (IS)	60°13'	24°24'
		30-Apr-95	SNR-8100					
SODA	10513M001	14-Aug-94	SNR-8100	DM T	Delft	2.5 m SG	67°25'	26°23'
		15-May-95	Ashtech Z-12					
TUOR		15-Aug-94	SNR-8100	DM T	-------	2.5 m SG	60°25'	22°27'
		21-Jan-95	Ashtech Z-12					
VIRO		15-Aug-94	SNR-8100	DM T	Delf	2.5 m SG	60°32'	27°33'
		24-Mar-95	Ashtech Z-12					
OLKI		19-Oct-94	SNR-8100	DM T	Delft	2 m CP	61°14'	21°28'
		19-Apr-95	Ashtech Z-12					
VAAS	10511M001	07-Apr-95	Ashtech Z-12	DM Ash	Ash	2.5 m SG	62°58'	21°46'
JOEN	10512M001	15-Jun-95	Ashtech Z-12	DM Ash	Ash	2.5 m SG	62°23'	30°06'
OULU		16-Sep-95	Ashtech Z-12	DM Ash	Ash	8 m (IS)	65°05'	25°54'
KIVE		05-Mar-96	Ashtech Z-12	DM Ash	Ash	2 m CP	62°49'	25°42'
ROMU		07-May-96	Ashtech Z-12	DM Ash	Ash	2 m CP	64°13'	29°56'
KEVO		05-Jul-96	Ashtech Z-12	DM Ash	Ash	5 m SG	69°45'	27°00'
KUUS		30-Oct-96	Ashtech Z-12	DM Ash	Ash	2.5 m SG	65°55'	29°02'

Table 1. *Station history.*

4. Station history

In the summer 1993 the first 2.5 m steel grid masts were built to Virolahti, Sodankylä, Tuorla, Vaasa and Joensuu. The first observations at the sites took place during DOSE'93 campaign and the first test observations were done in the end of 1994. We started the observations with Turbo Rogue SNR-8100 GPS receivers, but later they were replaced by Ashtech Z-12, because we were not satisfied with the functioning of the Rogues, Ashtech had 12 channels instead of 8 and also RTCM correction as an option. Table 1 gives an overwiev of the FinnRef history. The first column gives a 4 letter abbreviation of the station and the second an IERS Domex number. On the third column the installation day of the receiver type is given. In the case of Metsähovi we started the history from the date when the antenna was mounted to the current 25 m mast. The GPS measurements actually started in Metsähovi in an older tower already in 1991 when it became a part of the CIGNET network. Also the change day from Rogue to Ashtech is given, but receiver changes in case of the same type are not listed here. The fourth column shows the receiver type, SNR-8100 refers to Turbo Rogue SNR-8100. Fifth column tells the antenna type followed by the radome type on the sixth column. In all stations Choke Ring antennas are used. Metsähovi station has a Dorne Margolin B type antenna (DM B). On the other stations there are Dorne Margolin T (DM T) or Dorne Margolin Ash (DM Ash) antennas. T types are covered by Kootwijk (Delft) radomes (Except Tuorla, where we do not have a radome). All the Ash type antennas have a standard Ashtech Radome. Metsähovi station does not have a radome. The

seventh column tells on what platform the antenna is mounted. SG refers to steel grid mast, CP to concrete pillar and IS to Invar stabilised. Last two columns gives an approximate location of the stations.

5. The data flow and data processing

In our GPS control centre we have a 60 MHz Pentium running under MSDos 6.21 operating system. There is a simple Dos script running a timer which gives at 00:30 UT permission to activate the downloading script. A reason for this primitive operating system is that Ashtech's downloading program *Remote* runs best under it although more sophisticated systems are considered as one can read from (VERMEER, 1998). We have a modem connection to the stations and the script calls the stations one by one, downloads data and transfers it to the RINEX format. In the local computer we have 2 copies of the data on different hard disks and in addition one copy on DEC 3000 Workstation where the processing takes place as well. In addition the data is send to Onsala Space observatory where the EUREF processing is done and Metsähovi data is taken by the *Statens Kartverk* (Norway) to Hønefoss and further to IGS processing centre. The data is archived every second week to CDROM and Dat tapes.

Bernese 4.0 software is used for the processing. The procedures are described more detail in (KOIVULA, 1998). We process daily free network solutions saving normal equations and later combining them to weekly solutions.

6. Use of the FinnRef

6.1. International Campaigns and activities

Metsähovi station has been a part of CIGNET (Co-operative International GPS Network) since May 1, 1991 and IGS network since June, 1992 (KAKKURI et al, 1995). It is a part of FinnRef network, but is run by the FGI's Geodetic Observatory in Metsähovi instead of the Department of Geodesy that runs the rest of FinnRef.

The first observations of the permanent stations were done during the DOSE'93 (Dynamics of the Solid Earth) campaign, which was followed by several DOSE campaigns. In the first campaign the stations SODA, TUOR, VAAS, JOEN and VIRO masts were occupied by antennas and an additional benchmark of OULU station was observed. Later from the DOSE campaign grew the BIFROST project, for which FGI has provided also FinnRef data (BIFROST PROJECT, 1996).

Four FinnRef stations (Metsähovi, Vaasa, Joensuu and Sodankylä) are also EUREF stations. Metsähovi since 1996 and other 3 since 1997.

In May 21-29, 1997, Baltic Sea Level (BSL) campaign and EUVN (European Vertical GPS Reference Network) campaign was held. These campaigns overlapped on several common points so it was decided to have a one combined campaign. All EUVN points were observed during the whole 7 day period, on the contrary BSL points were measured only in 3-4 sessions. Data from FinnRef was available for both projects in order to create a strong backbone for the solution in Finland.

6.2. National campaigns and related measurements

During the year 1992 FGI, National Board of Survey and Finnish Maritime administration measured a network of 22 points including 3 original EUREF89 points. All these points were 1st order triangulation points with known N60 heights. This first big national GPS campaign created a GPS network that can be called the 0-class network of Finland. The results were used for determining the transformation between the Finnish national Grid Co-ordinate system (KKJ) and ED50 (OLLIKAINEN 1993, 1995). During the year 1994 the ties between all six existing FinnRef stations (Joensuu, Oulu, Sodankylä, Tuorla, Vaasa and Virolahti and 0-class GPS network was measured using Ashtech XII receivers and Microstrip antennas.

During the DOSE'94 campaign one receiver was visiting several levelled benchmarks around the Oulu station in order to determine the height of Oulu station, which was part of the campaign. Because the distance to the closest precise levelling point was around 11 km this method was implemented. Using the FIN95 geoid the orthometric height of Oulu station was calculated (OLLIKAINEN, 1997).

In Olkiluoto, Romuvaara and Kivetty stations FGI is measuring high precision local networks twice a year in order to find local deformations. These measurements are done for Posiva Oy which is responsible for finding a suitable place for disposal of nuclear waste. The first measurements were done in Olkiluoto in the end of 1994 and in Romuvaara and Kivetty in the end of 1995 (CHEN and KAKKURI, 1994, 1996, 1997).

In 1995 FGI made an agreement with the Finnish National Broadcasting Company (YLE) that 5 of FinnRef stations (Metsähovi, Vaasa, Joensuu, Oulu and Sodankylä) will provide RTCM corrections of type 1 and 2 which will be send for users via YLE's FM radio broadcasting. Later YLE has built their own reference stations the co-ordinates of which has been determined by FGI. At the moment Oulu is the only FinnRef station that provides RTCM corrections.

In the winter 1996 the Department of Gravimetry used FinnRef stations as a reference when they made gravity measurements on the ice of the Gulf of Bothnia. They used GPS for determining the velocity of the ice field in order to determine the Eötvös-correction more reliably (RUOTSALAINEN, 1997). GPS has also been used to determine heights of the relative gravity measurement points (RUOTSALAINEN 1998).

Eight FinnRef stations were connected to the precise levelling network by levelling during years 1995-1998. Tuorla, Virolahti, Joensuu and Vaasa were levelled in 1995; Oulu, Sodankylä and Kevo in 1996 and finally Kuusamo in the summer of 1997.

During the years 1996-1997 FGI measured a EUREF dencification network. The network consisted of 101 points of which 3 were precise levelling benchmarks, 6 tide gauges and 91 old 1st order triangulation points. The measurements were divided into two parts. The southern part of Finland was measured in 1996 and the northern part in 1997. All 12 FinnRef stations were used as a backbone for creating the EUREF-FIN reference frame.

The absolute gravity has been measured in some of the FinnRef points using JILAg-5 (owned by FGI) or FG5 (owned by NOAA) gravimetres. The JILAg-5 was used in Metsähovi in 1988 and 1995, in Vaasa 1995 and in Sodankylä at 1988, 1992 and 1998. FG5 was used in Metsähovi at 1993 and 1995, in Vaasa 1995. The Future plans includes measurements at Vaasa and Joensuu in this year (1998), five more stations in 1999 and again 5 more in 2000 (MÄKINEN, 1998).

On July 17th 1997 the stations VAASa, KUUSamo and KEVO were used by the Department of Photogrammetry of the FGI as base stations for a photogrammetric flight in the ORIENTATION-project. Observations were made with an interval of 1 second on the ground stations and in the airplane. The purpose was to study the influence of different baseline lengths on the camera coordinate solutions. More information can be found in (BILKER et al., 1998).

In addition anyone can purchase data for various purposes. It has been used as a static reference stations as well as a base station when mapping ski tracks and track profiles.

6.3. Activities at a moment and in the near future

At the moment the main task is to finish the processing data we have archived during years. At the moment data since 1996 is processed and the new data is processed as soon as precise orbits are available. But there is still plenty of data to process from years 1995 and 1994. These results lead us automatically to study the land uplift and horizontal deformations in Finland.

During the years 1998-1999 the FGI will measure some 300-400 new points in the EUREF-FIN system. These points can be used as a reference points by any GPS user.

In the summer of 1998 the field calibration of the antennas of FinnRef stations takes place. All the antennas will be calibrated in respect of one reference antenna using the method described in (Rothacher 1995).

In the Autumn 1998 we will install Vaisala PTU 220 type meteosensors for all FinnRef stations. These sensors will be connected straight to the receivers and will measure pressure, relative humidity and temperature. The data are downloaded together with the GPS data.

References

BIFROST PROJECT, 1996. GPS Measurements to Constrain Geodynamic Processes in Fennoscandia. EOS, transactions, American geophysical union, Vol 77, Number 35, August 27, 1996.

BILKER, M., HONKAVAARA, E., JAAKKOLA, J., 1998. GPS Supported Aerial Triangulation Using Untargeted Ground Control. In: International Archives of Photogrammetry and Remote Sensing, Vol. 32. ISPRS Com. III Symposium, Columbus, Ohio, USA.

CHEN, R AND KAKKURI, J., 1994. Feasibility study and technical proposal for long term observations of bedrock stability with GPS. Report YJT-02, Nuclear Waste Commission of Finnish Power Companies, Helsinki.

CHEN, R AND KAKKURI, J., 1996. GPS operations at Olkiluoto, Kivetty and Romuvaara for 1995. Project report, PATU -96-07e, Posiva Oy, 1996, Helsinki.

CHEN, R AND KAKKURI, J., 1997. GPS operations at Olkiluoto, Kivetty and Romuvaara for 1996. Project report, PATU -96-65e, Posiva Oy, 1996, Helsinki.

KAKKURI, J., KOIVULA,H., OLLIKAINEN, M., PAUNONEN, M., POUTANEN, M. AND VERMEER, M., 1995. The Finnish permanent GPS array FinnNet: Current status. Invited paper, IGS workshop, Potsdam, May 15-17, 1995.

KOIVULA, H., 1998. The first results of the Finnish permanent GPS network. Presented in the 13th General meeting of the Nordic Geodetic Commission, May 25-29, 1998, Gävle, Sweden.

MÄKINEN, 1998. Personal communication 19-May-1998.

OLLIKAINEN, M., 1993 (in Finnish). GPS-koordinaattien muuttaminen kartastokoordinaateiksi. Geodeettinen laitos. Tiedote 8.

OLLIKAINEN, M., 1995. The Finnish Geodetic Coordinate Systems and the Realisation of the EUREF-89 in Finland. Proceedings of Urgency Seminar: "Coordinate Systems, GPS and the Geoid", Hanasaari, Finland, June28-30, 1994. (Ed. M. Vermeer). Rep. of the FGI, No. 95:4, pp. 151-166. Helsinki.

OLLIKAINEN, M., 1997. Determination of orthometric heights using GPS levelling. Publ. Of the FGI, No. 123, pp. 67-75. Kirkkonummi.

PAUNONEN, M., 1993. Height stabilised 20-metre antenna mounting system of the CIGNET GPS station at Metsähovi, Newsletter of Space Geodetic Measurements Sites Subcommission (SGMS), IAG, IUGG, International Coordination of Space Techniques for Geodesy and Geodynamics (CSTG), Vol. 4, No. 1, May 1993, pp. 7-10.

RUOTSALAINEN, H., 1997. Determination of Ice field flow with the kinematic GPS method for the Eötvös correction in Gravity survey on the sea ice of Bothnian Bay. Proc. Int. Symp. On kinematic systems in geodesy, geomatics and navigation, Canada, University of Calgary.

RUOTSALAINEN, H., 1998. GPS-positioning in the gravity survey of Finnish Geodetic Institute. Geonickel project. International symposium in Geological Survey of Finland, 1998, Espoo, Finland.

ROTHACHER, M., SCHAER, S., MERVART, L. AND BEUTLER, G., 1995. Determination of antenna phase center variations using GPS data.

VERMEER, M., 1994. The Finnish National Permanent GPS Network: Current Status. Proceedings of the 12th General Meeting of the Nordic Geodetic Commission, Ullensvang, Norway, May 30 - June 3, 1994.

VERMEER, M., 1998. About GPS, Modems, and the meaning of life. Presented in the 13th General meeting of the Nordic Geodetic Commission, May 25-29, 1998, Gävle, Sweden.

Activities at the NKG GPS-data Analysis Center 1996-98

Jan Johansson, Onsala Space Observatory, Chalmers University of Technology, Sweden

Abstract
The development of a Nordic GPS observing network and its analysis center at Onsala Space Observatory is described, with special emphasis on its role as a contributor to EUREF, the European Reference Frame. Some stations have accumulated three years of data, but new sites continue to be added to the network. Selected examples of time series are presented to illustrate technical challenges, Nordic observing conditions, and the influence of post-glacial rebound on the results.

Introduction

The International Association for Geodesy appointed their EUREF subcommission in 1987 to establish, maintain, and enhance a 3-dimensional European geodetic reference frame. By definition the European Terrestrial Reference System (ETRS) is fixed to the stable part of the European tectonic plate and coincides with the International Terrestrial Reference System (ITRS) at epoch 1989.0. The EUREF subcommission consists of at least one representative from each European country. The operative part of EUREF is handled by the Technical Working Group (TWG).

The first step towards realization of ETRS was taken in 1989 with the EUREF-89 GPS observing campaign in Western Europe, involving more than 100 stations. Fiducials used for this campaign were SLR/VLBI sites fixed to their ITRF-89 coordinates at epoch 1989.0, which gave a straightforward realization of ETRS. Several later EUREF campaigns have been carried out ameliorating the results of previous campaigns and enlarging the coverage area in Europe.

Following the establishment of the International GPS Service (IGS), their permanent GPS sites are used as fiducials for the processing of GPS campaigns in EUREF. Further densification of the permanent GPS networks in Europe led to the establishment of the EUREF permanent GPS network and the EUREF data analysis center.

The EUREF permanent network

The EUREF network consists of permanently mounted GPS tracking stations (see Fig. 1), data centers for collection and distribution of observing data to the user community, and analysis centers which process the data from (their part of) the EUREF network (Bruyninx et al., 1996). A coordinating central bureau has been established at the Royal Observatory of Belgium (http://homepage.oma.be/euref).

The EUREF network of GPS tracking stations is comprised of all the European permanent IGS sites plus additional sites selected by the EUREF TWG. It now totals nearly 100 stations. Six European local data centers provide access to observing data from particular EUREF sub-networks. The global IGS data center at IGN, France and the regional IGS data center at BKG, Germany provide access to data from IGS stations (see Table 1 for abbreviations). All data are publicly available.

The data analysis scheme of the EUREF permanent network is based on distributed processing. The data from all stations in the network are processed by at least three analysis centers. The EUREF local network associated analysis centers listed in Table 1 routinely process the data from a particular EUREF sub-network. The EUREF data analysis follows IGS standards and uses precise IGS orbits and Earth Rotation Parameters. The local analysis centers deliver weekly free-network solutions to the IGS/EUREF regional data center. Precise GPS satellite orbits become available about two weeks after the observations are made. Thus, the products from the EUREF analysis centers are available within 2-3 weeks. The BKG analysis center combines all partial solutions into an official weekly EUREF solution.

The Nordic contribution

The NKG (Nordic Geodetic Commission) local analysis center for EUREF was formed in response to an invitation from the EUREF Technical Working Group. The task is to routinely process the GPS data from sites in Northern Europe for the extension and densification of the European reference frame. The NKG analysis center is located at Onsala Space Observatory after a decision by the NKG presidium May 15, 1996.

Networks of permanent GPS stations have been established and developed in the Nordic countries throughout the decade of the 1990s and now totals approximately 50 stations. The Nordic part of the EUREF permanent network consists of selected stations in the respective national networks. Each country has followed its own time scale of network development. A common driving force has been the quest to accurately describe and understand the phenomenon of post-glacial rebound. Some networks had the additional specific task of servicing real-time navigation applications and geodetic production. The data are also used for geodetic and atmospheric research.

The development history of each national network has led to diverse technical solutions. The 12 station FinnRef in Finland and 11 station SATREF in Norway employ mainly steel grid towers to carry the GPS antenna while the 21 station SWEPOS® in Sweden has temperature controlled concrete antenna towers. Different antenna types and receiver brands have been used. All stations are now equipped with same type of antenna after a decision taken within the NKG working group on permanent geodetic station in 1997. The Norwegian and Swedish networks transfer data in real time to national operation centers via TCP/IP computer networks. The Finnish stations are contacted by dial-up telephone and transfer data via modems. Figure 1 identifies, among other stations, the 4 Finnish, 6 Norwegian and 5 Swedish stations selected for the Nordic sub-network of EUREF. Some of them also serve as IGS stations. Other stations used in the NKG solution are 2 on Greenland, 2 on Iceland, one each in the three Baltic republics of Latvia, Lithuania, and Estonia, and one in Russia. Later additions include 3 stations in Denmark.

Members of the NKG Working Group on Permanent Geodetic Stations established the NKG analysis center in 1996 as a joint effort. The intention is to take an active part in the development of the EUREF permanent network, the EUREF processing strategies, and the products. This will help to facilitate integration of other Nordic permanent stations and GPS campaign sites into the EUREF/IERS and national geodetic reference systems in the region, aiming towards future extension and densification of such reference systems.

The standard analysis product is achieved by processing in an automatic mode, i.e. non-interactively, using Bernese Software 4.1 and the Bernese Processing Engine (Rothacher and Merwart, 1996). The Bernese software was chosen in view of the fact that most NKG member agencies use it and so does a majority of the EUREF analysis centers. The exchange of intermediate products can easily be facilitated. The daily analysis of 30 permanent GPS stations is handled using a cluster of HP-700 workstations and PC-Pentium Pro systems running under LINUX. The full system includes a disc capacity of about 50 Gbyte. The standard analysis uses an elevation cutoff angle of 15° for all sites. This give the smallest uncertainty values for the estimated horizontal and vertical baseline components (20° was used until April 1997). Due to different antenna types being selected for different sites, elevation-dependent phase-center corrections have been applied according to Rothacher and Schär (1996). Precise satellite orbits and earth orientation parameters are readily available from the IGS processing centers, and these are used to produce the NKG solutions. The data processing utilizes a regional free-network technique wherein the coordinates of site position have only weak *a priori* constraints. The coordinates of the sites are estimated as bias terms. Then constraints are applied to transfer the results into a terrestrial reference frame. The zenith values of the propagation delay due to water vapor are estimated as bias terms with a new parameter value for each site every second hour.

The daily and weekly analysis results are compared to the results of other techniques and to GPS results from other software and other analysis centers. This employs the same method as established for daily processing in the Bifrost project (BIFROST Project, 1996), where studies of station time series and their auto- and cross-correlation are undertaken, see e.g. Johansson (1998). Furthermore, the Power Spectral Density of all time series is used to detect periodic effects and address the problems associated with mechanical and electromagnetic stability of the sites.

Some preliminary results

The processing delivers valuable data for geophysical investigations and for the maintenance of the European reference frame. Furthermore it serves quality evaluation purposes and addresses the fundamental question of uncertainties and error sources in space geodetic techniques.

The official activity of the EUREF permanent network and the NKG local analysis center started in October 1996 and the time series now contain about three years of continuous results. The time series of station coordinates for the EUREF sites are created from the weekly EUREF combined solution. The combination of the different solutions obtained by the 11 processing centers is carried out using the Bernese software. The geodetic datum of the coordinates is defined by forcing the total free coordinate solution for a selected number of stations (fiducial stations) to have no translation and no rotation with respect to ITRF96. The fiducial stations are Brussels, Graz, Kootwijk, Matera, Onsala, Wettzell, and Zimmerwald. The combined solutions are produced by the BKG. At a later stage the EUREF solution is combined with the global IGS solutions and other regional solutions in order to obtain station coordinates and station velocities in a global reference frame such as ITRF96.

Figure 2 demonstrates the capability of the routine processing of data from the EUREF permanent network. The repeatability for the Onsala station coordinates is a few mm in the horizontal components and below 1 cm in the vertical component. Onsala is used as one of the

fiducial stations. Nevertheless, the time series show several interesting features such an apparent seasonal variation in the vertical component and a systematic trend in the North-South component. The trends may be due to real station motion in respect to the ITRF96 reference frame. Other possible explanations for these variations are found in various error sources such as satellite orbit errors, tension within the EUREF reference frame because the coordinates for the fixed stations are not all accurate, and seasonal variations in the electromagnetic and mechanical environment at the stations (Johansson, 1998).

In figure 3, problems associated with the GPS antenna and its environment are demonstrated. Jumps in the time series indicate changes of the antennas at the site. At the time of inclusion into the EUREF permanent network, four Norwegian stations were equipped with Trimble geodetic antennas. These were replaced in 1998 by Dorne-Margolin choke-ring antennas, the advantages being that the choke-ring antennas have very good characteristics and that stations in the Nordic countries thereby have the same type of antennas. However, the antenna change evidently introduced a jump in the Trondheim time series.

The time series from Sodankylä in Finland in plotted in figure 4. We note large variations and increased scatter in the time series during the winter periods. This higher noise level may be related to snow accumulating on top of the antenna as shown in earlier investigations (Johansson, 1998). This was confirmed in a separate investigation by the Finnish Geodetic Institute (Hannu Koivula, personal communication, 1998). This is a serious problem that most likely will affect the results obtained from several of the Finnish, Norwegian, and Swedish sites during wintertime.

In figure 5, the time series for the Swedish station in Vilhelmina is shown. Especially the vertical component deserves a more detailed investigation. The time series clearly indicates that the Vilhelmina station is rising with respect to the EUREF reference frame. In fact the motion is quite significant and could to some extent be explained by the land uplift associated with postglacial rebound. The capabilities of GPS-based space geodesy have been proposed to discern movements of surface in the course of postglacial rebound with bearing on the climate change. It is realized that only space techniques are able to separate vertical crustal movement from changes of the sea level and the geoid. The space-based methods have also been recognized as sufficiently sensitive to resolve the horizontal deformation expected in the course of the glacially induced isostatic rebound at rates of millimeters per year over distances between ten and several thousands kilometers [BIFROST Project, 1996].

The EUREF and IGS initiative could become a very powerful tool for different organizations. The Nordic Mapping Agencies may use the solutions to maintain the national reference systems by continuously relating the national GPS activities to the EUREF permanent network and to the International Reference Frame (ITRF). Today, the national reference systems do not handle the fact that reference sites have both inter- and intra-plate motion due to plate tectonics and postglacial rebound. Horizontal station motions associated with postglacial rebound are at the level of a few mm/year. Similarly, the vertical motions are from 0-10 mm/year dependent on station location. This will certainly have to be accounted for in future national reference systems. In Table 2, velocities are given for some of the stations routinely processed by the NKG analysis center.

Conclusion and future

The intention of the IGS, EUREF and NKG initiatives is to maintain and densify the European reference frame. Organizations who operate permanent stations or a network of stations will receive feedback about station performance and may also easily connect their own GPS observations to the NKG/EUREF solution in order to obtain station coordinates in a European or global reference frame. The future development of the EUREF permanent network certainly includes more stations. Over the period 1996-1999 at least 10 new stations have been added every year. This increase will most likely continue for many years to come.

The routine analysis is currently carried out by 11 centers handling daily data files. During 1999, some analysis centers started to process data every hour. The processing of the hourly data files is carried out immediately after the hour. The products from this type of data analysis will give information on both station and satellite performance. This information may easily be fed back to the organization responsible for the station or the network. Furthermore, the estimates of atmospheric propagation delay can be used in e.g. meteorological applications such as weather forecasting. The amount of water vapor in the lower atmosphere (troposphere) can be accurately determined by the use of GPS. In such a case hourly information may be required.

The NKG actively supports the establishment and integration of new GPS stations in the Baltic countries and Russia into EUREF and IGS. The intention is to provide information for routine use of our daily and weekly analysis products to organizations in the region.

Acknowledgements

The NKG permanent network and the NKG data analysis center have proven to be a fruitful Nordic cooperation. Important contributions have come from all Nordic Mapping Agencies through the channels of the NKG presidium and the working groups on Satellite Geodesy and Permanent Geodetic Stations. We would like to thank all people involved in different aspects of this work.

References

BIFROST Project, GPS Measurements to Constrain Geodynamic Processes in Fennoscandia, EOS Transactions (AGU), 35, 1996.

Bruyninx, C., W. Gurtner, A. Muls, (1996), The EUREF Permanent GPS network, Report on the Symposium of the IAG Subcommission for Europe (EUREF) held in Ankara 22-25 May 1996, Veröffentlichungen der Bayerischen Kommission für die Internationale Erdmessung.

Johansson, J.M, GPS Antenna and Site Effects, IAG Symposia: Advances in Positioning and Reference Frames (ed. F. Brunner), Vol. 18, Springer-Verlag, 1998.

Rothacher, M., L. Merwart, (1996), Bernese GPS Software Version 4.0, Technical Report, Astronomical Institute, Berne University, Switzerland.

Rothacher, M., S. Schär, (1996), Antenna Phase Center Offsets and Variations Estimated from GPS Data, Proc. IGS Analysis Center Workshop, Silver Spring, USA.

Agency	Location	Software
Italian Space Agency (ASI)	Matera, Italy	Microcosm
Bundesamt für Kartographie und Geodäsie (BKG)	Frankfurt, Germany	Bernese Software 4.0
Bayerische Akademie der Wissenschaften (BEK)	Munich, Germany	Bernese Software 4.0
Observatory Lustbuehel Graz (OLG)	Graz, Austria	Bernese Software 4.0
Bundesamt fuer Landestopographie (LPT)	Wabern, Switzerland	Bernese Software 4.0
Royal Observatory of Belgium (ROB)	Brussels, Belgium	Bernese Software 4.0
Geodetic Observatory Pecny (GOP)	Czech Republic	Bernese Software 4.0
Warsaw University of Technology (WUT)	Warsaw, Poland	Bernese Software 4.0
Center for Orbit Determination in Europe (CODE)	Berne, Switzerland	Bernese Software 4.1
Nordic Geodetic Commission (NKG)	Onsala, Sweden	Bernese Software 4.1
Institut Geographique National (IGN)	Paris, France	Bernese Software 4.0

Table 1. EUREF local network analysis centers. BKG is also responsible for the combination of all 11 solution into one single EUREF products.

Domes No.	Site name	Station ID	Velocity X (mm/year)	Velocity Y (mm/year)	Velocity Z (mm/year)
10202M001	Reykjavik	REYK	-20.1	-3.5	8.3
10204M002	Høfn	HOFN	-10.3	13.0	5.8
10302M006	Tromsø	TRO1	-17.5	7.6	5.0
10302M006	Oslo	OSLO	-13.1	-3.5	1.6
10317M001	Ny Ålesund	NYA1	-15.5	7.0	3.2
10322M002	Vardø	VARD	-13.9	20.2	22.8
10330M001	Stavanger	STAV	-6.4	6.5	15.9
10331M001	Trondheim	TRON	-21.2	25.5	1.9
10402M004	Onsala	ONSA	-13.6	14.7	8.4
10405M002	Mårtsbo	MAR6	-11.8	16.9	14.8
10422M001	Kiruna	KIR0	-13.9	11.5	10.6
10423M001	Visby	VIS0	-17.5	15.5	5.0
10424M001	Vilhelmina	VIL0	-13.6	14.5	10.8
10503S011	Metsähovi	METS	-17.6	13.9	4.9
10511M001	Vaasa	VAAS	-12.0	18.2	16.9
10512M001	Joensuu	JOEN	-18.7	17.8	7.9
10513M001	Sodankylä	SODA	-15.2	17.4	18.6
12302M002	Riga	RIGA	-17.4	13.9	3.8
12350M001	Svetloe	SVTL	-20.8	15.2	3.2
43001M001	Thule	THU1	-22.8	-3.1	-2.3
43005M001	Kellyville	KELY	-20.5	-3.1	0.3

Table 2. Velocities in the ITRF97 reference frame for a sample of the permanent stations processed by the NKG local network analysis center. The ITRF97 solution is available from

the International Earth Rotation Service (IERS) and Institut Geographic National (IGN) in France and based on observation up to the end of 1998.

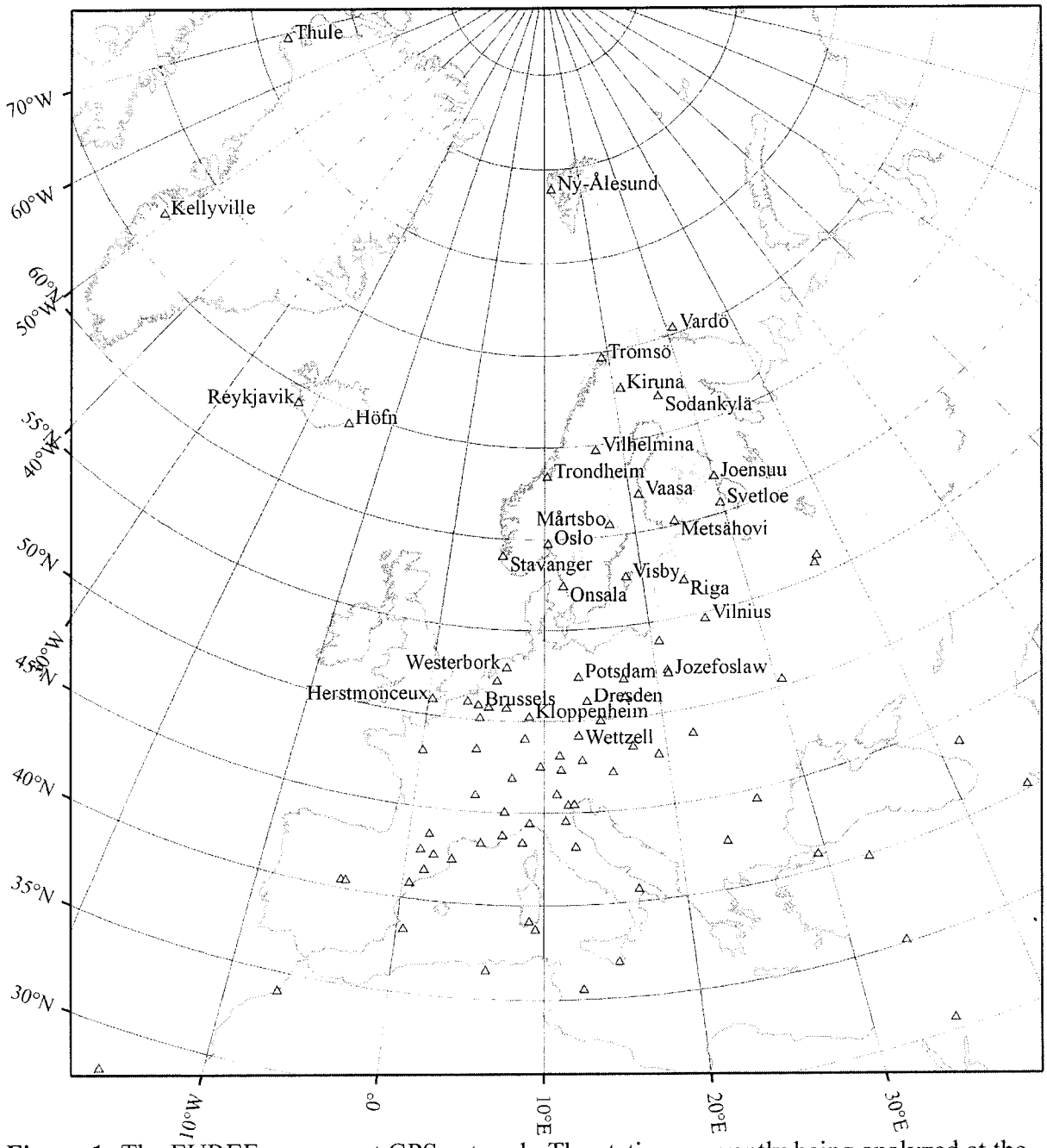

Figure 1: The EUREF permanent GPS network. The stations currently being analyzed at the NKG processing center are indicated as small triangles and the name of the stations. Other EUREF permanent stations are indicated without names. Three Danish stations will soon be ready for inclusion in the EUREF network.

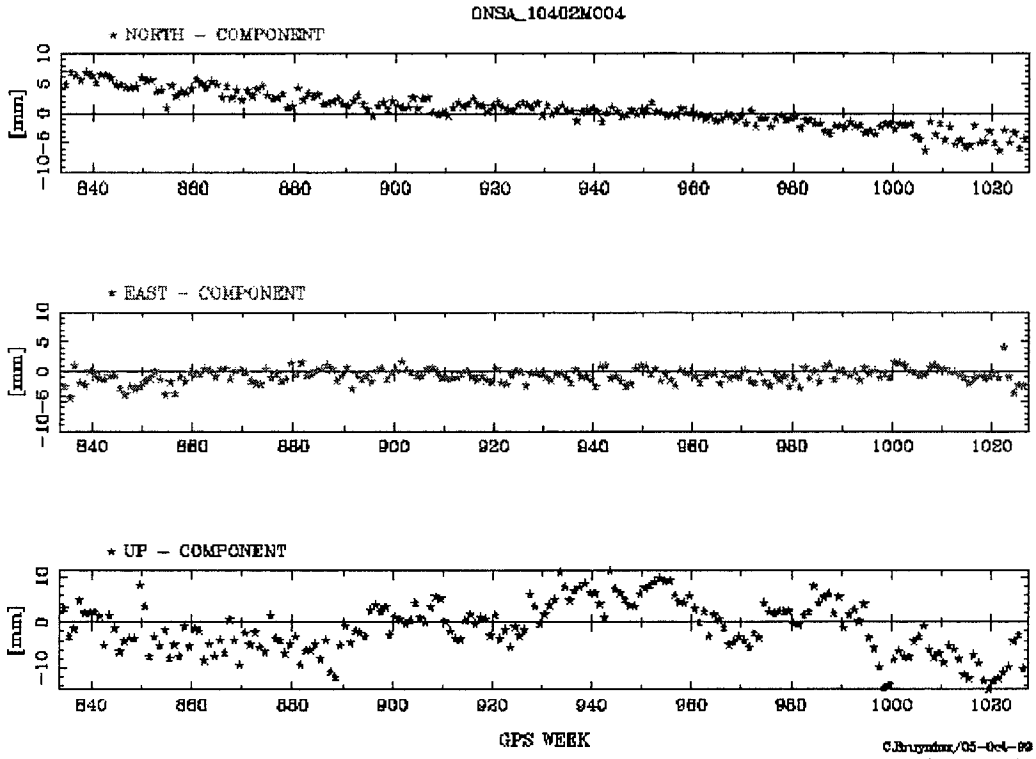

Figure 2: North, East, and Vertical time series for the Onsala (ONSA) site on the Swedish West Coast. The time series cover the time period January 1996 to September 1999, corresponding to GPS week 834-1027 (from http://homepage.oma.be/euref/series/onsa.html).

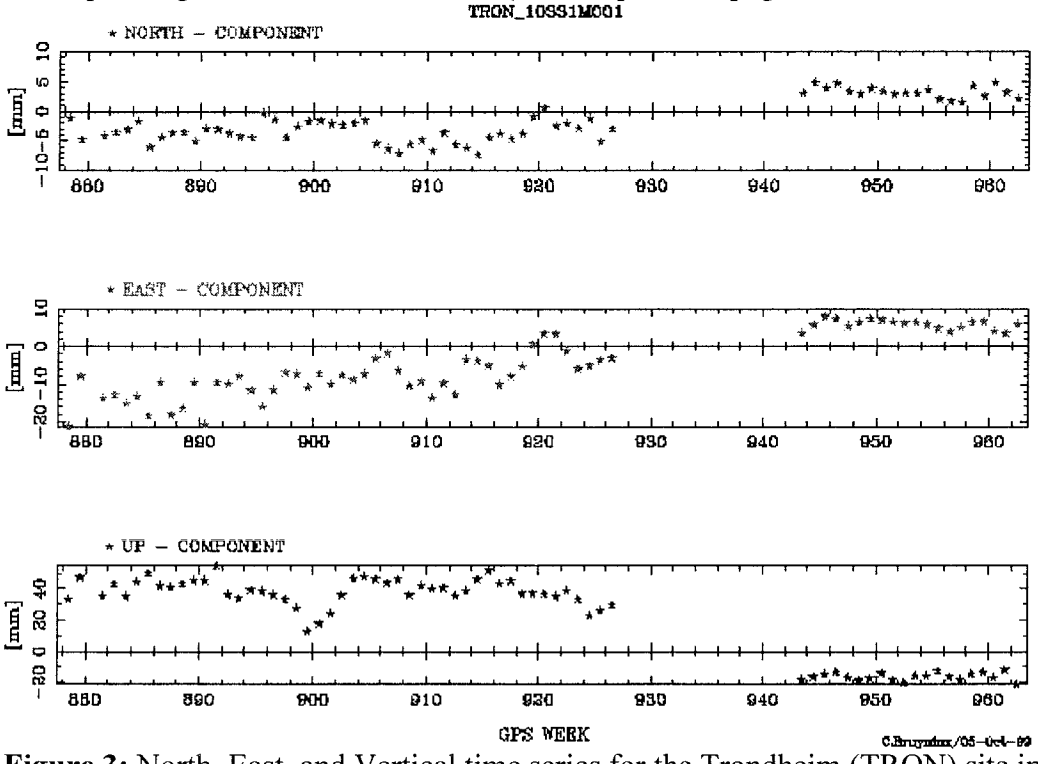

Figure 3: North, East, and Vertical time series for the Trondheim (TRON) site in Norway. The time series cover the time period November 1996 to September 1998, corresponding to GPS weeks 878-963. A clear jump is evident at the time when the antenna was change from a Trimble geodetic antenna to a choke-ring antenna (GPS week 943). In GPS week 964, the station was disrupted in order to re-arrange the mounting of the antenna (from http://homepage.oma.be/euref/series/tron.html).

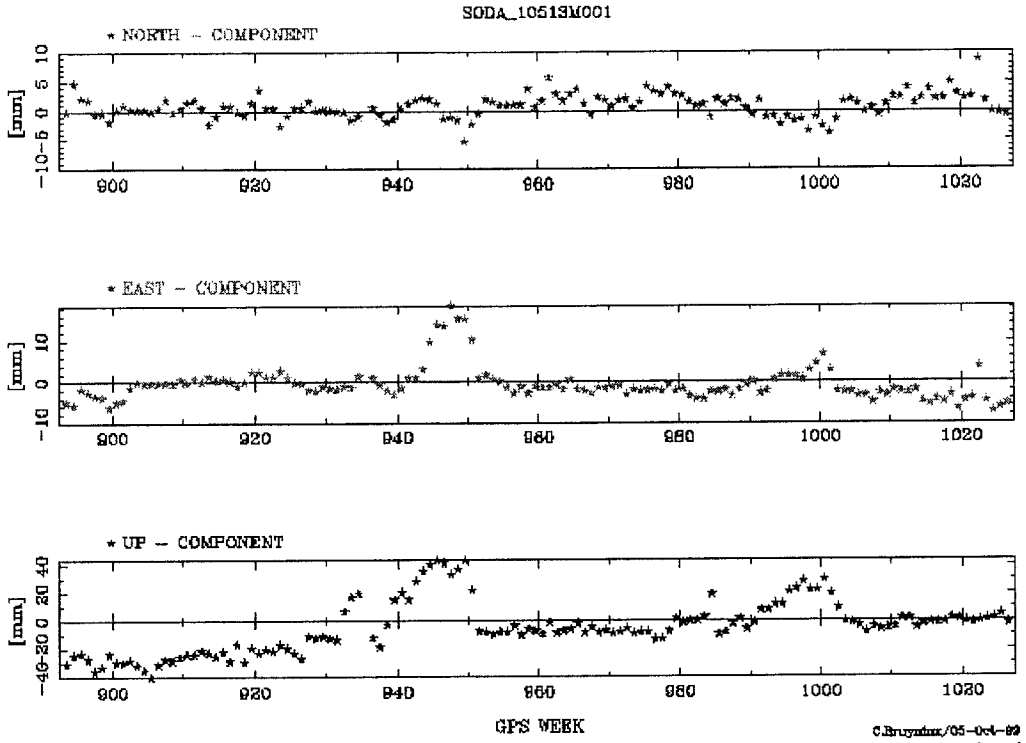

Figure 4: North, East, and Vertical time series for the Sodankylä (SODA) site in northern Finland. The time series cover the time period February 1997 to September 1999, corresponding to GPS week 894-1027. The results obtained during winter months appear to have more noise. This is most likely associated with snow accumulation on top of the antenna/pillar system (from http://homepage.oma.be/euref/series/soda.html).

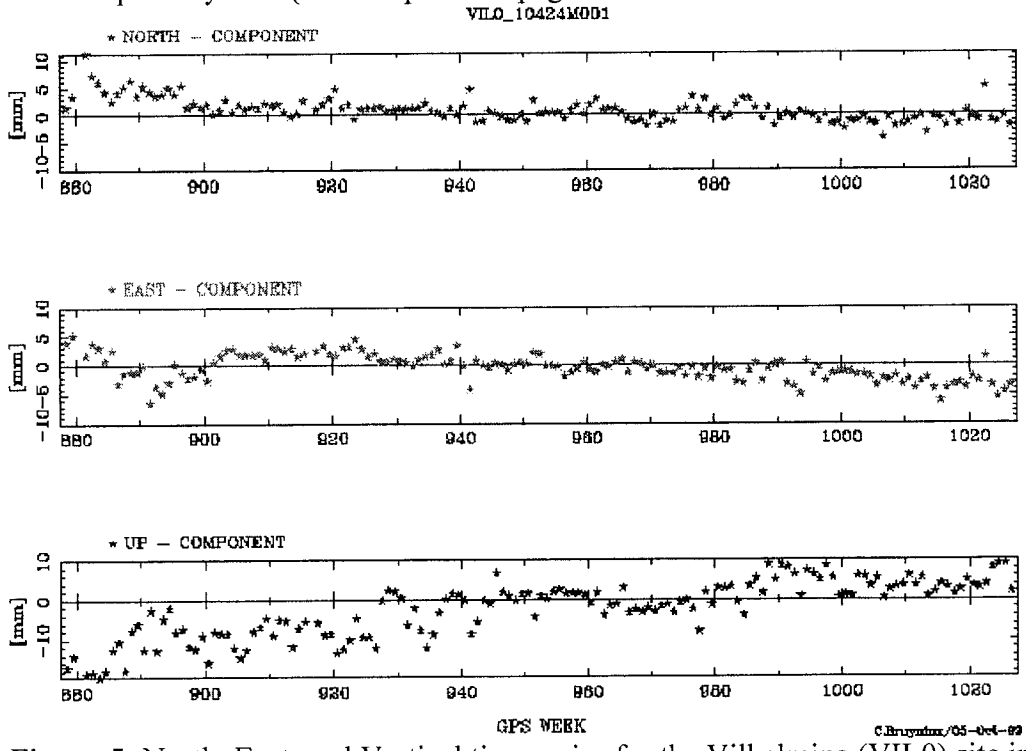

Figure 5: North, East, and Vertical time series for the Vilhelmina (VIL0) site in northern Sweden. The time series start in November 1996 and end in September 1999, corresponding to GPS week 878-1027. The results obtained during winter months appear to have more noise. This is most likely associated with snow accumulation on top of the antenna/pillar system. The up component indicates a trend that might be associated with land uplift.

Problems regarding the Estimation of Tropospheric Parameters in connection with the Determination of New Points in SWEREF 93

Jonas Ågren[1]

Abstract

Since 1995 the National Land Survey of Sweden has determined new points in SWEREF 93 relative to the SWEPOS stations. In the same year it was discovered that the estimated height of the new points depended considerably on the elevation cut off angle, when zenith tropospheric parameters were used. Because the estimation of these parameters obviously becomes disturbed by some kind of systematic difference in elevation dependent phase center variations (PCV) between a Dorne Margolin T on a tripod and the same antenna at a SWEPOS station, the decision was made in 1995 not to estimate tropospheric parameters.

This paper presents some investigations made by the National Land Survey to study this problem. It is found that the fibre-glass radomes used at the SWEPOS stations in 1995 and the first half of 1996, changed the elevation dependence of the phase center for the SWEPOS antennas. When these radomes were replaced by a plexiglass radomes, the distinct dependence of the height on the elevation cut off angle disappeared. On these reasons, tropospheric parameters have been estimated in the determination of new points in SWEREF 93, ever since the old fibre-glass radomes were removed.

1. Introduction

The Swedish network of permanent reference stations, SWEPOS, consists of 21 stations evenly distributed over Sweden. The average distance between the stations is approximately 200 km. The coordinates of the SWEPOS stations were determined in the GPS-campaign DOSE 93, and defines the Swedish reference system SWEREF 93.

Each SWEPOS station, with the exception of Onsala, is equipped with a Dorne Margolin T antenna from Turbo Rouge or with the counterpart from Ashtech (700936). Because these two antennas have been found to be very similar (Rothacher and Mader, 1996), Ashtech 700936 will always be called Dorne Margolin T in this report. In Onsala a Dorne Margolin B is used. The antenna is mounted on a metallic plate on top of a pillar, which for most of the stations is three meters high. Originally the antennas were covered by a Delft radome, which was mounted on a metallic cylinder. In the daily estimates of site positions made by Onsala Space Observatory, it could be seen that the vertical component for some of the stations varied several centimetres during the winter season. These jumps were suspected to be caused by snow accumulation on the radomes and on top of the pillar beside the antenna (Jaldehag, et al., 1996a). For that reason new conical radomes of fibre-glass were manufactured to replace the Delft radomes. These radomes not only covered the antenna, as before, but also completely covered the upper part of the pillar. The fibre-glass radomes were installed in the beginning of 1995. See Hedling and Jonsson (1996).

Since 1995, the National Land Survey of Sweden has determined new points in SWEREF 93. In the beginning, the main reasons for this densification were to study the quality of the Swedish national triangulation network RT 90 and to be able to improve the transformation between RT 90 and SWEREF 93. Today, the new points in SWEREF 93 are supposed to be used to compute transformations between various local systems and SWEREF 93.

To determine the new points in SWEREF 93, the following strategy is used: One point at a time is measured in 48 hours with the antenna on a tripod. In the beginning of 1995 an Ashtech Geodetic (700228) antenna was used, but after the summer 1995 this antenna was replaced by a Dorne Margolin T. The new SWEREF 93 point is determined relative to the eight closest SWEPOS stations. The processing is done in the Bernese Software, using precise orbits from CODE. Approximately 90 % of the ambiguities are solved. The final adjustment is made using the ionospheric free linear combination (L3) with one station held fixed. As a final step, the whole solution is transformed to SWEREF 93, using a 7-parameter Helmert transformation.

During 1995, an elevation cut off angle of 20 degrees was used. At the beginning of this year, however, it was discovered that when tropospheric parameters were estimated, the vertical component differed a couple of centimeters, depending on if 15 or 20 degrees was used as elevation cut off angle. Further studies showed that the estimated height differed as much as 6 - 10 cm, when the elevation cut off angle was changed from 10 to 25 degrees. The horizontal position was only affected by a few millimeters. When no tropospheric parameters were estimated, no such distinct dependence of the height could be observed. It seems like the estimation of tropospheric parameters becomes disturbed by some kind of difference

[1] Jonas Ågren; National Land Survey, S 801 82 Gävle, Sweden; Tel: +46 26 63 38 81; Fax: +46 26 61 06 76; E-mail: jonas.agren@lm.se.
Some of the tests presented have been made by Lars Harrie, who used to work at the National Land Survey (cf. Harrie, 1996). It is not pointed out which tests that were made by him.

in elevation dependent phase center variations (PCV) for the antennas involved and that this disturbance is different for different elevation cut off angles (cf. Rothacher, et al., 1995).

Sadly enough, this dependence on the elevation cut off angle did not disappear when the antenna type was changed from Ashtech Geodetic to Dorne Margolin T. Even though the same antenna type was used for all stations, the estimated height varied as before with the elevation cut off angle.

In this case it is not possible, without further ado, to be sure that there is not any systematic error involved for some specific elevation cut off angle. For this reason, it was decided in 1995 not to estimate tropospheric parameters, when new points are computed in SWEREF 93. Of course, the unmodelled part of the troposphere will result in an error in the height component in this case, but because the observation time is as long as 48 hours, and the new point is determined using as many as eight SWEPOS stations, this error can be suspected to become less than 3 - 4 centimetres, which has also been confirmed by a number of tests. However, if no tropospheric parameters are estimated, we do not risk that deviating elevation dependent PCV of different antennas will be interpreted as troposphere, which might result in a large systematic error (cf. Harrie, 1996). See further section 2.

In Jaldehag, et al. (1996b), elevation angle dependent errors are studied, which cause a dependence of the estimated height on the elevation cut off angle. They conclude that a large part of these errors seems to be caused by scattering from the pillar or from the devices mentioned above, which are used to mount the antenna and the radome. Thus, it is possible that this scattering effect might cause different elevation dependent errors on different SWEPOS stations and that the scattering is different for a Dorne Margolin T on a tripod and the same antenna type on a SWEPOS pillar.

Another possibility was suggested by Dr Jan M. Johansson at the Onsala Space Observatory. In the daily processing of the SWEPOS network with the Gipsy software, he could see that the residuals showed a clear dependence on the elevation angle, which was different for different SWEPOS stations. He suspected that the major part of this difference probably is caused by the fibre-glass radomes. Of course, it might also be effected by the metallic plate and the metallic cylinder used to mount the Delft radome. The latter was not removed on all stations when the Delft radomes were exchanged to the fibre-glass radomes.

For this reason it was decided that the fibre-glass radomes would be changed to a another type. So, in June 1996 they were removed and new ones took their place in October the same year. In connection with this, the redundant metallic cylinder was taken away. During June 1996 extensive tests were made by Jan Johansson with different types of radomes. On the basis of the results of these, the new radomes are made of plexiglass and are spherical over the antenna, with a conical collar covering the upper part of the pillar. The latter feature is supposed to prevent snow from accumulating around the antenna on top of the pillar. According to Jan Johansson the new radomes do not affect the phase pattern in the same way as the old ones apparently did. According to him, all of the SWEPOS stations now have almost the same elevation dependence pattern. One question that might be asked at this point, is whether the different SWEPOS stations have a similar elevation dependence of the phase center as a Dorne Margolin T on a tripod.

This paper presents some of the results from the investigations made of this problem by the National Land Survey of Sweden. The main purpose of the tests have been to find out whether it was the fibre-glass radome that caused the troubles, and to investigate whether it is safe to estimate trophospheric parameters in the determination of new points in SWEREF 93, when SWEPOS is equipped with the new plexiglass radomes.

This have been tested both with computations with different elevation cut off angles and by a number of antenna calibrations, where parameters for the elevation dependent PCV have been estimated in the Bernese Software. The latter tests were performed to show how the different radomes affect the elevation dependence of the phase center for a Dorne Margolin T antenna at a SWEPOS station. Because of the limited space in this paper, only a selection of the tests made are presented. The other tests show similar results though.

2. The effect of different elevation dependent PCV on the estimated relative height

The difference in elevation dependent phase center variations (PCV) between different antennas might cause an error in the vertical component. This error becomes larger in the case when the ionospheric free linear combination (L3) is used. If tropospheric parameters are estimated, the elevation dependence of the phase center might be interpreted as troposphere and cause a systematic shift in both the height and the tropospheric parameters (Rothacher, et al, 1995). This will cause an amplification of the resulting height error, compared to when no tropospheric parameters are used. This error will be similar for all baseline lengths.

When tropospheric parameters are estimated, a difference in elevation dependence of the phase center between two antennas is probable to amplify the height error more for higher elevation cut off angles. This can be motivated as follows. Imagine that the height of point B is going to be determined relative to another point A, which is kept fixed in the adjustment. We further assume that no horizontal coordinates are to be estimated. If a tropospheric parameter

T is estimated for point B only, the double difference observation equation will look like this:

$$\lambda + v = \left(\frac{1}{\cos z_1} - \frac{1}{\cos z_2}\right) \cdot dT - \left(\cos z_1 - \cos z_2\right) \cdot dH = A_1 \cdot dT + A_2 \cdot dH$$

where z_1 and z_2 are the zenith distances for the two satellites in the double difference. If we assume that the reference satellite 1 has the zenith distance $z_1 = 30°$, the coefficients A_1 and A_2 will have the following values, depending on z_2:

z_2	A_1	A_2
5	0.15	0.13
10	0.14	0.12
15	0.12	0.10
20	0.09	0.07
25	0.05	0.04
30	0	0
35	-0.07	-0.05
40	-0.15	-0.10

z_2	A_1	A_2
45	-0.26	-0.16
50	-0.40	-0.22
55	-0.59	-0.29
60	-0.84	-0.36
65	-1.21	-0.44
70	-1.77	-0.52
75	-2.71	-0.61
80	-4.60	-0.69

Table 2.1 The dependence of A_1 and A_2 on z_2. $z_1 = 30°$.

Similar values for the two columns in the design matrix result if different values for z_1 is chosen. The important thing to notice in table 2.1 is that A_1 and A_2 are very similar for small zenith distances, while A_1, but not A_2, becomes much bigger for the largest ones. Thus, the higher the elevation cut of angle is set, the more dependent the two columns in the design matrix become, which means that the estimation of the height and the tropspheric parameter will be more unstable for higher elevation cut off angles. Now, let us assume that there is a difference in the elevation dependence of the phase center between the two antennas at A and B. The resulting elevation dependent error is likely to be taken care of by a systematic shift in both dH and dT (with opposite signs), in such a way that the residuals become small according to the least square theory. What prevents this shift in dH and dT is the fact that A_1 gets larger for satellites on lower elevations. When the elevation cut off angle increases, the values for A_1 decreases for the lowest elevations, which means that the systematic shift might be larger.

Exactly how a specific difference in elevation dependence will disturb the estimation of tropospheric parameters is hard to say. That a difference in elevation dependent PCV might cause a large height error even for low elevation cut off angles, can be seen from the following test, where it is also clear that the height error increases rapidly when the elevation cut off angle is set to higher values.

An Ashtech 700718 antenna was mixed with the Dorne Margolin T at the SWEPOS station in Mårtsbo. The latter was equipped with a plexiglass radome. The Ashtech antenna was placed at the point SIB 1, situated about 100 m from the SWEPOS station. The height difference between these two points is known at the mm-level. Observations for 2×24 hours were used.

To see how these two antennas differ in the elevation dependence of the phase center, an antenna calibration was performed in the way that is described in Rothacher et al. (1995, 1996). No rotation of the antennas was made. The SWEPOS station was chosen as a reference and the official IGS model for Dorne Margolin T was used for this antenna, which means that the parameters for different elevations were set to zero for all elevations. As a first step, mean value offsets were estimated (L1 and L2) for the Ashtech antenna, using an elevation cut off angle of 15 degrees, without any modelling of the elevation dependent PCV for this antenna. After that, parameters for the elevation dependence of the phase center (piece-wise linear function), were estimated for L1 and L2, applying the estimated offsets. In fig. 2.1 the elevation dependent PCV for this antenna is shown for L1, L2 and L3.

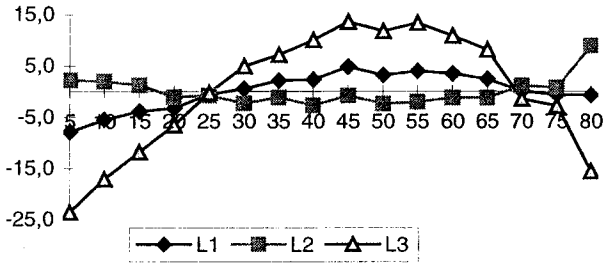

Fig. 2.1 Elevation dependence of the phase center in mm for a Ashtech 700718 relative to the SWEPOS station in Mårtsbo (Dorne Margolin T)

Here it can be seen that the elevation dependent PCV for the Ashtech antenna differs considerably from the Dorne Margolin T at the SWEPOS station and how this difference is magnified when the L3 combination is used.

To see how the difference in elevation dependent PCV affects the estimated height for different elevation cut off angles, the height for SIB 1 was estimated relative to the SWEPOS station. This was done with and without tropospheric parameters, using the ionospheric free linear combination L3. In the case with tropospheric parameters, one parameter every 24 hour session was estimated for one of the stations (SIB 1). No parameters for the elevation dependence of the phase center were used. The mean values of the two 24 hour sessions are presented in Table 2.1.

Cut off angle	Trop.		No trop.
	H	Tr. par.	H
10	56	-16	-14
15	94	-28	0
20	139	-47	16
25	175	-64	25

Table 2.1 Errors in mm for the height and the tropospheric parameter for different elevation cut off angles.

In this test, the estimated height depends a lot on the elevation cut off angle. This dependence is much more pronounced when tropospheric parameters are estimated. It is also interesting to notice that the different elevation dependence of the phase center for the Ashtech antenna causes such a large systematic shift in both the tropospheric parameter and the height (cf. Rothacher, et al., 1995).

Results such as this support the decision not to estimate tropospheric parameters when a distinct dependence of the height on the elevation cut of angle is present. This dependence indicates, that an elevation dependent error disturbs the estimation of tropospheric parameters at least for some elevation cut off angles. In this case there is no guarantee that a systematic shift is not involved for a cut off angle of 15 or 20 degrees.

3. Tests with different elevation cut off angles

As was mentioned in the introduction, Jan Johansson found that the fibre-glass radomes induced some kind of elevation dependent error for the SWEPOS antennas, which was different for different stations. In order to investigate, whether the distinct dependence of the height on the elevation cut off angle is caused by these radomes, a number of tests with different cut off angles have been made, with different radomes at the SWEPOS stations. It has also been tested if there is some kind of systematic difference between a Dorne Margolin T on a tripod and the same antenna type on a SWEPOS pillar and if the new plexiglass radomes cause a similar effect as the former type.

For all the tests presented below, the procedure described in the introduction has been used for the processing. When tropospheric parameters have been estimated, four parameters every 24 hours have been utilised for all stations. Furthermore, the horizontal components have only been affected a few millimeters, when the cut off angle has been changed. For this reason, only the results for the height component are presented. In all the tests the estimated heights have been compared to known coordinates in SWEREF 93.

What is studied in this section is what caused the large dependence of the height on the elevation cut off angle. Even though there is no difference in the elevation dependent PCV between the different antennas, the height might vary a bit for different cut off angles. One reason for this is that the troposphere is not correctly modelled by the mapping function (1/cosz), especially below 20 degrees.

In the introduction it was mentioned, that in 1995 the estimated height of a new SWEREF 93 point differed significantly for different elevation cut off angles, when tropospheric parameters were estimated. To find out if there is a systematic error involved, even for the lower cut off angles, the point SIB 1, close to the SWEPOS station Mårtsbo, was measured in 2x24 hours with a Dorne Margolin T on a tripod. Since this point participates in the precision network, surrounding the SWEPOS station, it has known coordinates in SWEREF 93 at the mm-level. The SWEPOS station in Mårtsbo was not used in the processing. At the time for this test, all the SWEPOS stations were equipped with fibre-glass radomes.

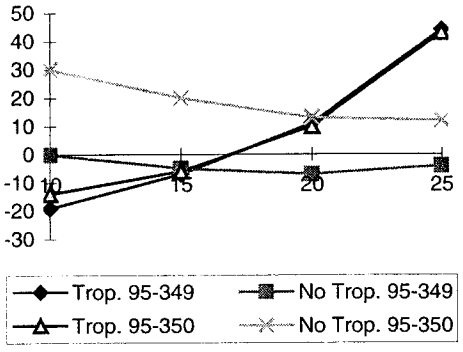

Fig. 3.1 Height error in mm for different elevation cut off angles. SIB 1 with the antenna on a tripod. Fibre-glass radomes at all SWEPOS stations.

The result shows a quite typical dependence of the height on the cut off angle, even though the dependence has been larger for other points, which have been determined relative to other SWEPOS stations. It seems like the estimated height is not shifted in a systematic way for the cut off angle 15 degrees. It can further be observed that the height does not depend that much on the cut off angle, when no tropospheric parameters are estimated. Not surprisingly, the height differs more between the two sessions, when no tropospheric parameters are estimated.

To find out if the fibre-glass radomes induce a similar elevation dependence of the phase center at all SWEPOS stations, two cut off angle tests were made, where the SWEPOS stations in Mårtsbo and Jönköping were determined relative to the surrounding SWEPOS stations, in the same way as in the determination of a new point in SWEREF 93. If the elevation dependent PCV is similar at all SWEPOS stations, it can be suspected that the estimated heights in these cases do not depend on the elevation cut off angle. For Jönköping, 2x24 hours of observations were used, while only 24 hours were utilised for Mårtsbo. All involved SWEPOS stations had a fibre-glass radome at the time of these tests.

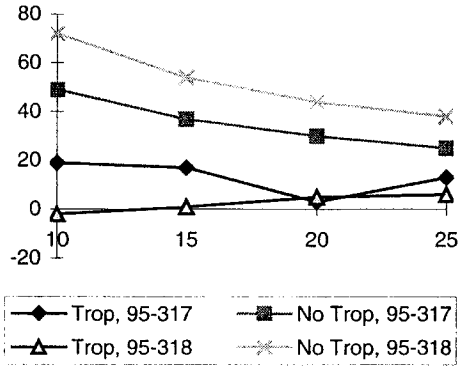

Fig 3.2 Height error in mm for different elevation cut off angles. The SWEPOS station in Jönköping. All involved stations have a fibre-glass radome.

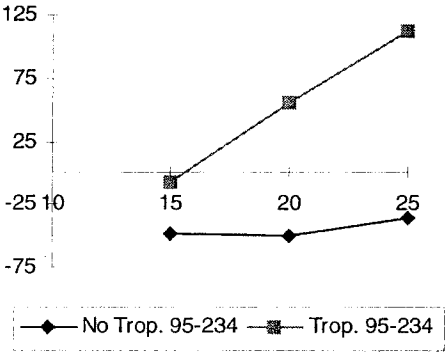

Fig 3.3 Height error in mm for different elevation cut off angles. The SWEPOS station in Mårtsbo. All involved stations have a fibre-glass radome.

These tests show that the dependence of the height on the cut off angle is very small in Jönköping, when tropospheric parameters are estimated. Thus, it seems like all the involved stations have a similar elevation dependence of the phase center in this case. However, this can not be said of the result from Mårtsbo. The dependence is very large and even more pronounced than what is usual for a point with an antenna on a tripod. These results seem to show, that some of the SWEPOS stations have a quite similar elevation dependent PCV, while others differ significantly from the rest of them. This is in accordance with what Jan Johannson observed from the daily processing.

That the fibre-glass radome seems to cause the dependence of the height on the elevation cut off angle, is supported by the following test. The SWEPOS station in Mårtsbo was again computed for 2×24 hours, but this time the fibre-glass radome had been removed from that station. All the other SWEPOS stations involved were still equipped with the fibre-glass radome, though.

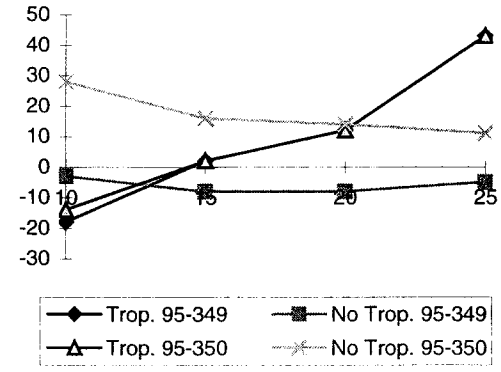

Fig 3.4 Height error in mm for different elevation cut off angles. The SWEPOS station in Mårtsbo without a radome. All other stations have a fibre-glass radome.

The result from this test is very similar to the result from the computation of the SIB 1 point in fig. 3.1. It seems like the SWEPOS station in Mårtsbo now behaves almost like a Dorne Margolin T on a tripod. This makes it probable that it is the fibre-glass radome that causes the dependence of the height on the elevation cut off angle.

This conclusion is further confirmed by the following test. When the fibre-glass radomes were removed in the middle of the summer 1996, some stations kept their radomes for a while. During that time, the SWEPOS station in Umeå was determined, both when it had a radom and when its radome had been taken away. In these tests all the other SWEPOS stations did not have a radome. Observations for 3×24 were used in both of the cases.

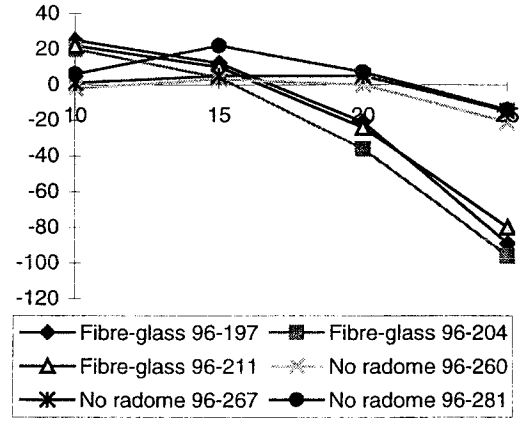

Fig. 3.5 Height error in mm for different elevation cut off angles. The SWEPOS station in Umeå with and without the fibre-glass radome. Tropospheric parameters only.

Here it is very clear, that the fibre-glass radome in Umeå causes a large dependence of the height on the elevation cut off angle. When that radome is removed, the height

shows no such distinct behaviour. Thus, it is obvious, that the fibre-glass radomes to a large extent are responsible for this dependence.

Another question that might be asked, is whether the new plexiglass radomes induce a similar height dependence on the cut off angle as the fibre-glass counterpart. To test this, the SWEPOS station Leksand, with and without a new radome, was determined relative to the surrounding SWEPOS stations, which all were free from coverage. Observations for 3×24 hours were used both when Leksand had a new radome and when it was without one.

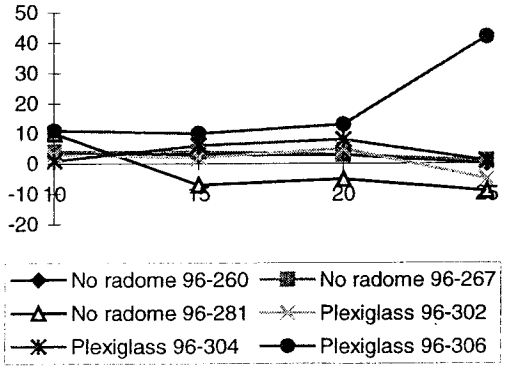

Fig 3.6 Height error in mm for different elevation cut off angles. The SWEPOS station in Leksand with and without the plexiglass radome. Tropospheric parameters only.

In large, this test confirms that the plexiglass radome does not cause any distinct dependence on the elevation cut off angle, even though for the last session, the height error gets quite large for an elevation cut off angle of 25 degrees.

However, it is still possible, that there is systematic difference between the SWEPOS stations and Dorne Margolin T on a tripod. Because the latter case is of utmost importance in the determination of new points in SWEREF 93, a test have been made, where the SIB 1 point used above (cf. Fig 1) was determined relative to SWEPOS stations equipped with the new plexiglass radomes. Observations for 2×24 hours were used.

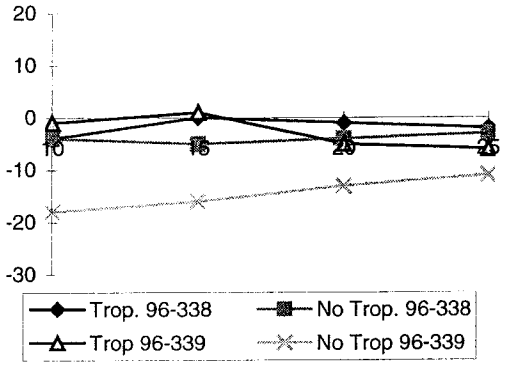

Fig. 3.7 Height error in mm for different elevation cut off angles. SIB 1 with the antenna on a tripod. Plexiglass radomes at all SWEPOS stations.

Compare this result with the result in fig 3.1. It is not possible to see any dependence of the height on the elevation cut off angle.

So far we have seen that the fibre-glass radomes have caused a distinct dependence of the height on the elevation cut off angle, which disappears when radomes are absent from the SWEPOS stations and when the plexiglass type is used.

Furthermore, there does not seem to be a systematic difference between a Dorne Margolin T an a tripod and a the same antenna type on a SWEPOS pillar. Of course, there might still be some deviating elevation dependence of the phase center between the different SWEPOS stations and between a SWEPOS station and a Dorne Margolin T on a tripod, caused for example by multipath, scattering or other disturbances. The importance of these tests, however, is that the very distinct dependence on the elevation cut off angle obviously has disappeared with the fibre-glass radomes.

4. Estimation of parameters for the elevation dependent PCV for different radomes

To study how the elevation dependent PCV of a SWEPOS station changes because of the different radomes, three antenna calibrations were performed in Mårtsbo The SWEPOS station was equipped first with the old fibre-glass radome, then with no radome at all, and finally with the new plexiglass device. In these three cases, the elevation dependence of the phase center was estimated relative to a Dorne Margolin T antenna, which was acting as reference. For the first calibration the reference antenna was placed on another pillar 6 meters away from the SWEPOS station. For the second and the third, the same antenna was put on a tripod at the SIB 1 point previously mentioned. This point is situated about 100 m from the SWEPOS station. In all cases the difference in height was known at the mm-level. Some uncertainty exists, though, in the measuring of the antenna height in calibration two and three.

The calibrations were performed as described in Rothacher et al. (1995,1996). No rotation of the antennas was done. For the reference antenna, the official IGS model was utilised, with the parameters for the elevation dependence set to zero for all elevations.

As a first step, the mean phase center offsets were estimated for L1 and L2 for the SWEPOS antenna with an elevation cut off angle of 15 degrees. In none of the cases, the difference from the IGS values was larger than 1-2 mm. For this reason, the estimation of elevation parameters for the SWEPOS station was done with the official IGS values

for the offsets. To model the elevation dependent PCV, a piece-wise linear function was used.

For the three cases, the estimated parameters for the elevation dependence of the phase center are presented in fig. 4.1, 4.2 and 4.3. In case one, only 24 hours of observation were used, while 2x24 hours were taken in case two and three. For the two 24 hour sessions the repeatability between the two days was very high, so only the mean values are presented. To see how the elevation dependence pattern become amplified, when the L3 combinations is used, the L3 pattern is also plotted.

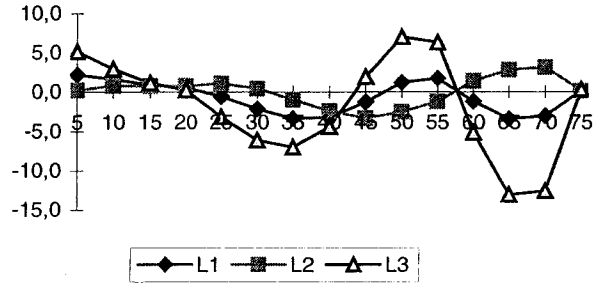

Fig. 4.1 Elevation dependent PCV in mm for the SWEPOS station Mårtsbo with a fibre-glass radome. Relative to Dorne Margolin T .

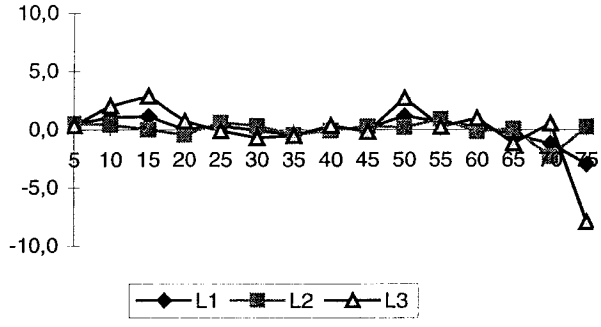

Fig 4.2 Elevation dependent PCV in mm for the SWEPOS station Mårtsbo without radome. Relative to Dorne Margolin T on a tripod.

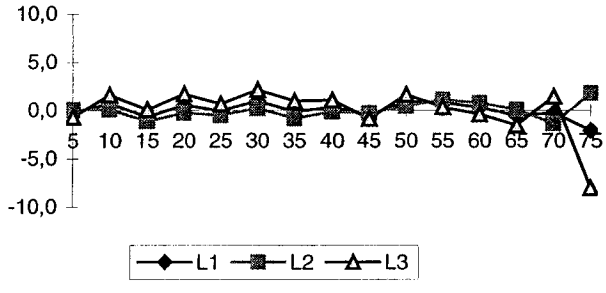

Fig 4.3 Elevation dependent PCV in mm for the SWEPOS station Mårtsbo with a plexiglass radome. Relative to Dorne Margolin T on a tripod.

These results show that the old fibre-glass radome in Mårtsbo affected the elevation dependence of the phase center quite heavily. If the estimated model in this case is used for the computation of the test presented in fig 3.3, the result is almost the same as when the radome was removed in Mårtsbo (cf. Fig. 3.4). It can further be seen that elevation pattern is similar in case two and three, which means that the new plexiglass radome does not seem to change the elevation dependence of the phase center in any significant way.

It can also be observed that the elevation dependent PCV is quite similar between a Dorne Margolin T on a tripod and the same antenna at the SWEPOS station in Mårtsbo (case 2 and 3), even though there is a difference for the lowest elevations. It is likely that this difference can be explained by multipath. The SWEPOS station is situated very close to Mårtsbo observatory, with a lot of possible "reflectors". Of course, this is not the only explanation of this deviation.

Finally, the following computations were made with the same data as in the calibration above. The height of the Dorne Margolin T not at the SWEPOS station was determined relative to the SWEPOS station in Mårtsbo. This was done without applying any parameters for the elevation dependence of the phase center. The height was computed for different elevation cut off angles with the L3 combination, both with and without tropospheric parameters (one parameter per 24 hour session for one of the two stations only). The results are presented in table 4.1, 4.2 and 4.3, which correspond to fig 4.1, 4.2 and 4.3.

Cut off angle	Trop.		No trop.
	H	Tr. par.	H
15	0	4	13
20	-53	26	16
25	-74	36	5

Table 4.1 Errors in mm. Relative to the SWEPOS station in Mårtsbo with a fibre-glass radome

Cut off angle	Trop.		No trop.
	H	Tr. par.	H
15	-9	4	4
20	-2	1	1
25	-1	0	1

Table 4.2 Errors in mm. Relative to the SWEPOS station in Mårtsbo without a radome

Cut off angle	Trop.		No trop.
	H	Tr. par.	H
15	-5	4	7
20	5	-1	3
25	-4	4	4

Table 4.3 Errors in mm. Relative to the SWEPOS station in Mårtsbo with plexiglass radome

As in section 3, the estimation of tropospheric parameters becomes disturbed by the fibre-glass radome, but in the other cases the results look promising.

5. Conclusion

The results in section 3 and 4 have shown quite clearly, that it was the old fibre-glass radomes that caused the distinct dependence of the vertical component on the elevation cut off angle in the case tropospheric parameters were estimated. These radomes seem to have affected the elevation dependence of the phase center rather similar for most of the SWEPOS stations, while some of the radomes, e.g. in Mårtsbo, obviously were deviating from the rest. The last remark is in accordance with Jan Johansson's observation, that the residuals for some of the SWEPOS stations showed a deviating dependence on the elevation angle from the rest. That the radomes differed from each other, can be explained by a careless manufacturing. The mould that was used to cast the radomes, was not cleaned properly between the making of the different radomes. The tests further show, that the new radomes do not affect the height in the same way. According to the tests, no significant difference in the elevation dependent PCV exists between a SWEPOS station with a plexiglass radome and a Dorne Margolin T on a tripod and it has not been possible to see a distinct dependence of the estimated height on the elevation cut off angle in this case.

On these grounds, it was decided that tropospheric parameters can be estimated, when new points are determined in SWEREF 93. So, since June 1996, all new points have been computed using eight tropospheric parameters every 24 hour session for all stations. The elevation cut off angle has been set to 15 degrees.

References

G. Hedling and B. Jonsson (1996). New developments in the SWEPOS network. Proceedings of ION GPS-96, pp. 1803 - 1808.

L. Harrie (1996). Automation of Bernese and determination of new Points in SWEREF 93. Unpublished report at the National Land Survey, Sweden.

R.T.K. Jaldehag, Jan M. Johansson, James L. Davis and Pedro Elósegui (1996a). Geodesy using the Swedish permanent GPS network: Effects of snow accumulation on estimates of site positions. Geophysical Research Letters, Volume 23, No. 13, June 15, 1996.

R.T.K. Jaldehag, J. M. Johansson, B.O Rönnäng, P. Elósegui, J.L. Davis, I.I. Shapiro and A.E. Neil (1996b). Geodesy using the Swedish permanent GPS network: Effects of signal scattering on estimates of relative site positions. J. Geophys. Res., Vol. 101, No. B8, August 10, 1996.

M. Rothacher and G. Mader (1996). Combination of Antenna Phase Center offsets and Variations.

M. Rothacher, S. Schaer, L. Mervart, G. Beutler (1995). Determination of Antenna Phase Center Variations using GPS data. Paper presented at the 1995 IGS Workshop, Potsdam, Germany, May 15 - 17, 1995.

M. Rothacher, L. Mervart, G. Beutler, E. Brockmann, S. Fankhauser, W.Gurtner, J. Johnsson, S. Schaer, T. Springer, R.Weber (1996). Manual for Bernese GPS Software Version 4.0. Astronomical Institute University of Berne.

The ionospheric problem in GPS phase ambiguity resolution and some possible solutions

by

Lars E. Sjöberg
Royal Institute of Technology
Department of Geodesy and Photogrammetry
S-100 44 STOCKHOLM, SWEDEN
Tel: +46 8 7907330
Fax: +46 8 7907343
Email: sjöberg@geomatics.kth.se

Abstract

It is a well-known fact that the ionospheric bias is a major source to impair long baseline determination by GPS. Generally, this bias is significant for baselines ranging from, say, 10 km and up, implying that the needed time for GPS phase ambiguity resolution is considerably increased. On the other hand, the correct resolution of the integer ambiguities is the key to precise positioning.

A common way to resolve the integer ambiguity for long baselines is to make use of the rather easily resolved widelane ambiguity in combination with the so-called ionosphere-free linear combination of phase observables. We show that this method can easily be replaced by a least squares combination that is about 1.5 times more efficient.

As an alternative to the above unbiased estimators we demonstrate a biased estimator called the Restricted Best Linear Estimator (RBLE). The RBLE is a compromise between the ionospheric bias and the observation noise.

Finally, we dwell upon the hypothetical disposal of a third GPS frequency, in which case the ionospheric bias might be efficiently eliminated for a proper choice of the frequency.

1. Introduction

For short baselines GPS phase ambiguities can be successfully resolved in a very short time from dual frequency phase and code data. In one way or another such methods rely on the accurately and reliably determination of the widelane ambiguity (N_w). For references, see e.g. Sjöberg (1996) and Almgren (1998). Also for long baselines N_w can be rather easily resolved, but the remaining problem to separate the original ambiguities (N_1 and N_2) becomes a hard task, in particular due to a generally significant ionospheric bias. This paper addresses this problem, and some possible solutions to it.

2. The observation equations and their solutions

The four observation equations for dual frequency phase ($\tilde{\ell}_1$ and $\tilde{\ell}_2$) and code ($\tilde{\ell}_3$ and $\tilde{\ell}_4$) data were first presented by Melbourne (1985):

$$u + \lambda_1 N_1 - \mu / f_1^2 = \tilde{\ell}_1 - \varepsilon_{11}$$

$$u + \lambda_2 N_2 - \mu / f_2^2 = \tilde{\ell}_2 - \varepsilon_{12}$$

$$u + \mu / f_1^2 = \tilde{\ell}_3 - \varepsilon_{21}$$

$$u + \mu / f_2^2 = \tilde{\ell}_4 - \varepsilon_{22} \ ,$$

where ε_{11}, ε_{12}, ε_{21} and ε_{22} are random observation errors, $u = \rho + c\Delta\delta$ is the sum of satellite-to-receiver range (ρ) and satellite-receiver clock bias ($\Delta\delta$) times velocity of light (c), μ is ionospheric bias and λ_1 and λ_2 are carrier wavelengths on frequencies f_1 and f_2, respectively. These 4 equations include 4 unknowns, and the direct solution becomes (Melbourne, ibid, and Sjöberg, 1997 a, b)

$$\begin{aligned} \hat{N}_1 &= \tilde{\phi}_1 + g\tilde{P}_2 - h\tilde{P}_1 \\ \hat{N}_2 &= \tilde{\phi}_2 - g\tilde{P}_1 + h\tilde{P}_2 \ , \end{aligned} \qquad (2)$$

where

$$g = 2f_1f_2 / \left(f_1^2 - f_2^2\right) = 2\nu / \left(\nu^2 - 1\right)$$
$$h = \left(f_1^2 + f_2^2\right) / \left(f_1^2 - f_2^2\right) = \left(\nu^2 + 1\right) / \left(\nu^2 - 1\right)$$
$$\nu = \left(f_1 / f_2\right) = \lambda_2 / \lambda_1$$
$$\tilde{P}_1 = \tilde{\ell}_3 / \lambda_1, \tilde{P}_2 = \tilde{\ell}_4 / \lambda_2, \tilde{\phi}_i = \tilde{\ell}_i / \lambda_i \ ; \ i = 1,2 .$$

The standard errors of these estimates are 7.86 for the standard error 3 mm and 30 cm for phase and code observables, respectively. On the contrary, the widelane ambiguity estimate

$$\hat{N}_w = \hat{N}_1 - \hat{N}_2 = \tilde{\phi}_1 - \tilde{\phi}_2 - \frac{f_1 - f_2}{f_1 + f_2}\left(\tilde{P}_1 + \tilde{P}_2\right) \qquad (3)$$

has the corresponding modest standard error 0.25. This shows that the widelane ambiguity is relatively easily resolved independent of ionospheric bias and baseline length. Subsequently, the correctly resolved N_w can be used as a tool for separating N_1 from N_2, and a most successful procedure for short baselines ($BLUE_1$) with insignificant ionospheric bias has been outlined in Sjöberg (1996) and (1997 a, b) and further developed and implemented in Almgren (1998). In this case the standard error of N_1 and N_2 is of order 0.08! However, in case of significant ionospheric bias the Best Linear Unbiased Estimator ($BLUE_2$) of eqs. (1) with the constraint N_w=N_1-N_2 (= known) yields the pessimistic standard error 7.80 of N_1 and N_2 (Sjöberg, 1997 b, c and 1998 a), and many times more data is needed for a correct fixing of the ambiguities.

Summarizing, the $BLUE_1$, which assumes no ionospheric effects, works excellent for short baselines, but it will be biased for medium and long baselines. The $BLUE_2$, that eliminates the effect of the ionospheric bias, is to inefficient, or, the prize to eliminate the bias is too high. See Sjöberg (1997 c) and (1998a).

So how can we improve the estimation of the primary integer ambiguities under these circumstances? Below we discuss some possibilities.

3. A prior information on u: The ionosphere-free linear combination

The ionosphere-free linear combination of the phase observables $\tilde{\ell}_1$ and $\tilde{\ell}_2$ of the system (1) reads

$$\tilde{L}_3 = \frac{\tilde{\ell}_1 f_1^2 - \tilde{\ell}_2 f_2^2}{f_1^2 - f_2^2} , \qquad (4)$$

and it corresponds to the observation equation

$$\tilde{L}_3 = u + B_3 + \varepsilon_3 \ , \tag{5 a}$$

where

$$B_3 = \frac{f_1^2\lambda_1 N_1 - f_2^2\lambda_2 N_2}{f_1^2 - f_2^2} = \text{ the } L_3 \text{ ambiguity bias} \tag{5 b}$$

and

$$\varepsilon_3 = \frac{\varepsilon_{11} f_1^2 - \varepsilon_{12} f_2^2}{f_1^2 - f_2^2} \tag{5 c}$$

The equation (5 a) includes the unknowns u and B_3, and it is clear that the ionospheric bias has been eliminated. As in section 2 we may now take advantage of that the widelane ambiguity (N_w) is relatively easily fixed. Moreover, u can be regarded as approximately known. Hence, inserting

$$N_2 = N_1 - N_w \tag{6}$$

for a fixed widelane ambiguity into eq. (5 b) and taking advantage of (5 a), one obtains the solution for N_1:

$$\hat{N}_1 = \frac{\lambda_1 + \lambda_2}{\lambda_1\lambda_2}\left(\tilde{L}_3 - \hat{u}\right) + \frac{\lambda_1}{\lambda_2 - \lambda_1} N_w \ , \tag{7}$$

where $\hat{u}$ is the a priori estimate for u. The variance of $\hat{N}_1$ becomes {in accord with (5 c)}

$$\sigma^2_{\hat{N}_1} = \frac{\lambda_1^4 + \lambda_2^4}{(\lambda_1\lambda_2)^2(\lambda_1 - \lambda_2)^2}\sigma^2_{\phi\lambda} + \left(\frac{\lambda_1 + \lambda_2}{\lambda_1\lambda_2}\right)^2 \sigma^2_{\hat{u}} \ . \tag{8}$$

For $\phi = 19{,}0$ cm, $\lambda_2 = 24{,}4$ cm and $\sigma_{\phi\lambda} = 3$ mm we get

$$\sigma^2_{\hat{N}_1} = 0.052 + 5.218\left(\frac{\sigma_{\hat{u}}}{\lambda_2}\right)^2 \ . \tag{9}$$

To be able to fix the correct integer ambiguity, $\sigma_{\hat{N}_1}$ must not exceed, say, 0.3, implying that $\sigma_{\hat{u}}$ must not exceed 2.1 cm.

This method to take advantage of the ionosphere-free linear combination for long baselines as well as a priori information on the satellite-to-receiver range was extensively discussed by

Blewitt (1989), (although he claims that it is sufficient that $\sigma_{\hat{u}}$ be less than 5.4 cm for 99% confidence in fixing the primary ambiguity). According to Sovers and Border (1987) ρ (and then u) can be modelled very accurately. However, for an uncertainty of u of 5.4 cm the standard error of $\hat{N}_1$ according to eq. (9) becomes 0.55, and it will not be practically possible to fix the correct integer ambiguity.

4. A priori information on u: Least squares solution

The additional information on u, say $\tilde{\ell}_5$ with error ε_5, can also be used together with the observation equation (1) to an improved estimate of N_1 (and N_2). Assuming that the wide-lane ambiguity has been fixed by formula (3), we may eliminate N_2 as an unknown. The system of observation equations becomes

$$\left.\begin{aligned} u + \lambda_1 N_1 - \frac{\mu}{f_1^2} &= \tilde{\ell}_1 - \varepsilon_{11} \\ u + \lambda_2 N_1 - \frac{\mu}{f_2^2} &= \ell'_2 - \varepsilon_{12} \\ u + \frac{\mu}{f_1^2} &= \tilde{\ell}_3 - \varepsilon_{21} \\ u + \frac{\mu}{f_2^2} &= \tilde{\ell}_4 - \varepsilon_{22} \\ u &= \tilde{\ell}_5 - \varepsilon_3 \end{aligned}\right\} \qquad (10)$$

where:

$\ell'_2 = \ell_2 + \lambda_2 N_w$

or, in matrix form with vector of unknowns X:

$$AX=L-\varepsilon \quad , \quad E(\varepsilon\varepsilon^T) = \sigma_o^2\, P^{-1} \qquad (11)$$

where

$$A = \begin{pmatrix} 1 & -1 & 1 \\ 1 & -\nu^2 & \nu \\ 1 & 1 & 0 \\ 1 & \nu^2 & 0 \\ 1 & 0 & 0 \end{pmatrix} \qquad X = \begin{pmatrix} u \\ \mu / f_1^2 \\ \lambda_1 N_1 \end{pmatrix} \qquad L^T = \left(\tilde{\ell}_1, \tilde{\ell}'_2, \ldots, \tilde{\ell}_5\right)$$

$P=\sigma_{\phi\lambda}^{-2}$ diagonal(1,1,k,k,a)

$\nu = f_1 / f_2 = \lambda_2 / \lambda_1$

$k = \left(\sigma_{\phi\lambda} / \sigma_R\right)^2 = 10^{-4}$

$a = \left(\sigma_{\phi\lambda} / \sigma_{\hat{u}}\right)^2$

σ_o^2 = variance of unit weight

$\sigma_{\hat{u}}^2$ = variance of $\tilde{\ell}_5$.

The least squares solution to eq. (11) is

$$\hat{X} = \left(A^T P A\right)^{-1} A^T P L, \tag{12}$$

where

$$A^T P A = \begin{pmatrix} 2(1+k)+a & (1+\nu^2)(k-1) & 1+\nu \\ (1+\nu^2)(k-1) & (1+\nu^4)(k+1) & -(1+\nu^{3)} \\ 1+\nu & -(1+\nu^3) & 1+\nu^2 \end{pmatrix} \sigma_{\phi\lambda}^{-2}$$

and

$$A^T P L = \begin{pmatrix} \tilde{\ell}_1 + \tilde{\ell}_2 + k\left(\tilde{\ell}_3 + \tilde{\ell}_4\right) + a\,\tilde{\ell}_5 \\ -\tilde{\ell}_1 - \nu^2\tilde{\ell}_2 + k\tilde{\ell}_3 + k\nu^2\tilde{\ell}_4 \\ \tilde{\ell}_1 + \nu\tilde{\ell}_2 \end{pmatrix} \sigma_{\phi\lambda}^{-2}.$$

For $\sigma_{\phi\lambda}$ = 3 mm and σ_R = 30 cm , k = 10^{-4}, and k can therefore be omitted. Then one obtains

$$\left(A^T P A\right)^{-1} = \frac{\sigma_{\phi\lambda}^2}{a\nu^2(1-\nu)^2} \begin{pmatrix} \nu^2(1-\nu)^2 & -\nu(1-\nu)^2 & -\nu(1-\nu)^2(1+\nu) \\ -\nu(1-\nu)^2 & 1-2\nu+a(1+\nu^2) & (1-\nu)^2(1+\nu)+a(1+\nu^3) \\ -\nu(1-\nu)^2(1+\nu) & (1-\nu)^2(1+\nu)+a(1+\nu^3) & (1-\nu^2)^2+a(1+\nu^4) \end{pmatrix}$$

and the solution for N_1 becomes

$$\lambda_1 \hat{N}_1 = \frac{\nu}{\nu-1}\tilde{\ell}_1 + \frac{\tilde{\ell}_2'}{\nu(1-\nu)} + \frac{\tilde{\ell}_5}{\nu^2(1-\nu)^2} \tag{13}$$

The covariance matrix of $\hat{X}$ is given by $\sigma_o^2(A^T P A)^{-1}$. Assuming that the variance of unit weight $\left(\sigma_o^2\right)$ is one, the variance of $\hat{N}_1$ becomes

$$\sigma^2_{\hat{N}_1} = \frac{\sigma^2_{\phi\lambda}}{\lambda_1^2 \nu^2}\left\{\frac{(1+\nu)^2}{a} + \frac{1+\nu^4}{(1-\nu)^2}\right\} \tag{14}$$

or, with $\lambda_1 = 19.0$ cm and $\lambda_2 = 24.4$ cm:

$$\sigma^2_{\hat{N}_1} = 1.51 \cdot 10^{-4}\left(\frac{5.22}{a} + 46.05\right) = 87.58\,\sigma^2_{\hat{u}} + 0.695 \cdot 10^{-2}, \tag{15}$$

where $\sigma_{\hat{u}}$ is given in metres.

If we require $\sigma_{\hat{N}_1}$ not to exceed 0.3, $\sigma_{\hat{u}}$ must not exceed 3.1 cm. Hence, the least squares solution (13) is slightly more efficient (about 1.5 times) than the solution by the L_3 ambiguity bias (7).

5. The Best Linear Estimator

One way to improve the estimation of N_1 and N_2 is to consider a compromise between the ionospheric bias and the noise. This implies that the estimator is biased, and the optimum estimator minimizing the so-called mean square error is the Best Linear Estimator (BLE). A Restricted Best Linear Estimator (RBLE), where the bias stems merely from the ionospheric effect, was derived by Sjöberg (1997 c).

The explicit form of the RBLE is

$$\hat{\tilde{N}}_1 = \hat{a}\,\tilde{\ell}_1 + \frac{1-\hat{a}\lambda_1}{\lambda_2}\tilde{\ell}_2 + \hat{b}\tilde{\ell}_3 - \left(\hat{a} + \hat{b} + \frac{1-\hat{a}\lambda_1}{\lambda_2}\right)\tilde{\ell}_4\,, \tag{16 a}$$

with

$$\hat{a} = \frac{1}{\lambda_1}\,\frac{-\alpha x^3\left(2\nu^2 + \nu + 1\right) + 2\kappa\nu^4 - x\nu^5}{D} \tag{16 b}$$

$$\hat{b} = \frac{1}{\lambda_1}\,\frac{-\alpha x^3(\nu+1) - \kappa\nu^4(\nu+1)}{D} \tag{16 c}$$

where

$$D = \alpha x^4(\nu^2+1) + 2\kappa\nu^4(\nu^2+1) + x^2\nu^4$$

$$x = \nu - 1$$

$$\alpha = \mu^2 / \left(f_2^4 \sigma_R^2\right)$$

$$\kappa = \left(\sigma_{\phi\lambda} / \sigma_R\right)^2 .$$

As κ is merely of the order 10^{-4}, all terms including κ can usually be neglected.

Then the mean square error becomes:

$$\mathrm{MSE}\left\{\hat{N}_1\right\} = \left(\frac{\sigma_R}{\lambda_2}\right)^2 \frac{\alpha x^2 \nu^2 (1+\nu)^2 + 2\kappa\nu^4}{\alpha x^4 (1+\nu^2) + x^2 \nu^4} \qquad (17)$$

It has the property

$$\sigma(\mathrm{BLUE}_1) \le \mathrm{RMSE(RBLE)} \le \sigma(\mathrm{BLUE}_2),$$

i.e. the Root Mean Square Error (RMSE) of the RBLE is limited by the standard errors of the BLUE:s. If the ionospheric effect is insignificant the RBLE equals BLUE_1, and if the ionospheric effect is the totally dominating error source RBLE equals BLUE_2. This method is demonstrated in Fig 1 for the code standard error 30 cm. It is obvious that the advantage with the RBLE will increase with a decreasing code standard error. This is the case, because the limiting error of this solution for an increasing ionospheric bias (R_1-R_2) is the standard error $\sigma(\mathrm{BLUE}_2)$, which is proportional to the code standard error. {See Formula (17).}

Fig 1 The figure shows the Root Mean Square Errors of the BLUE_1 and RBLE of N_1 (or N_2) as functions of the ionosphere range difference R_2-R_1. Shown are also the standard errors of the BLUE_1 and BLUE_2. $\sigma_{\phi\lambda}$ = 3 mm and σ_R = 30 cm.

Finally, formulas (16) demonstrate that the estimator $\hat{N}_1$ requires that there is a priori information on the ionospheric bias α. One such estimator was given in Sjöberg (1997 b). However, as is obvious from the above formulas all terms with α are multiplied by the factors $x^3 = 0.023$ and $x^4 = 6.5 \cdot 10^{-3}$, implying that very approximate information on the ionospheric bias is needed.

6. Triple frequency GPS

Today the US Department of Defence is considering to implement a second civil GPS signal, which might imply that future GPS satellites will transmit on three independent frequencies.

Sjöberg (1998 b) extended the observation model (1) with two additional equations for a third signal. This yields 6 instantaneous observation equations with 4 unknowns. The standard error of the least squares solution for the integer ambiguity N_1 is demonstrated in Fig. 2 (solid line) as a function of the ratio

$$\beta = f_1 / f_3 = \lambda_3 / \lambda_1 \ .$$

Shown in the figure is also the standard error of the widelane solution from f_1 and f_3:

Fig 2 The figure shows the standard errors of the base ambiguity N_1 (dashed line) and the widelane ambiguity N_{w13} (solid line) as functions of β. Constants: σ_R = 30.0 cm, σ_o = 3 mm, λ_1 = 19.0 cm.

$$\sigma_{NW13} = \frac{\sigma_R}{\lambda_1}\frac{|1-\beta|}{1+\beta}\left(1+\beta^{-1}\right) .$$

This curve (dotted) shows maxima for $f_1 = f_2$ and $f_2 = f_3$. For $\beta = 0.75$ and 1.58 both curves are close to 0.6. Obviously the optimum choice for β can be found for these values. Se also Table 1.

Table 1 Optimum choices of L_3 and corresponding standard error of N_1 and N_{w13}.

β	λ_3 (cm)	f_3	$\sigma_{\hat{N}_1}$	$\sigma_{N_{w13}}$
0.75	14.3	2100.6 MHz	0.56	0.53
1.58	30.0	997.1 MHz	0.59	0.58

7. Conclusions

The fast resolution of GPS phase ambiguities for a significant ionospheric bias is a challenging task. The most widely practised method is the one described by Blewitt (1989) to combine the widelane ambiguity with the ionophere-free bias, relying on a priori determined parameter u. We have demonstrated that in order to fix the correct integer ambiguity N_1 (with a standard error not exceeding 0.3) by Blewitt's method, the standard error of u must not exceed 2.1 cm. A corresponding least squares solution for the ambiguity allows the standard error of u to increase about 1.5 times.

We have also discussed our Restricted Best Linear Estimator, which is a compromise between the ionospheric bias and the random noise. This method is most important for low code noise GPS data.

Finally, we have shown that the problem related with the ionospheric bias can be satisfactory solved for a proper choice of a possible additional GPS signal frequency.

References

Almgren, K. (1998): A new method for GPS ambiguity resolution on-the-fly at short baselines. Division of Geodesy Report No. 1047, Royal Institute of Technology, Stockholm, Sweden.

Blewitt, G. (1989): Carrier phase ambiguity resolution for the Global Positioning System applied to geodetic baselines up to 2000 km. J Geophys Res, Vol. 94, No. 38, pp. 10187-10203.

Melbourne, W.G. (1985): The case for ranging in GPS-based geodetic systems. In: Proc First Int Symp on Precise Positioning with the Global Positioning System, Rockville, Maryland, Vol. 1, pp. 373-386.

Sjöberg, L.E. (1996): Application of GPS in detailed surveying, ZfV, Vol. 121, No. 10, pp. 485-491.

Sjöberg, L.E. (1997 a): On optimality and reliability for GPS base ambiguity resolution by combined phase and code observables. ZFV, Vol. 122, No. 6, pp. 270-275.

Sjöberg, L.E. (1997 b): Studies on a new method for GPS base ambiguity resolution by combined phase and code observables. In Bo Jonsson (ed.): Geodetic application of GPS, Lecture notes for Nordic Autumn Schools organised by the Nordic Geodetic Commission, LMV-rapport 1997:16, The National Land Survey, Gävle, Sweden, pp. 203-215.

Sjöberg, L.E. (1997 c): Linear estimation of GPS phase ambiguity from dual frequency code and phase observables. Submitted to J. of Geodesy.

Sjöberg, L.E. (1998 a): A new method for GPS base ambiguity resolution by combined phase and code observables. Accepted by Survey Review.

Sjöberg, L.E. (1998 b): On the estimation of GPS phase ambiguities by triple frequency phase and code data. ZfV, Vol. 123, No. 5, pp. 162-165.

Sovers, D.J. and J.S. Border (1987): Observation model and parameter partials for JPL geodetic modelling software, GPSOMC, JPL Publ. 87-21, Jet Propulsion Laboratory, Pasadena, Ca.

THE FIRST RESULTS OF THE FINNISH PERMANENT GPS NETWORK

Hannu Koivula
Finnish Geodetic Institute
Geodeetinrinne 2, FIN-02430, Masala, Finland
email: Hannu.Koivula@fgi.fi

The Finnish permanent GPS network, FinnRef, has been operational since 1994. The final coverage of 12 stations was reached in October, 1996. All stations, except Metsähovi, are equipped with Ashtech Z-12 receivers with Dorne Margolin antennas. The data is processed using Bernese 4.0 Software. From daily solutions the normal equations are saved and used later to produce weekly and monthly solutions. The network has this far served mainly as a data source for domestic and international GPS-campaigns. Now we have come to the point where we are ready to get the results processed on a routine basis. The present status and performance of the network as well as the daily data flow are described. Also we will show our first long term results and how they can be used for studying the post-glacial rebound and possible horizontal movements in Finland.

Introduction

The proposal of the establishment of the Fennoscandian Regional Permanent GPS network came from the Nordic Geodetic Commission in response to the initiative of the directors of the Nordic Mapping Agencies (KAKKURI *et al.* 1995). As a response to that the FGI started the planning the Finnish permanent GPS network, FinnRef, (Fig. 1). Planning started already at the end of 1992, when it was decided that the network of 12 stations will be established. The first stations were built in the summer of 1993 and the first test observations started in 1994. The last station (Kuusamo) became operational in the end of 1996.

All stations except Metsähovi are equipped with Ashtech Z-12 double frequency GPS receivers and Dorne Margolin type choke ring antennas. At Metsähovi we have a Turbo Rogue SNR-8100. The antennas are covered with radomes to avoid the snowload over the antenna. As we will see, the snow is playing an important role on the accuracy of GPS in wintertime. Olkiluoto, Romuvaara and Kivetty sites were established in co-operation with the company Posiva Oy. At those stations the antenna is mounted on a steel enforced concrete pillar, being part of high precision local GPS control networks which are periodically re-measured (CHEN and KAKKURI, 1994). Metsähovi and Oulu have an invar stabilized steel mast and all the other stations have a 2.5 m steel grid mast except Kevo, where we have a 5 m steel grid mast. The height changes due to the thermal expansion of the steel tower of 2.5 m are appr. 0.8 mm during the course of the year. We considered these changes to be insignificant and they will average out during the yearly cycle. All the stations have a 30 second observing interval and Oulu station disseminates an RTCM signal over the Finnish National Broadcasting Company's (YLE) FM radio network.

The orthometric heights of all stations except Romuvaara, Kivetty and Olkiluoto are determined by levelling. The absolute gravity is measured at Metsähovi, Vaasa and Sodankylä stations.

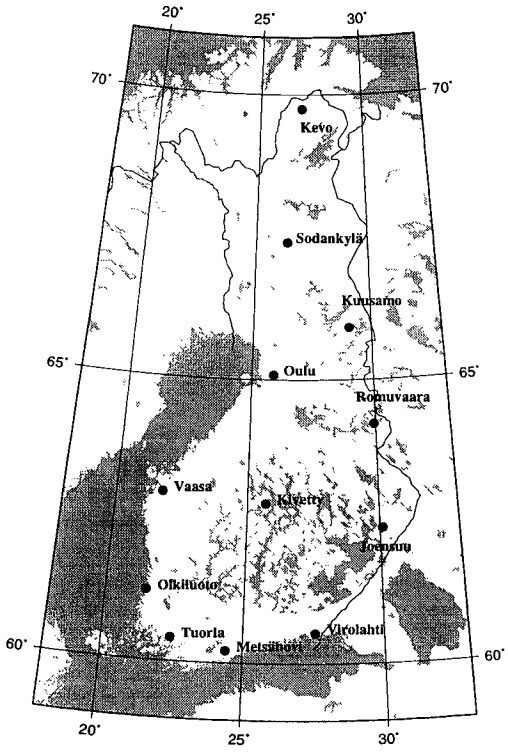

Fig. 1. *Finnish permanent GPS network - FinnRef*

At the FGI in Masala, Kirkkonummi, we have a PC with modem connection to all the stations. An automatic script calls to all the stations one after each other and downloads the data. The data is immediately transferred to RINEX format and backups are made on two different computers. Also the data is transferred to IGS and EUREF processing centres. Twice a month the data is also copied to dat tape and CDROM and stored into our data bank.

The FGI is responsible of establishing and maintaining the coordinate systems of Finland. The Finnish permanent GPS network offers for GPS users a homogeneous reference frame and a connection to international coordinate systems.

The base station of the permanent GPS network is Metsähovi Geodetic observatory which has been collaborating e.g. in international SLR observation programs during two decades. Today it belongs also to the IGS network producing GPS data for IGS orbit determinations.

FinnRef has been a part of numerous international GPS campaigns like DOSE, BIFROST, BSL and EUVN. FinnRef has been used as a reference frame in many national campaigns like EUREF-FIN densification where we measured a 100 point EUREF densification using FinnRef as a backbone. A more detailed list of FinnRef activities and its function can be found in (KOIVULA et al., 1998) and the publications and reports about the individual campaigns e.g. (MITROVICA *et al.*, 1997; POUTANEN, 1998; BIFROST PROJECT, 1996)

Data processing

The data processing is done with Bernese v4.0 software (ROTHACHER and MERVART, 1996) on a DEC 3000 workstation running an Open VMS operating system. We have built a script to allow a semiautomatic processing of the Bernese software. In the processing we use IGS

precise ephemerides which are given in the ITRFnn system. Here we describe step by step how the processing is done by our automatic processing tool.

The processing is done one GPS week at the time. First we collect the raw RINEX data from our archive where it is on CDROMs and dat tapes. TheIGS precise orbits are downloaded from the IGS data centre. Metsähovi is used as a fixed station. Its ITRFnn coordinates are transferred to the epoch of the observations using the velocity vectors given in the IERS catalogue.

The processing starts with transferring the RINEX data and IGS orbits to the Bernese format. From the orbit files also the satellite clock information is stored.

The cut off angle of 15 degrees is used throughout the computation. First the code observations of individual stations are used to synchronize the receiver clock with GPS time in the microsecond level.

The baselines are created by connecting each point to its 3 closest neighbours. In this way we believe to get a more robust network. We found this necessary because of the numerous problems with processing the winter time data of only a minimum number of baselines. The cycle slips are detected and corrected baseline by baseline using the *MAUPRP* program.

The station coordinates are estimated in two steps with the *GPSEST* program. In the first step the ambiguities are solved baseline by baseline keeping one end of the baseline fixed. In the second step we make a free network solution keeping Metsähovi's coordinates fixed to its ITRFnn values, using the L3 linear combination and pre-eliminating the ambiguities solved in the first step. The normal equations of one day solution are saved. When the whole GPS week is processed, the normal equations are combined to a weekly solution using the program *ADDNEQ*.

The First GPS results

The test setup

For this study we have used data from the years 1996, 1997 and the beginning of 1998. In the near future we reach our goal to process all the data "real time" and also we will process all the remaining data from the earlier days of the network. As one can see from the Fig. 2 some stations became operational during the year 1996, so the time series are not very long for e.g. postglacial rebound studies.

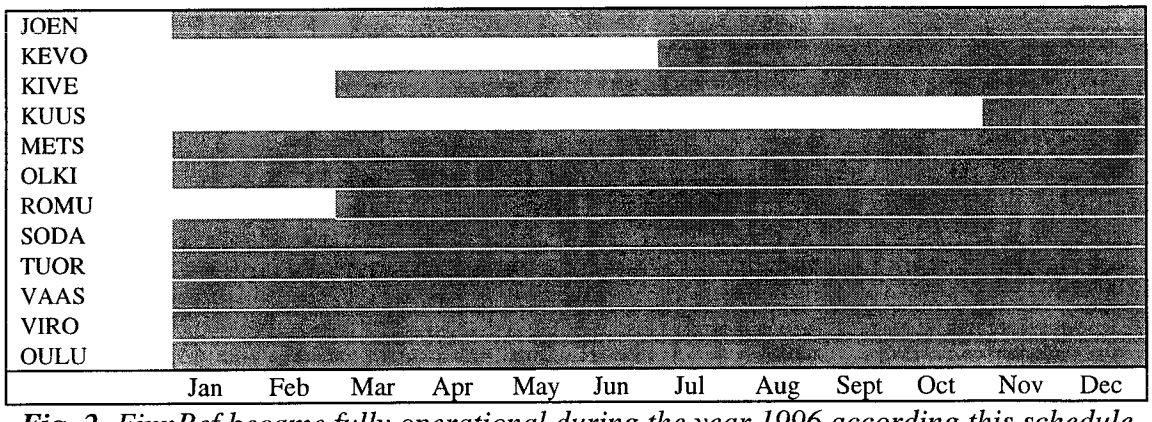

Fig. 2. *FinnRef became fully operational during the year 1996 according this schedule.*

The data used in this study has gone through the standard processing scenario as described in the previous chapter. One of our goals is to study the land uplift and possible horizontal movements on the Fennoscandian crust. At first stage we concentrate on the height differences and only mention that any statistically significant changes in baseline length were not detected. For this study we have chosen a set of baselines (Fig. 3) the results of which we take from the standard processing scenario.

The change of height differences are derived straight from the GPS solution so they reflect changes in ellipsoidal heights. As a "ground truth" we use the land uplift values derived from the recordings of the tide gauges and from the precise levellings of Finland (Fig. 4). Those heights are orthometric heights, but since the uplift of geoid is in order of 5 % or less of the land uplift value we neglected its effect at this stage.

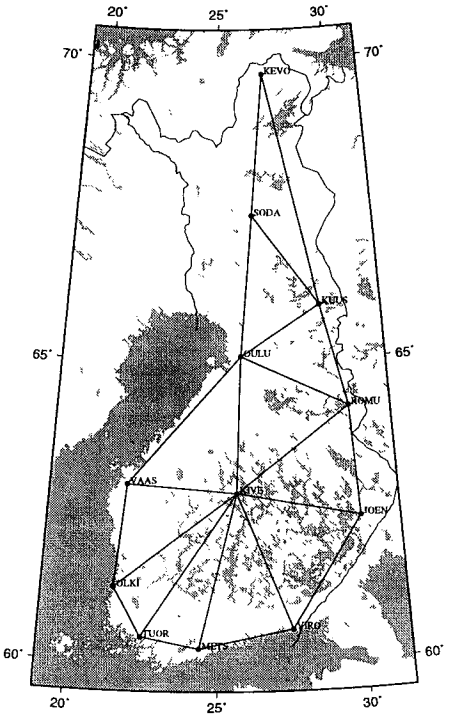

Fig. 3. The set of baselines from which the baseline lengths and height differences were studied.

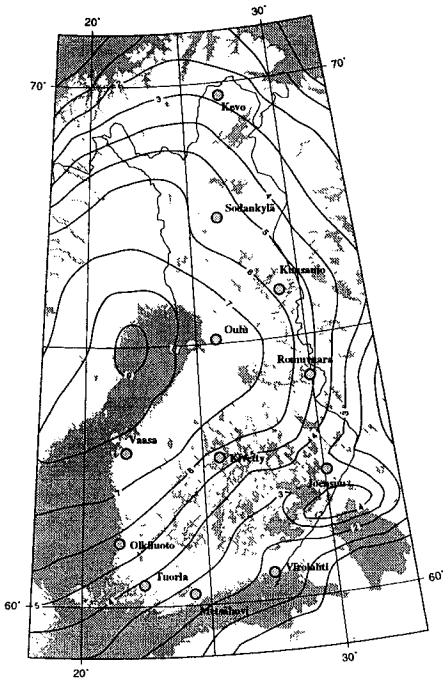

Fig. 4. Observed land uplift values in mm/year used as the "ground truth" (KAKKURI AND POUTANEN, 1996).

The results

In Fig. 5 we show an example of weekly height difference results from different baselines. The scale on the figures is the same, but the time scale varies because the stations have not been operational during the same time span (see Fig. 2). The pictures show that the scatter of the results is large during winter time. This kind of scatter in a dataset extended over short time span may cause significant errors in the estimation of the vertical velocities.

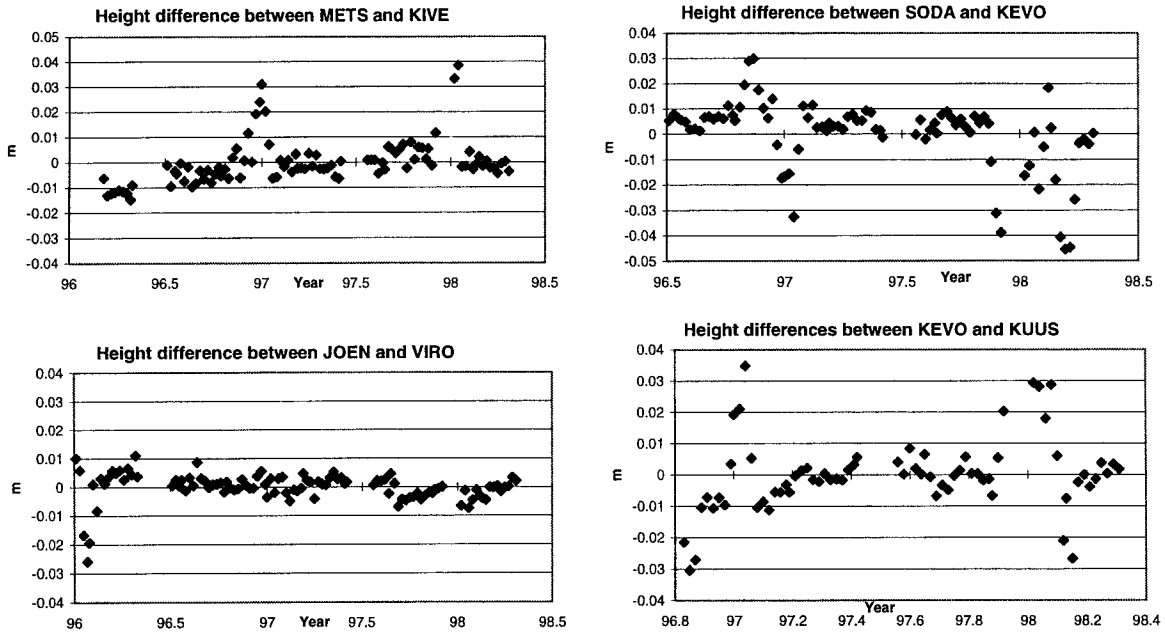

Fig. 5. The change of the height differences of four baselines. The winter effect can easily be seen.

We fitted a line to the height difference changes for all baselines and compared the results with the "ground truth". The line was fitted to the raw weekly results and also to the solution where the outliers deviating more than 3σ from the regression line were rejected. An overview of the results can be seen in Fig. 6. In the figure the size of the pie over the baseline is the difference between the uplift value of the ground truth and the one obtained by GPS. The colour of the pie tells only the trend. The black pie means the right direction and the grey one the wrong direction. It is easy to see from the figure that the results of the Northern Finland are bad when the Southern part of the network agree to the known uplift values very well.

The result is obvious if one looks at the large scatter of the height differences of the baselines SODA-KEVO and KEVO-KUUS in Fig. 5. The outliers of the winter time affect the solution, and for such a small data sets the 3σ values are too big to use reliably. On the other hand, 3σ rule improved the results of the southern part of Finland. Figs. 7 and 8 show the same phenomenon as Fig. 6 but more detailed. There the uplift values are plotted on the time scale of 10 years. The poor situation of northern Finland (above the OULU-ROMU baseline) is shown in Fig. 8 and the southern part in Fig. 7. When comparing the Fig. 7 and Fig. 8 one should notice that the scale of Fig 8. is 4 times bigger than in Fig. 7.

We will take a look first to Fig. 7. The uplift values obtained by GPS agree with the "ground truth" very well. In most cases the difference is less than 1mm/yr. Here the 3σ rule improved the result. From Fig. 8 we can see that the results of the Northern part are very bad and do not agree with the "ground truth". The reason for this is obvious. The results scatter in winter time so badly that the line fitting fails to find the major trend of the result (see Fig. 5). 3σ fails also because it's too big to really work because of the lack of data. The situation will of course improve with time when more data is collected and processed.

Another solution for this problem could be some kind of a robust regression that could filter out the "erroneous" data. That is the next step in our near future plan. Here we give an extremely rough example. Let's go back to Fig. 5 and look at the baseline SODA-KEVO. It is easy to see that the results of the summer time are nicely together with a deviation of some 0.5

cm, but the result "explodes" in winter time. In Fig. 9 we see the result if we just throw out the "bad" data of the wintertime. The comparison with the "ground truth" tells that the results are now much more realistic. This arises the question if we should throw away the data of the winter time from the northern part of Finland to get better and more reliable and realistic results.

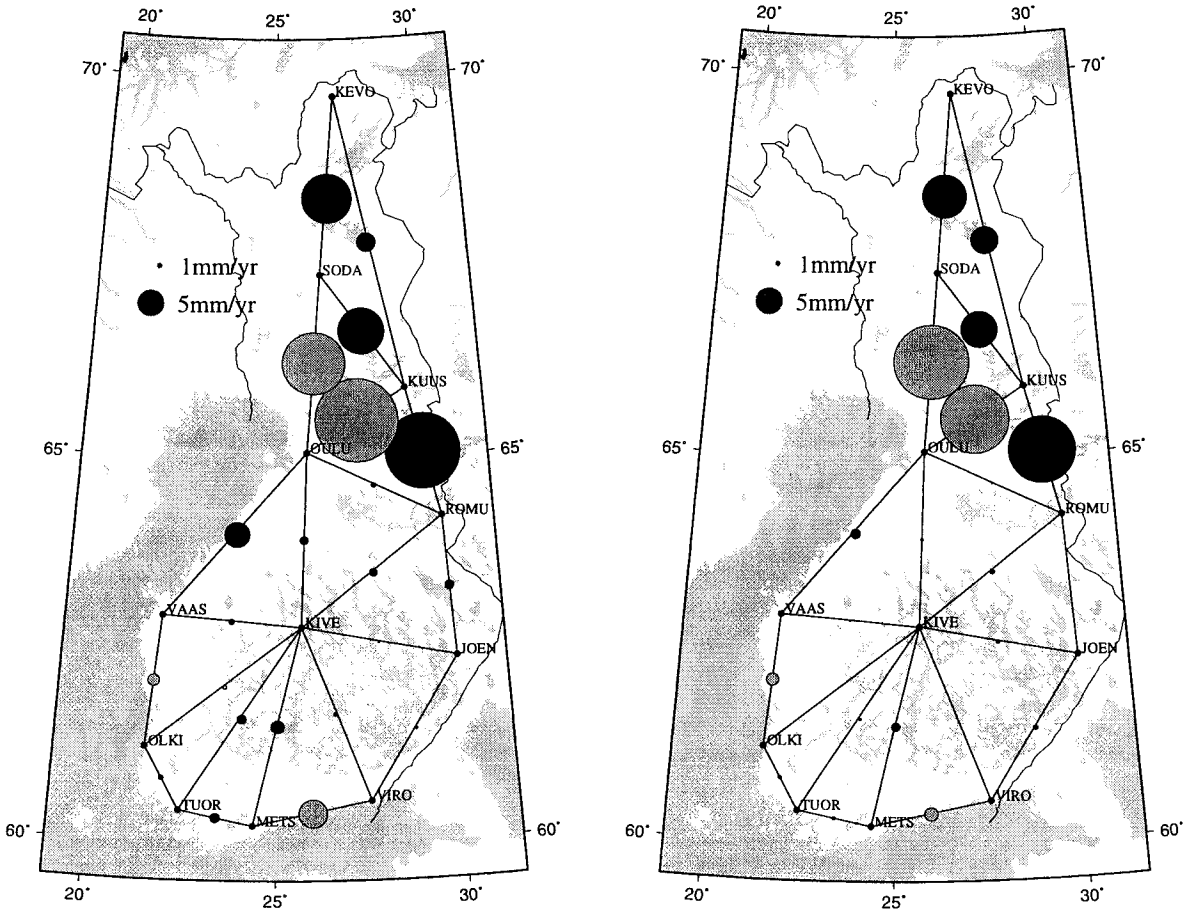

Fig. 6. *Comparison of the uplift rates between the "ground truth" and the ones obtained from the GPS solution. The left picture is from the raw data taken straight from the data processing. The right picture is the result after rejecting the results deviating more than 3σ from the regresion line. The size of the ball is the difference between the real uplift value and the one obtained by GPS. The black colour tells that of the land uplift is same in levelling and in GPS results, and grey that the direction is opposite.*

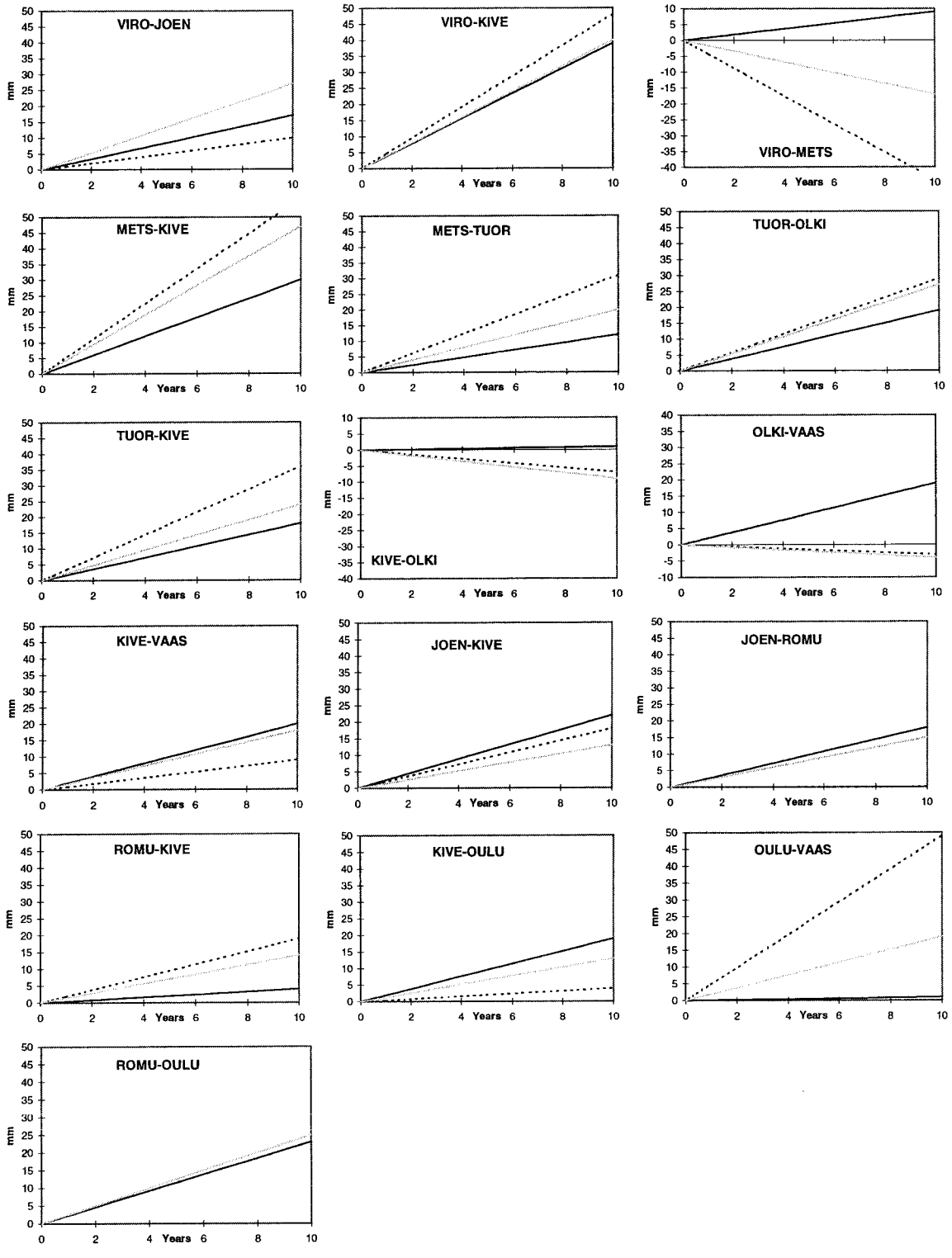

Fig. 7. The land uplift values for the test baselines south of the OULU-ROMU line. The time scale has been prolonged for 10 years so that the effects can be seen easier. The black line is the land uplift obtained from the levellings (Fig. 4). The dotted line is the land uplift obtained from the raw output of the processing and the grey line is the value after rejecting the results deviating more than 3σ from the regression line.

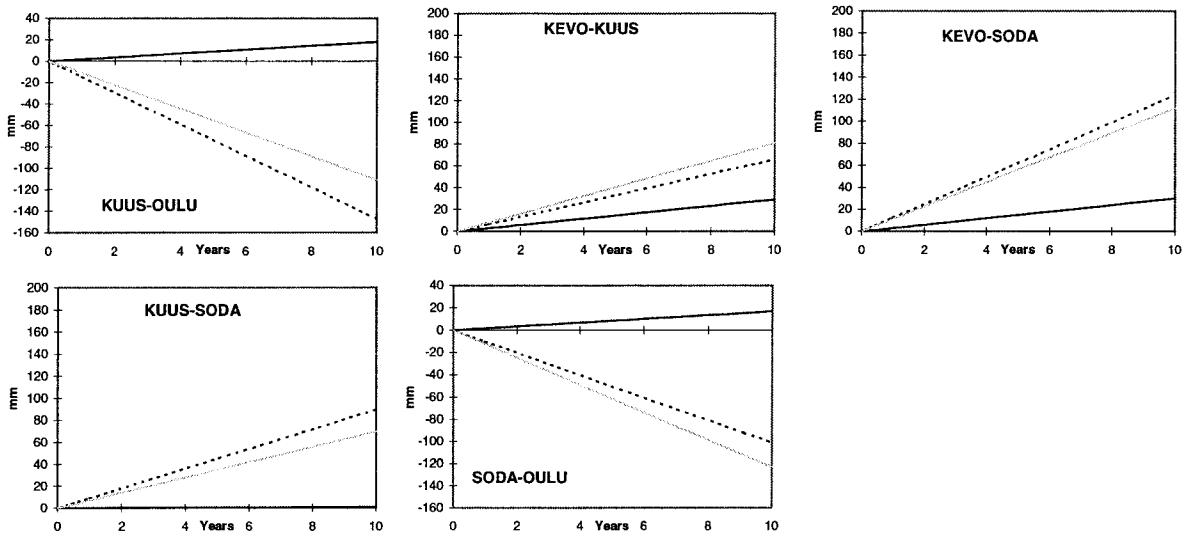

Fig. 8. The land uplift values for the test baselines south of the OULU-ROMU line. The time scale has been prolonged for 10 years so that the effects can be seen easier. The black line is the land uplift obtained from the levellings (Fig. 4). The dotted line is the land uplift obtained from the raw output of the processing and the grey line is the value after rejecting the results deviating more than 3σ from the regression line. Note that the mm scale is 4 times the scale of Fig. 7.

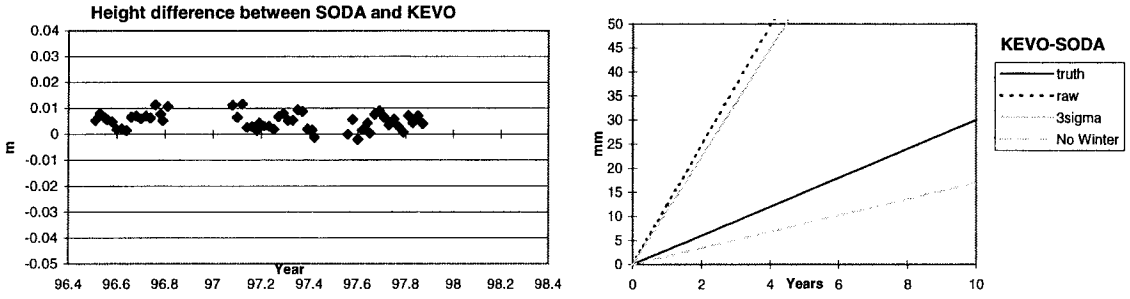

Fig.9. The results of the SODA-KEVO baseline when the data from the winters 1997 and 1998 is removed.

Case: Sodankylä's snow accumulation

During the winter 1997/98 we became aware of the fact that the results of the height component of SODA station wasn't very good. That made us think if we could find any simple connection between the meteorological data and the height problem. In Fig. 10 are shown the values of the height component of Sodankylä from the official EUREF solution between October 1997 and February 1998. (http://www.oma.be/KSB-ORB/EUREF/eurefhome.html). During this period the height component has behaved rather strangely. Below this there is a graph of the snow depth at Sodankylä observatory measured daily at 8 am, and the maximum daily temperatures. The meteorological information is from the database of the Finnish Meteorological Institute. As we can see, the up component starts increasing around the 15th of November. That is also the same time when the first

considerable amount of snow came to Sodankylä. The up component continues its anomalous behaviour together with the thickening of the snow layer. We believe that this is caused by the thicker and thicker snow layer on top of the antenna. After the 10th of December the height seems to go back to normal again. When we look at the daily maximum temperatures we do see that it happened to be above zero and could cause the melting of the snow hat. A similar, but smaller effect can be seen around 29th of December.

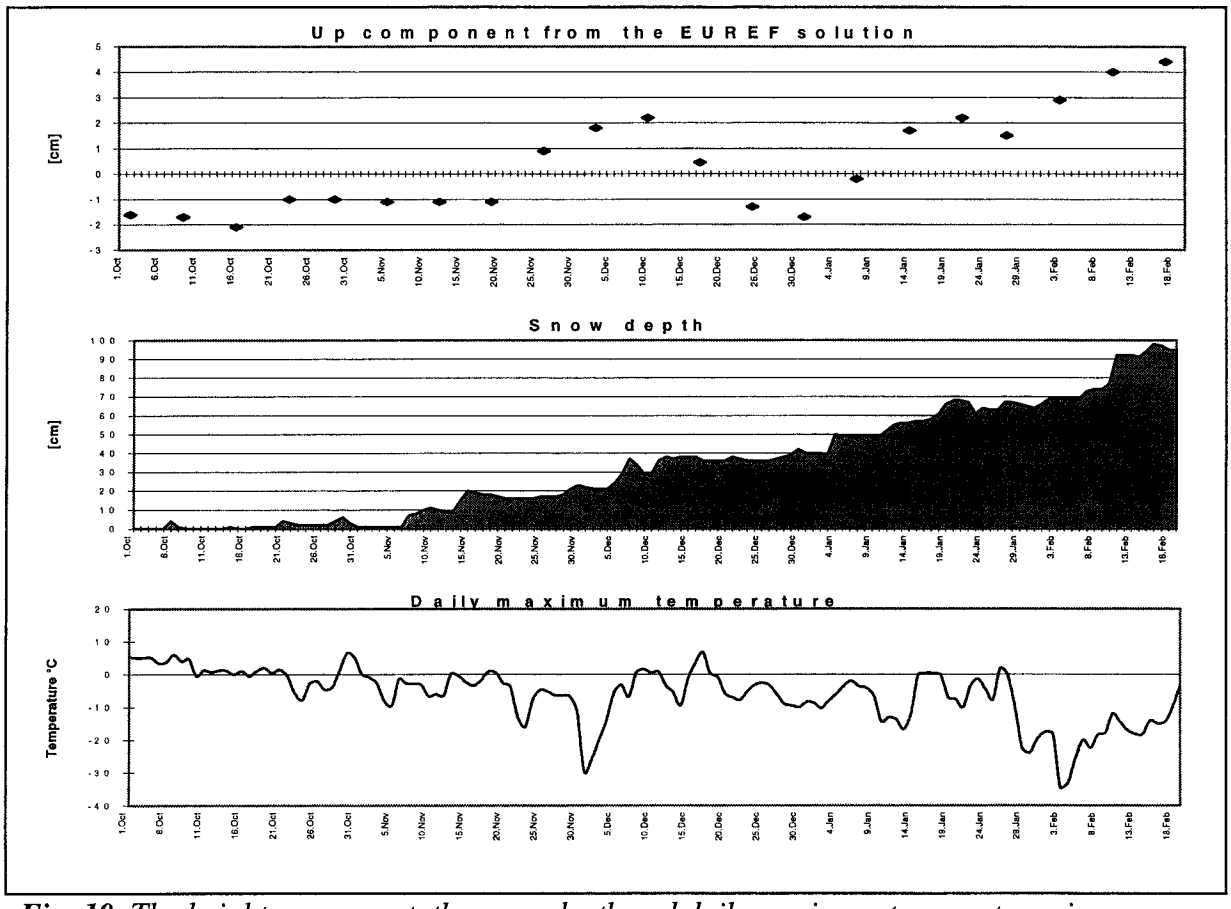

Fig. 10. The height component, the snow depth and daily maximum temperatures in Sodankylä station.

Conclusion and future work

This study shows that GPS can and will be a powerful tool for researching the postglacial rebound. There is still a lot of work to do in order to make the results more reliable. Especially the snow affects very badly on the height estimations. The winter time problems arise the question if these months of data should be sacrificed in the name of more accurate results. At least some more robust filtering methods have to be used. On the other hand the results of the southern part of Finland show that GPS can give good results in a relatively short time.

There are also lot of other possibilities for improving the repeatability. First attempt will be to decrease the cut off angle of the processing from the "safe 15°" to 10°. It gives more satisfactory results we may try even lower cut off angles using the elevation dependent weighting of the troposphere delay estimation. This procedure should improve the repeatability of the height component. During this year we will do a field calibration of all

GPS stations with respect to one reference antenna. So far the antennas have been believed to behave similarly. The mast and surroundings do affect on the antennas, so the field calibration may significantly improve especially vertical accuracy. After the first calibration, a winter calibration and some further tests may take place. The effect of the snow and frost to the results will be studied. The stations will also be equipped with Vaisala's meteo sensors. They are connected to the receivers and the data is downloaded together with the GPS data.

References

BIFROST PROJECT, 1996. GPS measurements to constrain geodynamic processes in Fennoscandia. EOS, transactions, American geophysical union. Vol. 77, Number 35, August 27, 1996, pages 337 and 341.

CHEN, R. and J. KAKKURI, 1994. Feasibility study and technical proposal for long-term observations of bedrock stability with GPS. Report YJT-94-02. Nuclear Waste Commission of Finnish Power Companies. Helsinki. 33 pp.

KAKKURI, J., H. KOIVULA, M. OLLIKAINEN, M. PAUNONEN, M. POUTANEN AND M. VERMEER (1995). The Finnish GPS Array FinnNet: Current Status. *Invited paper, IGS Workshop, Potsdam,* 15.-17.5. 1995.

KAKKURI, J. AND M. POUTANEN, 1996. Geodetic determination of the sea surface topography of the Baltic sea. Marine Geodesy, 20:307-316, 1997.

KOIVULA, H., M. OLLIKAINEN, AND M. POUTANEN, 1998. Finnish Permanent GPS Network-FinnRef. Presented in the 13th General meeting of the Nordic Geodetic Commission, May 25-29, 1998, Gävle, Sweden.

MITROVICA J.X., J.L. DAVIS, H.-G. SCHERNECK, AND J.M. JOHANSSON, 1997. BIFROST Project: GPS measurements to constrain geodynamic processes in Fennoscandia. *European Geophysical Society, XXII General Assembly*, Vienna, Austria 21–25 April, 1997. Annales Geophysicae, **15**, Supplement I, C81.

POUTANEN M., 1998. Results of the Baltic Sea Level 1997 GPS campaign. Presented in the 13th General meeting of the Nordic Geodetic Commission, May 25-29, 1998, Gävle, Sweden.

ROTHACHER AND MERVART, 1996. Manual to Bernese GPS Software Version 4.0. September, 1996, University of Berne.

Measuring water vapor with a permanent network of GPS receivers

T. Ragne EMARDSON and Jan M. JOHANSSON

Onsala Space Observatory, Chalmers University of Technology, SE-439 92 Onsala, Sweden

Abstract. Water vapor is difficult to measure using conventional techniques. The Global Positioning System has proven to be a useful tool for these kind of measurements. At least three aspects can be found on why to estimate water vapor with the GPS. The results can (1) be used in numerical weather prediction to improve the forecasts, (2) serve as information in climate change studies, and (3) be used as an independent data set to validate meteorological models. In this paper we review the the latest results in this area obtained using data from the Swedish Permanent GPS network.

1 Introduction

The Global Positioning System (GPS) was originally intended for precise positioning. During the last years, different groups have shown the possibility to use GPS also for determination of the total amount of water vapor in the atmosphere. The results from GPS have been assessed through comparisons with those from independent techniques such as microwave radiometry and radiosounding. The technique to estimate water vapor from GPS is based on the fact that the GPS signals are delayed by various gases in the atmosphere. The main part of this delay is due to the dry air and typically 10% is due to water vapor. The part due to the dry air can be modeled using surface pressure data. The residual part is the delay mainly due to water vapor, therefore often called the wet delay. This quantity is strongly correlated with the total amount of water vapor in the atmosphere and the relation between the water vapor content and the wet delay depends on the temperature profile of the atmosphere. Simple models do, however, exist using for example only surface temperature data.

The Swedish Permanent GPS network (SWEPOS) started to operate in August 1993. The network was originally intended for continuous measurements on contemporary vertical and horizontal crustal deformations in Sweden. The network consists today of 21 GPS sites. Figure 1 shows the location of the sites.

Apart from the role the wet delay plays in the estimation process of geodetic coordinates, there are several reasons on why to study the wet delay estimate itself. Information on the atmospheric water vapor can (1) be used in numerical weather prediction to improve the forecasts, (2) serve as information in climate change studies, and (3) be used as an independent data set to validate meteorological models. Although the atmospheric water vapor is such an important quantity in atmospheric research it is very difficult to measure with conventional techniques. The most commonly method used today to measure the water vapor is to launch weather balloons. Attatched to these balloons are sensors measuring for example, the pressure, temperature and humidity. These measurements can then be used to calculate the amount of water vapor. The main dis-advantage with these radiosondes is the man power which is needed for the activity. Also compared to GPS, the measurements from the radiosondes have a very sparse spatial and temporal resolution. In this paper we review the latest results obtained in this field using data from the SWEPOS network.

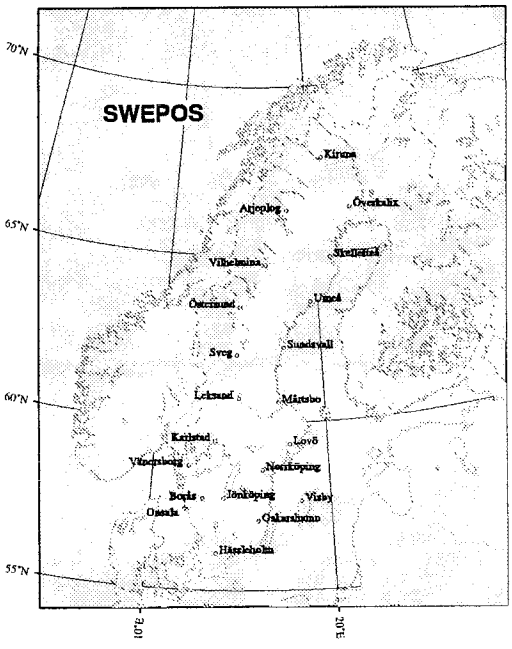

Figure 1: Locations of the 21 GPS sites in the SWEPOS network.

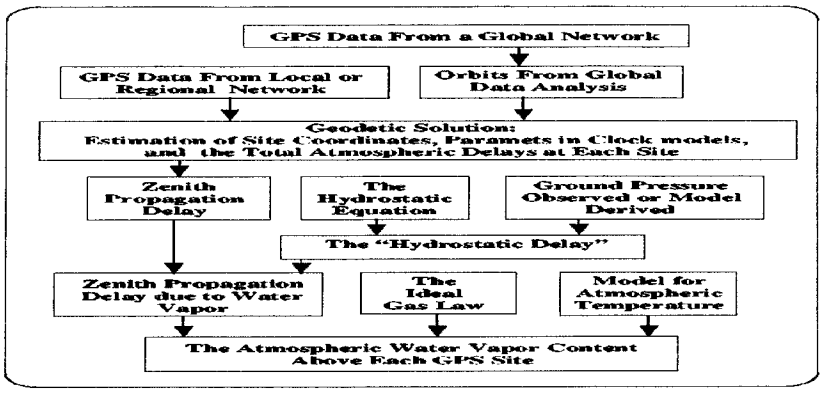

Figure 2: Flow chart over the algorithm used to derive the amount of atmospheric water vapor from the GPS data. (From *Emardson et al.* [1998a].)

2 Water vapor estimation

Figure 2 shows a flow chart describing the technique we use to estimate water vapor from GPS. We incorporate precise orbits distributed by the International GPS Service for Geodynamics (IGS) [*Noll and Gurtner*, 1996]. Using this a priori information we estimate site positions, satellite, and receiver clocks, and equivalent zenith propagation delay assuming a horizontally stratified atmosphere at all sites. The receiver clocks are estimated as white noise processes. To estimate the tropospheric delay, an a priori hydrostatic and wet component are subtracted from the total neutral delay. The residual delay is then estimated as a random walk process with a variance rate of 2.89×10^{-8} m^2/s, using the [*Lanyi*, 1984] mapping function to relate measurements at certain elevation angles to the zenith. The wet delay, ℓ_w is obtained by restoring the total delay from the residual and then subtracting the hydrostatic delay determined from pressure data at the different sites, and the [*Saastamoinen*, 1972] formula. Different algorithms can be used for the conversion between the wet delay and the IWV. [*Emardson and Derks*, 1998] used radiosonde data from 37 sites in Europe and one on Greenland to derive a conversion relation, Q, such that $IWV = Q \times \ell_w$ One model was based on ground temperature measurements, T.

$$Q = a_0 + a_1 T + a_2 T^2 \tag{1}$$

Such a model is also easily motivated by plotting Q against the surface temperature. Another relationship is based only on the annual change in Q due naturally to the seasonal variation in temperature.

$$Q = a_0 + a_1 \cdot \theta + a_2 \cdot \sin(2\pi \cdot \frac{t_D}{365}) + a_3 \cdot \cos(2\pi \cdot \frac{t_D}{365}) \tag{2}$$

where θ is the site latitude in degrees, t_D is the decimal day of the year, and a_n are constant parameters which can vary between different sites.

3 Result assessment

In order to evaluate the quality of the GPS estimated IWV we compare the result with those from independent techniques.

Radiometric measurements of the atmospheric emission can provide wet delay estimates along the signal propagation path and accordingly information on the integrated water vapor. A radiometer used for this purpose to measure

the water vapor will hereafter be referred to as a water vapor radiometer (WVR). The WVR at the Onsla Space Observatory is located approximately ten meters from the GPS monument and the difference in heights is less than 1 m. Figure 3 shows the time series for the three months of August to October 1995 of the GPS-estimated IWV at the Onsala site together with the data measured with the WVR. The top curves show the WVR data offset by 20 kg/m^2

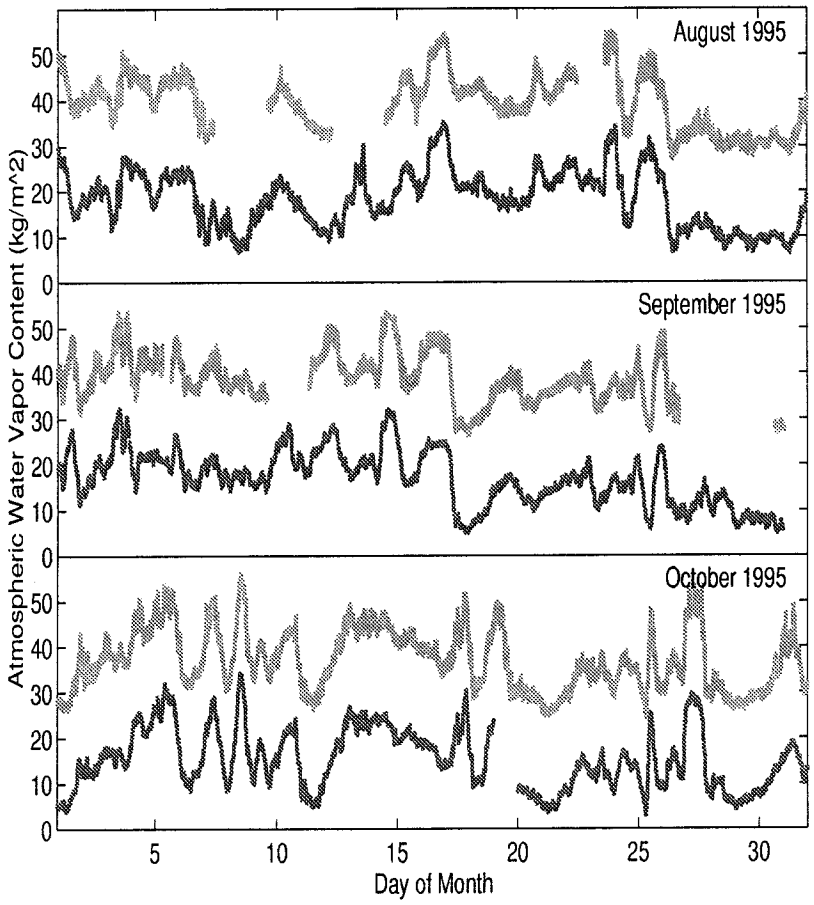

Figure 3: A comparison of the Integrated Water Vapor content estimated from GPS and water vapor radiometer data at the Onsala site. Note that the radiometer data have been offset by 20 units.

in order to improve the visual comparison. On the average, the WVR data are 0.9, 1.2, and 1.6 kg/m^2 above the GPS estimates for the months of August, September, and October, respectively. These numbers are of the same orders as reported by other groups for similar comparisons [*Duan et al.*, 1996] and [*Tregoning et al.*, 1998].

In order to study the long term stability of the GPS estimates [*Emardson et al.*, 1998b] compared four years of GPS results from the Onsala Space Observatory with WVR data. The comparison showed clear systematic variations, which were attributed to the GPS data. These variations were found to be correlated in time with occasions when radome changes were made at sites surrounding Onsala.

A straight-forward technique to measure the atmospheric water vapor is with radiosondes. These are hydrogen-filled balloons with attached sensors. While passing through the atmosphere the sensors are measuring altitude, pressure, temperature, and relative humidity, plus information not treated here such as wind speed and direction. Using the obtained profiles it is possible to calculate the IWV. At three sites in Sweden radiosondes are launched close enough to the SWEPOS sites for the results to be compared. These sites are Sundsvall, Frösön, and Landvetter. Figure 4 shows the GPS estimated IWV at the Sundsvall Station together with the radiosonde estimates from the same site. The formal error bars on the radiosonde data correspond to 5% of the total value, which is consistent with earlier comparison measurements between radiosondes and microwave radiometry [*Elgered*, 1993]. On the average, the radiosonde mea-

surements at Sundsvall are 1.2, 1.5, and 1.2 kg/m^2 above the the GPS estimates for the months of August, September, and October. The corresponding rms scatter of differences about the mean are 1.9, 1.7, and 1.5 kg/m^2.

In order to verify that the large variations seen in the comparison betwen the GPS and WVR data are due to problems with the GPS estimates and not, for example, to drifts in the WVR, we made a similar statistical comparison between the GPS estimates of the IWV and radiosonde data from Landvetter. This comparison showed similar variations as that of the GPS and WVR data and the variations were therefore attributed to the GPS data.

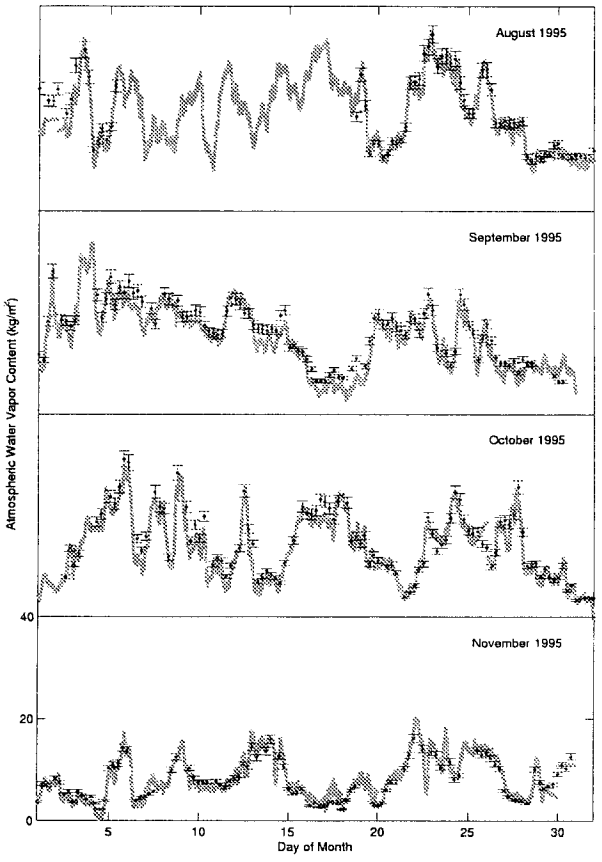

Figure 4: GPS-estimated IWV at the Sundsvall site together with integrated radiosonde measurements from the same site.

4 Applications

Some different studies have been carried out in order to evaluate the possibilities of using GPS results for climate studies and operational weather forecasting. [*Yang et al.*, 1998] compared estimates of the integrated water vapor from GPS and from a numerical weather prediction (NWP) model. The numerical prediction model used was the HIgh Resolution Limited Area Model (HIRLAM) and the data set was from 25 sites in Sweden and Finland during August to November, 1995. A mean offset between the estimated time series (HIRLAM−GPS) of 0.1 kg/m^2 and a rms difference of 2.4 kg/m^2 were reported. The results in the comparison indicate that the integrated water vapor obtained with GPS are useful in order to evaluate NWP models for meteorological applications.

An interesting prospective for GPS is the possibilities of using GPS data searching for climte trends ,e.g., [*Yuan et al.*, 1993]. [*Emardson et al.*, 1998b] showed the importance having a stable electromagnetic environment at each antenna site when applying GPS data to climate studies. This application may require the validation of systematic trends in the water vapor which are much smaller than such effects

GPS data from SWEPOS have also been used to produce maps of water vapor over Sweden, providing the possibility to study large scale weather systems as they move across the area [*Elgered et al.*, 1997].

References

J. Duan, M. Bevis, P. Fang, Y.Bock, S. Chiswell, S. Businger, C. Rocken, F. Solheim, T. VanHove, R. Ware, S. McClusky, T. A. Herring, and R. W. King, GPS Meteorology: Direct Estimation of the Absolute Value of Precipitable Water, *J. Appl. Meteor., 35*, 830-838, 1996.

Elgered, G., Tropospheric radio path delay from ground-based microwave radiometry, in *Atmospheric Remote Sensing by Microwave Radiometry*, edited by M. Janssen, pp. 215–258, John Wiley, New York, 1993.

Elgered, G., J.M. Johansson, B.O. Rönnäng, and J.L. Davis, Measuring regional atmospheric water vapor using the Swedish permanent GPS network, *Geophys. Res. Let., 24*, 2663–2666, 1997.

Emardson, T. R., G. Elgered, J. M. Johansson, Three months of continuous monitoring of atmospheric water vapor with a network of Global Positioning System receivers, J. Geophys. Res., 103, 1807–1820, 1998.

Emardson, T. R., J. M. Johansson, G. Elgered, The systematic behavior of water vapor estimates using four years of GPS observations, subm. to IEEE Trans. on Geosci. and remote sens., 1998.

Emardson, T.R, and H.J.P Derks, On the relation between the wet delay and the precipitable water in the European atmosphere, subm. to Meteorol. Applications, 1998.

Lanyi, G., Tropospheric delay affecting radio interferometry, *TDA Progr. Rep. 42–78* ,pp 152–159, Jet Propul. Lab., Pasadena, Calif., 1984.

Noll, C. E., W. Gurtner, Global GPS data flow from station to user within the IGS, in *GPS Trends in Precise Terrestrial Airborne, and Spaceborne Applications*, edited by G. Beutler, G. W. Hein, W. G. Melbourne, and G. Seeber, vol. 115, Springer-Verlag, New York, 1996.

Saastamoinen, J., Atmospheric correction for the troposphere and stratosphere in radio ranging of satellites, in *The Use of Artificial Satellites for Geodesy, Geophys. Monogr. Ser.*, vol. 15, edited by S.W. Henriksen et al., pp. 247–251, AGU, Washington, D. C., 1972.

Tregoning, P., R. Boers, D. M. O'Brien, and M. Hendy, Accuracy of absolute precipitable water estimates from GPS observations, J. Geophys. Res., 103, 28,701–28,710, 1998.

X. Yang, B. H. Sass, G. Elgered, J. M. Johansson, T. R. Emardson, A Comparison of the Integrated Water Vapor Estimation by a NWP Simulation and GPS Observation, *J. Appl. Meteor.*, in press, 1998.

L. Yuan, R. Anthes, R. Ware, C. Rocken, W. Bonner, M. Bevis, and S. Businger, Sensing global climate change using the Global Positioning System, *J. Geophys. Res., 98*, 14,925–14,937, 1993.

About GPS, Modems, and the Meaning of Life

by
Martin Vermeer
& The FinnRef Team*

June 2, 1998

Abstract

This is the tale of the FinnRef Team's quest to get the Finnish Permanent GPS Network's download system to work reliably. Going on for some three years now, the result is a system that succeeds in downloading all of the data from all twelve stations sometimes even for all days of a week. Most weeks, however, we are not that lucky.

The current system uses an MS-DOS script running on an ordinary PC, calling the Ashtech download program `remote` eleven times, and ProComm Plus once (for the Metsähovi Turbo Rogue), and takes care of RINEX conversion and `ftp` transmission to the NKG computing centre in Onsala. Our permanent receivers contain no less than seven different firmware versions, requiring three different versions of `remote` to be kept on our central PC.

Because of the linear nature of an MS-DOS script, when one of the downloads crashes or "hangs", the remaining download job will fail and must be restarted in the morning. Also when the modem fails to reset and release the phone line, subsequent downloads will fail.

In the course of our work, we of the Finnish Permanent GPS Team have thought up many creative approaches to making the download system more reliable. A time switch reboots the PC by midnight, so that during the weekend, if one download fails, it is tried again during the next night (`remote` will download all old files it finds in a receiver). This limits our cleanup job the following Monday.

A newer approach aims at replacing MS-DOS by a multitasking operating system. This has proven tough. We have played around a bit with both Windows95 and Linux; Ashtech warns against using `remote` under Windows, and trying it showed us one reason: it fails to work properly, producing lots of transmission errors. Under Linux, especially with older versions, speed is just a fraction of what it is under DOS alone... So, no final solution yet; just ideas. In the meantime, we muddle on. MURPHY rules![1]

*Matti OLLIKAINEN, Hannu KOIVULA, Markku POUTANEN; occasional others

[1]MS-DOS, Windows95 and Visual Basic are Microsoft trademarks. Ashtech is an Ashtech trademark.

1 Introduction

This article is intended to sketch our experiences with setting up FinnRef, the Finnish Permanent GPS network [Ollikainen97], [Koivula98], and especially its data download system. We describe the current system, the problems we have encountered and are encountering almost daily, and an investigation into possible alternatives. We also sketch relevant ongoing developments elsewhere.

2 Description of our system

Our system, which runs under MS-DOS 6.21, consists of two batch files, `finnnet.bat` and `purapa.bat`, and a lot of additional small configuration and control files. `finnnet.bat` is the main program; it calls purapa.bat once for each station (except Metsähovi, which is *sui generis*) with the arguments being the station four-letter word, the sequence number in the dialing list, the version of the `remote` software used (we have *four* different ones!), whether this data is to be transmitted for EUREF processing or not, the input configuration file name, and a flag which would require another half-page to explain so we let it be.

The batch file is started up by a small timer program (called – how did you guess – `timer`) written by Markku POUTANEN in Borland C, which, while awaiting the pre-set time of download, displays on the MS-DOS text screen a summary of earlier downloads, free disk space and time left to next download. See Fig 1.

Writing this script system had been a painful process. It took many months before most of the bugs were ironed out, and sometimes a small change made in a too carefree manner caused the whole download to fail in the following night. The download scripters (Markku POUTANEN and Hannu KOIVULA) expended a lot of effort on getting this script to work flawlessly.

The hardware that this system runs on is a ordinary Pentium running at (probably) 60 MHz; the disk drives are IDE, except the writable CD-ROM station used for archiving, which requires to be on a SCSI interface. (Actually, the CD-ROM write program, GEAR, requires Windows 95. Using two OS's with different, though supposedly compatible, native file systems on the same partition has also been causing some trouble, necessitating a few Windows re-installs. Currently it all seems to work OK.)

The modem is a Telebit World Blazer like the ones used at our (and Sweden's) permanent station sites also.

3 The firmware zoo

As mentioned above, we have no less than seven different firmware versions in our receivers, requiring three versions of remote to successfully download, a fourth one being needed

Turbo Rogue is a Allan Osborne trademark. ProComm is a Quarterdeck trademark. Linux is a registered trademark of Linus Benedict TORVALDS. UNIX is a trademark currently owned by The Open Group – or was it SCO? (Did I forget anybody? I wonder if **tcl/tk** and **perl** are trademarks?)

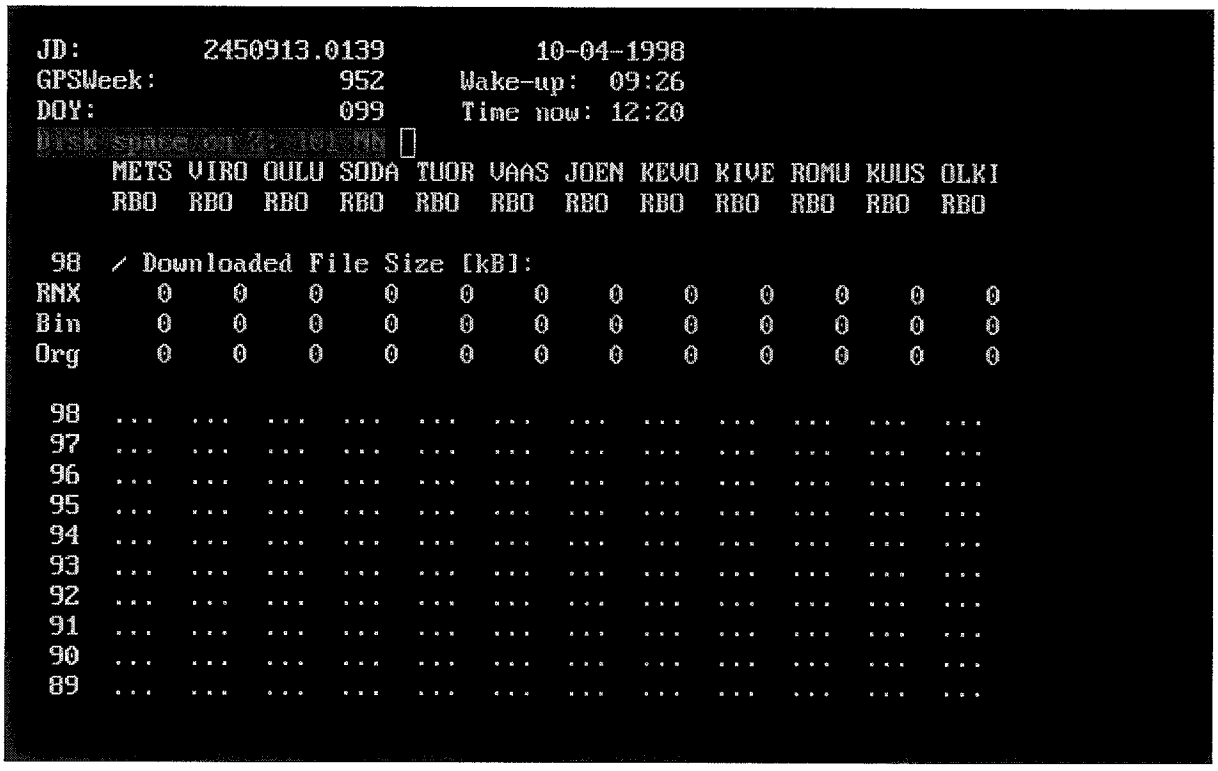

Figure 1: The display of the "timer" program. Here, the disk contains no downloaded data. For downloaded data files, in raw, binary or RINEX, the corresponding dot will change to an asterisk.

only to change parameter settings – long story. It would go perhaps too far here to recount the short but eventful history leading to the current state of affairs. "Version management" is an interesting little subdiscipline of GPS-downloadology. In the below Table 1 we list everything concerning firmware and download software.

4 Varied experiences

First of all, it is important to understand that we have a *linear* DOS script (batch file) which executes a download sequence – including conversions such as RINEX formation and `ftp` upload to the foreign servers expecting our data – *twelve* times in succession. If a download fails, but the software doesn't hang – or it does crash but comes out of it to the command interpreter –, we have no problem; the script just proceeds to the next station on the list. However, if one of the following happens:

- The download software hangs or crashes in a way that brings DOS down;
- One of the conversion routines crashes and brings DOS down;
- `ftp` hangs (as may occasionally happen with our MS-DOS `ftp`) because the server is not available;

Station	Code	Remote name	Remote version	Receiver firmware
Metsähovi	METS	PCPLUS		Turbo Rogue
Virolahti	VIRO	remote	5.2.01	1E00
Oulu	OULU	remt	5.000	1F60*
Sodankylä	SODA	remt	5.000	1E97
Tuorla	TUOR	remt	5.000	1E81
Vaasa	VAAS	remt	5.000	1E81
Joensuu	JOEN	remt	5.000	1E81
Kevo	KEVO	remt	5.000	1E97
Kivetty	KIVE	remo	5.3.00	1F00
Romuvaara	ROMU	remt	5.000	1F60*
Kuusamo	KUUS	remt	5.000	1E95
Olkiluoto	OLKI	remt	5.000	1E82

Table 1: The FinnRef Firmware Zoo (For *, `cgremote` 5.4.00 is needed to change RTCM settings).

...then the rest of the download for that night fails. Think of it statistically: If you have a total failure rate *per station* of only 5%, the resulting failure rate for the whole download – i.e. the probability to find the machine "hanging" next morning – is $(1 - 0.95^{12}) = 46\%$!

In order to make the system a little more robust, we installed a time switch behind the download machine; it reboots the machine every night, just before the download starts. The diskette drive contains a boot copy of MS-DOS 6.21, so that's the system the machine comes up in, and the download script is started automatically. This means that the only crashes that we are going to see, are those that happen in the night before a working day. Note that the system will try to download *all* the closed files it finds in a receiver's memory, also those that were not downloaded the previous day due to (e.g.) machine crash.

Statistics: during the beginning of 1998 (January 1 - April 9) we found the machine hanging or crashed on 17 of 66 working day mornings, i.e. 26% of cases. This corresponds to a single station download failure rate of only 2.5%.

The statistics presented here is probably rather representative. We have noticed that a problem never comes alone: weeks may pass without a single hang/crash, and then suddenly the machine hangs for five days in succession. There seem not to be certain stations causing problems, they are all represented in our lists. Also phone line quality is probably irrelevant: it may prevent a single station from being downloaded, but does not appear to crash our download PC.

Mr. MURPHY's presence is strongly felt.

5 About smoking disk drives and such things

We started deploying the permanent network in 1994. In those early days, download had to take place three times a day due to small receiver memory. The script contained a facility to ring, if a download failed, a specified phone number, e.g. the network operator's home number or pager. There were plans at some point to even allow this system to "phone home" during the night, but this was abandoned quickly...

During the summer of 1996, a big GPS campaign was going on in August-September, the First EUREF Densification Campaign, or EUREF-FIN96, as we called it. Those of us that were not in the field, were on holiday, and for a few days, Martin VERMEER was the only one on the spot.

Markku POUTANEN periodically checked in to make sure that our permanent GPS collection system was running properly, and noticed that something was wrong. One disk drive was not working properly. He decided to visit the Institute during his holiday, and when entering the computer room, smelled: *smoke*!

The disk drive that didn't work, was the one containing all the backed-up data from the ongoing campaign collected by the permanent stations, in other words, the data that would provide the "backbone" of the solution to be computed. Markku got a little nervous at that point.

Fortunately it was only the power supply that was broken. It was fixed, and no data was lost.

For Matti OLLIKAINEN, Vaasa has become a familiar piece of Finnish countryside. Several times he has driven five hours, pushed a reset button on either GPS receiver or modem (or both), and driven back for another five hours. Vaasa is located far from any human habitation.

Fortunately, Vaasa has behaved well of late [little prayer]. This experience has stressed, somewhat belatedly, the importance of choosing our sites close to an existing facility with people that can possibly help in such a situation. In Tuorla, Oulu, Sodankylä and Kevo, there is research station personnel that can be called upon for a helping hand, and in Olkiluoto, Romuvaara and Kivetty, the people of the Posiva Oy power company have helped us out also. Only Vaasa, Virolahti, Joensuu and Kuusamo are in the outback.

6 About "highly effective" data compression

There is an interesting thing called "data mode 3" in Ashtech. We found out by accident. It appears to be a variant of the geodetic data mode, a way to store this data in the receiver memory in compressed form, expanding it after download ([Ashtech97], p. 72). The compression factor is around 3. Of course, using this compression technique would be a very attractive way to make the receivers' memory last longer when phone lines are down, and to shorten the download times especially over bad lines. Perfect!

There lives a serpent in paradise. As we discovered to our ashtonishment and shame – *after* having collected data for a paying customer – this "mode 3" data does not contain doppler shifts! The manual ([Ashtech97]) mentions nothing of this.

Enter Markku POUTANEN, our fixer of insoluble problems. He quickly wrote a program using Bernese routines – in the process uncovering a bug in one of them – to *generate* the missing dopplers by software. This was supplied to the customer – who was made aware of the situation – and they have been very happy with it.

Markku also got software made that is able to interpolate observations to a higher sampling density than the one (30 s) under which they were originally collected. This may come in handy when aerial photographers want reference station data at, say, 1 s or 0.5 s interval. If this works (has not yet been operationally tested!) we will not have to manually change the sampling rate for our permanent stations any more ever. But... *don't* try to interpolate in this way the GPS data collected on board the aircraft. It only works for fixed stations!

7 Alternatives and prototypes

7.1 Reasons

As it is currently not possible to get hold of the source of the Ashtech `remote` download program, our only hope to improve the reliability of our download system is somehow to "encapsulate" this MS-DOS executable, in such a way that crashing or hanging this single application does not bring down the entire system. The obvious way to do this is to run `remote` as *one process* on a multitasking operating system. Clearly, the OS must be able to emulate MS-DOS in order to allow this; systems meeting these requirements are the various Windows versions and the various versions of UNIX, including Linux.

If, additionally, we would succeed in freeing up the modem and telephone line, we might have some hope of continuing the download process and limit the "damage" to data from only one GPS station.

Recently a second accident happened that reinforced the impression that a solution of this kind would be a good idea: the `ftp` server at Onsala went down, and our download PC remained hanging trying to do the impossible upload...

In our desperation we have even sometimes considered the option of putting up two or more separate PC's with their own modems working in parallel, brute-force multitasking indeed!

7.2 First try

Our first attempt exploring alternatives to the existing download system was simply trying to run the MS-DOS batch file system, `finnnet.bat` + `purapa.bat`, in a DOS emulator window under Linux. If we could do this, the argument ran, we could step-wise introduce multitasking and so on.

The emulator program, `dosemu`, was found to be quite stable and quite good; we tried out each of the DOS programs called from the script, the four versions of `remote`, `pcplus` used for Metsähovi, the rinexing software, the format conversion software (`hose` as well as `dc4`) and a few smaller things. Individually they worked fine. (This experimentation was

quite exciting: a "hurrah!" went up everytime the next program ran to finish. Emulation, and running software under an operating system it was not originally designed for, is always a gamble.).

However, when running the complete script, things were not so good. The script remained "hanging", possibly at a point where it called back to UNIX to execute a UNIX `ftp` command, or when calling a DOS memory extender – features known to be somewhat fragile. We never identified what precisely went wrong, but the system was hanging badly. It was decided then, that instead of trying to port the system unchanged, we should try to make it run under Linux natively for as great a part as was possible, calling the emulator only for software for which there was no Linux counterpart, such as the four `remote`'s.

7.3 A visual download script prototype

The first author chose to try out his ideas for a better download system by writing a script in the **tcl/tk** language, calling the DOS emulator only for running `remote` and `hose`.

tcl/tk is a pretty language; **tcl** is basically just a scripting language ("shell") for doing the things that shell scripts are used for, while **tk** again provides the building blocks for a graphic user interface (GUI). While **tcl** is somewhat obtuse and takes some effort to learn – but very powerful, allowing on-the-fly addition of functionality, just like **lisp**! – **tk** is the UNIX counterpart of Visual Basic.

tcl and **tk** were developed by John OUSTERHOUT [Ousterhout94]. Like Java, it is a free software product running on many different OS platforms.

To get an idea what a GUI built in **tcl/tk** looks like, have a look at Figure 2, which was taken from our working prototype.

We have done some timing experiments. A typical download, which would take 10-15 minutes per station, under version 5.000 of `remote` would take as much as half an hour in the Linux MS-DOS emulator (As for the Windows 95 DOS emulator, it didn't even get that far with the any of the `remote` versions, mostly producing lots of errors and failing on that). With the older 1E00 firmware and `remote` v. 5.2.01, the download under emulation even slowed down to more than an hour, totally unacceptable.

Operating environment	Download time	Remarks
MS-DOS raw	11 min	
Windows 95 +DOS	~18 min	
Linux + DosEmu	~18 min	Different machine (probably faster)

Table 2: Download testing of operating environments

However, we will have to upgrade all our receiver firmware anyway this year, due to the addition of the VAISALA Oy meteo sensors, and switch to using `cgremote` (cg = "Continuous Geodetic"), so this old stuff will be phased out. `cgremote` is designed to be (and is) Windows-compatible, apparently by not using any "dirty tricks" to access the serial port.

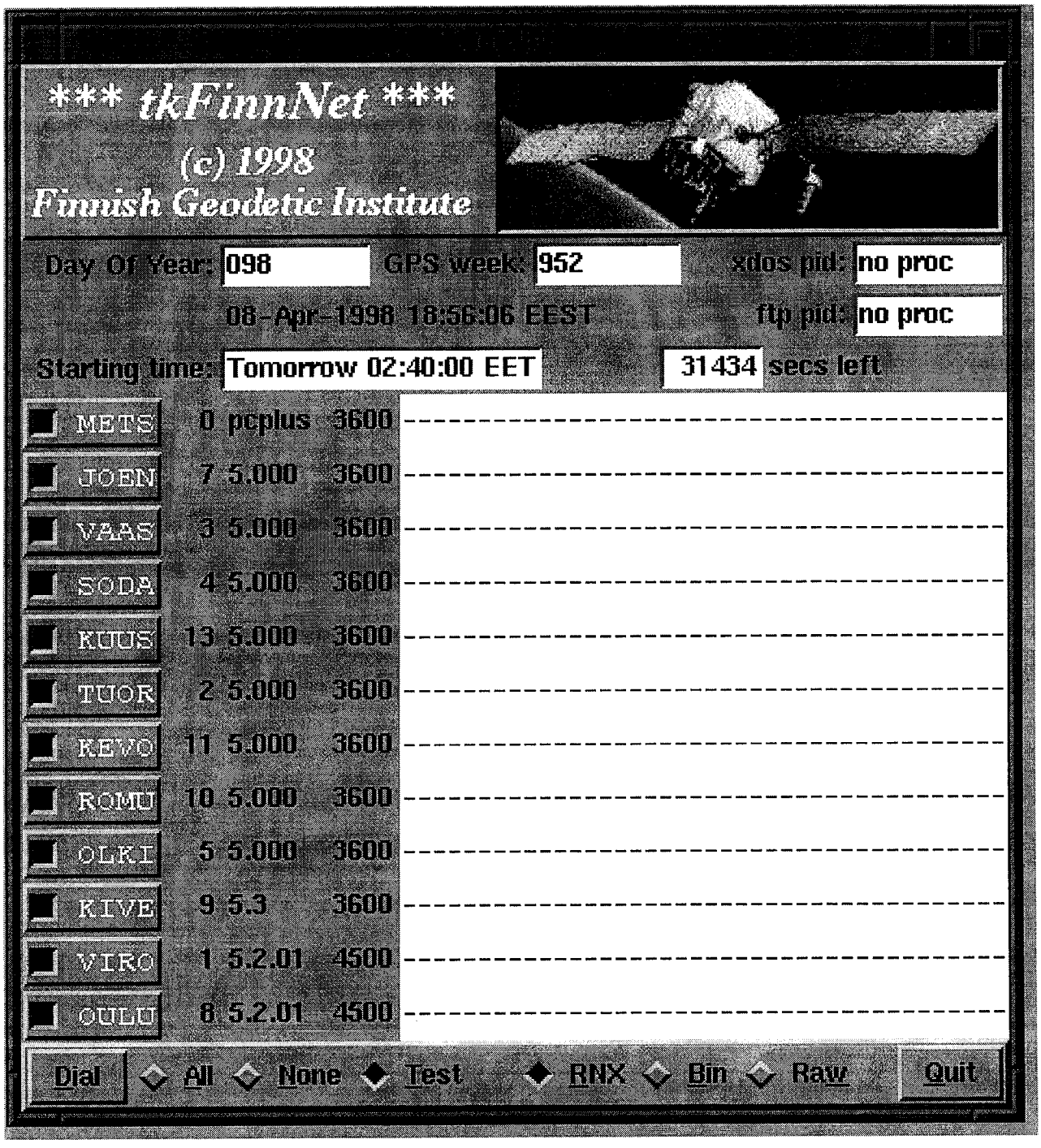

Figure 2: The prototype GUI, written in **tcl/tk**. Currently 700 lines of code.

We recently tested one download of the station Romuvaara (Kuhmo) under MS-DOS raw, Windows 95 and Linux, using the new software `cgremote`. The results are given in Table 2. It is seen that emulation makes the speed drop by nearly half. This is probably due to a technical property of emulating access to the serial hardware which is the same for

all operating systems. The speed loss, which is the price for improved reliability until a native Linux version of the software comes up, means a significant growth of our phone bill.

8 UNAVCO and geodetic GPS

Also UNAVCO is looking into the problem of geodetic GPS data collection. A system exists (LAPDOGS) for downloading data from Trimble and Turbo Rogue GPS receivers, with Ashtech support to be added during 1998 (Wayne S. SHIVER, personal comm.)

The LAPDOGS software has been ported to a number of platforms including most UNIXes and Linux. Also Windows is supported, but less well tested, as it is apparently not the preferred platform for UNAVCO.

The UNAVCO software has been written in **perl**, a scripting language designed by Larry WALL [Wall96] originally for UNIX and the Internet, and freely available for a number of different platforms. It is somewhat similar to **tcl**, but more mature and widespread. It can also be integrated with **tk** for building graphical user interfaces.

We are following this development with interest; even if we would choose not to use the package ourselves, still an open software solution to the problem of Ashtech data download is inevitably of great interest to us.

I heard (Erricos PAVLIS, personal comm.) that the UNAVCO group works with Ashtech Inc., who were found to be cooperative as UNAVCO represents potentially a huge market. That this market, and the American scientific establishment in general, favours UNIX solutions, is interesting. UNIX isn't dead yet [Byte98], [Petreley98]!

As I see it, if Ashtech Inc. had been wise (i.e. listened to their engineers instead of their lawyers), they would have long ago thrown that part of `remote` that handles the actual downloading, out into the open, i.e. publish the source code. One must understand that Ashtech is not in the software business; they are in the complete system business, selling systems for geodynamic GPS monitoring of which `remote` is only a small part.

All that would be needed to be made public is the part of `remote` that does the *actual x-modem download*, taken apart as a separate program; the user interface for changing receiver settings etc. can stay where it is. Ashtech is not in any position to effectively debug this download code; the international GPS geodynamics community, running these systems around the clock year in year out, is in this position, and also has the motive to do so. Scientists are used to having source available for the critical software they use. By publishing the source code, Ashtech would lose very little; they would gain, in time, a properly debugged component – running as well in operating environments that scientists and engineers prefer for sound technical reasons over MS-DOS or Windows –, adding value and competitiveness to one of Ashtech's stategic products.

For a general discussion of these issues, which not only is worthwhile reading, but also highly relevant in this specific context, see [Raymond98] ("Widget Frosting").

9 The effect of future developments

Currently, of the data path leading from the field to the international data centres working with our GPS data, the first segment, the download by modem to Masala, is the weakest link by far. This situation will become unacceptable on the longer term; we have to raise this link to the same level of robustness that the Internet enjoys thanks to its well-tested open software base.

We must be aware that the present way of functioning of the permanent GPS network and its download system may not be maintainable in the future. Currently data from the network is available on average slightly over 12 hours after the moment at which it was collected; for some fields of application, especially the use of GPS-determined integrated water vapour columns for operational weather prediction, this delay may not be acceptable.

There has been talk in the GPS meteorology community about shortening this "latency" to something around three hours; this would mean that the GPS data has to be downloaded in pieces of three hours length, and every three hours a download would have to take place from *every* station.

Please try to imagine what this would mean: during a evening and night of 16 hours, no less than $12 \times 16/3 = 64$ station downloads would have to take place! At the reliability level quoted above of 97.5%, this means a total success rate overnight of $0.975^{64} = 20\%$!

Obviously this is totally unacceptable. So, either we have to permanently hire some guardsmen to sit watch through the night and restart the machine whenever it goes down – joking, of course – *or* we have completely re-think, and re-implement the system on an operating system platform that is known to be *absolutely stable* and cannot be brought down by one application crashing. Our prototype experiments seem to indicate that this would be a fruitful avenue of research.

Late breaking news: The GPS meteorologists are even proposing a download interval of one hour (Werner GURTNER, personal comm.), with a merging into a larger file – to be submitted in the regular way – scheduled every 24 hours!

10 Choosing the operating system

Besides Windows 95 – which is application-crashable – one could of course consider Windows NT. This is a true 32-bit multitasking system, and known to be much stabler than Win95, while supporting most of its software. It is already quite fashionable in business circles.

Undoubtedly a system like the one sketched here could be implemented under Windows NT... after purchasing the licence, probably upgrading the existing PC to meet the higher resource requirements of this demanding OS, and possibly changing some hardware for compatibility reasons. With Linux, we just started experimenting using the CD purchased privately (US$49) by one of us, out of general curiosity. But originally also with a notion

that it might have to offer us something useful – we are scientists, and trying out new things is very much our business!

In my own personal (MV) estimation, Linux (and UNIX in general) wins on three counts here: maturity of the basic OS including networking, track record in server applications, and quality of technical support. Concerning *maturity*, Linux was made to conform to UNIX industrial standards, developed and tested in real life for over twenty years. And UNIX has always been the OS of the Internet.

Linux has also a good track record in various *server applications*. The FGI is among many users running a small `ftp` server[2] under Red Hat Linux 4.2 (Washington University's `ftp` daemon `wu-ftpd`), as well as a Samba file server networking our Windows machines running on our Digital UNIX Alpha "mainframe". Installing Samba, a powerful but complex package, was done by Juha JAAKKOLA, our system administrator.

It is also a well kept secret that Apache, the freely available UNIX/Linux Web server software, runs nearly half of the world's `www` servers ([Berst97]).

By *technical support* I don't mean hand-holding non-professional computer users. It's in-depth assistance when you're trying to do something nobody has done before, from the people that actually wrote the software ([Foster98]). For that kind of support, Linux is in my experience second to none.

There is a broad consensus in the industry (e.g., [Aberdeen97a], [Coffee98]; spectacularly, [Aberdeen97b]), that there continue to be serious stability and other issues with Windows NT, limiting its penetration into the mission-critical server marketplace. While this does not exactly project a good image, it is probably not a primary concern for us. What is, is that most of the problems we have had in our business simply stem from trying to fit together a number of "black boxes" that we cannot look into and that we have no in-depth understanding of. Windows NT would be just one more such black box. This is not the way a serious scientist is supposed to work, and not an experience we are eager to renew.

References

[Aberdeen97a] The Aberdeen Group, October 1997: Windows NT Server 4.0: First Anniversary Review. Executive White Paper.
`http://www.aberdeen.com/research/comp/whtpaper/1997/nt/97100199.htm`

[Aberdeen97b] The Aberdeen Group, autumn 1997: Case study: Migration Migraines.
`http://www.aberdeen.com/research/comp/onsite/case1/body.htm`

[Ashtech97] Ashtech Inc: Continuous Geodetic Reference Station (CGRS)™ Operation and Technical Manual. Sunnyvale, 1997

[2]
```
[mv@ftp mv]$ date
Fri May 8 13:50:08 EET DST 1998
[mv@ftp mv]$ uptime
1:50pm up 130 days, 1:19, 1 user, load average: 0.00, 0.01, 0.00
```

[Berst97] Jesse BERST: The World's Cheapest Web Server. The World's Most Popular Web Server. (Psst! It's the Same One!). Sept. 1997. *Anchordesk*, Sept. 26, 1997. See especially attached discussions.
`http://www.zdnet.com:80/anchordesk/story/story_1284.html`

[Byte98] BYTE magazine, Jan. 1998: Putting Unix in All the Right Places; The reports of Unix's death are greatly exaggerated. John Montgomery.
`http://www.byte.com/art/9801/sec19/art4.htm`.

[Coffee98] Peter COFFEE: We have no failure to communicate. PC Week, April 13, 1998.
`http://www.zdnet.com/pcweek/opinion/0413/13coff.html`

[Foster98] Ed FOSTER: InfoWorld Best Technical Support Award. 1998.
`http://www.infoworld.com/cgi-bin/displayTC.pl?97poy.supp.htm`

[Koivula98] Hannu KOIVULA, Matti OLLIKAINEN, M. POUTANEN: The Finnish Permanent GPS Network – FinnRef. These Proceedings. Gävle, 1998.

[Ollikainen97] Matti OLLIKAINEN, Hannu KOIVULA, Markku POUTANEN, Ruizhi CHEN: Suomen kiinteiden GSP-asemien verkko (in Finnish; contains maps and figures). Geodeettisen laitoksen tiedote 16. Masala, 1997.

[Ousterhout94] J. K. OUSTERHOUT: TCL and the TK Toolkit. Addison-Wesley, Reading, MA, 1994

[Petreley98] Nicholas PETRELEY: The new Unix alters NT's orbit. The re-emergence of Unix threatens to modify the future direction of NT. *NC World*, April 1998
`http://www.ncworldmag.com/ncworld/ncw-04-1998/ncw-04-nextten.html`

[Raymond98] Eric S. RAYMOND: The Business Case for Open-Source. 23 Feb. 1998.
`http://www.opensource.org/for-suits.html`

[Wall96] Larry WALL: Programming Perl 2nd edition. O'Reilly & Associates, 1996.

Computation of land uplift from the three precise levellings in Finland

Jaakko Mäkinen and Veikko Saaranen
Finnish Geodetic Institute
P.O.Box 15
FIN-02431 Masala, Finland
tel +358 9 255550
fax +358 9 29555200
e-mail Jaakko.Makinen@fgi.fi

Abstract

We present a land uplift map based on the three precise levellings in Finland, with central epochs 1902, 1946, and 1986, and compare it with earlier results.

1. Introduction, observation material

The exposition here is not self-contained but leans on Mäkinen and Saaranen (1998), which the reader should consult for details and references where necessary. In the sequel we refer to it as Paper 1. In part we present a summary of it, in part we expand on some aspects in it. We also have additional material from 1996–1997 which we incorporate in a new land uplift map.

The Third Levelling of Finland, still in progress, already covers the area common to the First Levelling (Blomqvist and Renqvist 1910) and to the Second Levelling (Kääriäinen 1966). We use all three levellings and work with two different data sets. First, we have the benchmarks and lines which belong to all three levellings. We call this the common network. In it we can solve for velocities from any combination of the levellings, and thus for changes in velocities as well. However, we can solve for velocities in a larger network. It suffices that the bench marks belong to any two of the three levellings. We call this the maximum network. It is used to draw the land uplift map. Figure 1 and Table 1 summarize the observation material. We only use bench marks in bedrock.

Table 1. Network statistics. The precision figure is the a-priori estimate from loop misclosures. Both it and the mean epoch refer to the common network. There are 199 bench marks (BM) in the common network and 369 BMs in the maximum network.

Levelling	Performed years	Mean epoch	Precision mgpu/$\sqrt{\text{km}}$	Number of loops in	
				common net	maximum net
First	1892–1910	1902	1.254	9	11
Second	1935–1955	1946	0.460	9	14
Third	1978–	1986	0.854	9	22

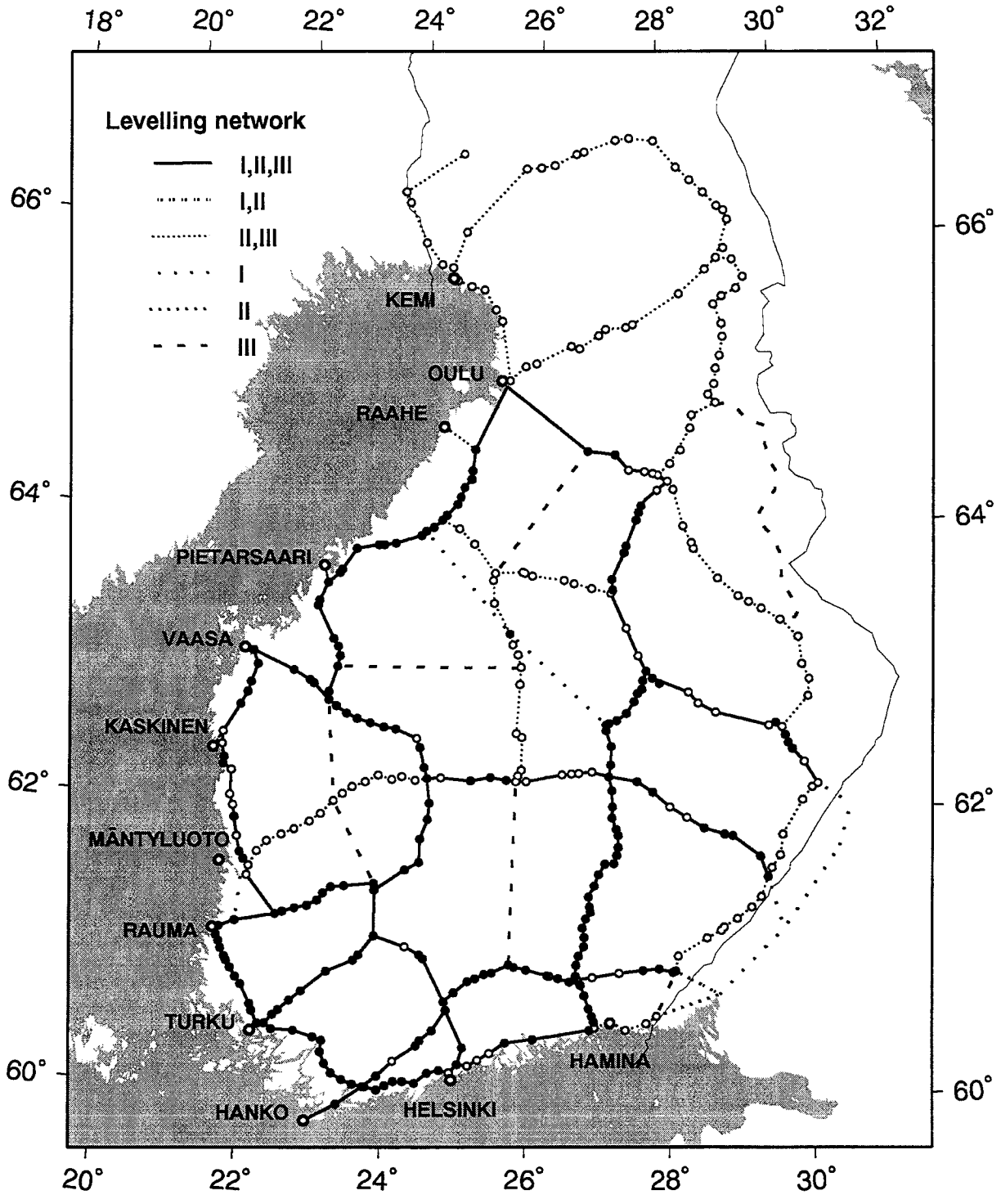

Figure 1. The networks we use. Third Levelling results up to and including work in 1997 are included. Bench marks which belong to all three levellings are marked with solid circles, bench marks which belong to two levellings are marked with open circles. Tide gauges (we only use Hanko in this paper) are marked with large open circles. The maximum network consists of the totality of bench marks and lines. The common network consists of the BMs marked with solid circles and of the solid lines, plus two lines in the southeastern part of the network, which run along different routes but can be used between their end points.

2. Models and solution strategies

In forming the model, three aspects must be considered:

Model	Approach adopted
Temporal	Velocities. Irregularities are investigated by allowing different velocities between levellings 1→2 and 2→3. This is approximately equivalent with including acceleration. Acceleration model explored for comparison (results not shown here).
Spatial	No assumptions, e.g., no "velocity surface".
Stochastic	Classical, i.e., with error variance proportional to line length. Intra-levelling correlations: are not modelled. But we have applied multivariate modelling with a full (3×3) covariance matrix between levellings, in order to interpret our univariate solutions (Paper 1).

This leads to the observation equation

$$y(i,j,k) = h(j,t_0) - h(i,t_0) + \left[\dot{h}(j) - \dot{h}(i)\right]\left[t(i,j,k) - t_0\right] + e(i,j,k) \qquad (1)$$

where the notation is

$y(i,j,k)$	observed height difference between BMs i and j in the levelling $k, k = 1,2,3$
$t(i,j,k)$	epoch of the observation
t_0	reference epoch of the heights
$h(i,t_0), h(j,t_0)$	heights of the BMs i and j at epoch t_0, unknowns
$\dot{h}(i), \dot{h}(j)$	vertical velocities of the BMs i and j, unknowns
$e(i,j,k)$	error in the observation

We could call (1) the "master" observation equation, as new equations can be derived from it. First, we may eliminate the heights $h(i,t_0), h(j,t_0)$, which are nuisance parameters for the velocity problem. Subtracting levelling 1 from levelling 2 we have

$$y(i,j,2) - y(i,j,1) = \left[\dot{h}_{12}(j) - \dot{h}_{12}(i)\right]\left[t(i,j,2) - t(i,j,1)\right] + e(i,j,2) - e(i,j,1) \qquad (2)$$

where $\dot{h}_{12}(i), \dot{h}_{12}(j)$ are velocities between levellings 1 and 2. Similarly, subtracting levelling 2 from levelling 3

$$y(i,j,3) - y(i,j,2) = \left[\dot{h}_{23}(j) - \dot{h}_{23}(i)\right]\left[t(i,j,3) - t(i,j,2)\right] + e(i,j,3) - e(i,j,2) \qquad (3)$$

We then can solve for velocities from (2) and (3), either putting $\dot{h}_{12}(i) \equiv \dot{h}_{23}(i)$ for all i, or allowing $\dot{h}_{12}(i) \neq \dot{h}_{23}(i)$. If we are only interested in the velocity change in time, i.e. in

$\dot{h}_\Delta(i) = \dot{h}_{23}(i) - \dot{h}_{12}(i)$ then we can again eliminate $\dot{h}_{12}(i)$ and $\dot{h}_{23}(i)$ from (2) and (3) to leave just the change $\dot{h}_\Delta(i)$:

$$\begin{aligned}&\left[t(i,j,3) - t(i,j,2)\right]^{-1}\left[y(i,j,3) - y(i,j,2)\right] - \left[t(i,j,2) - t(i,j,1)\right]^{-1}\left[y(i,j,2) - y(i,j,1\right] \\ &= \left[\dot{h}_\Delta(j) - \dot{h}_\Delta(i)\right] + error\end{aligned} \tag{4}$$

We do not write out the error term in detail. In essence, (4) is the second difference of the three levellings, divided by 40 years.

Remark: It should be kept in mind that heights are not estimable from levellings, only height differences between points are (and linear functions of height differences of course). Similarly, neither velocities nor velocity changes in time (or accelerations) are estimable, only their differences between points. Physically this just expresses the fact that vertical motion which is the same for all points in the network cannot show up in repeated levellings. For instance, it does not make sense to formulate the hypothesis of no velocity change as "$\dot{h}_\Delta(i) = 0$ for all i". The correct phrasing is that "all estimable functions of the $\dot{h}_\Delta(i)$ are zero". To formulate all relevant sentences rigorously in terms of the estimable quantities only (height differences, velocity differences etc.) would make our writing very clogged, so we just ask the reader to remember this.

3. Modelling investigations in the common network

We have determined velocities from all four combinations of the levellings, (I,II), (II,III), (I,III) and (I,II,III), by two methods, i.e., keeping the heights (observation equation 1) or eliminating them by forming differences (equations 2, 3),. This gives 8 solutions. It turns out (cf. Paper 1) that

(A) for any combination, the subtraction has only a small effect on the *estimated velocities*, but
(B) for some combinations, it has a large effect on the a-posteriori *error estimation.*

In Section 7 (Figure 7b) we show an example of (A). The interpretation of (A) revolves around the closing errors of the loops: There are two kinds of velocity signals present in the data. First, we have the differences between the levellings. This is the major signal. Second, we have the misclosures of the loops in the individual levellings. They contain a contribution from velocities, as the lines of the loops were levelled at different epochs. However, this spread in epochs is small compared with the time difference between the levellings, and the second signal is a minor one. Now, when we subtract the levellings from each other, the first signal is unchanged, but we lose track of the second signal (Vaníček et al. 1987, p.170).

It is sometimes conjectured (Vaníček et al. 1987, p. 171) that in the presence of unmodelled systematic levelling errors the velocity estimate from differences might be the better one, as some of these errors are eliminated in subtraction. However, we show in Paper 1 that even in this case the estimates cannot differ much.

Item (B) can be interpreted using misclosures as well. With two levellings in the same network and heights retained, the velocity model primarily absorbs the difference between the levellings and when that is the important signal the model cannot pay much attention to improving their internal consistencies[1] (cf. remarks above and Paper 1, Table 3). The fitting process thus is left with misclosures of approximately the original size for error estimation. In the alternative model, when the levellings are subtracted from each other, the error estimation comes from the misclosures of the difference, i.e., from the differences of the misclosures. If misclosures in the same loops have predominantly the same sign, they are attenuated in the difference and the error estimate will be lower than that expected from the minuend and the subtrahend. If misclosures have predominantly different signs, they are amplified and a high error estimate for the difference obtained.

The coherence in the misclosures can be formulated in terms of correlations between the levellings (Paper 1) which then can be tested for significance. However, even when the empirical correlations are not high enough to be statistically significant they still may have appreciable effects on the error estimation, and this independently whether we are even conscious of their existence. And on the other hand, a statistically significant correlation can be spurious all the same.

4. Estimating the error of velocity change

The uncertainty in the error estimation does not perhaps matter much in the velocity context. After all, the errors of the velocities are in any case small compared with the velocities themselves, there is no controversy on whether uplift is taking place or not. However, for estimation of velocity change in time we have the same uncertainty. We have three alternative models:

(i) Append an acceleration term (i.e., a term with second power in time) to observation equation (1) and determine heights, velocities, and accelerations.
(ii) Use observation equations (2) and (3) (the pairwise differences of the levellings) to determine two sets of velocities $\dot{h}_{23}(i), \dot{h}_{12}(i)$ and subsequently velocity change $\dot{h}_{\Delta}(i) = \dot{h}_{23}(i) - \dot{h}_{12}(i)$.
(iii) Use observation equation (4) (the second difference of the three levellings) to determine just velocity change $\dot{h}_{\Delta}(i)$.

These models produce almost the same velocity change but rather different error estimates. And here error estimation is critical since tests of significance for velocity change depend on it.

Now, in all models (i),(ii),(iii) only misclosures of the three levellings are left for error estimation as the parametrisation exhausts other discrepancies. In all models the information about velocity change resides essentially in the second difference of the three levellings and

[1] This apparently is often overlooked. For instance, Andersen and Remmer (1982) discovered that they could considerably decrease the misclosures of the First and Second Levellings by just multiplying Kääriäinen's (1966) velocities with a constant. But it seems that they have not checked how well the scaled velocities explain the observed height differences.

their misclosures are combined to estimate its error. However, the combination steps are different and the covariances between the levellings influence the outcome in different ways. We state somewhat loosely and without proof the following result:

Result: Denote by Σ the empirical (3×3) variance-covariance matrix of the three levellings.

$$\Sigma = \begin{pmatrix} \sigma_1^2 & \sigma_{12} & \sigma_{13} \\ \sigma_{12} & \sigma_2^2 & \sigma_{23} \\ \sigma_{13} & \sigma_{23} & \sigma_3^2 \end{pmatrix} \qquad (5)$$

The elements on the diagonal of Σ are the empirical variances per distance unit, and the off-diagonal elements are the corresponding covariances. (They are determined either from loop misclosures or from the residuals of a preliminary adjustment, see Paper 1). The second difference of the three levellings (I,II,III) can be symbolically written

$$(\mathrm{III} - \mathrm{II}) - (\mathrm{II} - \mathrm{I}) = 1\times\mathrm{I} - 2\times\mathrm{II} + 1\times\mathrm{III} = (1 \;\; -2 \;\; 1)(\mathrm{I} \;\; \mathrm{II} \;\; \mathrm{III})^T = c^T(\mathrm{I} \;\; \mathrm{II} \;\; \mathrm{III})^T \qquad (6)$$

where the coefficient vector $c = (1 \;\; -2 \;\; 1)^T$. Denote the variance estimate for the second difference by σ_Δ^2. Then it can be shown that in the three models (i),(ii),(iii) it is computed approximately as

(i) $\sigma_\Delta^2 = \sigma_1^2 + 4\sigma_2^2 + \sigma_3^2$

(ii) $\sigma_\Delta^2 = (\sigma_1^2 - 2\sigma_{12} + \sigma_2^2) + 2\sigma_2^2 + (\sigma_2^2 - 2\sigma_{23} + \sigma_3^2) = \sigma_1^2 + 4\sigma_2^2 + \sigma_3^2 - 2\sigma_{12} - 2\sigma_{23}$

(iii) $\sigma_\Delta^2 = c^T\Sigma\, c = \sigma_1^2 + 4\sigma_2^2 + \sigma_3^2 - 4\sigma_{12} - 4\sigma_{23} + 2\sigma_{13}$

We note that (i) uses only the diagonal elements of Σ, (iii) uses Σ in full, and (ii) uses its 2×2 submatrices (I,II) and (II,III), taking into account their intersection σ_2^2.

In our data there is a significant negative correlation between the First and the Third Levelling (cf. Paper 1). This has the consequence that in (iii) the accuracy of the second difference of the three levellings is estimated to be better than the accuracy of the First Levelling alone! The result is a high statistical significance for velocity change in (iii). But even the non-significant correlations between other pairs influence the tests. To avoid misunderstandings, we would like to point out that the dependence of error estimation on the model and on the empirical covariances between epochs is not due to any pathological characteristics in our data, but is present in any deformation analysis (cf. Paper 1).

Beyond the play with covariances there is another, perhaps more basic problem in estimating velocity change from three levellings. As previously mentioned, the model is then capable of explaining all differences between the levellings and only loop misclosures remain to estimate error. One could advance the suspicion that loop misclosures in general may provide underestimates. From this viewpoint, one would need two levellings to estimate levelling error in the absence of vertical motion, three levellings to estimate it in the case of constant velocities, and four levellings in case of accelerations. Alternatively, one might try to introduce prior information on, say, spatial wavelengths, to separate vertical motion from levelling error.

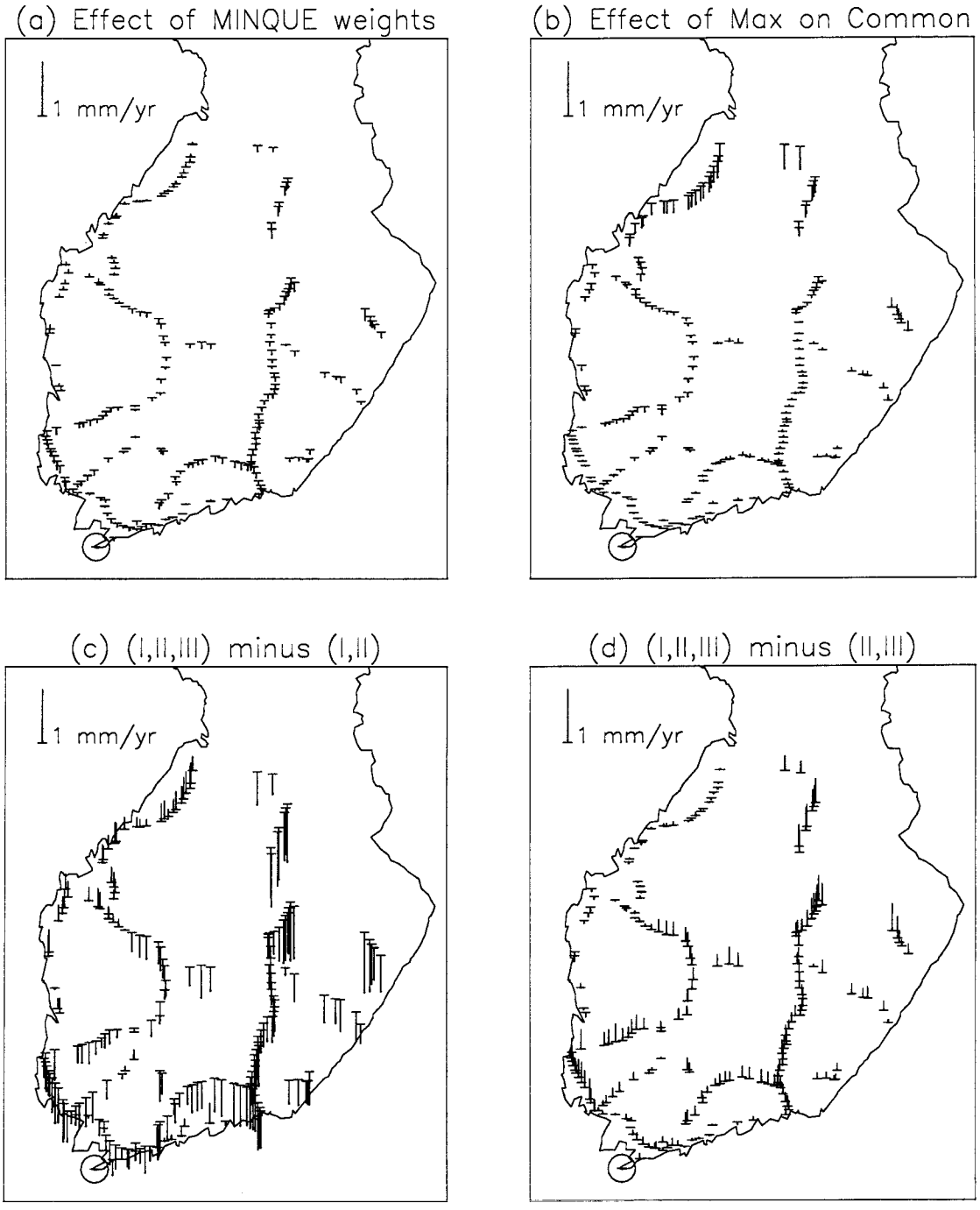

Figure 3. The effects of weights and levellings used on estimated velocities in the common network. All comparisons are relative to Hanko (circled).

(a) All three levellings, solution with MINQUE weights (7) minus solution with a-priori weights (Table 1).

(b) All three levellings, solution using the maximum network minus solution using only the common network. MINQUE weights were used in both.

(c) Solution using all three levellings minus solution using First and Second Levellings only.

(d) Solution using all three levellings minus solution using Second and Third Levellings only.

See Section 5 for comments on (a), (c) and (d), Section 6 for (b).

5. Variance component estimation

Fitting the model (1) with constant velocities to the three levellings in the common network, using the a-priori weights derived from loop misclosures (Table 1) results in the a-posteriori variance factor of $\hat{\sigma}_0^2 = 1.85$ which differs significantly from unity. In Paper 1 we have adopted the working hypotheses that this is not due to change in velocities but to an a-priori overestimation of weights, and that the covariances between the levellings are spurious. For error estimation, the assumption of constant velocities yields 207–9 = 198 additional discrepancies on the 207 BM intervals we use in the common net. Otherwise we only have the 3×9 = 27 loop misclosures. We have used the iterated MINQUE (Minimum Norm Quadratic Unbiased Estimation) technique (Rao 1971). Interestingly, this does not lead to a uniform scaling of the a-priori errors of Table 1 by $\sqrt{1.85} = 1.36$. The final iterated variance estimates for the three levellings are

$$\begin{aligned} \hat{m}_1^2 &= 1.61^2 \times 1.254^2 = (2.01^2 \quad \text{mgpu} / \sqrt{\text{km}})^2 \\ \hat{m}_2^2 &= 1.23^2 \times 0.460^2 = (0.57^2 \quad \text{mgpu} / \sqrt{\text{km}})^2 \\ \hat{m}_3^2 &= 1.03^2 \times 0.854^2 = (0.88^2 \quad \text{mgpu} / \sqrt{\text{km}})^2 \end{aligned} \qquad (7)$$

The velocity estimates change little in the process (Figure 3a). Independently of weights, the solution using all three levellings (I,II,III) is bound to lie between the pairwise solutions from (I,II) and (II,III). It is closer to the latter because of the low weight of the First Levelling compared with the Third (Figure 3c,d).

6. Land uplift map

We have solved for velocities in the maximum network (Figure 1), using the MINQUE weights (7) estimated in the common network, and the model (1) with constant velocities through all the three levellings. The a-posteriori variance factor was $\hat{\sigma}_0^2 = 0.87$, but since the maximum network includes several lines with one or two levellings only, we consider the MINQUE variances (7) determined in the common network better and apply unity instead. The numerous additional lines in the maximum network have only locally some influence on the solution within the common network (Figure 3b).

Repeated levellings only provide velocity differences. We have joined them to the tide gauge result by Vermeer et al. (1988) at Hanko (Figure 1), where they obtained the uplift 2.73 mm/yr relative to mean sea level (MSL). The resulting land uplift map is shown in Figure 4 and the standard errors relative to Hanko in Figure 5. They are maximally about 0.5 mm/yr. For comparisons at other tide gauges and with other tide gauge computations see Paper 1.

7. Comparisons with other results

In comparing our map (Figure 4) with the maps by Kääriäinen (1966) and Suutarinen (1983) the difference in zeroes should be kept in mind. Both aforementioned maps include an estimate for the eustatic rise in MSL, and thus show uplift relative to the geoid, while our map

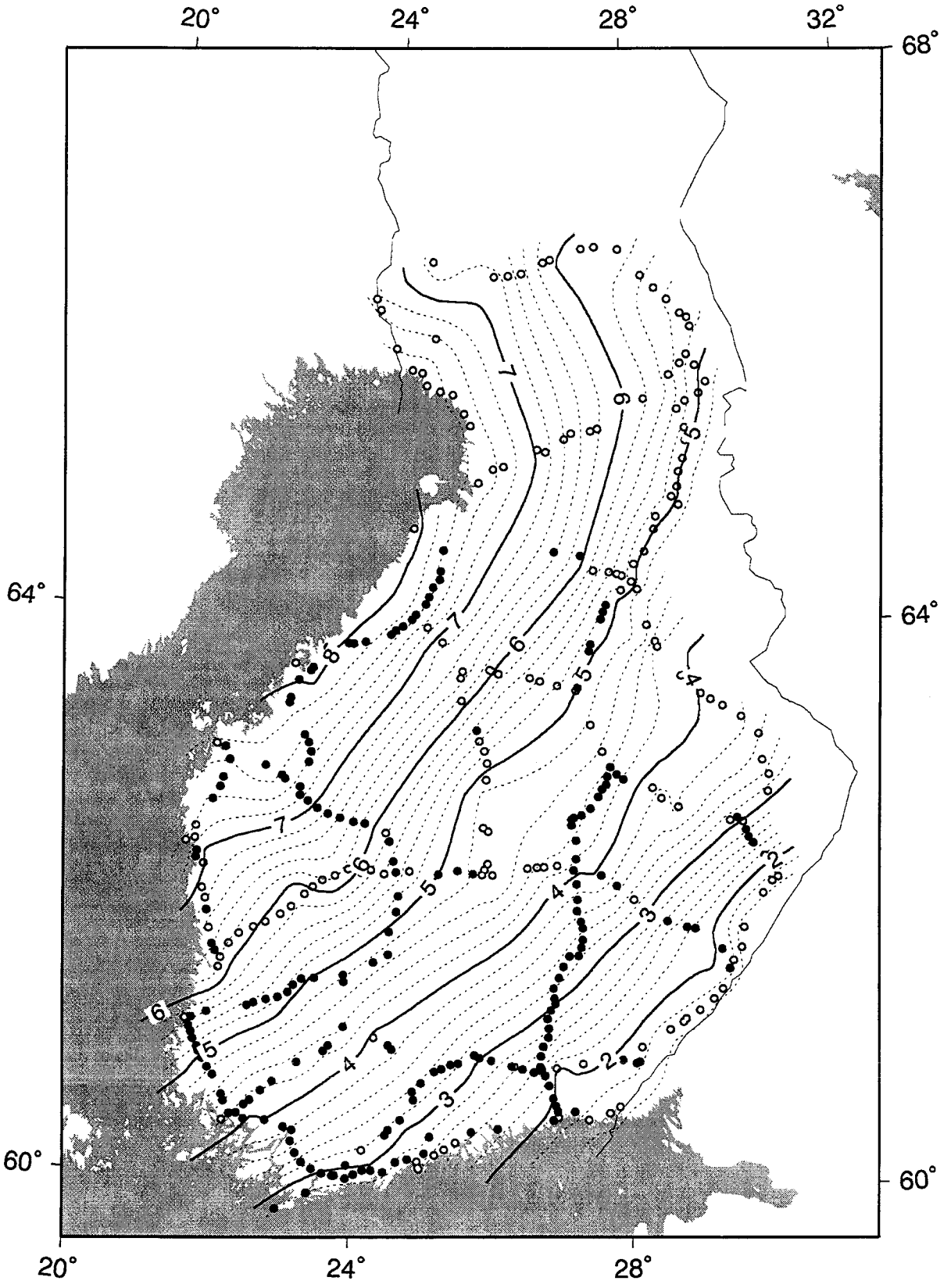

Figure 4. Land uplift relative to mean sea level in mm/yr, computed in the maximum network using all three levellings, MINQUE weights and assuming constant velocity. Solid circles are the bench marks which belong to all three levellings, open circles belong to two levellings only. See Section 6.

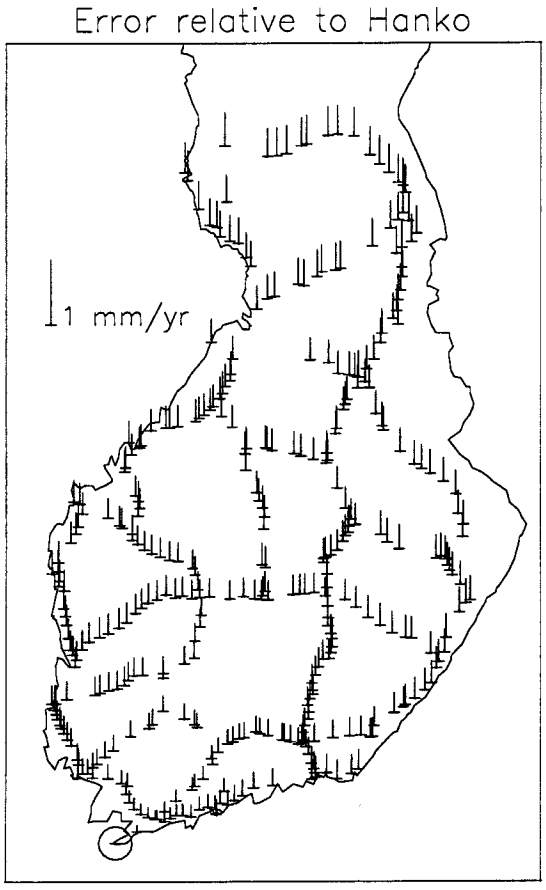

Figure 5. Standard errors (one-sigma) of velocities relative to Hanko (circled). The velocities are those of Figure 4. For details see Section 6.

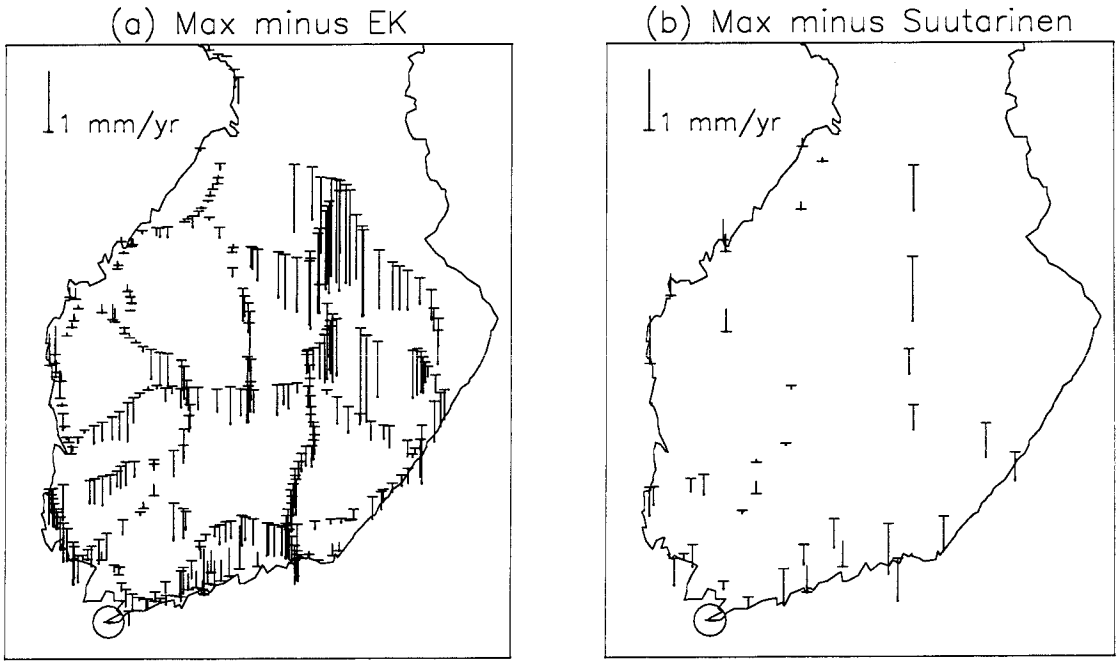

Figure 6. (a) Velocities of Figure 4 minus the velocities of Kääriäinen (1966). (b) Velocities of Figure 4 minus the velocities of Suutarinen (1983), "observation variance" weights. Both are relative to Hanko (circled). Comments in Section 7.

shows uplift relative to MSL ("apparent uplift"). Moreover, Kääriäinen (1966) and Suutarinen (1983) join the velocity differences, not to a single tide gauge result as we do, but to a weighted mean of several tide gauges. All the same, their maps are "levelling-only" in the sense that land uplift differences are determined from repeated levellings alone and tide gauges only contribute the zero term. With their estimate (0.8 mm/yr) for the eustatic rise we would have 3.53 mm/yr at the tide gauge in Hanko, where Kääriäinen (1966) has 3.66 mm/yr and Suutarinen (1983) has 4.0 mm/yr.

In Figure 6 we compare, not the maps but the numerical values which went into the drafting of the maps. Kääriäinen (1966) and Suutarinen (1983) only had the First and Second Levellings, so the Figures 6a and 6b are similar with each other and with Figure 3c as well. It is then of interest to check to which extent our solution using First and Second Levellings only can reproduce theirs. Actually, notwithstanding his much sparser set of bench marks, Suutarinen's (1983) data is nearly identical with First and Second Levellings in our common network and differences to our solution (I,II) turn out to depend solely on his unconventional weights using "observation variance" (results not shown here).

The comparison with Kääriäinen (1966) is more interesting (Figure 7) since with his approximate adjustment method he was able to incorporate lines where the limiting BMs belonged to one levelling only (by interpolating land uplift corrections for them), and to include land uplift information which did not come from the two levellings. We can isolate the influence of his extra data by simulating his adjustment method. Vaníček et al. (1987, p. 208) have demonstrated that in the case of two levellings in identical networks (and no extra data) Kääriäinen's approximate method is equivalent with

(u) eliminating the heights by forming the difference of the levellings, i.e. with using observation equation (2) instead of (1), and then
(v) applying weights which diminish the importance of long time spans.

We have applied steps (u) and (v) to our own data in the common network (Figure 7b, c). The "legitimate" step (u) has some effect (Figure 7b); in the modelling investigations of Paper 1 the pair (I,II) was the one most influenced by elimination of the heights. This was discussed as item (A) in Section 3. The "illegitimate" step (v) has hardly any effect at all (Figure 7c). Most of the difference in Figure 7a is retained in Figure 7d and thus appears to be due to Kääriäinen's additional material and not to his adjustment method.

8. Conclusions

We have determined differences in land uplift rates (vertical velocities) up to the latitude 66.5°N using the three precise levellings in Finland. The standard errors (one-sigma) between the extremities of the network are around 0.5 mm/yr. The fit with constant (in time) velocities is not as good as could be expected from accuracy estimates of the three levellings using loop misclosures. Further work is needed to clarify whether this is due to changes in velocities or to underestimated levelling errors.

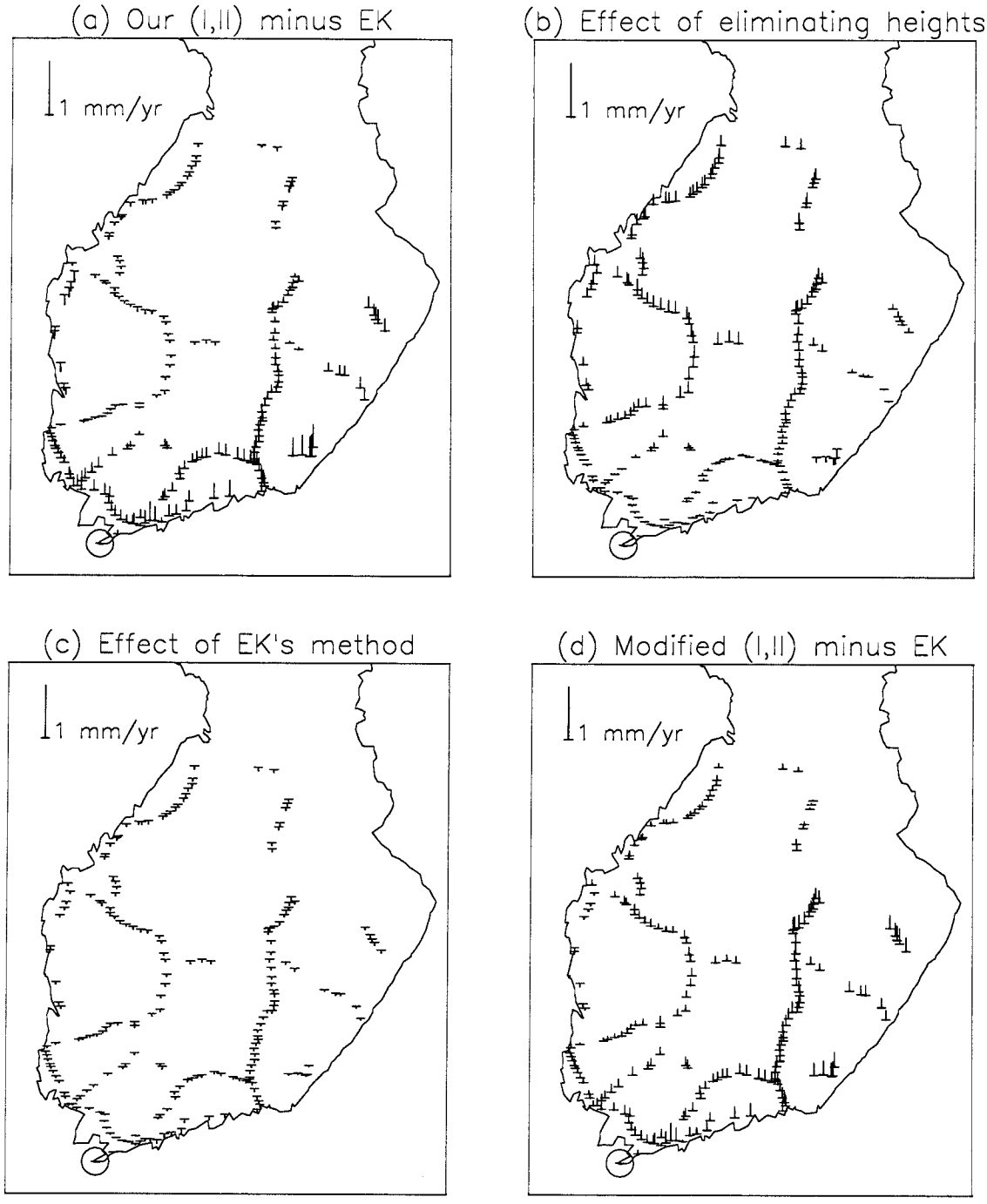

Figure 7. Comparison of our velocities from the First and Second Levellings in the common network with the velocities of Kääriäinen (1966). Everything is relative to Hanko (circled).

(a) Our (I,II) using observation equation (1) minus Kääriäinen (1966)

(b) Our (I,II) using observation equation (2) minus our (I,II) using observation equation (1), i.e., the effect of step (u) in Section 7.

(c) The effect of step (v) in Section 7, i.e., of the "illegitimate" part of Kääriäinen's approximate method.

(d) The sum of (a), (b), and (c), i.e., our (I,II) adjusted with the approximate method of Kääriäinen minus his own result, i.e., the influence of his extra data.

References

Remark: A more complete list appears in Mäkinen and Saaranen (1998).

Andersen O.B. and O. Remmer (1982): Non-random effects in the Finnish levellings of high precision. manuscripta geodetica 7: 353–373.

Blomqvist E. and H. Renqvist (1910): Das Präcisionsnivellement Finlands 1892–1910. Fennia 31:2, 1–265.

Mäkinen J. and V. Saaranen (1998): Determination of postglacial land uplift from the three precise levellings in Finland. J. Geodesy, accepted for publication.

Kääriäinen E. (1966): The Second Levelling of Finland in 1935–1955. Publ. Finn. Geod. Inst. 61.

Rao C.R. (1971): Estimation of variance and covariance components–Minque Theory. J. Multivariate Analysis 1: 257–275.

Suutarinen O. (1983): Recomputation of land uplift values in Finland. Rep. Finn. Geod. Inst. 83:1.

Vaníček P. et al. (1987): Four-dimensional geodetic positioning. manuscripta geodaetica, 12: 147–222.

Vermeer M., J. Kakkuri, P. Mälkki, H. Boman, K.K. Kahma and M. Leppäranta (1988): Land uplift and sea level variability spectrum using fully measured monthly means of tide gauge readings. Finnish Marine Research 256: 3–75.

Vertical secular movements in Denmark from repeated levellings and sea-level observations during the last 100 years

by

Klaus Schmidt
National Survey and Cadastre (KMS)

Rentemestervej 8, DK 2400 København N, Danmark

presented at the 13th General Meeting of the NGC
Gävle, 1998

Abstract: Since the end of the sixties Danish geodesists had to accept that land uplift determined from precise levellings didn't agree with the uplift from sea-level records. A few years ago the third precise levelling was completed. Therefore, secular movements in Denmark have bee recomputed and recompared with the results from sea-level observations, and a much better agreement could be established. The paper presented is an extract from the author's Ph.D. thesis at the Univerity of Copenhagen, 1997.

Chapter 1: Historical and theoretical background

1. Historical remarks on the determination of the land uplift in Denmark

The postglacial land uplift of Fennoscandia is a still on-going phenomenon, which already has been studied for more than two and a half centuries. A presentation of this phenomenon from the geo-physical point of view is given e.g. by Kakkuri, (1985).

The latest contour map of recent apparent land uplift rates, i.e. values relative to sea level, has been published by Ekman (1996), see fig.1. The map is based on sea/lake level records and on repeated national levellings of high precision; dashed lines mean interpolation.

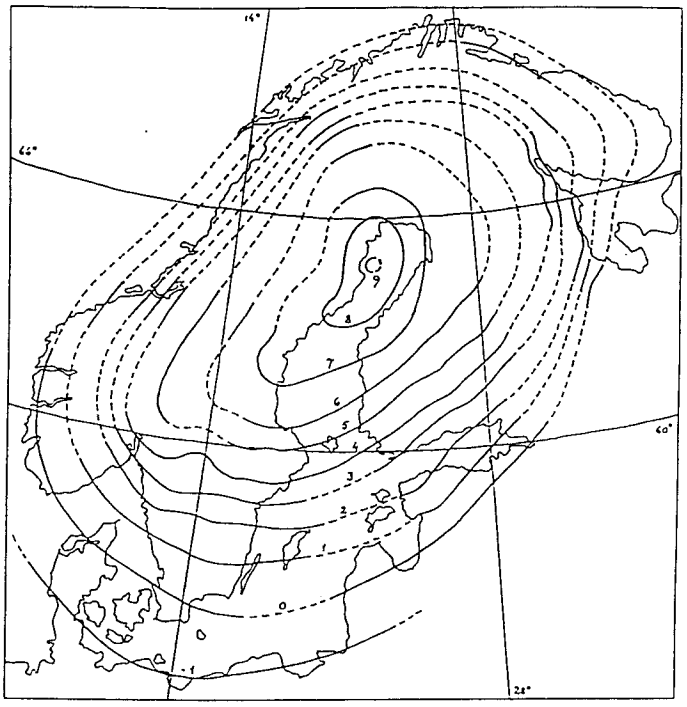

Figure 1. Apparent postglacial uplift of Fennoscandia 1892 - 1991 in mm/yr.

Fig.1 indicates that the apparent land uplift in Denmark is part of the Fennoscandian uplift. It can be described very roughly as a tilt of a rigid plane along an axis in a north-west south-east direction. Uplift rate differences of about 2 mm/yr can be expected between Skagen (the most northern place in Denmark) and the German border.

This, of course, is in agreement with the results published by Egedal (1945), since both authors applied uncorrected annual means from sea level records starting at the end of the last century. Egedal's results, concerning position, direction of the tilt axis, and the tilt's velocity, were determined by an adjustment of linearly adjusted apparent land uplift rates at 10 tide gauge stations. These results can be found in Simonsen (1949), including the map below, fig.2, where the position of the tilt axis is based on different assumptions of sea level rise. Applying the usual value of 1mm/yr the corresponding tilt axis, indicated by '-1 mm/Aar', is almost passing through the town of Esbjerg. The straight line indicated by '0 mm/Aar' is the line where land uplift and sea level rise are of the same size.

After the completion of the second precise levelling new heights were computed. Comparing them on Zealand with the old ones from the first precise levelling and assuming the benchmarks had moved linearly in time, a bar graph of relative secular movements of 225 points was produced, Simonsen (1949, p.116), and a tilt axis for Zealand, shown on fig.2, was computed. Taking into account the mean square errors of the direction, ±4.6° from sea level records (Egedal) and ±2.8° from levelling, cf. Simonsen (1949, p.111 and p.115), there seems to be a significant directional deviation (about 39°) between the two tilt axes. It should be

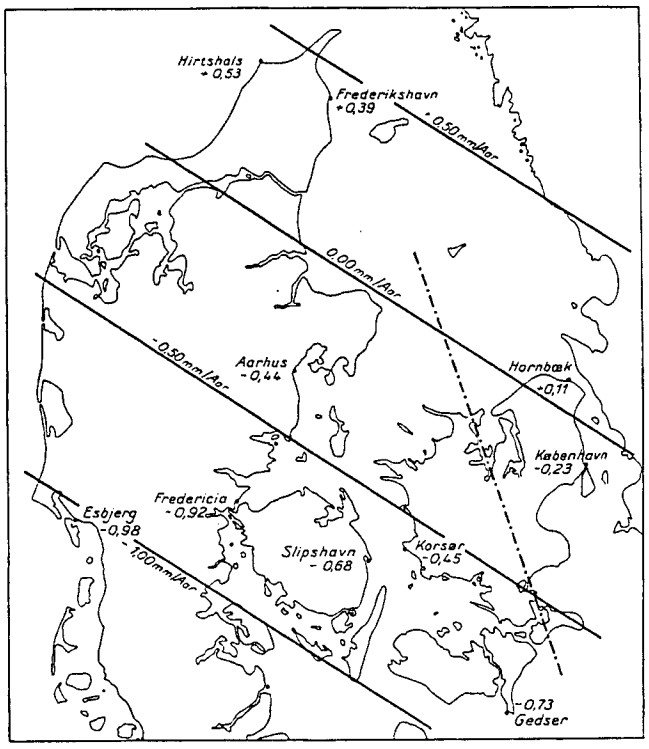

Fig.2: Apparent land uplift in mm/yr, determined from sea level observations at 10 Danish tide gauge stations. From Simonsen (1949)

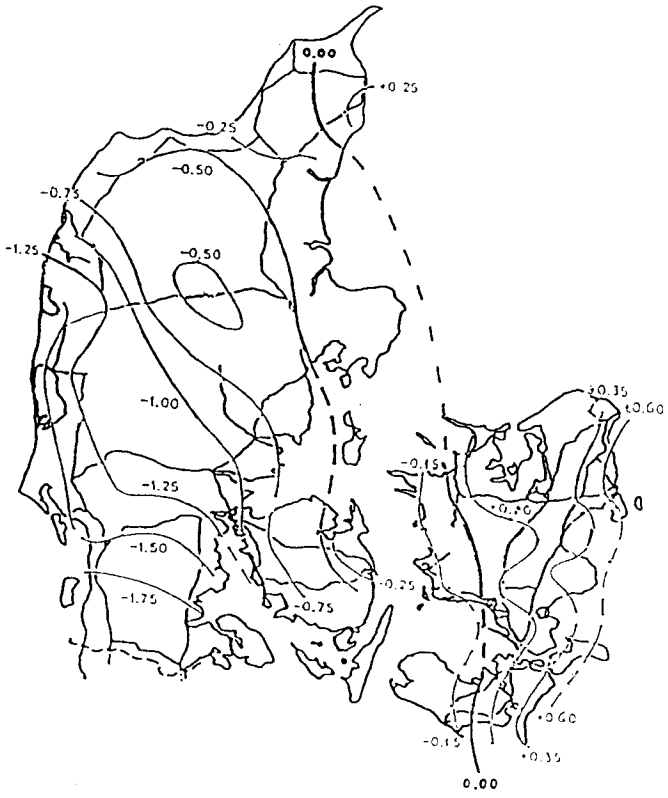

Fig.3: Land uplift in mm/year relative to mean sea level in Århus, determined from the first and the second levelling of high precision. From N. Andersen (1992)

added, that new and old heights on Zealand were directly comparable, since they were computed in the same way without any geopotential or tidal corrections.

In 1964 secular benchmark movements within Jutland, relative to the fundamental benchmark GM 902 (Århus cathedral), were determined, performing a joint adjustment of the first and the second precise levelling (epochs 1890.5 and 1950.5), published by Bedsted Andersen et al. (1974). The publication includes a bar graph of relative secular movements during the last 60 years. Before the adjustment the astronomical correction was applied to the measurements of the second precise levelling and all of the height differences from the first and the second precise levelling were converted into geopotential differences. The astronomical correction applied is a kind of tidal correction, removing the time dependent influence of the moon and the sun on the earth's gravity potential and shape. As pointed out by the authors (p.11) the astronomical correction of the first levelling would have removed the tilt introduced by correcting the second levelling. The amount of this tilt is ca. 7 mm from North Jutland to the German frontier. However, this is less than 5% of the land uplift difference that actually occured.

From the results of the joint adjustment and by comparing new and old water crossings as well as new and old heights as described above, but now also comprising Funen and Falster, Simonsen (1968) produced, by eye, a strongly generalized contour map of the land uplift rates in Denmark (relative to the mean sea level at the Århus tide gauge). This map was later revised by N. Andersen (1992), according to the results from the hydrostatic levellings across Great Belt in 1938 and 1990, implying that a small constant value had to be added to the uplift rates on the Danish islands east from Great Belt. This latest version is shown in fig.3. One should have in mind, that the map is based on benchmarks from the first

precise levelling, i.e. mainly on subsoil benchmarks.

Obviously, there is a significant discrepancy between the apparent land uplift, computed from the sea level observations (Egedal) and from the first and second levelling (Simonsen). Therefore several attempts have been made in the past to correct the sea level observations for meteorological and oceanographic effects, cf. Rossiter (1967), Simonsen (1968), and Borre (1970), but it seems, they haven't been quite succesful. To the authors knowledge such corrected observations are still not available.

Furthermore, comparing the tilt axis of Zealand in fig.2 with fig.3 there seems to be a rather great change of direction. Also, in fig.3, there is a considerable deviation between the directions of the tilt axes for Jutland and Zealand. Therefore, the recomputation of these tilt axes, using uncorrected sea level records up to 1993 as well as a joint adjustment of the three levellings, was the principle task.

2. Precise levelling and sea level observation during the last 100 years

All of the three levellings available today have been performed in accordance with the standard guidelines for levelling of high precision, i.e. all sections have been measured in both directions, the maximum sight length is 50 m, etc., cf. Becker and Bedsted Andersen (1984). Maps of the simplified network configurations can be found in the appendix.

The first levelling was performed (mainly) from 1885 to 1904. It started in Jutland and was continued on the Danish islands, which were tied to the network by optical water crossings. The results were published in Den Danske Gradmaaling (1909) and (1911).

Measured height differences were corrected using an average rod meter, which was currently determined. The network consisted of about 1500 points, most of them subsoil benchmarks in a depth of about 1 meter.

The network has been enhanced with data from German levellings, taken from Trigonometrische Abtheilung der Landesaufnahme (1894), comprising the most southern loop in Jutland, measured in 1889 and fully comparable with Danish levellings.

About 50 years later, the second precise levelling was executed, mainly from 1938 to 1953. This time the Danish islands were measured first. A lot of new benchmarks were established, some of them as subsoil benchmarks, but the majority were placed less stable (houses, walls, etc.). Some results are published by Simonsen (1949) and by Bedsted Andersen et al. (1974). Eastern and western part of the network were connected in 1938 by the hydrostatic levelling across the Great Belt.

Invar rods were applied and the measured height differences were corrected with respect to an average rod meter and the thermal expansion.

Finally, the third levelling was measured by motorized levelling, cf. Widmark and Becker (1984), mainly from 1986 to 1992. Like in the first levelling, Jutland was measured before the Danish islands. Again, a considerable point establishment had to take place. Final results will be published in the near future. The network was connected by optical water crossings and the hydrostatic levelling in 1990.

It should be mentioned, that the measurements in the Great Belt area before 1990 are excluded. The reason is the construction work of tunnel and bridge across the Belt, causing the ground water level to change significantly and the whole area to subside. Also, the measurements in certain harbour areas are omitted in this work, because they haven't been adjusted yet due to irregular ground movements.

The levels applied were all of the type Zeiss NI 002. The measured height differences were corrected with respect to the thermal expansion as well as the scale graduation errors, which were currently determined from laser interferometer measurements.

Sea level observations have been recorded in Denmark since the end of the last century and the mean of the annual mean sea level heights at 10 tide gauge stations has been used to fix the origins of the first, DNN GM 1891, and the third, (DNN KMS 1990), national height system. These stations are located at Esbjerg, Fredericia, Frederikshavn, Gedser, Hirtshals, Hornbæk, Korsør, København, Slipshavn, and Århus; their geographical position can be seen in fig. 2. The corresponding height values, referring to the first height system, have been retained up to today for those of the original TGBMs, which are still in use. The other ones, which turned out to be unstable in relation to their surroundings, or simply got lost, had to be replaced computationally or physically. Then the associated height value of the new TGBM had to be determined such, that future mean sea level heights could continue apparently undisturbed, i.e. the new TGBM should have the same movement as the old one, before it was disturbed or destroyed, and the difference between the height values associated with the new and the old TGBM should be the constant height difference between them. At some of the stations such a replacement took place up to five times during the last 100 years. Problems with the unstable or destroyed TGBMs led in 1964 to a comprehensive revision of the mean sea level heights.

3. Remarks on the applicability of levelling and sea level records to determine secular movements

Geometrical levelling has been and still is one of the most accurate measuring techniques for the determination of height differences. In addition, since levelling has been applied in many countries over a long time, a great deal of information on height changes is available through repeated levellings. However, there are limiting factors.

The levelling technique requires a dense physical network, which has to be established and maintained. Levelling is expensive, if applied to longer distances, because it is slow and great effort has to be made to control the accumulation of systematic errors, primarily, the sinking of the rods and of the level during the scale readings, the refraction and the instrumental errors, which may result in a seeming land uplift. It should be mentioned, that the Danish levellings are not corrected for refraction.

Concerning the instrumental errors, the article of Rumpf and Meurisch (1981) created great concerns, because the influence of the geomagnetic field on compensators of automatic levels had been observed and repeated levelling with that kind of instrument was going on in many countries at that time. This error factor cannot be detected from loop closing errors, and if older spirit levellings are compared with new compensator levellings a seeming north-south tilt can be found. In Denmark, the response of the NI 002 levels to magnetic fields was investigated during 5 years. The result is that the errors from magnetic fields can be neglected, cf. Stampe Villadsen and N. Andersen (1990).

Another limitation is that the main purpose of national levelling networks is the physical realization of heights closely covering the whole country. In Denmark, the networks and benchmarks are not specially designed or established to monitor height changes. Hence, by repeated levelling basically one only can achieve relative benchmark movements, caused

by the Fennoscandian land uplift in addition to regional and local effects. Regional disturbances may occur by e.g. exploitation of raw material from the ground, including natural gas and water, or by extensive construction or drainage works. Local disturbances are often caused by a benchmark establishment, which is inexpedient with respect to the soil conditions. Hence, when benchmark movements have been computed, it is a matter of discussion to which extend they really reflect the land uplift.

The Danish coast line allows to establish tide gauge stations all over the area of interest, but this probably causes rather different regional impacts on the sea level or on the TGBM's (for example, the oceanographic conditions at the Gedser station presumably are quite different from those at the Esbjerg station near by the open sea). In particular, the local influences should be kept as small as possible. That means, for example, TGBMs should move in accordance with the secular movement of the land. Since the height value associated with a TGBM is retained as long as the TGBM is in use, the local height system defining sea level height can move correspondingly to the movement of the TGBM. Consequentely, sea level heights reflect the movements of both the TGBM and the sea level. Hence, a change of mean sea level heights indicates either a change of the meteorological or oceanographic conditions, or a change of the TGBM's movement. A change of mean sea level heights may also occur, if a new TGBM, moving differently from the old one, has been introduced during the period of observations. There also may occur jumps, caused by sudden subsidence of the TGBM or by a new TGBM with an associated height value badly determined. Sudden changes of sea current conditions, caused by reestablishment of the tide gauge board at a new place or by rebuilding of the harbour, may also cause a jump. Due to the great natural variation of the sea level, a rather long time of observation is needed to establish significant changes.

4. Levelling and geopotential differences

In principle, levelling measurements are performed at each set up with a horizontal sight line, i.e. orthogonal to the gravity vector at the location of the set up. Because of the nonparallelism of the equipotential surfaces of the earth this implies, that the levelled height difference between two benchmarks depends on the actual path of levelling. Furthermore, the closing errors of levelling loops computed from the levelled height differences do not vanish completely, even if the measurements were perfect. Geopotential differences, however, don't have these theoretical drawbacks. In flat areas or areas, which are moderately mountaineous, they can be determined from the levelled height differences by multiplication with the mean gravity at the two benchmarks involved. The theoretical background can be found in Heiskanen and Moritz (1967), chapt.4. Geopotential differences fulfil the usual observation equations of levelling.

From a theoretical point of view levelled height differences should be tidally corrected before they are converted into geopotential differences. The same type of tidal correction should be applied to all of the measurements, used to determine secular movements from repeated levellings. However, for old levellings, often only the year of observation is indicated, thus tidal corrections cannot be computed. In this case, the geopotential differences are approximately referring to the mean gravity potential of the earth, cf. Ekman (1989), chapt.2.. Consequentely, to be consistent, the tidal correction of modern levellings either should be left undone or the correction should refer to the mean geoid. This is achieved by correcting the measured height differences astronomically, resulting in non-tidal height

differences, and then converting them into mean height differences, applying formula (31) from Ekman (1989). After this, the mean height differences can be converted into geopotential differences applying gravity, referring to the International Gravity Standardization Net 1971 (IGSN 71), i.e. in Denmark, gravity according to the Danish reference network, cf. Bedsted Andersen and Forsberg (1996).

Furthermore, geoid and gravity changes have an impact on secular movements determined from repeated levelling. This topic has beeen treated in numerous papers, but in practice geoid changes are assumed to be insignificant and old levellings are converted by means of modern gravity values.

5. Kinematic models

Various kinds of kinematic models for the determination of vertical movements from repeated levelling exist. In general, the motion of the benchmark P_i as a function of time is modelled by means of a polynomial of p'th degree corresponding to the truncated Taylor expansion

$$h_i(t)=h_i(t_0)+g_i\Delta t+\tfrac{1}{2}a_i\Delta t^2+ \ldots +(1/p!)c_{p,i}\Delta t^p$$

where $\Delta t=t-t_0$, $h_i(t)$ is the height of P_i at the moment t, t_0 is a reference time, and g_i and a_i are constant velocity and acceleration of P_i. For repeated national levellings degrees higher than 2 normally are not applied.

Regardless of which model is chosen the usual procedure is, preliminarily to divide the network with respect to epochs into geometrically connected subnetworks, each of which is considered measured at the same time (specified by the epoch). This procedure is followed in order to detect errors and to get an estimate of the measuring accuracy. In addition, multivariate adjustment, cf. Koch (1988), p.278, should be applied to these subnetworks to detect correlations between different epochs, but then some of the measurements possibly have to be omitted to obtain subnetworks with exactly the same configuration, i.e. the same observation equation matrix.

In Pelzer and Niemeyer (1987) and Mälzer (1990) several kinematic models and brief evaluations are presented. Models from these two publications can be classified as follows:

I. Deterministic parameters of movements
   - A. Individual parameters for each benchmark
     1. the same polynomial degree p for all benchmarks (p=0: static model, p=1: linear model, p=2: quadratic model)
     2. individual degree for each point
   - B. Linear(quadratic) models, where velocity(and acceleration) are surface funtions determined by
     1. interpolation
     2. polynomials

II. Linear models, where velocity (partly) is considered random

Models of type I are adjusted by a least-squares adjustment, whereas collocation, cf. Koch (1988), p.258, is applied to type II.

Chapter 2: Joint adjustment of Danish levellings of high precision

1. Method: In the following the kinematic model and its adjustment is described. It will turn out, that some of the theoretical and practical aspects have been ignored owing to the limited amount of time at the disposal. Consequences from this will be discussed.

The adjustment method applied by the author is based on the traditional model I.A.1, p=1, i.e. the observation equation of the levelled height difference between the benchmarks P_i and P_j at the time t is given by

$$E(\Delta H_{ij}(t))=H_j(t_0)-H_i(t_0)+(\alpha_j-\alpha_i)(t-t_0)$$

where t_0 is a fixed reference time, H is the height and α the velocity. Furthermore, it is assumed that all the measured height differences are normally distributed and stochastically independent with a variance determined by the levelling

$$Var(\Delta H_{ij}(t))=\sigma^2 L_{ij}$$

where L_{ij} is the levelled distance between the benchmarks and σ^2 is the levelling variance of unit weight.

The basic data to be adjusted are scale corrected, metric height differences from single runs between consecutive benchmarks. This includes all of the measurements from the three precise levellings. Geopotential or tidal corrections have not been applied.

Measurements from the same precise levelling are considered to be measured at the same time, i.e. the epoch 1890, 1950 or 1990, which appoximately is the mean of the moments of observation of the levelling in question. The same variance of unit weight σ_i^2, i=1,2,3, (i.e. the variance of 1 km single run), is assumed for measurements from the same epoch. Corresponding to the epochs the joined network from the precise levellings is divided epochwise into three subnetworks. Then, each of these subnetworks is geometrically connected, i.e. there is just one singularity, and they all have at least one benchmark in common. Hence, fixing the reference height and the velocity of a single point, the corresponding quantities, relative to the point kept fixed, can be computed for all of the benchmarks, which have been measured at different times.

The following notation will be applied:

$\Delta \mathbf{H}_i$: the vector of levelled height differences from the i'th epoch
n_i : number of these measurements
m_i : number of benchmarks involved
m' : $m_1+m_2+m_3$
$\Delta \mathbf{H}$: the total vector of observations, $\Delta \mathbf{H}^T=(\Delta \mathbf{H}_1^T,\Delta \mathbf{H}_2^T,\Delta \mathbf{H}_3^T)$
n : $n_1+n_2+n_3$, the total number of observations
m : the total number of benchmarks of the joined network
A : the observation equation matrix

In order to detect errors, and to get an estimate of measuring accuracy, each epoch is adjusted statically in the usual way keeping fixed the height of one single point, i.e. the number of freedom is $f_i=n_i-(m_i-1)$. From this we get the usual least-squares estimates s_i^2 of σ_i^2. Applying Bartlett's test, cf. Hald (1952), p.290, it is tested, if it is reasonable to assume the same variance of unit weight for all of three epochs. Alternatively, one can use the Fischer-test from Hald, p.374, pairwise. Concerning repeated national levellings, it is quite

usual, that the hypothesis on equal variances is rejected, and this is also the case for the Danish levellings.

Since $f_i s_i^2/\sigma_i^2 \sim \chi^2(f_i)$, i.e. the statistic on the left-hand side is χ^2-distributed with f_i degrees of freedom, and the s_i^2 are stochastically independent in accordance with the previous assumptions, it follows that $(s_3^2/\sigma_3^2)/(s_1^2/\sigma_1^2) \sim F(f_3,f_1)$, which means the Fisher distribution with f_3 and f_1 degrees of freedom. Hence, denoting the p%-fractile of this distribution by $F(f_3,f_1)_p$, the confidence interval of σ_1^2/σ_3^2 at the confidence level 5% is given by

$$[\ q_1/F(f_1,f_3)_{97.5}\ ,\ q_1F(f_3,f_1)_{97.5}\ ] \qquad (1)$$

where $q_1=s_1^2/s_3^2$. This result is valid, too, if the subindex 1 is replaced by subindex 2.

In order to handle different variances of unit weight, it is assumed from now on that the confidence intervals of σ_1^2/σ_3^2 and σ_2^2/σ_3^2 are sufficiently small to consider $q_1=s_1^2/s_3^2$ and $q_2=s_2^2/s_3^2$ as true values. That means, denoting the cofactor matrix of $\Delta\mathbf{H}_i$ by $\mathbf{D}_i$, the covariance matrix of $\Delta\mathbf{H}$ is assigned by

$$\mathbf{COV}\Delta\mathbf{H}=\sigma_3^2\cdot\mathrm{diag}(q_1\mathbf{D_1},q_2\mathbf{D_2},\mathbf{D_3}) \qquad (2)$$

Formally, the entire network should be readjusted, applying the new weight matrix $(q_1\mathbf{D_1},q_2\mathbf{D_2},\mathbf{D_3})^{-1}$. However, one would obtain the same results, i.e. the adjusted observations and the estimate s_3^2, determined previously from the epochwise adjustments, can be regarded as the results from this readjustment.

Though estimation methods of variance components are available, cf. Koch (1988), p.264, the approach above seems to be a common practice. In any case, it has been used in Bedsted Andersen et al. (1974), p.13, applying a weight ratio of 3.6 between the new and the old measurements. It should be noted, that the different variances of unit weight are implying a kind of Fisher-Behrens problem, cf. Hald (1955), p.397, when linear hypotheses are tested. In the tests below this problem is ignored as usual.

The hypothesis on stability of all of the network points can be tested by the statistic T

$$T=\frac{f}{f_0-f}\left(\frac{f_0 s_{03}^2}{f s_3^2}-1\right) \quad \sim \quad F(f_0-f,\ f)$$

i.e. T is Fisher-distributed with the degrees of freedom f_0-f and f, if the hypothesis is true. Here f=n-(m'-3), f_0=n-(m-1), and s_{03}^2 is the usual least-squares estimate of σ_3^2 from the static adjustment of the entire network (with f_0 degrees of freedom), assuming overall stability. Hence, rejecting the hypothesis, whenever $T>F(f_0\text{-}f,f)_{95}$ is a test at the significance level of 5%. This test is an application of the Fisher-test in Pruscha (1989), p.107. However, there is no reason to apply this test in the present case, cf. Bedsted Andersen et al., p.21.

More important is the test on linear movements, which is quite similar to the test above. Let $\mathbf{A}$ be the observation equation matrix of the entire network and $s_{\ell 3}^2$ the usual least-squares estimator of σ_3^2, obtained from the linear model adjustment, according to the covariance matrix (2), with f_ℓ=n-rank$\mathbf{A}$ degrees of freedom. Then the hypothesis of overall linear movements is tested by the statistic

$$T_\ell=\frac{f}{f_\ell-f}\left(\frac{f_\ell s_{\ell 3}^2}{f s_3^2}-1\right) \quad \sim \quad F(f_\ell-f,\ f) \qquad (3)$$

Again, the hypothesis has to be rejected, if $T_\ell>F(f_\ell\text{-}f,f)_{95}$.

As seen from the above several aspects have been left out of consideration. By the missing geopotential corrections a tilt in a north-south direction of about 8 mm is introduced into each levelling. However, the errors are approx. of the same size, due to the similar configurations of the three levellings.

The present investigation should be considered only as a first step towards a determination of modellized movements in Denmark. To begin with, one should prefere single point determination, based on a linear model, without smoothing effects. This makes it easier to find local irregular movements and to compare new results with the old ones from Simonsen (1949), (1968), and from Bedsted et al. (1974), in particular with respect to the discrepancy between land uplift found either from levelling or from sea level records.

Furthermore, as mentioned above, all of the measurements have been assumed to be stochastically independent with a variance proportional to the section length. This takes the levelling accuracy into account but not random deviations from linerarity of the vertical movements. However, usually the latter is ignored, when a traditional pointwise least-squares adjustment is performed. Probably the reason is, that the stochastical model of the measurements becomes more complicated, if the deviations are introduced as stochastical variables. Then an additional term, independent of section length, must be added to the variance of measured height differences. Furthermore, consecutive height differences from the same epoch become correlated. Besides, normally it is not possible to model the covariances between these deviations realistically.

Our treatment can be critisized further, because observations are weighted with respect to the levelling accuracies achieved. If it is assumed that the variances of the random deviations in question are much larger than the levelling variances, it would be better to leave the weighting undone.

The main objection to the present investigation could be, that all of the benchmarks available, subsoil or not, have been included. However, the elimination of benchmarks, preserving as many observations as possible, is a very time consuming work which lies outside the scope of this investigation.

Last, but not least, we have to admit, that the replacement of the individual years of observation by the corresponding epochs affects the results negatively. Especially, because the time spans between the epochs are rather short compared to the epoch lengths. However, this replacement was necessary, because the joint adjustment with the original years of observation preserved, gave an unexpected computational problem. Most of the computed velocities were much too small, compared to what could be expected from the adjusted epoch heights.

2.Results: In table 1 we have listed some of the results from the separate static adjustments of the three epochs. It should be noticed, that a single observation may be the result of several levelling runs, which is taken into account by its variance. This is the case especially with respect to the first levelling, i.e. the number of observations, compared with the second and the third levelling, is not as small as it appears. It is seen that the second and the third levelling have to be weighted almost equally in the succeeding joint adjustment, whereas the first levelling is weighted about 9 times less.

epoch	no. of observations	no. of benchmarks	s_i	q_i
i=1: 1890	1723	1503	1.84mm	9.00
2: 1950	18733	9222	.64	1.09
3: 1990	18044	7669	.61	

table 1: results from different epochs (s_i and q_i are defined in sect.1)

Of course, the variance σ_1^2 is significantly different from the other two. The confidence interval, eq.(1), is [7.4,11.0], which is considered to be sufficiently small. The corresponding interval with respect to σ_2^2/σ_3^2 is practically vanishing. Hence, q_1 and q_2 are adopted as true values, and the covariance matrix of the joint adjustment is assigned by eq.(2).

The joined network consists of 38496 observations including 14521 benchmarks, but only approx. 400 benchmarks have been measured in all of the three epochs. About 3400 benchmarks have been measured in at least two different epochs. The benchmark kept fixed in the joint adjustment is the Danish fundamental benchmark GM 902, Århus Cathedral, which is supposed to be stable. Thus all of the 3430 computed point velocities are relative to the velocity of GM 902.

Since it is rather inappropriate to illustrate several thousands of velocity values by a bar diagram, applying the paper format used in this presentation, it has been decided to produce a contour map, shown on the next page. This map is based on predicted relative velocity values at regular grid points. The prediction was accomplished by the collocation of the computed benchmark velocities, applying the KMS-program 'geogrid'. From the grid point values contour lines have been drawn by means of the program PV-Wave. Covariances between the input data to these programs have been ignored. The values indicated in the contour map are relative velocities in mm/year, contour interval=.2mm, the dark area is subsiding relative to GM 902 with a velocity greater than .5mm/year. One should remember that contour lines in areas not covered by the levellings are irrelevant. Furthermore, the contour lines are very sensitive to irregular movementsor and errors in the data.

The square root of the least-squares estimate of σ_3^2, cf. (2), is $s_{\ell 3}$=.78mm, and the computed value of the statistic T_ℓ, cf.(3), is 31.22. Since the Fisher fractile $F(441,20105)_{95}$ is equal to 1.12 the hypothesis of linearity of the movements has to be rejected, as expected.

The joint adjustment passed off unproblematically after the replacement of the individual years of observation by epochs. The number of observations to be corrected or rejected was no more than 1‰ of the total number. The program applied was the KMS network adjustment system (for details, see Engsager (1997)). This program solves the normal equation system by means of the Cholesky procedure. Applying an appropriate ordering of the unknowns, and using sparse matrix technique, the number of elements of the upper tringle normal equation matrix could be reduced from 161 mill. to 0.6 mill.. The computation time on a Sun-Sparc20 computer was about 14 min..

Regarding the estimated mean square errors of the computed relative velocities, such an error is the product of $s_{\ell 3}$ and the square root of the corresponding diagonal element of the inverse of the normal equation matrix. The majority of these errors has values between .1 and .2mm.

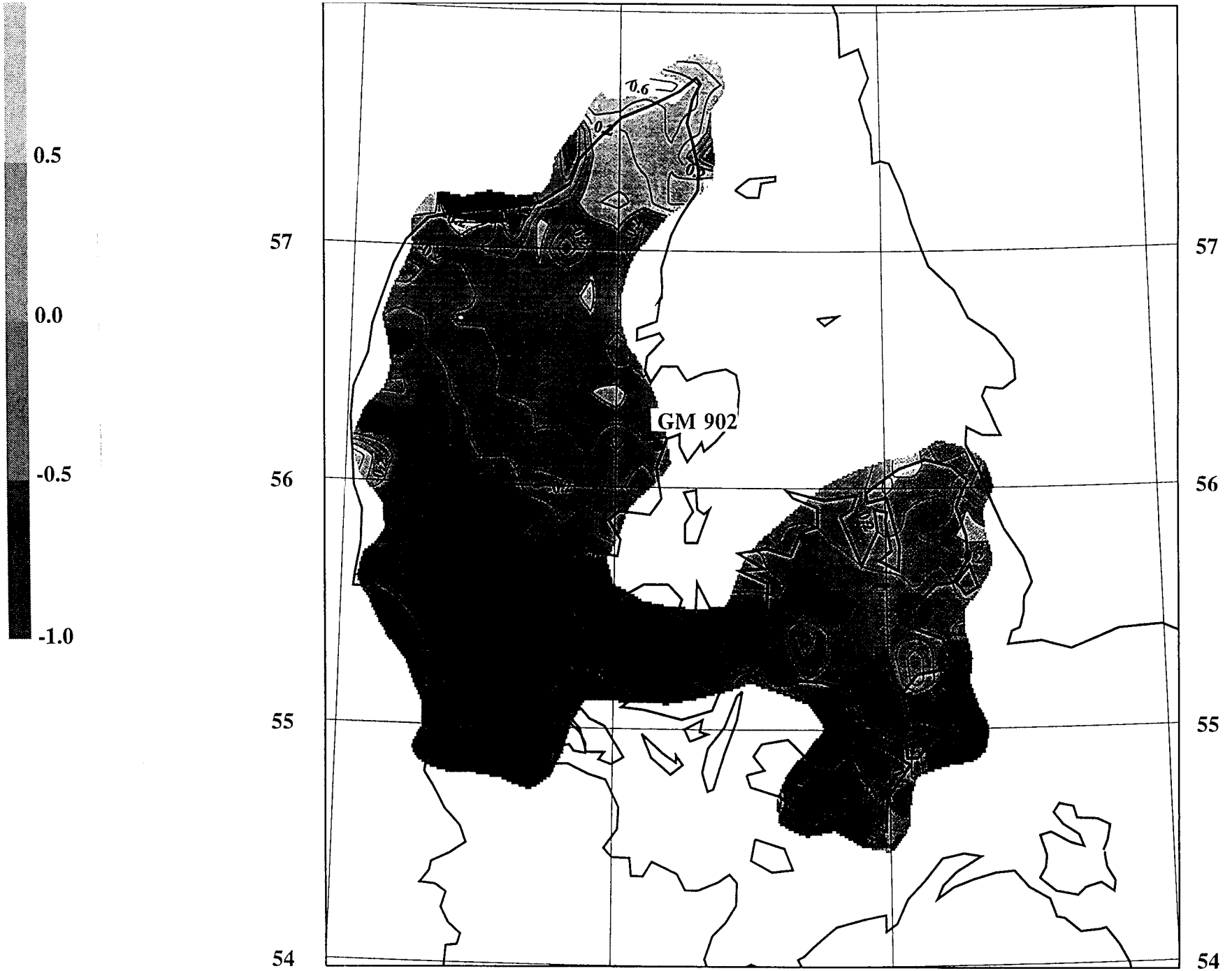

Annual land uplift (mm), rel. to GM 902, from precise levellings (cont.int.=.2mm)

Chapter 3: Adjustment of Danish sea level observations

The monthly means of the local sea level heights at Danish tide gauge stations are kept in a database 'klimadb', established and administrated by the Danish Meteorological Institute. These heights are not corrected for oceanographic or meteorological influences.

The author's investigations of the monthly means are omitted here, i.e. annual means, from 1893-1993, are applied in all what follows.

1. Preliminary investigations:

Based on the annual means it has been checked, whether the continuity of the mean sea level records has been kept, when TGBMs had to be replaced. In accordance with the dates of replacement, the entire time span from 1893 to 1993 has been divided into subintervals with unchanged TGBM. For each subinterval it has been assumed, that the annual means have the same variance and follow a straight line. Applying the formulas of linear regression, an estimate of the variance of an annual mean has been computed for each subinterval, and the equality of the corresponding variances has been tested at the 5%-level. This test has never been rejected. After this, it has been tested, if the straight lines from the subintervals are part of a common line valid for the entire time span. The test has been accepted for all stations except Hirtshals, but this was caused by a very short interval of 4 years. Thus, we may conclude, the annual means do not indicate that the introduction of new TGBMs has not been handled carefully.

Furthermore, it has been investigated at each station, if annual means continue undisturbed without discontinuities or changes of slope. To achieve this, the entire time span 1893-1993 has been divided into 2 consecutive subintervals. The first one of an initial length of 10 years, which is successively increased by 1 year until the length of the second subinterval becomes smaller than 10 years. The hypothesis on a common straight line has been tested for each pair of such subintervals. There has been only one clear rejection, namely at the Frederikshavn tide gauge with respect to the subintervals 1893-1942 and 1943-1993.

Referring to Jessen (1970), a sudden subsidence of 4.45 cm took place in Sept./Oct. 1942 at the Frederikshavn station, caused by the exploitation of natural gas during the second world-war. This was indicated by mean sea level records and by repeated levellings as well. Based on the annual means available to the present investigation, the values from 1893-1941 and 1943-1993 have been adjusted separately. The Fisher-test on equal variance and the Student-test on equal slope have both been accepted. Applying the adjusted common slope, Jessen's value of subsidence has been confirmed. Consequentely, 4.5 cm have been added to all of the annual means from 1943 on.

2.Results from annual means: For each station we have computed by linear regression an estimated value $\hat{b}_i$ of the slope of the annual means, the corresponding mean square error, as well as the mean square error of a single mean. In addition, the estimated interannual correlation r_{nb} has been computed from Grenander (1956).These values are listed in table 1.

	slope $\hat{b}_i$	mse($\hat{b}_i$)	mse(a. mean)	r_{nb}
Esbjerg	1.08 mm/yr	.16 mm/yr	4.7 cm/yr	.14
Fredericia	.95	.08	2.5	.24
Frederikshavn	-.58	.10	2.8	.14
Gedser	.93	.11	3.3	.05
Hirtshals	-.41	.13	3.8	.26
Hornbæk	.06	.13	3.9	.11
Korsør	.63	.10	3.0	.08
København	.23	.13	3.7	.04
Slipshavn	.79	.10	2.8	.19
Århus	.46	.09	2.6	.17

table 1: results from annual means

Ignoring the expected small positive neighbour correlations we will consider the annual means from the same station as uncorrelated. Furthermore, for any given pair of stations there is assumed an identical covariance between annual means from the same year, whereas means from different years are assumed uncorrelated. The corresponding covariance matrix is denoted by Σ. Based on these assumptions estimated covariances $s_{k\ell}$ as well as correlation coefficients $r_{k\ell}$ between annual means from the same year at different stations, no.k and no.ℓ, have been computed in the usual way. The computed values are given in table 2. In accordance with our assumptions $\hat{b}_k$ and $\hat{b}_\ell$ have the same correlation coefficient as the annual means from the same year at station no.k and no.ℓ. Hence, the values in table 2 are also representing estimates of the correlation coefficient of estimated apparent land uplift rates at different stations.

Esbj.	Frc.	Frhv.	Geds.	Hirts.	Horn.	Kors.	Køb.	Slips.	Århus
1.00	0.69	0.82	0.62	0.81	0.81	0.75	0.77	0.73	0.79
	1.00	0.83	0.84	0.72	0.81	0.87	0.85	0.91	0.91
		1.00	0.69	0.84	0.84	0.80	0.83	0.84	0.88
			1.00	0.64	0.81	0.89	0.86	0.88	0.82
				1.00	0.84	0.79	0.79	0.79	0.80
					1.00	0.88	0.96	0.91	0.90
						1.00	0.90	0.92	0.89
							1.00	0.93	0.91
								1.00	0.92
									1.00

table 2: correlation coefficients between annual means from the same year at different stations

Finally, we compare the uplift of the TGBMs, relative to GM 902, computed from the sea level observations and from the joint adjustment of the levellings. The uplift values are given in table 3. Assuming the same sea level rise at all tide gauges the values from sea level observations have been computed from the first column of table 1 and the relative uplift of the Århus TGBM from the joint adjustment, i.e. from the expression $(-\hat{b}_{TGBM}+\hat{b}_{TGBM\ Århus}+\hat{\alpha}_{GM\ 902,TGBM\ Århus})$. The corresponding mean square errors have been found from the second column of table 1 and from the values in table 2. Taking the mean square errors into account the agreement between the first and the second column of table 3 is fairly good with reference to the tide gauges at Esbjerg, Fredericia, and Gedser.

	from sea level obs.		from levellings	
Esbjerg	-0.53 mm	± 0.11 mm	-0.64 mm	± 0.13 mm
Fredericia	-0.40	± 0.04	-0.58	± 0.12
Frederikshavn	1.13	± 0.05	-	
Gedser	-0.38	± 0.06	-0.56	± 0.21
Hirtshals	0.96	± 0.08	-	
Hornbæk	0.49	± 0.06	-0.16	± 0.20
Korsør	-0.08	± 0.05	-0.46	± 0.16
København	0.32	± 0.06	-	
Slipshavn	-0.24	± 0.04	-0.58	± 0.16
Århus	-		0.09	± 0.01

table 3: annual uplift of TGBMs, rel. to GM 902, and corresponding mean square errors from sea level observations and repeated levellings

As regards the great deviation at the Hornbæk station it is perhaps not fair to compare the values above, since the TGBM has not been included in the the first precise levelling. Restricting the annual means of the sea level to the years 1936-1993 and excluding the first levelling we get the corresponding values 0.18 mm ± 0.16 mm and -0.21 mm ± 0.21 mm.

Chapter 4: Computations of tilt and conclusions

Let us consider the computation of tilt from the annual apparent land uplift rates $\hat{\alpha}_i=-\hat{b}_i$ as shown in the appendix. We want to determine the tilting plane minimizing the average of quadratic differences between observed rates $\hat{\alpha}_i$ and the rates α_i corresponding to the plane in question, i.e. we have to minimize $\|\hat{\alpha}-\mathbf{Bu}\|_I^2$ on $\mathbb{R}_3$. Hence, the minimizing plane is given by $\hat{\mathbf{u}}$, determined by $\mathbf{B}\hat{\mathbf{u}}=pr_{B,I}(\hat{\alpha})$, i.e. $\hat{\mathbf{u}}=(\mathbf{B}^T\mathbf{B})^{-1}\mathbf{B}^T\hat{\alpha}$. The associated parameter values $\hat{\gamma}$, $\hat{w}$, and $\hat{q}$, as well as the corresponding mean square errors are computed from the formulas in the appendix, replacing $\mathbf{u}$ by $\hat{\mathbf{u}}$, and estimating the covariance matrix

$$\mathbf{COV}\hat{\mathbf{U}}=(\mathbf{B}^T\mathbf{B})^{-1}\mathbf{B}^T\mathbf{COV}\hat{\alpha}\mathbf{B}(\mathbf{B}^T\mathbf{B})^{-1}$$

by replacing the covariance matrix Σ, mentioned above in chapt.3, in $\mathbf{COV}\hat{\alpha}=1/\Sigma_{i=1}^{n}dx_i^2\cdot\Sigma$, $dx_i=x_i-\bar{x}$, $x_i=i$, by $S=(s_{k\ell})$, cf. chapt.3, which is an unbiased estimate of Σ. In table 1 we have listed the results from Simonsen (1949) and the new results. The parameter γ is the velocity of tilt, w is the angle of the tilt axis, and q is the perpendicular distance of the tilt axis, marked on the map Danmark, 1:750000, from the south eastern corner of the map. This map has been used already by Simonsen (1949). The distance q is determined by the assumption on no sea level rise. With regard to the corresponding mean square errors it has to be noted, that Simonsen replaced the covariance matrix of $\hat{\alpha}$ by $\sigma^2\mathbf{I}$, but in table 1 we have applied the estimate based on S.

	$\hat{w}$(°)	$\hat{q}$(cm)	$\hat{\gamma}$("/year)
Simonsen:	-57.1±7.0	15.9±7.4	-.0012±.00010
1893-1993:	-60.9±2.8	18.7±2.7	-.0013±.00004

table 1: tilt parameters from sea level records (no sea level rise)

The same kind of approximating planes have been computed from the relative velocities determined from the repeated levellings. Here the tilt axes is determined by velocity=0, relative to GM 902. The results are listed in table 2.

	$\hat{w}$(°)	$\hat{q}$(cm)	$\hat{\gamma}$"/year)	nmb. of velocities
east from Great Belt	-70			1093
west from Great Belt	-55			2338
the whole country	-68	24.1	-.0009	3431

table 2: tilt parameters from repeated levellings (rel. to GM 902)

Below we have shown the direction of the tilt axes determined from the sea level records and from the precise levellings.

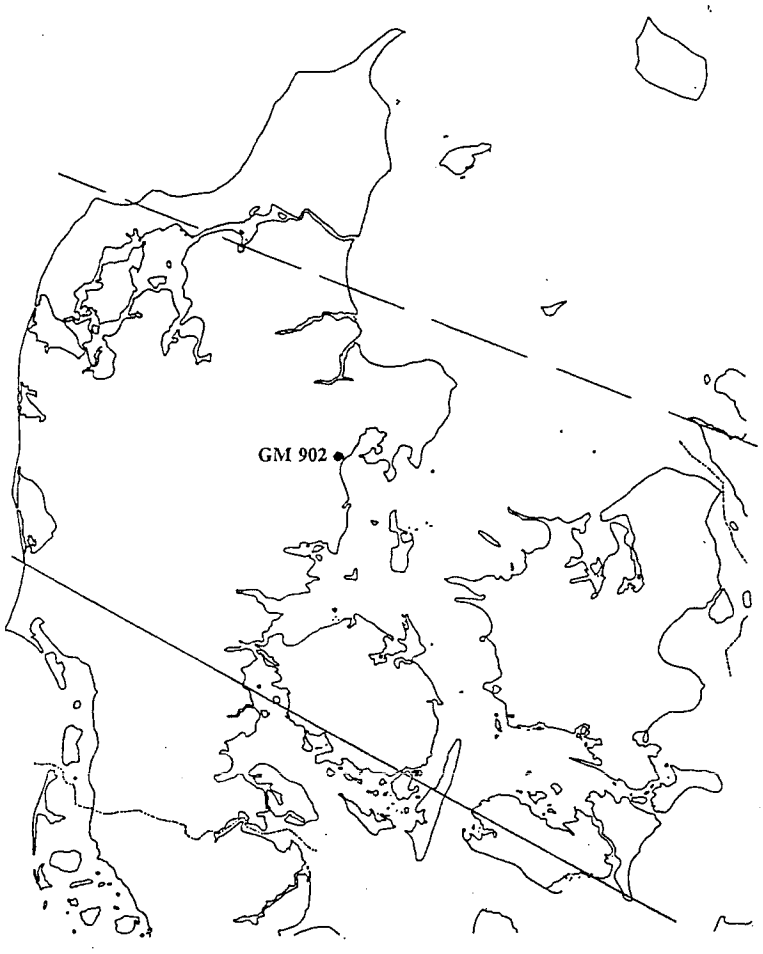

fig.1: solid line: tilt axis from sea-level records, eustatic rise=1mm/yr
dashed line: tilt axis from repeated levellings, GM 902 stable

Conclusions: The readjustment of the sea level records didn't give new results, and as long as meteorological and oceanographic corrections are not available, the results can hardly be improved, even though the time span of observations would be considerably longer than today. The joint adjustment of the levellings, however, gave completely new results concerning the region east from the Great Belt. Here, the north-south direction of the old tilt axis is changed to a north-west south-east direction, which is in much better agreement with the axis determined from the sea level observations.

One still may say that the gap between the results from the two methods is too big. As indicated by the contour map in chapt.2 there seems to be some points with irregular movements, in particular in the south of Zealand, on Falster, and on Lolland. A restriction of the present investigation to the subsoil benchmarks could improve the results.

The fact, that the 0-isoline of the annual land uplift relative to the fundamental benchmark GM 902, i.e. the dashed line in fig.1, is crossing the country much more to the north as it should be expected, might indicate an irregular movement of the fundamental benchmark.

References:

Andersen, N. (1992): The hydrostatic levellings in Denmark. In: Sea Level Changes: Determination and Effects, Geophysical Monograph 69, IUGG Volume 11, pp. 107-111

Becker, J.M., Bedsted Andersen, O. (1984): Guidelines for motorized 1.order precise levelling. Accepted by the Nordic Levelling Group at the Helsinki meeting.

Bedsted Andersen, O., Kejlsø, E., Remmer, O. (1974): Secular movements within Jutland as determined from repeated precise levellings 1885-94 and 1943-53. Geodætisk Instituts Skrifter 3.Række Bind XL, Bianco Lunos Bogtrykkeri A/S

Bedsted Andersen, O., Forsberg, R. (1996): Danish precision gravity reference network. Publications 4.series, volume 4. National Survey and Cadastre, Denmark

Borre, K. (1970): The influence of current and meteorological forces on the mean sea level in the Danish straits. Geodætisk Institut, meddelelse no.47. København

Den Danske Gradmaaling (1909): Præcisionsnivellement Jylland. Ny Række, hefte nr.3

Den Danske Gradmaaling (1909): Nivellement over bredere vandarealer. Ny Række, hefte nr.4

Den Danske Gradmaaling (1911): Præcisionsnivellement Fyn, Sjælland og Falster.Ny Række,hefte nr.8

Egedal, J. (1945): On the variations of the Normal Height of the sea-level round the Danish coasts. Published by the Danish Meteorological Institute, supplement to Nautical Meteorological annual, 1945

Ekman, M. (1989): The impact of geodynamic phenomena on systems for height and gravity. In: Modern techniques in geodesy and surveying. National Survey and Cadastre, Denmark. Publications 4.series vol.1

Ekman, M. (1996): A consistent map of the postglacial uplift of Fennoscandia. Terra Nova,8,p.158

Engsager, K. (1997): Integration of satellite data in local geodetic networks. Ph.D.-thesis. National Survey and cadastre in Denmark, 1997

Grenander, U., Rosenblatt, M. (1956): Statistical analysis of stationary time series. 1956

Hald, A. (1955): Statistical theory with engineering applications. John Wiley & Sons, New York

Heiskanen, W.A., Moritz, H. (1967): Physical geodesy. Freeman and comp., San Francisco & London

Jessen, A. (1970): Jordsætningen i Frederikshavn 1942. Geodætisk Institut, Meddelelse no.46. København

Kakkuri, J. (1985): Die Landhebung in Fennoscandien im Lichte der heutigen Wissenschaft. ZfV, 2/1985, pp.51-59

Koch, K.R. (1988): Parameter estimation and hypothesis testing linear models. Springer Verlag, Berlin

Mälzer, H. (1990): Berechnung von Höhenänderungen im Bayerischen Haupthöhennetz unter Verwendung unterschiedlicher Modelle. DGK, Reihe B, Heft Nr.293. Verlag der Bayerischen Akademie der Wissenschaften, München

Pelzer, H., Niemeyer, W. (1987): Determination of heights and height changes, pp.571-631. Dümmler Verlag, Bonn.

Pruscha, H. (1989): Angewandte Methoden der mathematischen Statistik. B.G.Teubner, Stuttgart

Rossiter, J.R. (1967): An analysis of annual sea level variations in European waters. Geophysical Journal of the Royal Astr. Society, vol.12, pp.259-299.

Rumpf, W.E., Meurisch, H. (1981): Systematische Änderungen der Ziellinie eines Präzisionskompensator-Nivelliers - insbesondere des Zeiss NI1 - durch magnetische Gleich- und Wechselfelder. XVI. FIG-Kongress, Montreux, 1981

Simonsen, O. (1968): Some remarks in May 1968 on secular movements in Denmark. Third Symposium on Recent Crustal Movements, Leningrad, 1968

Simonsen, O. (1949): Nivellements-nul på Sjælland, Møn og Lolland-Falster med særligt henblik på København og Frederiksberg 1845-1945. København, Bianco Lunos Bogtrykkeri, 1949

Stampe Villadsen, S., Andersen, N. (1990): On the DC-AC effect on automatic levelling instruments. Proceedings of the 11'th general meeting of the Nordic Geodetic Comission, 1990, p.225-233. Kort- og Matrikelstyrelsen (National Survey and Cadastre), Copenhagen, 1990

Trigonometrische Abtheilung der Landesaufnahme (1894): Nivellements der Trigonometrischen Abtheilung der Landesaufnahme, achter Band. Berlin

Widmark, J., Becker, J.M. (1984): The motorized levelling technique - the Swedish experience. LMV-rapport, 1984:15. Gävle

Appendix 1

1. Danish levellings of high precision.

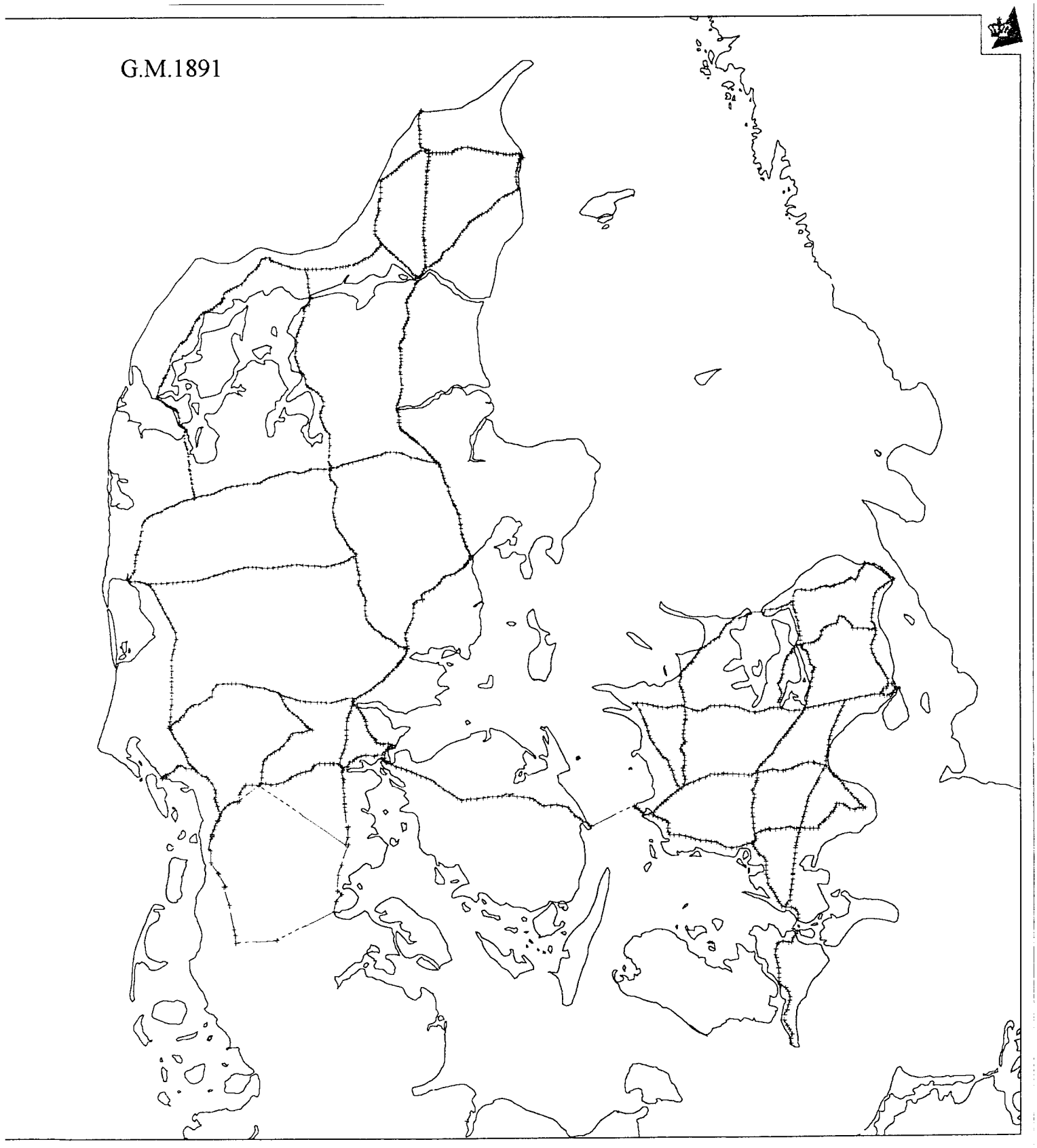

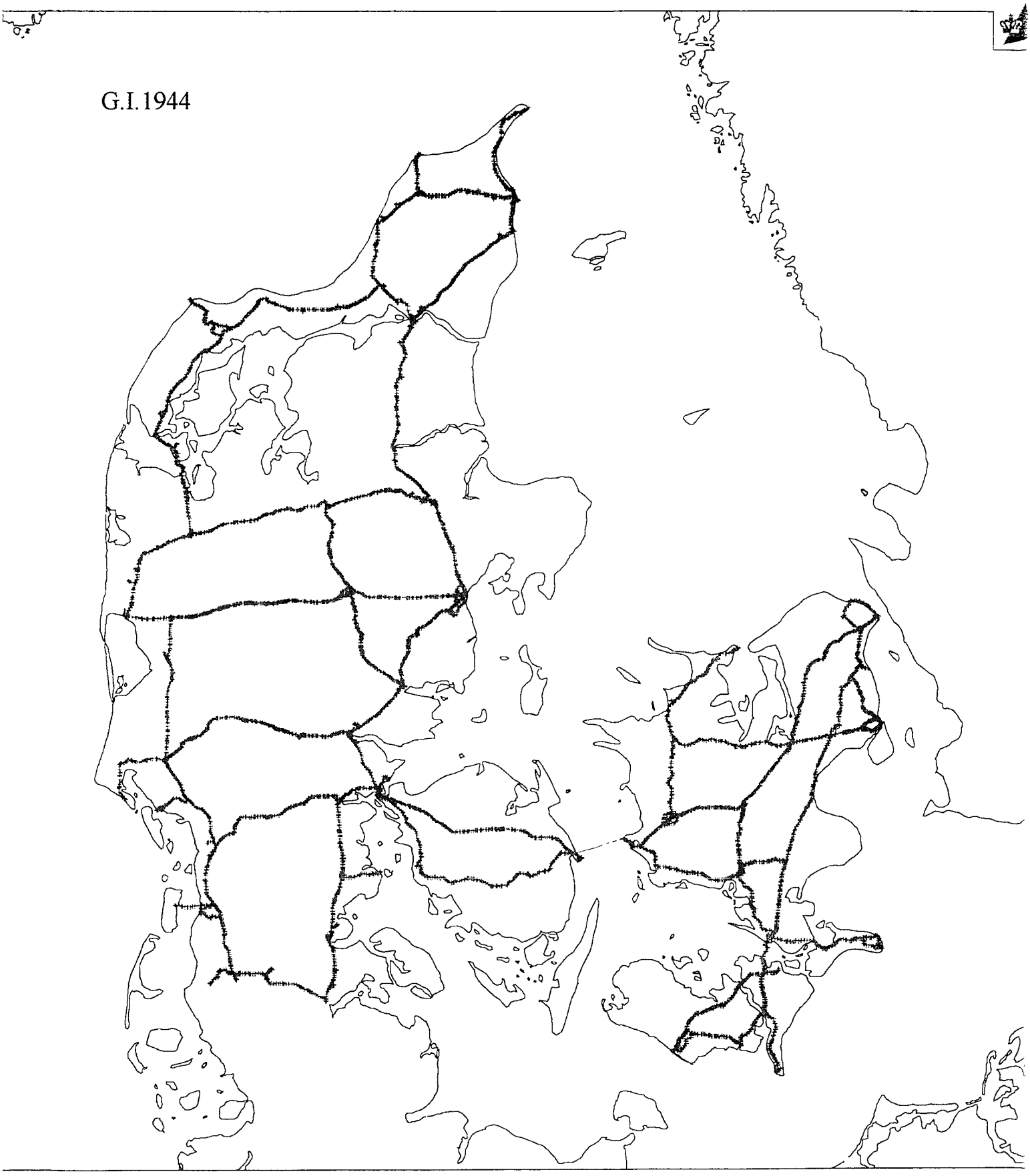

cond levelling of high precision (1938 - 1953)

50 km

Program: GDisp 1:1840000 Mon Jan 05 17:32:49 1998 KJ/KM

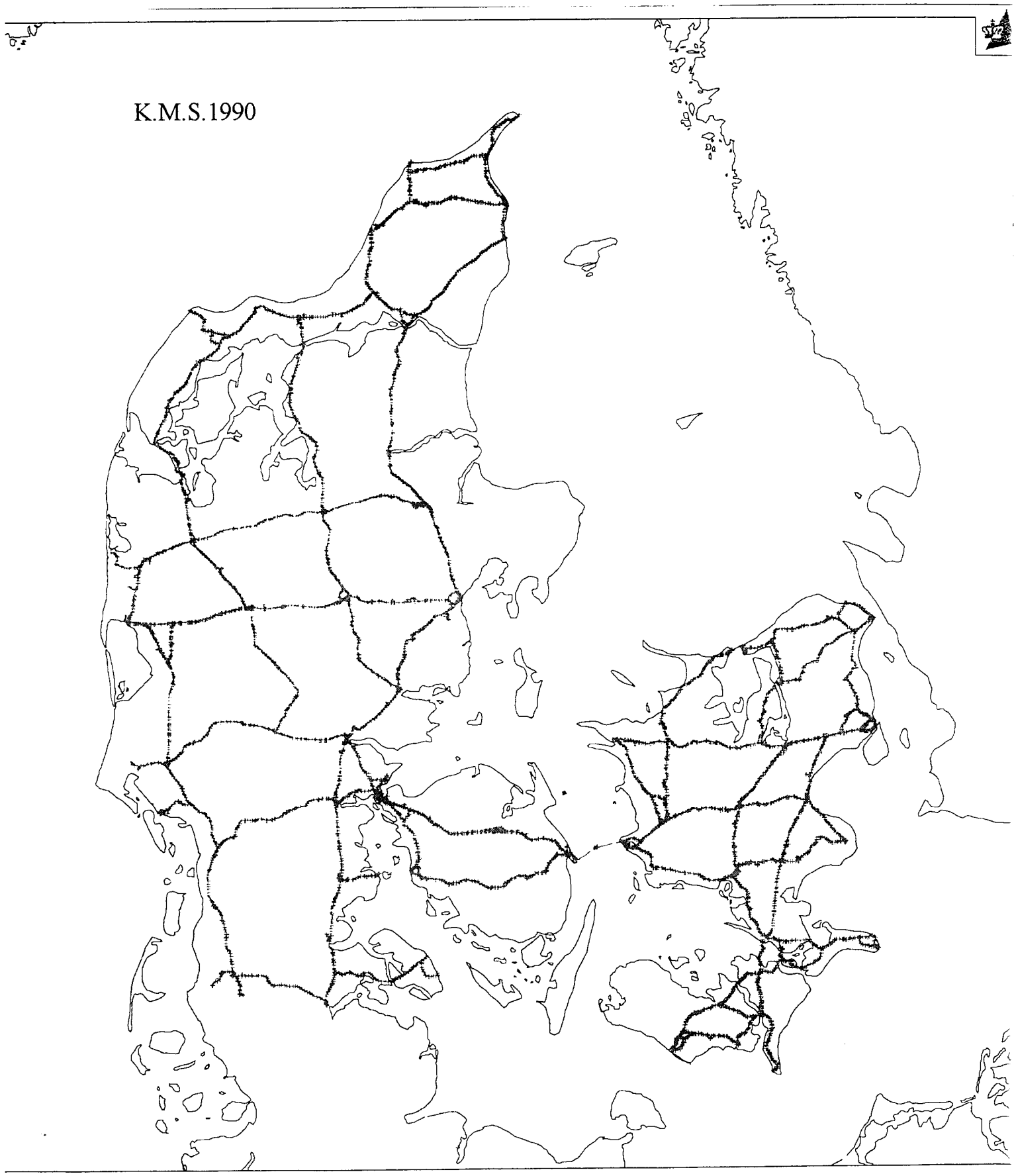

ird levelling of high precision (1986 - 1992)

50 km

Program: GDisp 1:1840000 Mon Jan 05 17:37:12 1998 KJ/KN

2. Computation of tilt.

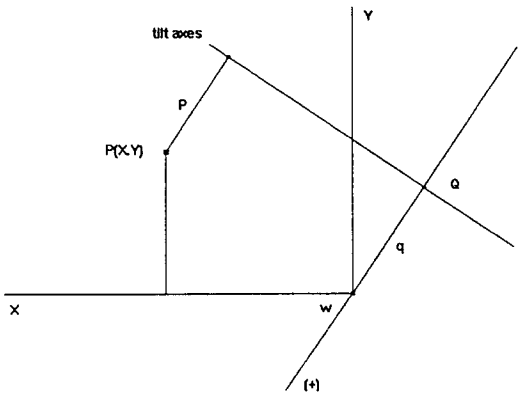

The figure on the right-hand side is illustrating a plane, containing an x,y-coordinate system, a line perpendicular to a tilt axes, the axes itself, and a point P with coordinates x and y. The distance from the tilt axes to P is denoted by p, counted positive or negative in accordance with the direction of the perpendicular line, q is the distance from the tilt axes to the origin, counted in the same way as p, and w is the angle between x-axes and perpendicular line, counted negative counter clockwise. Assuming the plane is tilting with angle velocity γ, counted negative counter clockwise seen from the point Q, the velocity α of P can be written

$$\alpha=\gamma p=\gamma(q+x\cos w+y\sin w)$$

Assigning

$$u_1=\gamma\cos w, \quad u_2=\gamma\sin w, \quad u_3=\gamma q$$

it holds

$$\gamma=\text{sign}(u_1)\,\text{sqrt}(u_1^2+u_2^2), \quad \tan w=u_2/u_1, \quad q=u_3/\gamma$$

Inserting u_1, u_2, and u_3 into the formula of α we obtain $\alpha=xu_1+yu_2+u_3$. Hence, given the velocities of n points, this can be written

$$\alpha=\mathbf{Bu}, \quad \mathbf{B}=(x,y,1)$$

If $\mathbf{u}=(u_1,u_2,u_3)^T$ is computed from observations, i.e. $\mathbf{u}$ is an outcome of a stochastical variable $\mathbf{U}$, then linearizing w, q, and γ with respect to u_1, u_2, and u_3 and applying the law of error propagation yields with $k=1/(u_1^2+u_2^2)$ and $\mathbf{U}_{12}=(U_1,U_2)^T$

$$\text{Var}w=k^2(-u_2,\ u_1)\mathbf{COVU}_{12}(-u_2,\ u_1)^T$$

$$\text{Var}\gamma=k(u_1,\ u_2)\mathbf{COVU}_{12}(u_1,\ u_2)^T$$

$$\text{Var}q=k^3(u_1u_3,\ u_2u_3,\ -1/k)\mathbf{COVU}(u_1u_3,\ u_2u_3,\ -1/k)^T$$

BIFROST Project: Horizontal and Vertical Crustal Motion in Fennoscandia from 1500 days of GPS observations

Hans-Georg Scherneck * Jan M. Johansson * James L. Davis ‡
Jerry X. Mitrovica § Martin Vermeer ¶

Abstract

This presentation compares results from continuous GPS observations in Fennoscandia and neighbour regions with other types of postglacial rebound related data. Vertical movements are compared to tide gauge and precise levelling. Baseline length changes are compared with a visco-elastic model. In the course of the data preparation we carefully examine reference frame issues. In post-processing stage we obtain refined rates (reduced by a best-fitting common mode) by means of Empirical Orthogonal Functions constructed from the motion residuals of neighbour stations.

Our results seem to indicate high rates in the centre of the uplift area—so high that we suspect a large bias. A likely explanation is the still short duration of the experiment compared to the original plan of 10 years. Also, during the first stages, changes of antenna characterstics may have had a large influence. We characterize these results as highly preliminary.

Horizontal motion can be inferred from baseline length changes with the advantage that this parameter is invariant under rotation and translation. Also, radome issues affect the horizontal components less than the vertical. Using only the swedish stations we obtain a pattern of unilateral extension, indicating that horizontal crustal shear on a continent-wide scale is an order of magnitude less important than postglacial rebound.

Background

The BIFROST project has been described earlier (BIFROST, 1996; Scherneck et al., 1998). In short, we use continuous GPS observations obtained at the permanent stations of the SWEPOS network in Sweden. In addition we incorporate observations from the equivalent network in Finland, FinnRef (Koivula et al., this volume). But, due to a different deployment schedule, part of the Finnish stations have been online shorter than 1500 days by varying amounts. Observations at number of IGS stations in Europe are used together with ITRF position and velocity information to map the regional positions into a well controlled geocentric reference frame.

Data analysis

Station positions in this presentation have been obtained with the GIPSY programme (Lichten and Border, 1987; Webb and Zumberge, 1993) using a nonfiducial strategy (Heflin et al., 1992). Bifrost solutions start in August 1993. Since then a number of versions of the reference frame have been issued: ITRF92, ITRF93, and ITRF94 (Boucher et al., 1996). Most recently, in conjunction with a transition to using JPL nonfiducial orbits we have used a JPL reference frame solution (Heflin, 1997; Heflin et al., 1992) that we will call Hef97 henceforth.

The nonfiducial positions are mapped into the most recent reference frame evaluated at the actual date using reference site positions and velocities. The position evolution thus obtained is dominated

* *Onsala Space Observatory, Chalmers University of Technology, S-439 92 ONSALA, Sweden*
phone +46 31 7725500, fax +46 31 7725590, corresponding author: Scherneck, e-mail: hgs@oso.chalmers.se
‡ *Center for Astrophysics, Harvard-Smithsonian, Cambridge, Mass.*
§ *University of Toronto, Canada*
¶ *Finnish Geodetic Institute, Masala, Finland*

by the tectonic plate motion with respect to a no-net-rotation origin. Our objective, however, is to discriminate deformation in the plate interior.

While station positions can readily be mapped into an arbitrary reference frame using a seven parameter transformation, we need to remember that the positions may contain systematic errors due to orbit errors. Some of these errors have very-long time behaviour and may be related to e.g. slow migrations of the orbit centre with respect to the reference frame origin. The accuracies of orbits and tracking station positions evolve by mutually gaining from each other. Moreover, positions that are computed with orbits that themselves refer to, say, ITRF92 but are mapped into Hef97 obtain an inconsistency.

Therefore, we need to compensate for the relative translations and rotations between individual issues of the frames. At some stations, Wettzell and Onsala being good examples, the reference velocities differ significantly. Anticipating that reference information becomes more certain as the data base at the IGS processing centres grows, we decided to use the most recently available ITRF (incl. Hef) and account for the interframe discrepancies in the post-processing stage.

We compute small rotations and translations using the catalogue velocities at all GPS stations that contributed to the respective ITRF's. The position of each station relative to its starting position is then corrected by the inverse of these frame motions. (The effect enters with a negative sign as it propagates via the satellites.)

The positions so corrected are once more reduced by the motion of a rigid frame that travels with the subset of those IGS stations the observations at which have been used in the Bifrost solutions. This frame will be called ARF (accompanying rigid frame). For this we use the most recent reference frame. There are two options, either to use a six parameter rotation and translation mapping or a three parameter rotation-only mapping. It can be shown that the latter case the ARF rotates around a fixed geocentre whereas in the former case the ARF is free to move vertically. The vertical motion of the regional sites is then reckoned relative to this motion which might pick up spurious tilts or other vertical motion which might be erroneous or even part of the signal we aim at. For that reason, the three-parameter rotation-only ARF would be preferable; it relies implicitly on the geocenter as derived from all Hef97 GPS stations world-wide.

In either case we obtain a mode of motion of the network that is deformation dominated. (It would also be possible to subtract a field that yields no-net motion at these sites, but in the present way we obtain Bifrost descrepancies with respect to the "official" reference information site by site.

If a station (Matera) is not on the same tectonic plate as the others we reduce its catalogue velocity with the Nuvel-1a (DeMets et al., 1994) relative motion.

Rates and refined rates

Least-squares adjustment of the single-site position time-series fits a rate that is assumed to be constant throughout the length of the time-series and generalized seasonal variations $s_j(t)$, individually for each spatial component. In addition, at each known instance when changes were made to the antenna (exchange of radomes), a bias term $H(t - t_j)$ (Heaviside's distribution) is introduced (and of course at $t_1 = 0$ to adjust to the reference position). We also condidered side-effects due to changing a large number of antennas possibly affecting sites where conditions were kept constant.

$$x_{kt} = \sum_j p_{kj}\ s_j(t) + a_k\ t + \sum_j b_{kj}\ H(t - t_j)$$

or more symbolically

$$\mathbf{x} = \mathbf{Y}\mathbf{p}$$

for each of the spatial components $k = X, Y, Z$. In the above we have weighted the data with the formal sigmas obtained from the GIPSY solution. There are M parameters and N data samples.

Inversion uses Generalized Inverse (GI) method of Lanczos (Aki and Richards, 1980, Chap. 12.3) with M eigenvalues λ, dataspace eigenvectors $\mathbf{v}$ and modelspace eigenvectors $\mathbf{u}$.

$$\begin{aligned} \mathbf{Y}\mathbf{u} &= \lambda\mathbf{v} \\ \mathbf{Y}^\top\mathbf{v} &= \lambda\mathbf{u} \end{aligned}$$

We delete eigenvalues by a magnitude ratio criterion $1{:}10^{-8}$. At this point there is only little difference to ordinary weighted least-squares; e.g. the GI manages singular matrices as due to coinciding bias

events, that happen frequently when baseline vectors are processed instead of single-site positions. The inversion is given by

$$\mathbf{p} = \mathbf{V}\Lambda\mathbf{U}^{\top}\mathbf{x}$$

Empirical Orthogonal Functions

In our analysis for refined rates we try to remove a common mode signal from the position time-series. The common mode is determined in a separate stage of the least-squares inversion

$$x_{kt} = \sum_j p_{kj}\, s_j(t) + p_k^{pl}\, s_{kt}^{pl} + a_k\, t + \sum_j b_{kj}\, H(t - t_j) + \sum_j q_{kj}\, r_{kt}^j$$

where the residuals of station j in the previous stage, r_{kt}^j, are "recycled". We have also added an atmospheric pressure loading time-series s^{pl} to the signal model.

A set of Empirical Orthogonal Functions (EOF) are constructed from r_{kt}. If only these were present in the signal model, we would retain just one (the greatest) eigenvalue. In the mixed case where EOF's are constructed from only a subset of the components of the signal model, the work amounts to identifying what the eigenvectors represent. Let p_1 to p_K be the parameters of the recycled residuals. In parameter space, the common mode is associated with an eigenvector having elements 1 to K of the same sign and similar magnitude, and K+1 to M much smaller elements. The eigenvalues to be deleted have equally low magnitude in elements K+1 to M, but other (mixed-sign) combinations of elements 1 to K.

In data space, the eigenvectors representative of the residuals are characterized as being similar to white noise. The common mode is easily singled out as it pertains to the largest eigenvalue, while the others can be searched with a white-noise detection method. We propose application of Structure Function methodology (Davis et al., 1994), searching for the K-1 eigenvectors with the smallest power index to remove them from the GI. This can be automated.

The common mode is obtained from

$$\sum_j q_{kj}\, r_{kt}^j$$

It is seen to pick up features at all time scales. The weighted residual has a normalized χ^2 typically about 50% of the case without EOF. The solutions for the rates are only moderately affected.

Inspection of joint confidence limits for Skellefteå as an example shows high correlation between the estimates of rates and offsets; however, the 95% confidence ellipse indicates a rate between 16.7 to 17.1 mm/yr (cf Fig. 1).

Vertical rates

We show Bifrost vertical rates versus results from tide gauges and precise levelling (Ekman, 1998, this issue). The steepness of the regression line between both data types is indicative of the geoid rebound while the zero intercept of the Bifrost results points out the negative of a general sea level change.

Our results (Fig. 2) show high inclination of the regression line. A geoid rebound of 55% of the vertical rate appears unrealistic to suggest.

The large correlation between offsets and rates suggests that the rates obtained in BIFROST may be biased. Therefore, rate results should be considered preliminary. Since all antenna changes occurred at approximately the same time, and since the rates correlate with the height of the jumps, an amplification of the rates can be expected rather than a constant offset. A dichotomy between stations that underwent changes and those that did not is difficult to establish since all stations with high rates and low variances are SWEPOS stations, i.e. have had their radomes exchanged.

Horizontal motion and deformation style

Since BIFROST baselines are short compared to the earth radius, baselines length is dominated by horizontal movements. The length component has the advantage that it is invariant under rotation. Baseline length time series have been used to fit rates. These rates are compared with contemporary baseline rates from the postglacial rebound model of Mitrovica et al. (1994).

We have used only those baselines where there have been more than 800 (500) daily solutions.

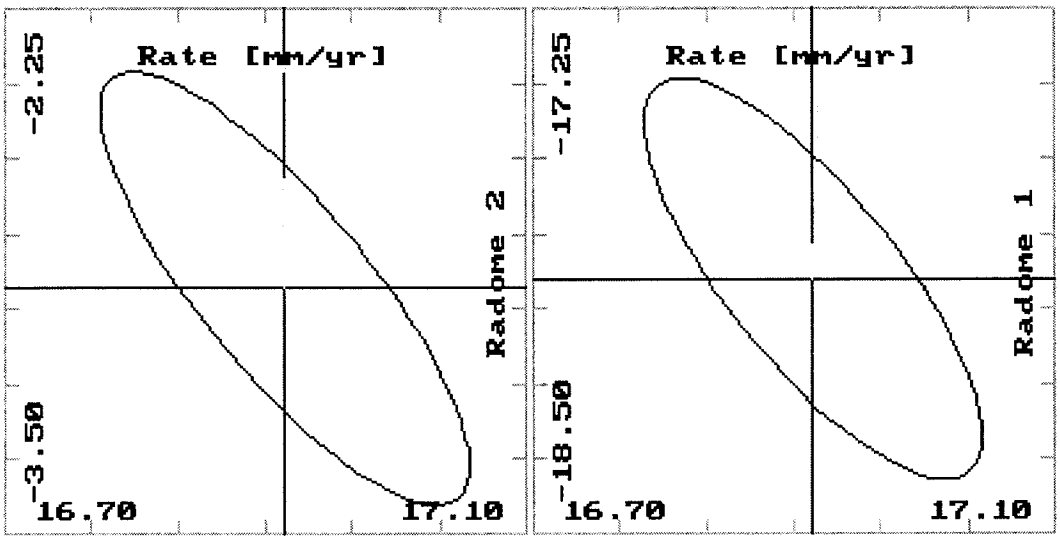

Figure 1: Joint confidence limits (95%) for rates and offsets at Skellefteå

A scatter diagram of observations versus model (Fig. 3) shows a noticeable degree of correlation between both ($\chi^2/\nu = 57$, $\nu = 165$). Eliminating the GPS station SAAR improves the fit to within 5σ. Using the larger set with minimum 800 solutions containing 250 baselines gives $\chi^2/\nu = 50$, respectively $\chi^2/\nu = 30$ when SAAR is removed.

We suspect the anomalous motion at SAAR to relate to the fact that the antenna is not mounted on a standard SWEPOS pillar. The station operated by ESA has the antenna mounted on the roof of a building instead.

It is important to observe that the only set of baselines showing shortening involves the Wettzell station, and that this shortening is predicted by the model. If major zones of crustal shear were the dominating style of deformation, pairs of extending and shortening would be expected. If such a style exists, it is obviously hidden below the unilateral extensional style. Drawing a rose diagram with baseline deformation $\delta l/l$ shown along the azimuth of the baseline, using the unit circle's sectors III and IV to plot shortening, does not indicate a preferred direction.

After the model rates have been subtracted shortening baselines are found at preferred NE-SW azimuth. This is not expected from e.g. the European stress map (Müller et al., 1992) which for most of central Europe shows maximum compression along a NW-SE azimuth. In northern Europe, maximum stress directions scatter, which may be taken as yet another indication that surface extension in the course of the rebound is a prevailing feature.

At this point, however, it is important to point out that most of the baselines to Finland fall short of the 800 days threshold. In the future we expect a more homogeneous coverage of the whole area and perhaps more clear results as regards tectonic signatures.

Conclusions

The issues of reference frame and orbit which we encountered in the BIFROST work are considered to be cumbersome by us. An optimum strategy would deconstrain the site positions that were used in orbit determination and thus to compute a station position solution that is more fully internally consistent.

The high inclination of the regression line found by us between vertical motion observed with GPS versus mareographs, as shown in our figures, certainly has no justifyable physical interpretation as large geoidal rebound signature. We suggest instead that the GPS determined vertical rates are correlated with the estimated temporary offsets that had to be introduced in order to account for changes in the antenna characteristics in connection with changes of antenna radomes. As the BIFROST project is likely to continue for another five years, this bias will become smaller. And as more data are collected

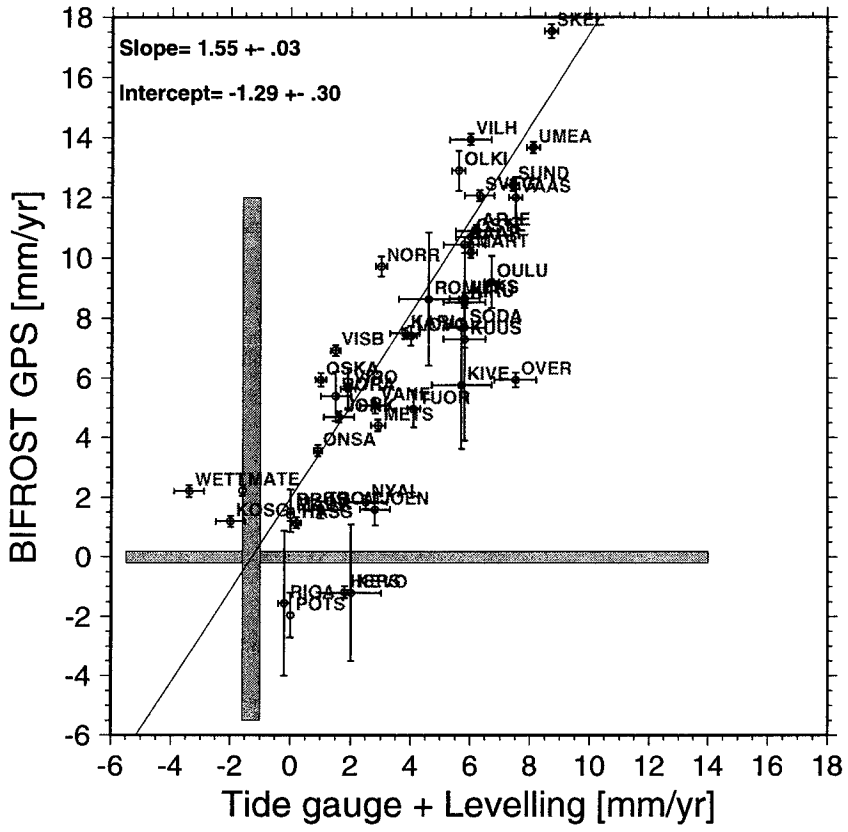

Figure 2: Bifrost GPS-determined rates versus tide gauge and precise levelling results.

and analyzed undisturbed time-series will soon become long enough to provide reasonable confidence limits. Thus, the results presented here will have to be lookeded upon as preliminary. This uncertainty extends also to the zero intercept of the GPS-mareograph regression, which is indicative of a constant sea level rise in the region, and is one of the key quantities to be determined in BIFROST.

Horizontal components of GPS determined positions are to a lesser degree affected by antenna characteristics. The baseline length components draw from this advantage and in addition are invariant to reference frame rotations and translations. We are therefore more confident when interpreting the regression between observed and modelled baseline length variations. Our findings hint at a predominant style of extension and high correlation with the deformation pattern expected from postglacial rebound, including a near-unity slope of the regression. A clear anomaly has been found in one case. Considering that the monumentation of the particular site on top of a building is not complient with the SWEPOS standard, we tend to attribute the anomalous motion to local deformation external to the bedrock or possibly to effects from varying conditions for signal propagation including multipath. The exceptional case underlines the rule that SWEPOS observing stations appear to have good baserock coupling and undisrupted observing conditions in the horizontal components in particular.

References

Aki, K. and Richards, P. G., 1980. *Quantitative Seismology, Theory and Methods, Volume II,* Freeman, San Francisco, pp. 559–935.

BIFROST Project, Bennett, R.A., Carlsson, T.R., Carlsson, T.M., Chen, R., Davis, J.L., Ekman, M., Elgered, G., Elósegui, P., Hedling, G., Jaldehag, R.T.K., Jarlemark, P.O.J., Johansson, J.M., Jonsson, B., Kakkuri, J., Koivula, H., Milne, G.A., Mitrovica, J.X.,

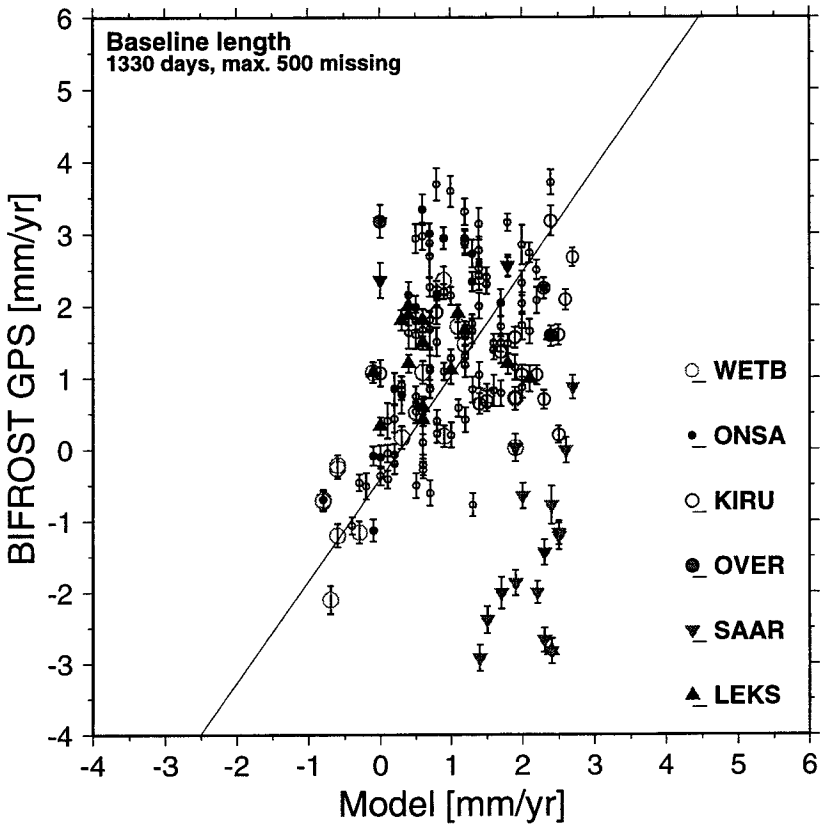

Figure 3: Baseline rates determined by Bifrost GPS compared to the rebound model of Mitrovica et al. (1995). Some baselines have been coded to emphasize particular stations. Noteworthy are WETB in the peripheral subsidence zone where shortening baselines are expected. SAAR is mounted on a building near Kiruna. LEKS has been subject to frequent monument monitoring and antenna remounting in its course.

Nilsson, B.I., Ollikainen, M., Paunonen, M., Poutanen, M., Pysklywec, R.N., Rönnäng, B.O., Scherneck, H.-G., Shapiro, I.I., and Vermeer, M., 1996. GPS measurements to constrain geodynamic processes in Fennoscandia, *EOS Trans. American Geophys. Union,* **77**, p.337+339.

Boucher, C., Altamimi, Z., Feissel, M., and Sillard, P., 1996. *Results and Analysis of the ITRF94*, IERS Technical Note 20, Observatoire de Paris, 157pp.

Davis, A., Marshak, A., Wiscombe, W., and Cahalan, R., 1994. Multifractal charaterizations of nonstationarity and intermittency in geophysical fields: Observed, retrieved, or simulated, *J. Geophys. Res.*, **99**, 8055–8072.

DeMets, C., Gordon, R. G., Argus, D. F., and Stein, S., 1994. Effect of recent revisions to the geomagnetic reversal timescale on estimates of current plate motions, *Geophys. Res. Letters, 21*, 2191–2194.

Ekman, M., 1998. On postglacial uplift rates for reducing vertical positions in geodetic reference systems, in Jonsson, B. (ed.) *Proc. 13th NKG General Assembly, Gävle.* Nordic Geodetic Commission, National Land Survey, Gävle, Sweden. This issue.

Heflin, M.B., 1997. `http://sideshow.jpl.nasa.gov/mbh/all/table.txt`

Heflin, M.B., Bertiger, W., Blewitt, G., Freedman, A., Hurst, K., Lichten, S., Lindqwister, U., Vigue, Y., Webb, F.H., Yunck, T., and Zumberge, J.F., 1992. Global geodesy using GPS without fiducial sites, *Geophys. Res. Lett.*, **19**, 131–134.

Koivula, H., Ollikainen, M., and Poutanen, M., 1998. The Finnish Permanent GPS Network - Finn Ref, in Jonsson, B. (ed.) *Proc. 13th NKG General Assembly, Gävle.* Nordic Geodetic Commission, National Land Survey, Gävle, Sweden. This issue.

Lichten, S.M. and Border, J.S., 1987. Strategies for high precision Global Positioning System orbit determination, *J. Geophys. Res.*, **92,** 12,751-12,762.

Mitrovica, J.X., Davis, J.L., and Shapiro, I.I., 1994. A spectral formalism for computing three-dimensional deformations due to surface loads, 2. Present-day glacial isostatic adjustment, *J. Geophys. Res.*, **99,** 7075–7101.

Müller, B., Zoback, M.L., Fuchs, K., Mastin, L., Gregersen, S., Pavoni, N.,Stephansson, O., Ljunggren, C., 1992. Regional patterns of tectonic stress in Europe, *J. Geophys. Res.*, **92,** 11,783–11,803.

Scherneck, H.-G., Johansson, J.M., Mitrovica, J.X., and Davis, J.L., The BIFROST project: GPS determined 3-D displacement rates in Fennoscandia from 800 days of continuous observations in the SWEPOS network. *Tectonophysics,* in print, 1998.

Webb, F.H. and Zumberge, J.F., 1993. *An Introduction to GIPSY/OASIS–II Precision Software for the Analysis of Data from the Global Positioning System,* JPL, Pasadena, CA.

Nordic Geodetic Commission, 13th General Meeting
1998

Postglacial uplift rates for reducing vertical positions in geodetic reference systems

Martin Ekman

Geodetic Research Division
National Land Survey
SE - 801 82 Gävle
Sweden

Abstract

Rates of postglacial uplift are presented for the permanent geodetic stations in Fennoscandia, including mareographs, GPS reference stations and colocated absolute gravity stations. The uplift rates are of all possible kinds: crustal uplift relative to the sea level, crustal uplift relative to the geoid, rise of the geoid (relative to the ellipsoid), crustal uplift relative to the ellipsoid, and gravity decrease on the surface of the crust. A brief discussion of the reliability of the results, partly in the light of a recent geophysical model, concludes the paper.

1. Introduction

Accurate rates of postglacial rebound are needed for reduction of vertical positions to specified epochs. The need is not only confined to old shore lines and heights above the geoid in traditional height systems, but nowadays also cover heights above the ellipsoid in three-dimensional reference systems as well as gravity values in gravity systems. Especially, postglacial uplift rates for these different purposes are required at the various permanent geodetic stations in the Nordic and Baltic countries, i.e. at mareographs, GPS reference stations and absolute gravity stations. We will here present complete tables of such uplift rates and briefly discuss their reliability.

2. Uplift rates at permanent geodetic stations

In Tables 1 and 2 we list postglacial uplift rates at more than 100 permanent geodetic stations in Fennoscandia. Table 1 contains mareographs, and Table 2 GPS reference stations, often co-located with absolute gravity stations. The stations are grouped by countries in an anti-clockwise order around the Baltic.

The tables are the same as in Ekman (1998), and are computed according to the methods described there; for details see Ekman (1996) and Ekman & Mäkinen (1996). The various uplift rates listed are the following.

$\dot{H}_a$ is the apparent uplift, i.e. the uplift of the crust relative to the sea level, during the 100-year-period 1892 - 1991. These rates are taken from Ekman (1996), a computation founded on sea level data, inland densified by repeated levellings.

$\dot{H}$ is the uplift of the crust relative to the geoid. These rates are obtained by adding a eustatic rise of sea level of $\dot{H}_e = 1.2$ mm/yr to the $\dot{H}_a$ values.

$\dot{N}$ is the rise of the geoid (relative to the ellipsoid). These rates are computed on the basis of the formulae of Ekman & Mäkinen (1996).

$\dot{h}$ is the absolute uplift, i.e. the uplift of the crust relative to the ellipsoid. These rates are obtained by adding the geoid rise $\dot{N}$ to the $\dot{H}$ values.

$\dot{g}$ (in Table 2) is the gravity decrease, i.e. the rate of change of gravity on the surface of the crust. These rates are computed by multiplying the $\dot{h}$ values by the factor $\dot{g}/\dot{h} = -0.20$ μgal/mm.

The largest uplift rates occur at the mareograph Furuögrund and the closely situated GPS reference station Skellefteå, the latter co-located with an absolute gravity station: $\dot{H}_a = 8.75$ mm/yr, $\dot{H} = 10.0$ mm/yr, $\dot{N} = 0.6$ mm/yr, $\dot{h} = 10.6$ mm/yr, and $\dot{g} = -2.1$ μgal/yr.

3. Reliability of the uplift rates

A few words should be said about the accuracy of the contents of Tables 1 and 2. To start with, the standard errors of the $\dot{H}_a$ values are about 0.2 mm/yr in Table 1 (Ekman, 1996a), and 0.2 - 0.5 mm/yr in Table 2 (Ekman, 1996), the latter values depending on the location of the reference station relative to mareographs. The standard error of an uplift difference between two stations is usually smaller. The standard errors of $\dot{H}$ become slightly larger, about 0.3 mm/yr in Table 1 and 0.3 - 0.5 mm/yr in Table 2, since the standard error of $\dot{H}_e$ may be estimated at 0.2 mm/yr. The standard error of an uplift difference is unchanged, as $\dot{H}_e$ is just a constant not contributing to the difference. The standard errors of $\dot{h}$ become more or less the same as those of $\dot{H}$, since the standard error of $\dot{N}$ should be less than 0.1 mm/yr. Finally, the standard errors of $\dot{g}$ are about 0.2 μgal/yr (cf. Ekman & Mäkinen, 1996).

It is interesting to compare the above error estimates for the $\dot{H}_a$ values with recent results from a geophysical model of the Earth. This model is developed by Lambeck, Smither & Johnston (1998), based on a very large amount of geological shore line data from northwestern Europe, and then improved by Lambeck, Smither & Ekman (1998), using the mareograph results of Ekman (1996). The improved model has a lower mantle viscosity of $2 \cdot 10^{22}$ Pas, an upper mantle viscosity of $5 \cdot 10^{20}$ Pas, and a lithosphere thickness of 110 km. Furthermore, it has an ice shape and thickness with a comparatively thin ice over eastern and southern Fennoscandia, equal to the original model, although the mareograph results indicate that slight improvements can be made also in this respect.

Using the improved model for calculating and comparing $\dot{H}_a$ at the mareographs in Table 1 yields a standard deviation of 0.36 mm/yr. Compared to the 0.2 mm/yr above, this shows that the model is able to reproduce the mareograph results successfully. Hence it is also of interest to compare the model with the inland results in Table 2. This yields a good agreement, too, complying with the uncertainty figures of 0.2 - 0.5 mm/yr above. The largest discrepancies between the model and Table 2, around 1.0 mm/yr, occur for some of the interpolated stations marked by an asterisk in the $\dot{H}_a$ column.

Since the model is partly based on the mareograph results used for the uplift map of Ekman (1996), the model is not directly comparable with other uplift maps, like that of Kakkuri (1997). The irregular shape of the (inland) isobases in the latter map is, nevertheless, difficult to reconcile with the fact that the mareographs alone yield a quite regular pattern (Ekman, 1996).

Finally it should be noted that improved inland uplift rates can be expected in the future from GPS recordings at the permanent reference stations; see Johansson & Scherneck (1997).

Table 1. Apparent and absolute uplift rates etc. at mareographs. Unit: mm/yr. ($\dot{H}_a$ from Ekman, 1996.)

Station	Lat.	Long.	$\dot{H}_a$	$\dot{H}$	$\dot{N}$	$\dot{h}$
Liepaja	56 32	20 59	- 0.30	0.9	0.0	0.9
Kronstadt	59 59	29 47	0.09	1.3	0.1	1.4
Hamina	60 34	27 11	1.67	2.9	0.2	3.1
Helsinki	60 09	24 58	2.28	3.5	0.2	3.7
Hanko	59 49	22 58	2.99	4.2	0.2	4.4
Turku	60 25	22 06	4.05	5.2	0.3	5.5
Degerby (Åland)	60 02	20 23	4.11	5.3	0.3	5.6
Lemström (Åland)	60 06	20 01	4.57	5.8	0.3	6.1
Lypyrtti	60 36	21 14	5.06	6.3	0.4	6.7
Rauma	61 08	21 29	5.22	6.4	0.4	6.8
Mäntyluoto	61 36	21 29	6.31	7.5	0.4	7.9
Kaskinen	62 23	21 13	7.11	8.3	0.5	8.8
Vaasa	63 06	21 34	7.62	8.8	0.5	9.3
Pietarsaari	63 42	22 42	8.04	9.2	0.5	9.7
Raahe	64 42	24 30	7.54	8.7	0.5	9.2
Oulu	65 02	25 26	6.66	7.9	0.4	8.3
Kemi	65 44	24 33	7.14	8.3	0.5	8.8
Furuögrund	64 55	21 14	8.75	10.0	0.6	10.6
Ratan	64 00	20 55	8.16	9.4	0.5	9.9
Draghällan	62 20	17 28	7.57	8.8	0.5	9.3
Gävle	60 41	17 10	5.90	7.1	0.4	7.5
Björn	60 38	17 58	5.95	7.2	0.4	7.6
Stockholm	59 19	18 05	3.98	5.2	0.3	5.5
Grönskär	59 16	19 02	3.97	5.2	0.3	5.5
Södertälje	59 12	17 38	3.66	4.9	0.3	5.2
Landsort	58 45	17 52	3.06	4.3	0.2	4.5
Visby (Gotland)	57 39	18 18	1.45	2.6	0.2	2.8
Ölands norra udde	57 22	17 06	1.29	2.5	0.1	2.6
Kungsholmsfort	56 06	15 35	0.20	1.4	0.1	1.5
Ystad	55 25	13 49	- 0.62	0.6	0.0	0.6
Klagshamn	55 31	12 55	- 0.04	1.2	0.1	1.3
Varberg	57 06	12 13	0.77	2.0	0.1	2.1
Smögen	58 22	11 13	1.99	3.2	0.2	3.4

Oslo	59 54	10 45	4.10	5.3	0.3	5.6
Nevlunghavn	58 58	9 53	1.56	2.8	0.2	3.0
Tregde	58 00	7 34	- 0.05	1.2	0.1	1.3
Stavanger	58 58	5 44	- 0.19	1.0	0.1	1.1
Bergen	60 24	5 18	0.24	1.4	0.1	1.5
Heimsjø	63 26	9 04	1.47	2.7	0.2	2.9
Narvik	68 26	17 25	3.06	4.3	0.2	4.5
Vardø	70 20	31 06	0.81	2.0	0.1	2.1
Esbjerg	55 28	8 27	- 1.04	0.2	0.0	0.2
Hirtshals	57 36	9 57	0.38	1.6	0.1	1.7
Frederikshavn	57 26	10 34	0.49	1.7	0.1	1.8
Århus	56 09	10 13	- 0.49	0.7	0.0	0.7
Fredericia	55 34	9 46	- 0.96	0.2	0.0	0.2
Slipshavn	55 17	10 50	- 0.83	0.4	0.0	0.4
Korsør	55 20	11 08	- 0.61	0.6	0.0	0.6
Hornbæk	56 06	12 28	- 0.08	1.1	0.1	1.2
København	55 41	12 36	- 0.24	1.0	0.1	1.1
Gedser	54 34	11 58	- 0.94	0.3	0.0	0.3
Marienleuchte	54 30	11 15	- 0.72	0.5	0.0	0.5
Travemünde	53 58	10 52	- 1.80	- 0.6	0.0	- 0.6
Wismar	53 54	11 28	- 1.31	- 0.1	0.0	- 0.1
Warnemünde	54 11	12 05	- 1.06	0.1	0.0	0.1
Swinemünde	53 55	14 16	- 0.77	0.4	0.0	0.4
Kolberg	54 11	15 34	- 0.95	0.2	0.0	0.2
Pillau	54 39	19 54	- 1.22	0.0	0.0	0.0

* * *

Table 2. Apparent and absolute uplift rates, gravity change rates etc. at permanent GPS stations, including co-located absolute gravity stations. Units: mm/yr and (for $\dot{g}$) μgal/yr. (Asterisk in the $\dot{H}_a$ column marks uncertain value, relying on interpolation.)

Station	Lat.	Long.	$\dot{H}_a$	$\dot{H}$	$\dot{N}$	$\dot{h}$	$\dot{g}$
Riga	56 57	24 04	- 0.2	1.0	0.1	1.1	0.2
Suurupi	59 30	24 25	2.3	3.5	0.2	3.7	0.7
Svetloe	60 32	29 47	0.8	2.0	0.1	2.1	0.4
Virolahti	60 32	27 33	1.9	3.1	0.2	3.3	0.7
Metsähovi	60 13	24 24	2.9	4.1	0.2	4.3	0.9
Tuorla	60 25	22 27	4.1	5.3	0.3	5.6	1.1
Olkiluoto	61 14	21 28	5.6	6.8	0.4	7.2	1.4
Vaasa	62 58	21 46	7.5	8.7	0.5	9.2	1.8
Konginkangas	62 49	25 42	5.7	6.9	0.4	7.3	1.5
Joensuu	62 23	30 06	2.8	4.0	0.2	4.2	0.8
Kuhmo	64 13	29 56	5.0	6.2	0.4	6.6	1.3
Oulu	65 05	25 54	6.7	7.9	0.4	8.3	1.7
Kuusamo	65 55	29 03	5.8*	7.0	0.4	7.4	1.5
Sodankylä	67 25	26 23	5.8*	7.0	0.4	7.4	1.5
Kevo	69 45	27 01	2.0*	3.2	0.2	3.4	0.7
Kiruna	67 53	21 04	5.8	7.0	0.4	7.4	1.5
Överkalix	66 19	22 47	7.5	8.7	0.5	9.2	1.8
Arjeplog	66 19	18 08	6.2*	7.4	0.4	7.8	1.6
Skellefteå	64 53	21 03	8.7	9.9	0.6	10.5	2.1
Vilhelmina	62 42	16 34	6.0*	7.2	0.4	7.6	1.5
Umeå	63 35	19 31	8.1	9.3	0.5	9.8	2.0
Östersund	63 27	14 52	6.0	7.2	0.4	7.6	1.5
Sundsvall	62 14	17 40	7.4	8.6	0.5	9.1	1.8
Sveg	62 01	14 42	6.3	7.5	0.4	7.9	1.6
Leksand	60 43	14 53	5.8	7.0	0.4	7.4	1.5
Mårtsbo	60 36	17 16	6.0	7.2	0.4	7.6	1.5
Karlstad	59 27	13 31	3.8	5.0	0.3	5.3	1.1
Lovö	59 20	17 50	4.0	5.2	0.3	5.5	1.1
Vänersborg	58 42	12 02	2.8	4.0	0.2	4.2	0.8
Norrköping	58 35	16 15	3.0	4.2	0.2	4.4	0.9
Jönköping	57 45	14 04	1.6	2.8	0.2	3.0	0.6
Visby	57 39	18 22	1.5	2.7	0.2	2.9	0.6
Onsala	57 24	11 56	0.9	2.1	0.1	2.2	0.4
Oskarshamn	57 04	16 00	1.0	2.2	0.1	2.3	0.5
Hässleholm	56 06	13 43	0.2	1.4	0.1	1.5	0.3

Oslo	59 44	10 22	4.0	5.2	0.3	5.5	1.1
Kristiansand	58 05	7 54	0.3	1.5	0.1	1.6	0.3
Stavanger	59 01	5 36	- 0.2	1.0	0.1	1.1	0.2
Bergen	60 17	5 16	0.2	1.4	0.1	1.5	0.3
Ålesund	62 29	6 12	0.3	1.5	0.1	1.6	0.3
Trondheim	63 22	10 19	3.1	4.3	0.2	4.5	0.9
Bodø	67 16	14 21	1.5*	2.7	0.2	2.9	0.6
Tromsø	69 40	18 56	1.0*	2.2	0.1	2.3	0.5
Vardø	70 20	31 02	0.8	2.0	0.1	2.1	0.4
Himmerland	56 51	9 45	0.0	1.2	0.1	1.3	0.3
Skærup	55 38	9 34	- 0.9	0.3	0.0	0.3	0.1
Buddinge	55 44	12 30	- 0.3	0.9	0.0	0.9	0.2

References

Ekman, M (1996): A consistent map of the postglacial uplift of Fennoscandia. Terra Nova, 8, 158-165.

Ekman, M (1996a): A common pattern for interannual and periodical sea level variations in the Baltic Sea and adjacent waters. Geophysica, 32, 261-272.

Ekman, M (1998): Recent postglacial rebound of Fennoscandia - a short review and some numerical results. In Wu (ed): Dynamics of the Ice Age Earth: A modern perspective; Trans Tech Publications, in press.

Ekman, M, & Mäkinen, J (1996): Recent postglacial rebound, gravity change and mantle flow in Fennoscandia. Geophysical Journal International, 126, 229-234.

Johansson, J & Scherneck, H-G (1997): Three years of continuous observations in the SWEPOS network. In Jonsson (ed): Geodetic Applications of GPS; Reports in Geodesy and Geographical Information Systems of the National Land Survey of Sweden, 1977:16, 181-202.

Kakkuri, J (1997): Postglacial deformation of the Fennoscandian crust. Geophysica, 33, 99-109.

Lambeck, K, Smither, C & Johnston, P (1998): Sea-level change, glacial rebound and mantle viscosity for northern Europe. Geophysical Journal International, in press.

Lambeck, K, Smither, C & Ekman, M (1998): Tests of glacial rebound models for Fennoscandinavia based on instrumented sea- and lake-level records. Geophysical Journal International, accepted.

Nordic Geodetic Commission, 13th General Meeting
1998

An example of the impact of winter climate on interannual sea level variations

Martin Ekman

Summer Institute for Historical Geophysics
Bomarsund
ÅL - 225 30 Sund
Åland

(Ordinary address: Geodetic Research Division, National Land Survey,
SE - 801 82 Gävle, Sweden)

Abstract

Weather during winter plays a central role in influencing annual mean values of the sea level in the Baltic Sea. Using air temperature data and sea level data from Stockholm from 1774 onwards, a simple investigation is made of the interannual variabilities of sea level and winter climate. Both the interannual sea level variability and the interannual winter temperature variability decrease from the end of the 1700s to the beginning of the 1900s, and then increase again; the changes are statistically significant at the 94 - 98 % level. The common origin of these changes should be changes of the winter wind conditions over the Baltic entrance and southern Scandinavia.

1. Background

Annual mean values of the sea level are used in geodesy for studying mean sea surface topography as well as for computing postglacial land uplift rates. It is known that a single annual mean might deviate from normal sea level, i.e. from the regression line of a long sea level series, by more than 10 cm in the Baltic Sea. In two recent studies by Ekman (1996, 1997) it has been revealed that extreme annual mean sea levels in the Baltic Sea are mainly due to extreme sea levels during winters, caused by anomalous winter climate. The effect of winter climate on annual sea level will here be studied from a different point of view, using, as before, the long sea level series of Stockholm, commencing 1774 (Ekman, 1988), as well as the long air temperature series of Stockholm, commencing 1756 (Moberg & Bergström, 1997).

2. Investigation

From Ekman (1997) it is known that a special relation is valid for extreme sea level years, which are defined by the annual sea level deviation exceeding twice the standard deviation, or 11.5 cm at Stockholm: Extreme high water years have persistent winter winds from SW and winter temperatures about 3 - 4 °C above normal (with only about 20 % ice cover in the Baltic Sea), extreme low water years have persistent winter winds from ENE and winter temperatures 3 - 4 °C below normal (with as much as 85 % ice cover in the Baltic Sea). Unfortunately, this relation does not work the other way around. Considering all winters with a temperature deviation exceeding 3 °C, one cannot predict the annual mean sea level from that information only. Nevertheless, of all such years, 85 % (25 out of 30) do show a sea level deviation of the same sign as the temperature deviation. Altogether, we should expect some co-variation between winter temperatures and annual mean sea levels.

Let us, therefore, study the interannual variability of the sea level as well as of the winter temperature. As measures of the variability we use their respective standard deviations, $\sigma(H)$ and $\sigma(t_w)$. The results of the computations for both sea level and winter temperature are given in Table 1, where the whole time span of approximately 200 years has been dividied into four 50-year-periods.

Table 1. Standard deviations of annual sea levels (cm) and of winter temperatures (January - March, °C).

Years	$\sigma(H)$	$\sigma(t_w)$
1774 - 1834	7.4	2.5
1835 - 1884	5.8	2.1
1885 - 1934	4.7	1.8
1935 - 1984	6.2	2.4

Table 1 indicates that $\sigma(H)$ as well as $\sigma(t_w)$ decrease from the first period to the third, and then increase from the third period to the fourth. A minor reservation should be made for the earliest period; here the sparseness of sea level data might exaggerate that figure slightly. F-tests applied to the standard deviations squared show that the changes from the first period to the third as well as from the third period to the fourth are statistically significant at the 94 - 98 % level. Hence, the columns of Table 1 most probably reflect real changes in both temperature and sea level. These should then originate from corresponding changes of the wind conditions over southern Scandinavia and the Baltic entrance. It should also be noted that long-term sea level changes at Stockholm are typical for more or less the whole Baltic Sea (and the adjacent part of the North Sea); cf. Samuelsson & Stigebrandt (1996).

A wider study, including winds, is in preparation (Ekman, 1998). For a different example of winter climate changes causing long-term sea level changes, see Ekman (1998a).

3. Conclusion

The interannual sea level variability and the interannual winter temperature variability have both decreased significantly from the end of the 1700s to the beginning of the 1900s; after that they have both increased significantly again. The common origin of these changes should be changes of the winter wind conditions over the Baltic entrance and southern Scandinavia.

References

Ekman, M (1988): The world's longest continued series of sea level observations. Pure and Applied Geophysics, 127, 73-77.

Ekman, M (1996): Extreme annual means in the Baltic Sea level during 200 years. Small Publications in Historical Geophysics, 2, 15 pp.

Ekman, M (1997): Anomalous winter climate coupled to extreme annual means in the Baltic Sea level during the last 200 years. Small Publications in Historical Geophysics, 3, 14 pp.

Ekman, M (1998): Long-term changes of interannual sea level variability in the Baltic Sea and related changes of winter climate. In preparation.

Ekman, M (1998a): Secular change of the seasonal sea level variation in the Baltic Sea and secular change of the winter climate. Submitted for publication.

Moberg, A, & Bergström, H (1997): Homogenization of Swedish temperature data, part III: The long temperature records from Uppsala and Stockholm. International Journal of Climatology, 17, 667-699.

Samuelsson, M, & Stigebrandt, A (1996): Main characteristics of the long-term sea level variability in the Baltic Sea. Tellus, 48 A, 672-683.

Tidal gravity measurements at 79 degrees North on Svalbard - results from Ny-Ålesund

by

Knut Røthing

Norwegian Mapping Authority, Geodetic Institute

Abstract

We here report on the results of an analysis of one year of data from NMA's tidal gravity meter located in Ny-Ålesund on Svalbard. The measurements indicate a significant loading effect particularly at semidiurnal frequencies. The admittance factor, the regression factor between tidal gravity and air pressure, indicates a seasonal variation. The same type of variation seems to show up in tidal constituents. In addition tidal gravity results from NMA's gravimeter in Trysil will be presented.

Introduction

Ny-Ålesund tidal gravity station is situated at 79 degrees north and is the northernmost tidal gravity station in the world (figure 1). Gravity changes at the Earth surface result from elevation changes, redistribution of mass below the surface, oceanic or atmospheric loading, changes in the relative positions of the sun and the moon [4]. Continuous measurements of gravity can provide information about a variety of geophysical processes.

Description of the site

Ny-Ålesund tidal gravity station is situated about 1 km from the coast (figure 2) and approximately 40 meter above the sea level. The gravimeter is of type Lacoste–Romberg, G863F, and is located in a seismic vault on a concrete pillar. The pillar is founded on bedrock and is situated 5 meter below the surface. The instrument has been upgraded with an electronic feed back system from Hannover IfE (Institutt fur Erdmessung). The output voltage from the feedback system is measured by a digital voltmeter, PREMA 5000. Air pressure - and temperature transducer are located inside the vault. The recording system consists of a pentium

pc equipped with UPS as backup power supply. The computer clock is updated every minute by a GPS-clock receiver. Temperature data are sampled by a rate of 1 minute. The air temperature inside the station is typically stable within 0.5 degree (figure 3). The data are daily transferred by modem connection between the tidal station and Ny-Ålesund Geodetic Observatory which is situated 2 km NW of the tidal gravity station. The recording program was originally written by Prof. H.-G Wenzel, Technical University of Karlsruhe. Significant changes has been made and the code has been changed from Quick Basic to C.

Calibration

The gravimeter is calibrated at NMA's vertical calibration line in Oslo. The accuracy is estimated to 0.5 percent. The air pressure transducer was calibrated by SINTEF, a company in Oslo before starting the tidal gravity measurements. The RMS values were estimated to 0.3 hektoPascal.

Data processing

By modem connection, the data are daily transferred from the station to Ny-Ålesund Geodetic Observatory. Gravity,-and air pressure data are sampled by an interval of 5 seconds. The data have been filtered by a zero shift filter [1] to one-minute data. By using standard software as PREGRED, PRETERNA from the ETERNA-package [3], the time series have been edited for "spikes" and "steps". Small gaps of some minutes up to one hour have been refilled by theoretical values. The gaps migth be caused by micro seismic activity and strong winds. The edited data were filtered to hourly data. Estimation of the instrumental phase lag of the gravimeter is obtained by using "impulse step response method" [2]. The instrumental time lag is estimated to 16 seconds.

Tidal Analysis, Ny-Ålesund

Figure 4 shows observed hourly tidal gravity values. The instrumental drift is big and the drift rate is approximately -330 nms-2 pr. day. The instrumental drift is removed by high pass filtering. Computation of tidal parameters were computed by the earth tide analysis program ETERNA [3]. Earth tidal measurements in Ny-Ålesund indicate a significant tidal loading effect particularly at semi-diurnal frequencies (table 1). For the main semi-diurnal constituent, M2, the theoretical transfer function for a visco elastic ocean less Earth is delta factor 1.155 and phase approximately zero. However, at Ny-Ålesund, the observed delta factor for M2 is 0.540 and the phase is 58.0 degrees (table 1).

Table 1:

wave	amplitude theoretical [nms-2]	amplitude observed [nms-2]	ampl.fac.	stdv. [nms-2]	ph.lead [deg]	stdv.
Q1	22,4756	23,837	1,0606	0,00995	0,447	0,5700
O1	117,3888	132,861	1,1318	0,00187	1,045	0,1070
M1	9,2322	10,981	1,1894	0,01499	-1,977	0,8582
K1	165,0943	187,001	1,1327	0,00111	-1,214	0,0636
J1	9,2319	10,25	1,1103	0,02445	0,627	1,3993
OO1	5,0514	6,494	1,2856	0,05891	1,084	3,3787
2N2	0,8503	1,278	1,5028	0,20500	2,109	11,7562
N2	5,3244	0,841	0,1579	0,04072	37,888	2,3328
M2	27,8096	15,011	0,5398	0,00755	58,004	0,4325
L2	0,786	1,004	1,2772	0,19033	46,015	10,9052
S2	12,9385	14,163	1,0947	0,01668	35,284	0,9532
M3	0,1054	0,054	0,5097	0,55757	43,085	31,9478

*Regression coefficient: **-3.57** nm/s**2pr.hPa stdv: 0.097. Number of recorded days: **340.** TAMURA 1987* [5] *tidal potential used.. WAHR-DEHANT-ZSCHAU inelastic Earth model used.. UNITY window used for least squares adjustment. Numerical filter is PERTZEV 1959 with 51 coefficients. Estimation of noise by FOURIER-spectrum of residuals*

Atmospheric Pressure, admittance factor

The plot in Figure 5 shows hourly values of the air pressure. The variation is big, approximately 70 hectoPascal, and is what we would expect at high latitudes. ETERNA allows the simultaneous determination of the tidal parameters and the local air pressure admittance factor by least squares adjustment. An admittance factor of -3.57 nms-2/hPascal resulted from the adjustments. However, the admittance factor indicates a seasonal variation (figure 6). The admittance factor is dominated by 2 geophysical phenomena. One part is caused by the direct gravity attraction from the air masses. The second is caused by changes in the vertical position due to deformation of the earth. The first part is responsible for approximately -4 nms-2/hPascal. The deformational part acts in the opposite direction. Separate analysis of 3 months length were carried out of the time series by one month of overlap from autumn 96 to autumn 97. A change in the admittance seems to show up in mars 97. This might indicate a variation of the extension of air pressure at Svalbard and the surrounding ocean (personal comment from Hans-Peter Plag). In early April 1997 the ice broke up on the fjord close to Ny-Ålesund. This might also complicate the picture of the admittance. Figure 7 shows a plot of the same type as of figure 6, but from the tidal constituent Q1. The same type of variation seems to show up at this plot.

Tidal Analysis, Trysil

Earth tidal analysis was carried out from 107 days of tidal gravity observations from Trysil with the same instrument used in Ny-Ålesund. Table 2 shows the tidal parameters. The parameters from Trysil are closer to the theoretical values than the parameters from Ny-Ålesund. The

admittance factor is estimated to –2.84 nms-2 pr. hPascal (table 2). This might indicate a larger gravity effect from the deformational part. Trysil is an inland station in southern Norway (more land to deform) and a higher admittance is what we would expect.

Table 2:

wave	amplitude theoretical [nms-2]	amplitude observed [nms-2]	ampl.fac.	stdv	ph.lead [deg]	stdv. [deg]
Q1	50.0160	56.733	1.13429	.00459	-1.0329	.2607
O1	261.2311	299.560	1.14673	.00092	.3081	.0528
M1	20.5448	24.113	1.17366	.00759	.3158	.4357
K1	367.3919	417.809	1.13723	.00071	.1296	.0406
J1	20.5441	23.757	1.15641	.01135	.4611	.6498
OO1	11.2415	12.727	1.13215	.02032	-.0257	1.1646
2N2	5.2610	5.888	1.11920	.01760		
N2	32.9439	37.689	1.14404	.00398	.1705	.2280
M2	172.0666	197.246	1.14634	.00078	.4969	.0444
L2	4.8635	5.378	1.10582	.01787	.0369	1.0231
S2	80.0545	92.069	1.15008	.00150	-.1014	.0849
M3	1.6213	1.806	1.11385	.04729	4.7695	2.7092

*Regression coefficient: **-2.84** nm/s**2pr.hPa stdv: 0.078. Number of recorded days: **107.** TAMURA 1987* [5] *tidal potential used. WAHR-DEHANT-ZSCHAU inelastic Earth model used. UNITY window used for least squares adjustment. Numerical filter is PERTZEV 1959 with 51 coefficients. Estimation of noise by FOURIER-spectrum of residuals.*

Ocean Loading

In figure 8 the length of the horizontal arrow indicates the theoretical amplitude for the semi-diurnal constituent M2. The other arrow with same origin has an angle of 58 degrees (the phase lag of M2) from the horizontal line. The length indicates the observed amplitude. The three arrows that origin from the ending point of the theoretical tide are obtained from ocean loading models. The longest is from Schwiderski ocean load model (provided by H-.G. Scherneck), the 2 shorter one comes from Texas Ocean and Grenoble models (provided by Trevor Baker). It must be pointed out that the tidal gravity are at this stage preliminary results. We need to correct the tidal gravity for the influence of the direct attraction from ocean tide from the nearby area. However, Figure 8 indicates a difference between the Schwiderski-model and Texas Ocean/Grenoble models.

Conclusions

Significant loading effect particularly at semidiurnal frequencies. The admittance factor, the regression factor between tidal gravity and air pressure, indicates a seasonal variation. The same type of variation seems to show up in tidal constituent Q1. Indication of difference between the Schwiderski-model and Texas Ocean/Grenoble models.

Acknowledgements

The author would like to thank Hans-Peter Plag for his support in the preparation of this paper. Hans-Georg Scherneck and Trevor Baker for kindly providing ocean tide loading computations. Reidar Bjørnstad is thanked for transferring data from Trysil to Hønefoss. NMA's local staff in Ny-Ålesund for excellent operation of the gravity station.

References

[1] Zero shift filter, Dr. Prof. Hans-Georg Wenzel , *Bull. Inf. Marees Terrestres*

[2] Stepresponse , Dr. Prof. Hans-Georg Wenzel , *Bull. Inf. Marees Terrestres*

[3] Wenzel, H.-G., 1996: *Earth Tide Data Processing package, ETERNA 3.20, Black Forest Observatory, Schiltach, Karlsruhe, 1996.*

[4] T.Hartmann and H.-G. *Wenzel.The harmonic development of the Earth tide generating potential due to the direct effect of the planets. Geophys. Res. Lett., 21:1991-1993,1994*

[5] Y. Tamura. *A harmonic development of the tide generating potential. Bull. Inf. Marees Terrestres, 99:6813-6855, 1987.*

Figure 1

STATENS KARTVERK

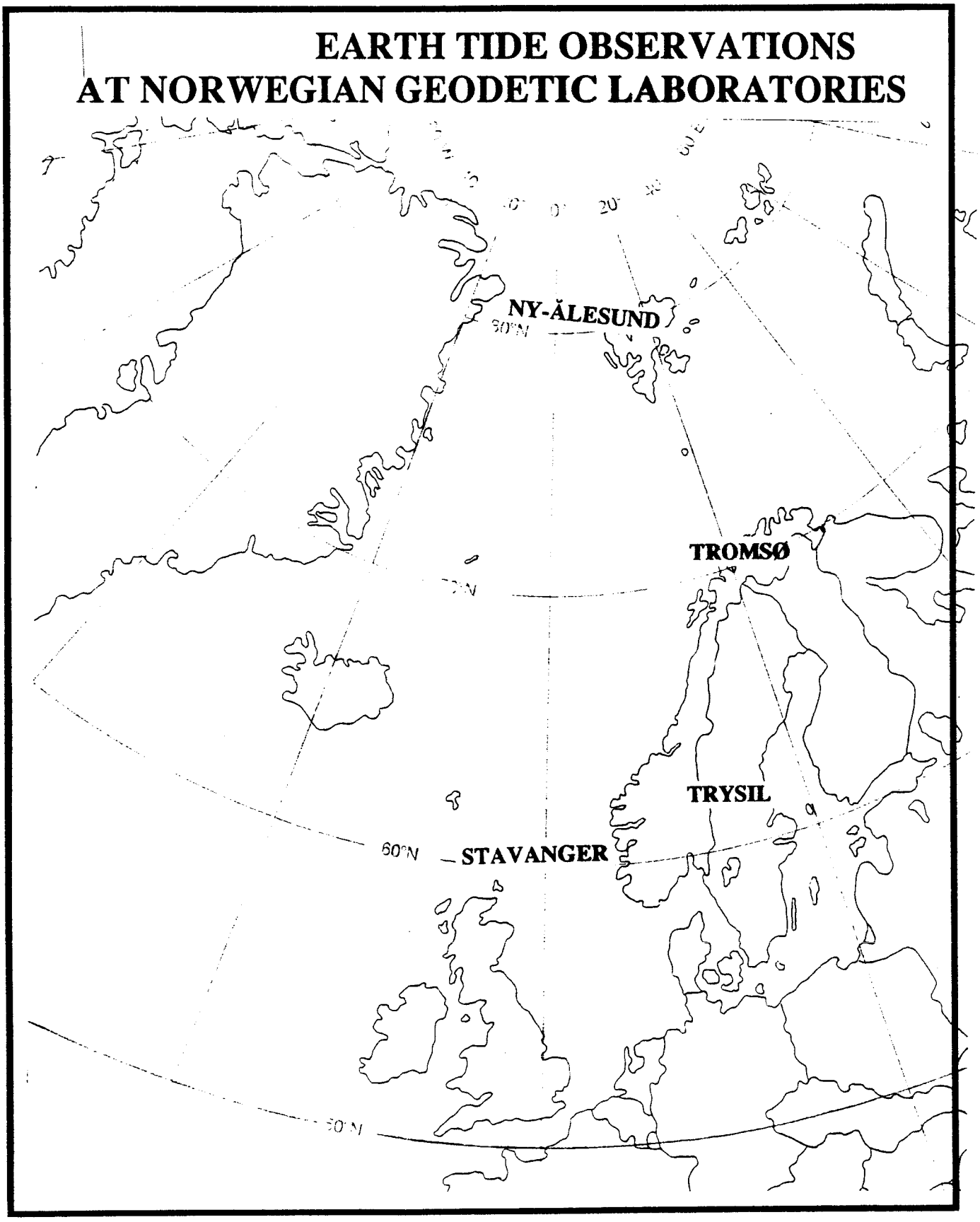

Figure 2

STATENS KARTVERK

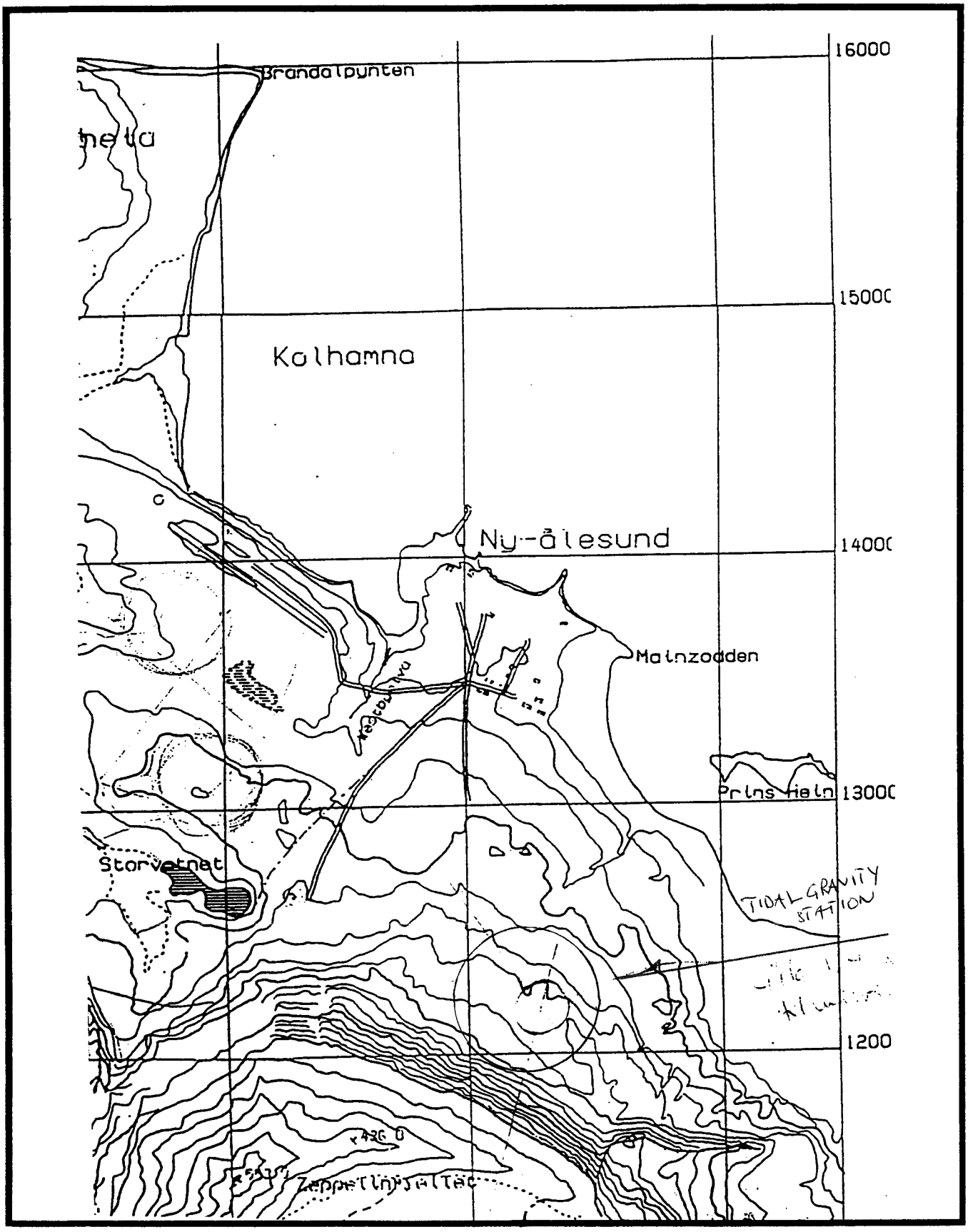

1 km

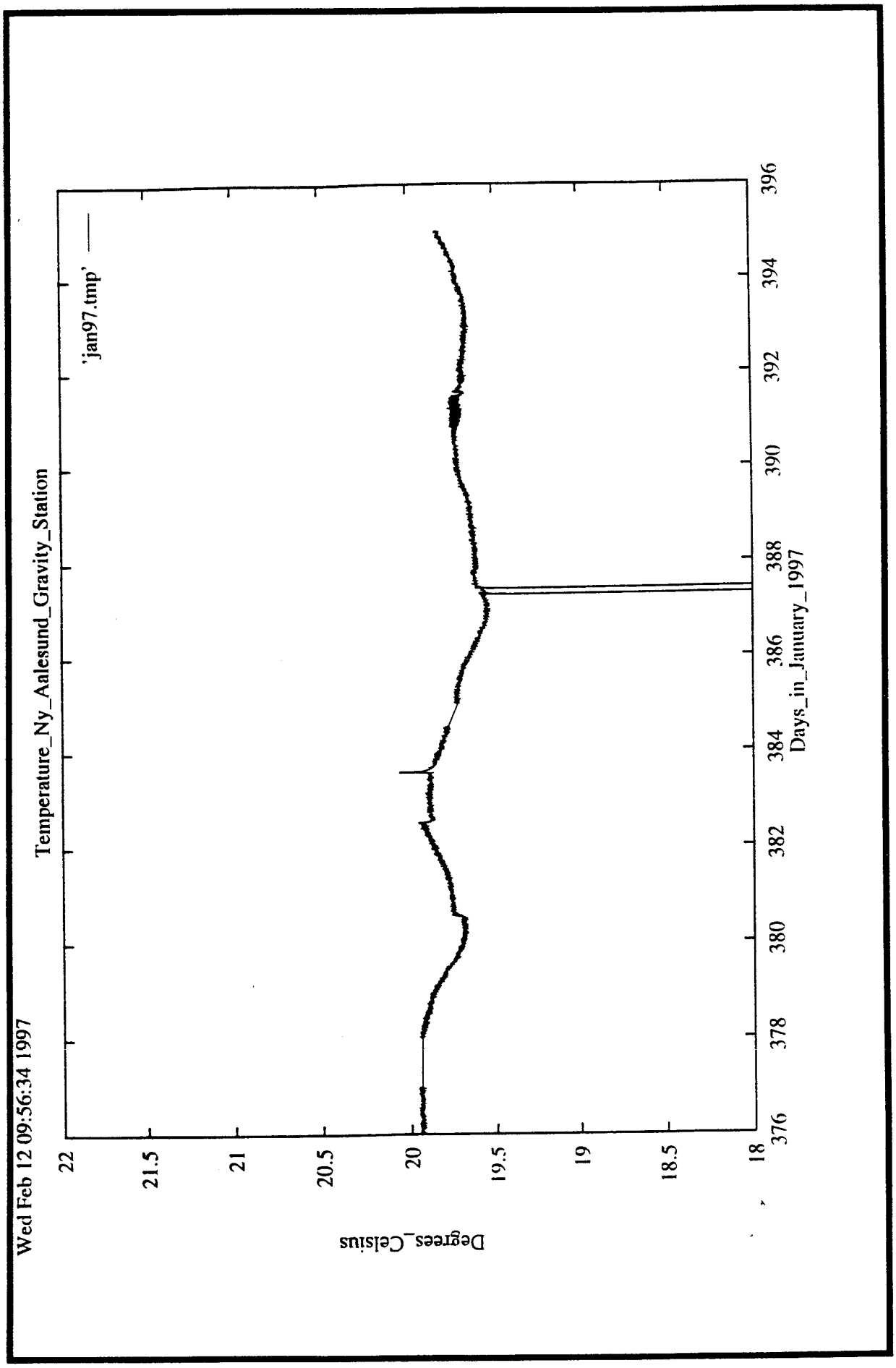
STATENS KARTVERK
Wed Feb 12 09:56:34 1997
Temperature_Ny_Aalesund_Gravity_Station
'jan97.tmp'
Degrees_Celsius
Days_in_January_1997
22
21.5
21
20.5
20
19.5
19
18.5
18
376
378
380
382
384
386
388
390
392
394
396

Figure 3

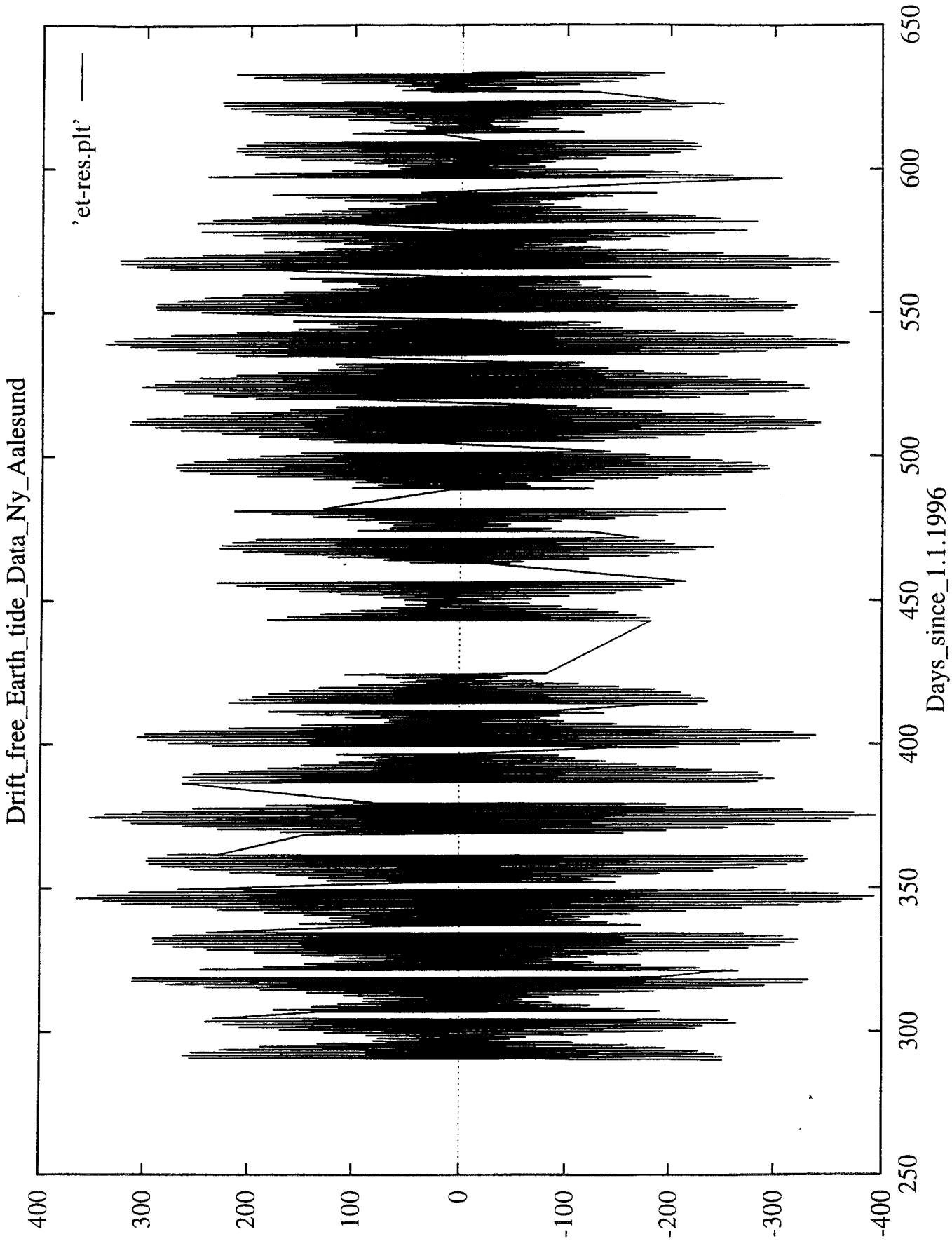
Drift_free_Earth_tide_Data_Ny_Aalesund
'et-res.plt'
nms-2
Days_since_1.1.1996
400
300
200
100
0
-100
-200
-300
-400
250
300
350
400
450
500
550
600
650

Figure 4

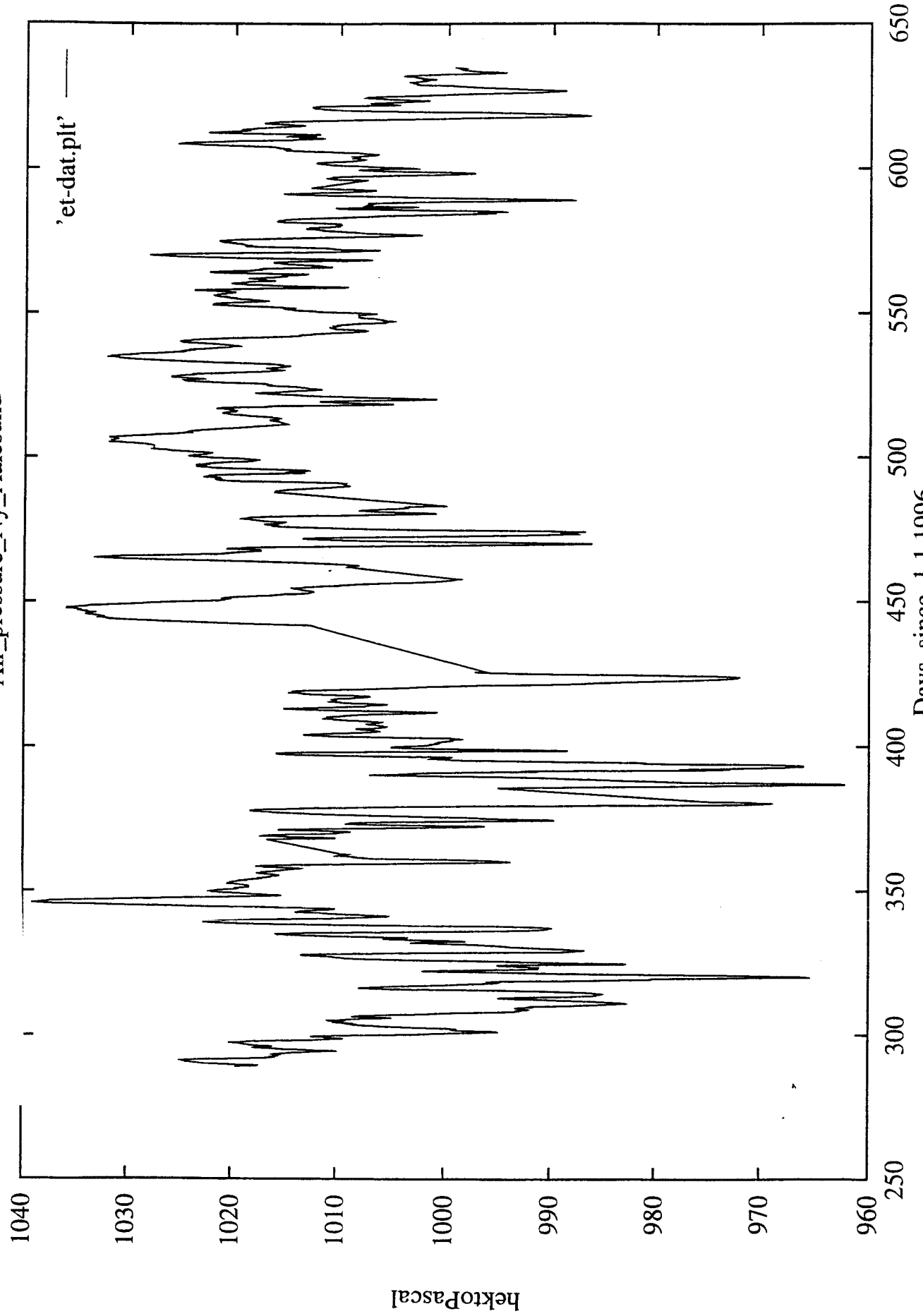
Air_pressure_Ny_Aalesund
'et-dat.plt'
hektoPascal
Days_since_1.1.1996
1040
1030
1020
1010
1000
990
980
970
960
250
300
350
400
450
500
550
600
650

Figure 5

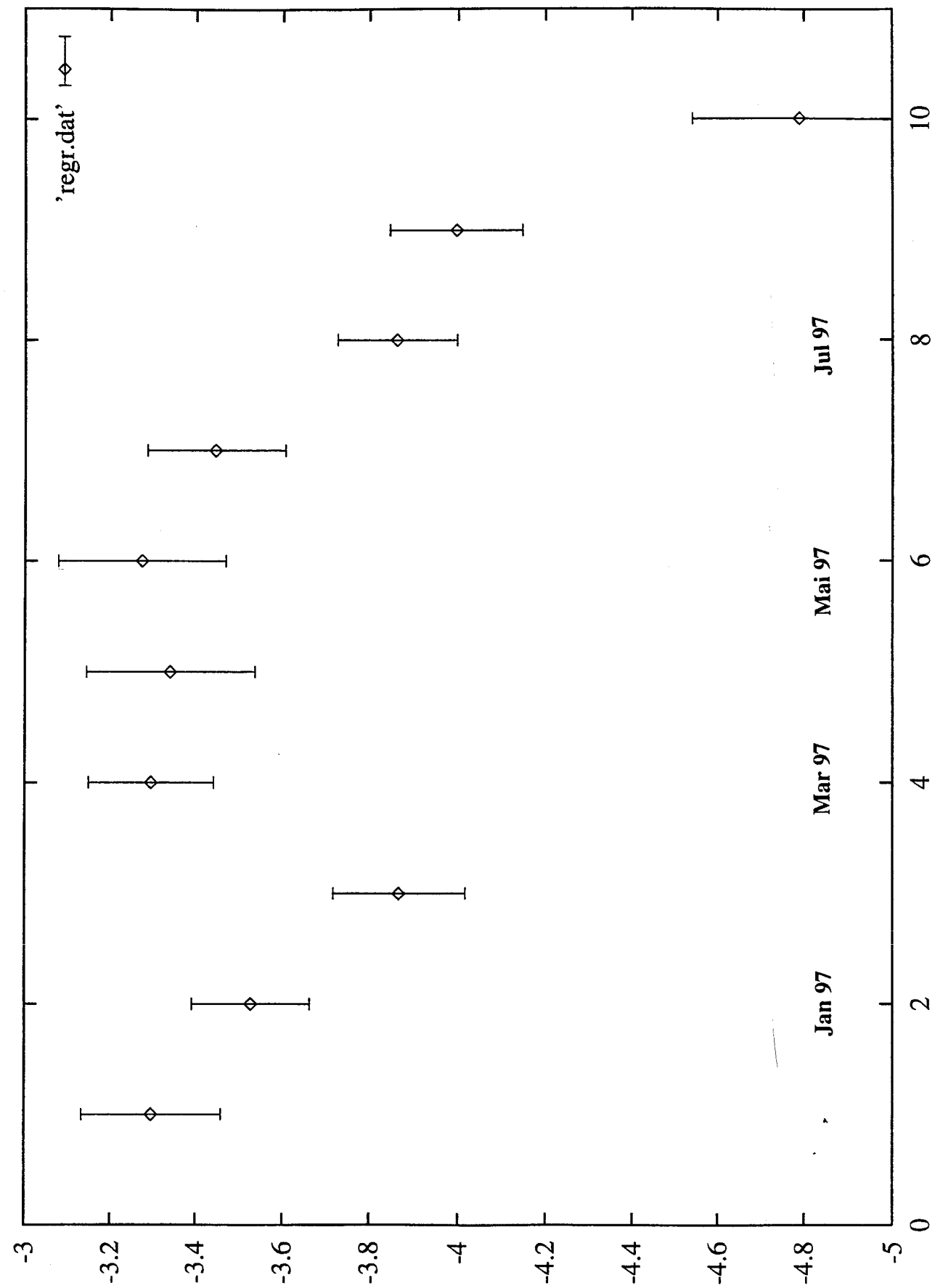
'regr.dat'
Jan 97
Mar 97
Mai 97
Jul 97
-3
-3.2
-3.4
-3.6
-3.8
-4
-4.2
-4.4
-4.6
-4.8
-5
0
2
4
6
8
10

Figure 6

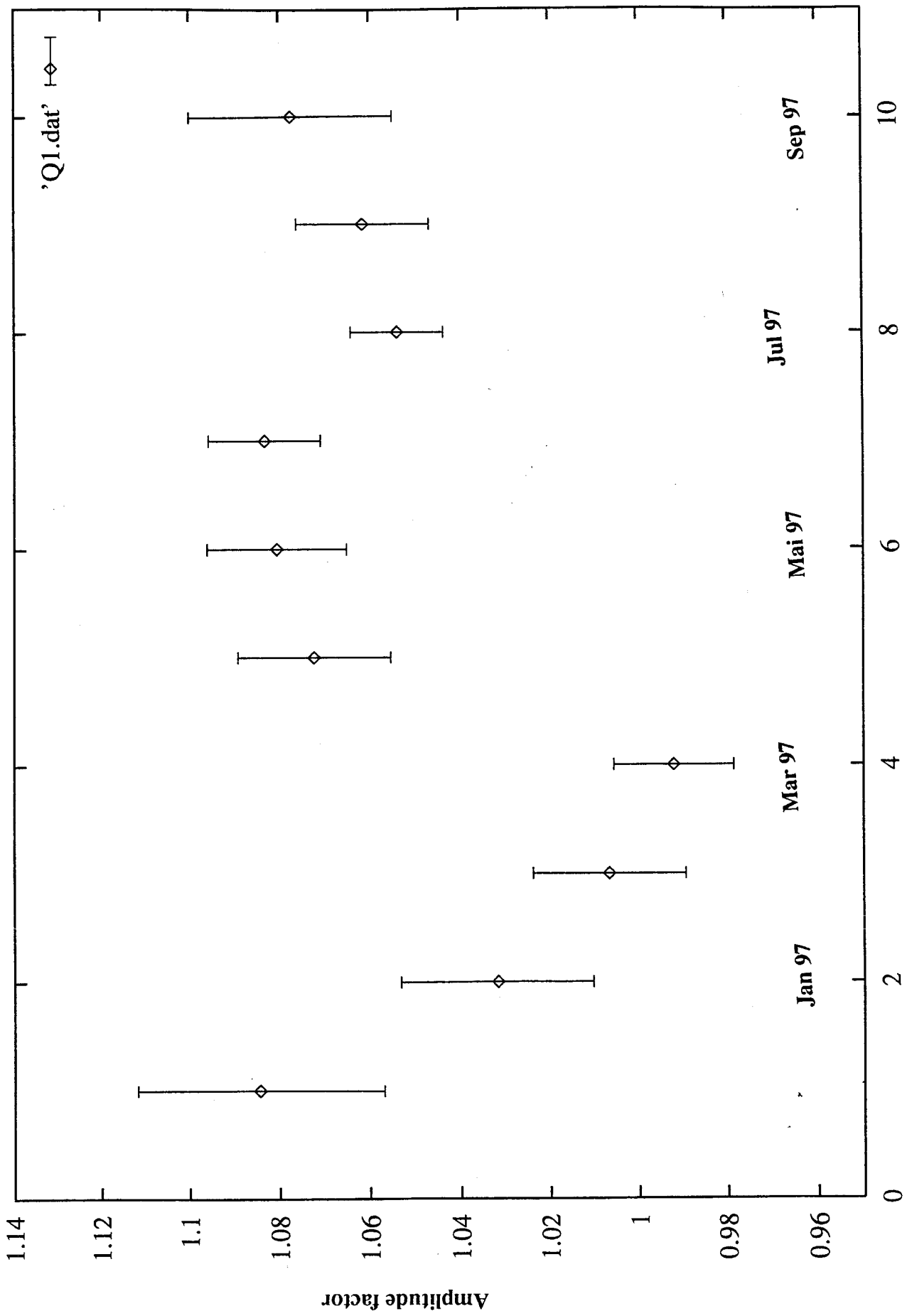
'Q1.dat'
Amplitude factor
1.14
1.12
1.1
1.08
1.06
1.04
1.02
1
0.98
0.96
0
2
4
6
8
10
Jan 97
Mar 97
Mai 97
Jul 97
Sep 97

Figure 7

Figure 8

STATENS KARTVERK

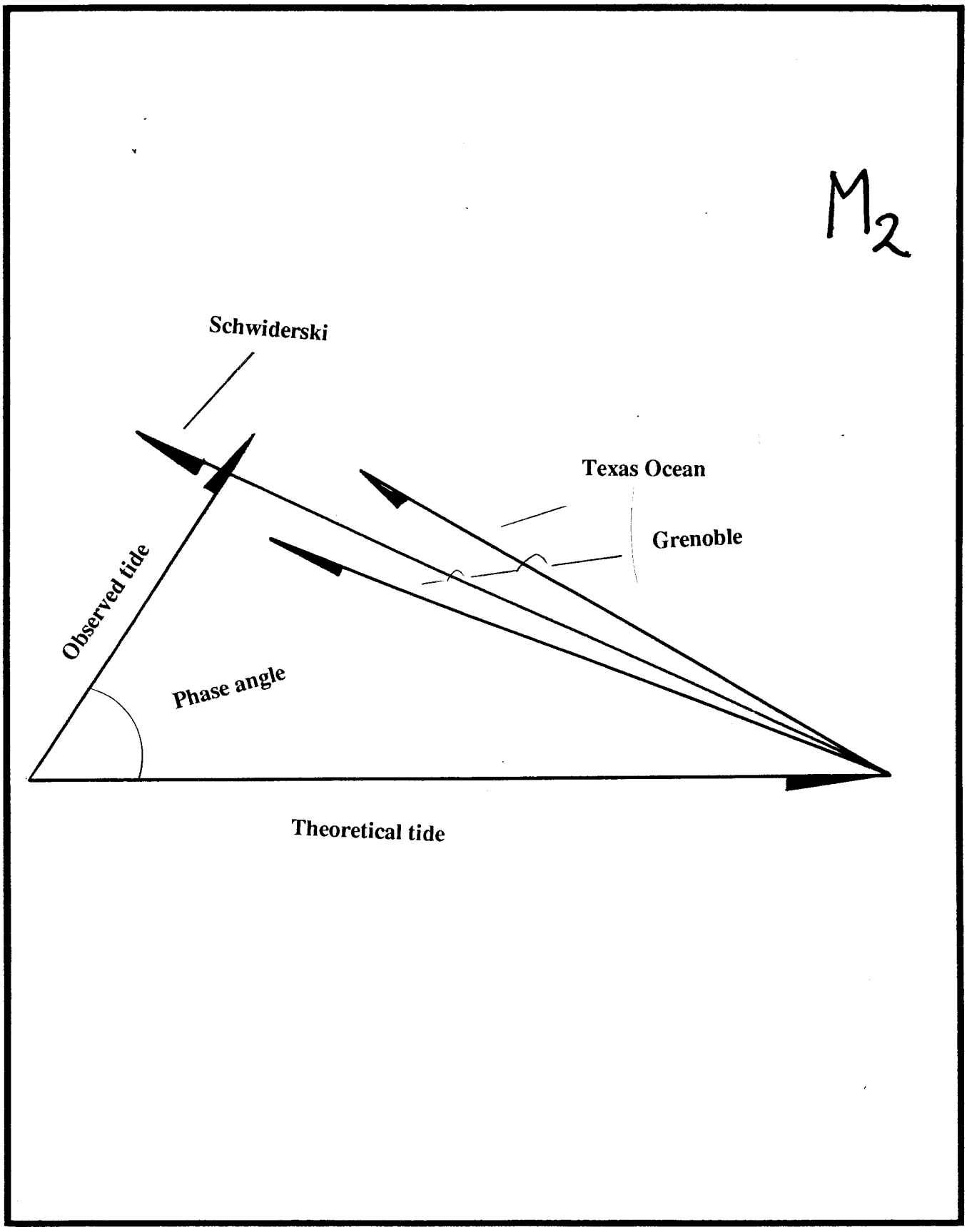

Ocean loading tides in space techniques and implications for mass centre variations

Hans-Georg Scherneck* Rüdiger Haas * Frank H. Webb §

Abstract

Ocean tide loading in VLBI and GPS is examined at a limited set of stations. We highlight the problem of discriminating the frame motion induced by the time varying component of the centre of mass of the ocean, which is to cause a counterbalancing tide in the mass centre of the solid earth. We find that the frame origin of the GPS system is not susceptable to these tides.

Our route of attack is to use VLBI to assess the quality of the loading model and to compute variants of ocean loading for testing them with GPS.The situation for studying tidal site and frame motion is anticipated to be favorable when precise point position is used in contrast to baseline or network solutions. Using more that one year long time-series of GPS point positions at two hour interval we obtain estimates of tide related parameters at submillimeter precision. This is sufficient for resolving particularly some lunar effects as these are less perturbed by environmental effects than their solar counterparts.

We find further that motion due to ocean loading tides is detected in VLBI in all three spatial components, of which the horizontal results are new.

Introduction

Activities in ocean tide loading at Onsala Space Observatory comprise presently a new model for the IERS and verification/assessment of models using VLBI and GPS. Ocean loading tides are computed from a given ocean tide model using a convolution integral with the point load function as a kernel. The point load function is the Green's function of the deformation problem and is derived from the elastic and density structure of an earth model. For a background refer to Farrell (1972), and Scherneck (1991).

For use as an international standard in space geodesy the IERS endorses an ocean loading model in their Conventions document (McCarthy, 1996). The crustal motion due to ocean loading tides is regularly at the one to ten millimetre level. The maximum displacement at any one of the fundamental stations listed in the ITRF catalogue is found at Fortaleza (Brasil) with 66 mm in the vertical and 15 mm the horizontal (scanned inside an 18.6 yr interval). With an increasing resolving power of the methods and more and more data being available for analysis, the need for more and more accurate ocean loading parameters at more and more stations continues.

As ocean tide matters mature after the conclusion of a number of modelling and observation efforts, the idea behind the suggestion for an update of the standards, IERS Conventions 2000, is to achive a greater level of consistency between different chapters of the standards, and to come up with a model that is internally more consistent at the same time. To get perspective on that issue, the previous loading model is based on Le Provost et al. (1994) tides with augmentation for missing oceanic areas from other models or, as in the case of the Bay of Fundy, without. The Bay of Fundy is an area with extremely large semidiurnal tides, complicated coastlines and therefore difficult to model—in particular in a hydrodynamic model that at the same time attempts to represent the ocean on global scales. This piecemeal situation is somewhat relaxed now with the advent of the CSR3.0 ocean tide of Eanes and Bettadpur (1995). Still, the Bay of Fundy is absent, but the Mediterranean (and Kattegatt) is well represented. Additional virtues are that TOPEX/Poseidon satellite altimetry has been used to assimilate long-wavelength features, and that these have considerably improved the parameters representing the centre of mass of the ocean.

*Onsala Space Observatory, Chalmers University of Technology, S-439 92 ONSALA, Sweden
phone +46 31 7725500, fax +46 31 7725590, corresponding author: Scherneck, e-mail: hgs@oso.chalmers.se
§Jet Propulsion Laboratory, Pasadena, Calif.

In the centre of the scope of this paper is the attempt to discern tide induced motion in space-based determinations of point positions on the solid earth. Earlier work in this respect has been presented by Sovers (1994), observing vertical ocean tide loading effects in VLBI. Haas (1996) and Haas and Schuh (1998) have analyzed and discussed these effects primarily in conjunction with devising an improved observation model for solid earth tides in VLBI (Schuh and Haas, 1998).

Centre of mass tides

At first, ocean loading tides are concieved as a deformation of the earth. The traditional reference point has been the centre of mass of the earth excluding the load itself. Seen from space, the centre of mass of the solid earth (and core) moves in a mirror fashion to the centre of mass of the load in order to preserve the joint centre of mass as fixed.

The centre of mass of the tide is

$$\mathbf{X}_{tide} = \frac{1}{M_{tide}} \int_{\mathcal{O}} \mathbf{x}\, dm$$

where M is the mass of the earth and dm is the tidal mass distribution in the ocean $\mathcal{O}$. It is counterbalanced by the condition

$$M_{Earth}\mathbf{X}_{earth} + M_{tide}\mathbf{X}_{tide} = 0$$

This motion is observable with satellite techniques only, since the physical centre of the orbits is in the joint mass centre. In VLBI, as the technique is tied to nearly infinitely distant quasars, the translational motion of a baseline vector cannot be resolved. Surface geodetic techniques are insensitive to this motion. This is seen in inspecting Love number relations. The differences k'_1 - h'_1, k'_1 - l'_1, and k'_1 - l'_1 are invariant, and k'_1 = -1 is the value of the load Love number for the secondary potential corresponding to a reference origin in the joint mass centre (to first order in perturbations). The combinations apply to e.g. the components tilt $(1 + k' - h')$, gravity $(1 + 2h' - [(n + 1)/n]k')$, vertical deflection $(1 + k' - l')$, areal strain $(2h' - n(n + 1)l')$ with spherical harmonic degree $n = 1$ for this style of motion.

The implication of the joint centre of mass of load and deformed body as the physical centre of the gravitational forces acting on the satellites and thus the fixing of translation of the reference frame might appear strong at first sight. However, when orbital parameters are solved from GPS observations at tracking stations, a number of parameters have to be solved for which independent control does not exist (e.g. clock drift, dissipative forces on the spacecrafts) and a number of modelling conditions are used that influence the orbit solutions. Among others, effects due to ocean tide loading and atmospheric loading are usually neglected. Thus, estimated parameters might be biased at a comparatively high degree by systematic effects. To put it simply: if the cohorent, translational motions of sites in the tracking network is not properly reduced in the orbital analysis, the motion is propagated into the orbital parameters. From there the bias propagates into the site positions estimated at an observer's station. In consequence, the differential motion between tracking stations and user stations is to a great extent (probably 100 percent) unaffected by the bias. The bias will therefore only potentially appear as a problem when different satellite techniques are used together inconsistently.

Data analysis

To test the sensitivity of space techniques to ocean loading effects we have compared predicted ocean tide loading parameters with solutions from VLBI and GPS.

VLBI data

For VLBI the data analysis is described in Haas (1996). The data sets analyzed here come from the archive at Goddard Space Flight Center and comprise about 2000 observing sessions, or 1.6 Mio. individual radio source observations, round 70 percent of the available stock. Since VLBI is a baseline network method, the retrieval of residual tidal motion at one station requires that the remaining stations are modelled. The choice of model will therefore cause a side-effect on the residual of the free station. In the analysis a number interesting stations (typically 10 to 20) are freed (model set to null) and the remaining ones (80 to 90) are fixed to the modelled motion. The estimated parameters consider cotidal

motion (amplitude and phase with respect to the astronomical partial tide). The new ingredient in this study is the extension to include horizontal components in the analysis of the baseline residual of each observation. Only cotidal parameters for M_2 and O_1, i.e. significant lunar tides, were targeted. Haas and Schuh (1998) have been successful to retrieve vertical tidal motion at both lunar, solar, and sidereal frequencies. In this study, however, we excluded the latter terms for the sake of comparison with GPS data.

GPS point positioning data

For GPS, the precise single point positioning method available in the GIPSY/OASIS-II software has been employed (Webb and Zumberge, 1993; Zumberge et al., 1997). We have chosen this processing mode since it does not perform range differencing, and since it is free from the interdependencies of motions and errors at simultatneous observations typically experienced in network solutions. Thus the data is expected to preserve a more complete set of range variations between the satellite and the receiver. Spacecraft positions are taken from JPL orbit solutions which include an accurate clock parameter as a prerequisite to solve single point positions accurately. The huge amount of available observations allows to solve for long, almost uninterrupted time-series at sampling rates suitable for tide analysis.

Positions were estimated with the GIPSY Kalman filter at two hours interval, atmospheric parameter at 5 minutes interval assuming a random walk noise model of the zenith delay. Each sample was taken to represent the mean position of the station at the central time of the two-hour interval. The 3-D series were transformed into a local system with east, north, and vertical axes. Solid earth tide displacements were subtracted as usual in GIPSY. The point-positioning time-series were then analyzed with a standard least-squares tidal analysis program.

Loading models

On the modelling side different sets of loading coefficients were computed from three global ocean tide models, NSWC - Schwiderski and Szeto (1982), Grenoble - Le Provost et al. (1994), and CSR3.0 - Eanes and Bettadpur (1995). For details concerning the computation see Scherneck, (1991). These computations are identical (and some variants) from those available from the IERS standards (McCarthy, 1996). For the GPS analysis alternate options to include or not include the centre of mass tide were applied (Scherneck and Webb, 1998).

We have used various methods and options to model and discriminate atmospheric loading, but the results are hitherto too unsystematic and weak for coming into the focus of the discussion.

Discussion

In GPS we generally find very large perturbations at solar and sidereal cycles. The origin of the solar cycles (24/n hours period) is most probably found in the reinitiation of the Kalman filter each midnight. The sidereal period and its upper harmonics, however, might have a less clear origin, one candidate being satellite orbit errors (range effective features that are fixed in the orbital frame will cause near sidereal (sub-) periods seen from an earth-fixed point). We therefore limit the discussion to lunar species in both techniques.

Ocean loading models appear to generally explain a greater amount of the tidal residuals at the lunar frequencies. This is particularly true of VLBI where even most of the horizontal motion can be explained by ocean loading tides. Results for the stations of this survey are compiled in Table 1. A general finding is that the models leave residuals in all components that are significant as compared to the confidence limit of the observations. Reasons may be threefold: There are possible errors in the ocean tide, biases in the VLBI analysis due to the loading model at the fixed stations, and biases due to the solid earth tide model. The discrepancies, however, are larger than what could be explained by loading effects as propagated through different earth rheologies. Take Wettzell as an example. The continental structure of central Europe departs only slightly from the continental PREM model (Dziewonski and Anderson, 1981), which was used to compute the loading Green's function. Yet at this station the weakest reduction of tide motion is found. Of course, the unexplained motion could arise due to various combinations of the problems pointed out, being different at each site.

As an example we show a phasor diagram for Westford, Massachusetts (Fig. 1) where we include different models and variants. The CSR3.0 model has been used in the VLBI analysis at the other stations. We find a good agreement with the Schwiderski model (Schwiderski and Szeto, 1982) and in

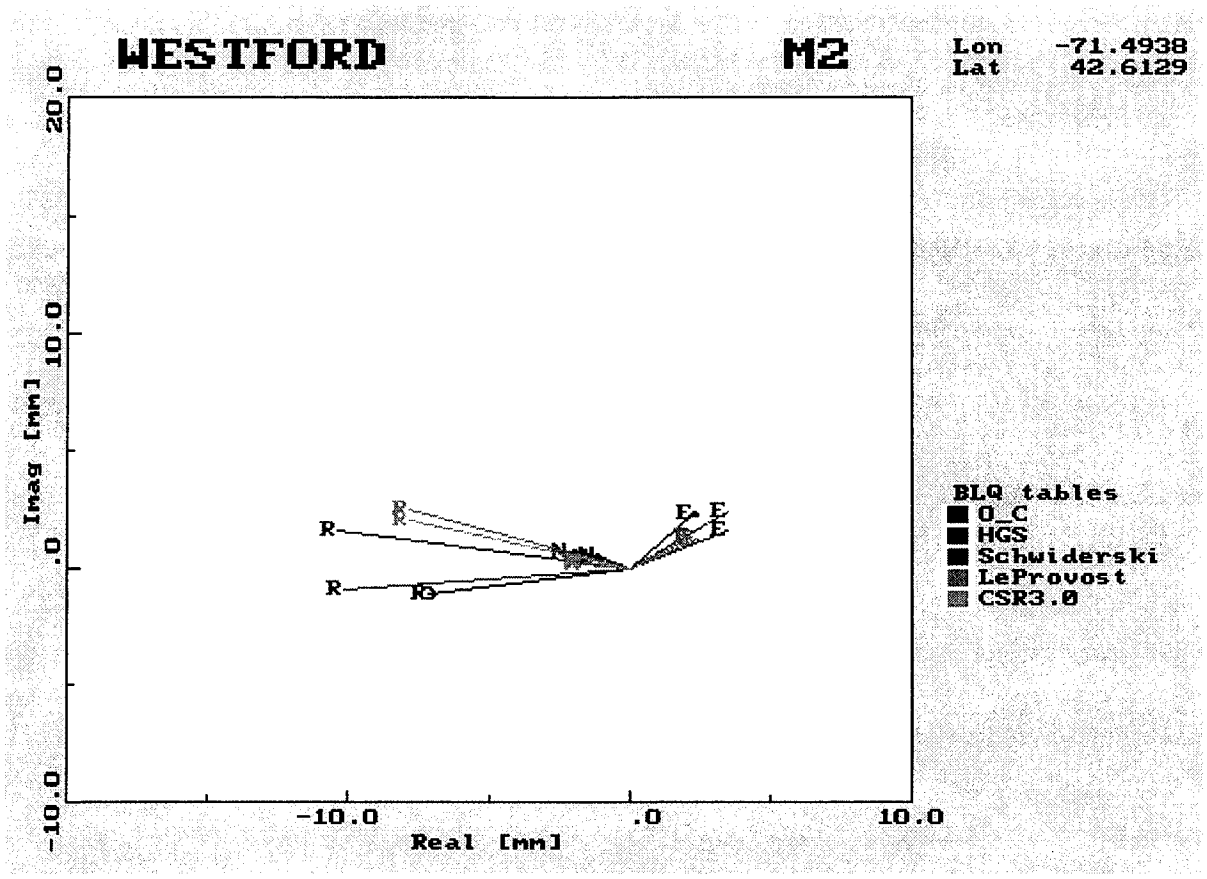

Figure 1: M_2 tide at Westford, Massachusetts. Observed motion in VLBI is indicated by light grey arrows with 95% confidence circle. Components Radial (=vertical), North and East are indicated by the capital letters. Ocean loading models are coded by grey-scale, see the legend.

a few cases less good agreement with the others; the Grenoble model (Le Provost et al., 1994) CSR3.0 (Eanes and Bettadpur, 1995), have not modelled the Bay of Fundy. The model labelled HGS is along the lines of Scherneck (1991a) and augments the Grenoble model in the missing area. It is generally found that Schwiderski's models compete quite well with more recent ones when loading on the shelves is considered. This is probably the effect of using a large number of coastal tide gauges, from which there is a great amount of high-quality data available particularly in the Atlantic area. In Fig. 2 a more abridged plot of the situation at three VLBI stations is shown. The diagrams shows all spatial components separately; the M_2 and O_1 tides have been combined (root square sum), first the observed effect and subsequently the residual when each model is applied.

GPS results are compiled in Tab. 2 for a comparison of loading due to the NSWC model (Naval Surface Weapons Center, Schwiderski and Szeto, 1982), the CSR3.0 model (Eanes and Bettadpur, 1995), and two model versions where we have added the centre of mass tide, denoting them CSR3.0-CMC and CSR3.1-CMC. The latter model has been adjusted to produce the centre of mass terms as reported in Watkins and Eanes (1997).

The test for the admittance of centre of mass tide into GPS is most sensitive at stations located far inland. One suitable site is Irkoutsk in Siberia. In Fig. 4 we show the model misfit at three locations (Irkoutsk, Ascension Island, Pie Town), and Fig. 3 details the situation for the M_2 tide at Irkoutsk. As suspected, the centre of mass components are not visible in the GPS data. We have investigated ten stations altogether (Reykjavik, Mauna Kea, Ascension Island, Onsala; Sundsvall, Yarragadee, Pie Town, Mendeleevo, Hartebeesthook) and found the results to point in the same direction, however less clear as crustal deformation components are regularly larger at coastal stations, particularly those in the first group.

More surprising with Irkoutsk is that the observed motion is close to the predicted motion although the signals are below one millimeter in amplitude. The error limit is based on the assumption of a phase

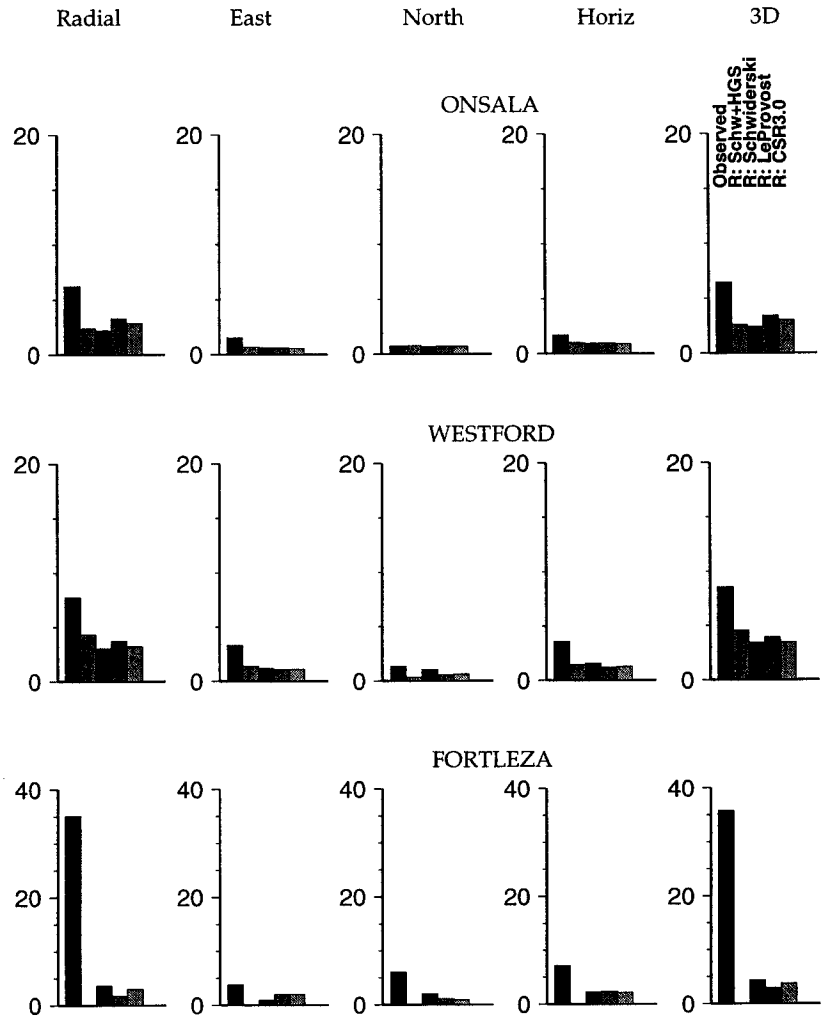

Figure 2: Modelling misfit for O_1 and M_2 tides at three VLBI stations. First column is radial (=vertical) direction, second east, third north, fourth horizontal (root square sum of east and north) and fifth the total root square sum. In each frame the first bar shows the observed effect and the other bars the residual effect (observed minus model, always vectorial amplitudes).

measurement accuracy of 10 cm and from that front-end assumption carried through the analysis. For more details, especially the accuracy of the satellite clock parameter that is crucial in single point positioning refer to Zumberge et al. (1997). The tidal post-fit normalized residual χ^2 is only slightly greater than unity in the vertical component and less than unity in the horizontal components, which hints at a resolution capability of subdiurnal motion of much less than a millimeter from two years of GPS. The method of interleaving of data batches over the day boundary, however, requires reformulation in order to avoid the biases we are seeing at solar synchronous cycles. They are not supposed to leak into the lunar frequencies, though, since the total length of the data assertains frequency selectivity narrower than one cycle per year, while only two cycles per month are required here.

Conclusions

We could show that ocean loading effects are observable with VLBI and GPS. We have restricted our scan to lunar species as these are largely unaffected by environmental perturbations and spurious effects due to earth rotation variations and satellite orbits. In VLBI the detectability of horizontal components due to ocean loading tides mark new, previously unreported results. In GPS the level of noise is greater, and horizontal motion is only marginally significant. As the vertical components of tide loading is

Table 1: Ocean loading at VLBI stations. Results show combined (root square sum) lunar effects at the diurnal period of O_1 and the semidurnal M_2. Lines marked R show vertical component, H horizontal. Values are in mm. Uncertainty σ is specified for M_2; for O_1 the uncertainty is about 30 percent greater. All cases show significant reduction of effect in all spatial components. Loading effects are computed from the models of NSWC - Schwiderski and Szeto (1982), Grenoble - Le Provost et al. (1994), and CSR3.0 - Eanes and Bettadpur (1995).

Site	C	σ	Observed	Residuals		
				NSWC	Grenoble	CSR3.0
FORTLEZA	R	0.7	35.1	3.7	1.8	3.0
	H	0.3	7.1	2.3	2.3	2.2
GILCREEK	R	0.3	9.7	1.5	1.2	0.8
	H	0.1	3.2	0.8	1.0	0.9
HARTEBEE	R	0.9	17.3	3.6	3.0	3.1
	H	0.5	2.9	2.2	1.8	2.0
KOKEE	R	0.4	13.7	3.4	3.4	2.3
	H	0.2	5.0	0.8	0.7	0.7
MOJAVE12	R	0.5	7.3	2.2	2.0	2.1
	H	0.2	4.2	1.5	0.6	0.7
ONSALA60	R	0.4	6.2	2.2	3.3	2.9
	H	0.2	1.7	0.9	1.0	0.9
RICHMOND	R	0.5	7.1	2.1	3.4	1.9
	H	0.2	4.2	0.8	0.8	0.9
WESTFORD	R	0.2	7.7	3.0	3.7	3.2
	H	0.1	3.6	1.6	1.2	1.3
WETTZELL	R	0.2	5.4	0.9	1.3	1.0
	H	0.1	1.9	1.3	1.1	1.0

regularly larger than a few millimeters, this component can be resolved with a better signal to noise ratio.

It appears most clear that differential frame motion between the stations and the satellite orbits is not affected by the centre of mass tide. This is probably a consequence of the treatment of the tracking stations in the orbit analysis where this effect is ignored, while the contribution from deformation at these stations is corrected for.

References

Dziewonski, A. and Anderson, D.L., 1981. Preliminary reference earth model, *Phys. Earth Planet. Int.*, **25**, 297–356.

Eanes R.J. and Bettadpur S., 1995: The CSR 3.0 global ocean tide model, *Technical Memorandum CSR-TM-95-06,* Center for Space Research, University of Texas, Austin, Tx.

Farrell, W.E., 1972. Deformation of the earth by surface loads, *Rev. Geophys. Space Phys.*, **10**, 761-797.

Haas, R., 1996. *Untersuchungen zu Erddeformationsmodellen für die Auswertung von geodätischen VLBI-Messungen*, PhD-thesis, Deutsche Geodätische Kommission, Reihe C, Heft Nr. 466, 103 pp.

Haas, R. and Schuh, H., 1998. Ocean loading observed by geodetic VLBI, in Ducarme, B. (ed.), *Proc. 13'th Int. Symp. Earth Tides Brussels 1996,* in print.

Le Provost, C., Genco, M. L., Lyard, F., Vincent, P., and Canceil, P., 1994: Spectroscopy

Table 2: Ocean loading at GPS stations. Results show combined (root square sum) lunar effects at the diurnal periods of O_1 and Q_1 and the semidurnal M_2 and N_2. See caption of Tab. 1 for notations. Two versions of centre of mass tides are accounted for (label -CMC, CSR3.1-CMC being due to Watkins and Eanes, 1997). Error values apply to detection of a semidurnal oscillation.

Site	C	σ	Observed	Residuals			
				NSWC	CSR3.0	CSR3.0 -CMC	CSR3.1 -CMC
Reykjavik	R	0.9	18.9	5.5	5.4	6.0	8.1
	H	0.6	5.2	2.6	2.6	4.7	8.1
Sundsvall	R	0.8	2.9	2.1	1.7	3.5	5.6
	H	0.6	2.3	2.3	2.2	3.5	7.7
Pietown	R	1.0	4.8	1.7	0.9	2.9	5.1
	H	0.8	2.8	1.7	1.8	3.9	7.4
Hartebeesthoek	R	2.2	15.7	11.6	10.7	9.0	10.3
	H	2.0	4.9	4.8	5.0	5.9	7.5
Irkoutsk	R	0.9	1.6	2.0	1.9	2.2	3.3
	H	0.7	1.4	1.9	2.0	4.9	9.4
Ascension Isl.	R	1.4	12.8	10.4	11.9	10.2	11.2
	H	1.2	2.5	5.4	4.9	7.1	10.0
Yarragadee	R	1.2	6.8	13.3	13.3	13.7	13.7
	H	1.0	3.1	3.7	3.8	6.3	9.8
Mauna Kea	R	1.2	13.7	3.3	5.5	7.1	9.8
	H	1.0	4.7	2.2	2.7	5.1	7.5
Mendeleevo	R	1.0	2.1	1.4	1.6	3.1	5.5
	H	0.7	1.5	1.4	1.2	3.9	7.7
Onsala	R	0.7	5.1	1.7	2.0	3.7	6.6
	H	0.5	13.1	12.3	12.4	12.4	14.7

of the world ocean tides from a finite element hydrological model, *J. Geophys. Res.*, **99**, 24777–24798.

McCarthy, D. D. (ed): *IERS Conventions* IERS Technical Notes 21, Observatoire de Paris, 94 pp. 1996, and `http://hpiers.obspm.fr/webiers/general/syframes/convent/CONV.html`

Scherneck, H.-G., 1991. A parametrized solid earth tide model and ocean tide loading effects for global geodetic baseline measurements, *Geophys. J. Int.*, **106**, 677–694.

Scherneck, H.-G., 1991a. Regional ocean tide modelling, in *Proc. Eleventh Int. Symp. Earth Tides,* pp. 345-354, ed. Kakkuri, J., Schweizerbart, Stuttgart.

Scherneck, H.-G., and Webb, F.H., 1998. Ocean tide loading and diurnal tidal motion of the solid earth centre, *IERS(1998) Technical Note No 25.*, Observatoire de Paris, in print.

Schuh, H. and Haas, R., 1998. Earth tides in VLBI observations, in Ducarme, B. (ed.), *Proc. 13'th Int. Symp. Earth Tides Brussels 1996*, in print.

Schwiderski E. W. and Szeto, L. T., 1981, The NSWC global ocean tide data tape (GOTD), its features and application, random-point tide program, *NSWC-TR 81-254,* Naval Surface Weapons Center, Dahlgren Va., 19 pp.

Sovers, O. J., 1994. Vertical ocean loading amplitudes from VLBI measurements, *Geophys. Res. Letters,* **21**, 357–360.

Watkins M.M. and Eanes R.J., 1997: Observations of tidally coherent diurnal and semidiurnal variations in the geocenter, *Geophys. Res. Letters,* **24**, 2231–2234.

Webb F H, Zumberge J F, 1993: An Introduction to GIPSY/OASIS-II Precision Software

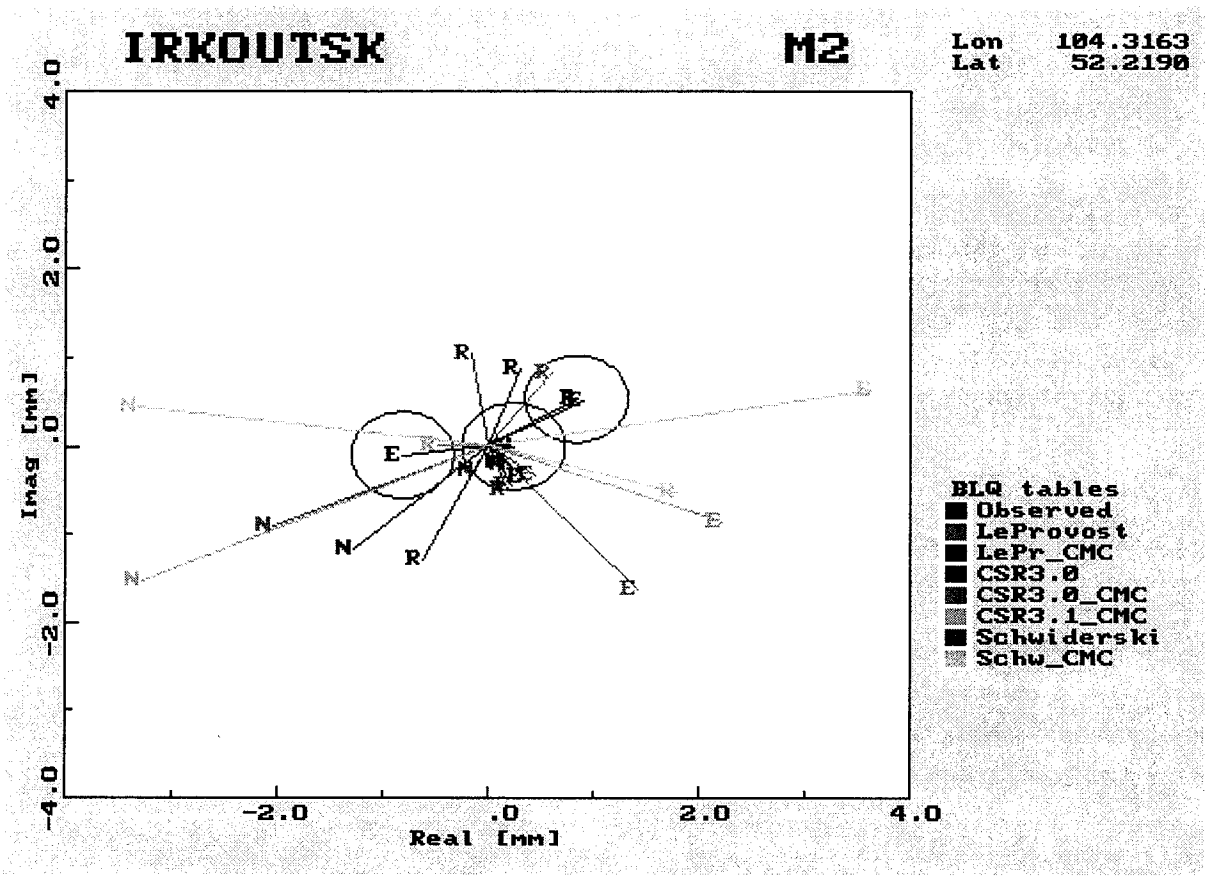

Figure 3: Like Fig. 1, but GPS at Irkoutsk, Siberia. This is an extreme inland station, which therefore is prone to exhibit global frame related motion. The loading models that incorporate frame translations are labelled _CMC and shown in light greys. They predict much larger motion than what is oberved.

for the Analysis of Data from the Global Positioning System, *JPL Publ. No. D-11088,* Jet Propulsion Laboratory, Pasadena, Cal.

Zumberge J F, Heflin M B, Jefferson D C, Watkins M M, Webb F H, 1997: Precise point positioning for the efficient and robust analysis of GPS data from large networks. *J. Geophys. Res.*, **102**, 5005–5017.

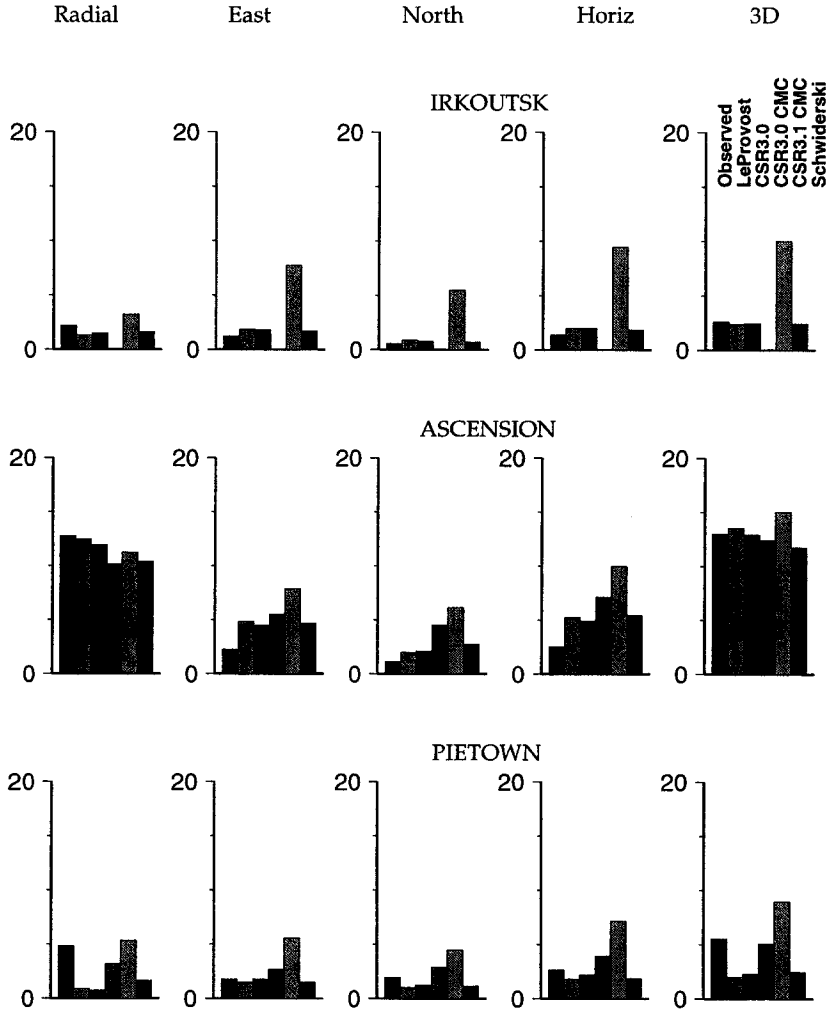

Figure 4: Like Fig. 2, but for GPS. Model and misfits consider four lunar tides, O_1, Q_1, N_2 and M_2. A general tendency is difficult to extract from this figure alone. Where residuals are low, the largest misfit occurs with the use of centre of mass tides. This seems to indicate that the GPS satellite orbit data is affected by the earth-fixed frame translations (as the tracking stations are not corrected for this motion), and thus the range to user stations is unaffected. The motion due to deformation, however, is visible since it is regularly modelled at the GPS orbit analysis stage, and it is geographically variable.

Crustal motion in Europe determined with geodetic Very Long Baseline Interferometry

Rüdiger Haas [1] and Axel Nothnagel [2]

[1] Onsala Space Observatory (OSO), S-43992 Onsala, Sweden, (haas@oso.chalmers.se)

[2] Geodätisches Institut der Universität Bonn (GIUB), D-53115 Bonn, Germany, (nothnagel@uni-bonn.de)

Abstract Since 1990 the European fixed station geodetic Very Long Baseline Interferometry [VLBI] network has been observing on a regular basis in order to determine crustal motion in Europe. Usually 6 European geodetic VLBI sessions are performed each year. In the first years the network was limited to central and southern Europe but with the inclusion of Ny Ålesund on Spitsbergen and Simeiz on the Crimean peninsula it received valuable extensions to the North and to the East. Meanwhile 8 years of observations allow the determination of crustal motion in Europe with high accuracy. Resulting baseline evolution and individual station drifts will be presented. In the future special emphasis will be placed on the vertical components.

1 Introduction

In January 1990 the European geodetic Very Long Baseline Interferometry [VLBI] group, a community formed by members of institutions involved in carrying out geodetic VLBI observations joint their efforts to start a purely European geodetic VLBI programme on a regular basis. From January 1990 to December 1997 a total number of 40 sessions has been carried out. Currently 6 European geodetic VLBI sessions are observed every year. In addition to the fixed station observations two campaigns have been observed with mobile VLBI equipment occupying several sites in Europe which are now corner-stones of the EUREF network [SEEGER, 1992].

The aim of the project is the determination of crustal motion in Europe with geodetic VLBI and to provide a stable reference network for other geodetic techniques used in the area, e.g. regional Global Positioning System [GPS] networks. The observing programme is coordinated by the Geodetic Institute of the University of Bonn (GIUB) and the data is correlated with the Mark-IIIA correlator of the Max-Planck-Institute for Radio Astronomy (MPIfR) in Bonn by members of the Geodetic Institute. The European Union [EU] (European Community [EC] until 1994) provides financial support for the operation of the network in the 'European Commission Framework Programme for Research and Technical Development'. In the first phase of the project the main aspect has been the determination of horizontal crustal motion while the second phase of the project now concentrates on the vertical component.

2 The European geodetic VLBI network

Today the fixed station European geodetic VLBI network consists of 10 stations: Effelsberg (Germany), Madrid (Spain), Matera (Italy), Medicina (Italy), Noto (Italy), Ny Ålesund (Norway), Onsala (Sweden), Simeiz (Ukraine), Wettzell (Germany) and Yebes (Spain). Table 1 lists the VLBI sites, the size of the telescopes and the operating institutions. Figure 1 displays the current configuration of the network.

In figure 2 the participation of European VLBI stations in high precision geodetic measurements is depicted. Prerequisites for precise geodetic VLBI measurements are that the stations are equipped with a Mark III VLBI system, S/X-band receivers for simultaneous dual frequency observations and a Hydrogen maser atomic clock for precise time keeping and frequency generation. The first VLBI observatories equipped compatibly for precise geodetic VLBI measurements were Onsala and Effelsberg which performed the first observations in 1980. In these days Effelsberg was only supplied temporarily with a Mark III terminal on loan for testing purposes permitting first epoch measurments. In 1991 all hardware components for precise geodetic observations were available on-site and observations were made possible on a once to twice per year basis. With Wettzell coming on line in late 1984 the first routine observations within intercontinental geodetic VLBI sessions were started. In the late-eighties, the Italian stations Medicina, Noto and Matera and the NASA Deep Space station near Madrid, Spain, were completed. With these stations the first observations were scheduled in a purely European network in January 1990. In recent years the two stations Simeiz and Ny Ålesund extended the geodetic network to the East and to the North. With the Yebes observatory an additional observatory in Spain is in line for routine observations in the European network.

Table 1: European geodetic VLBI stations with name, diameter D of the telescopes and operating institution.

Station	D [m]	operating institution
Effelsberg	100.0	Max-Planck Institut für Radioastronomy, Bonn, Germany
Madrid	34.0	Consejo Superior de Investigaciones Cientificas - Centre d'Estudis i Avancats de Blanes (CSIC-CEAB), NASA Deep Space Communications Complex (MDSCC), Madrid, Spain
Matera	20.0	Instituto di Tecnologia Informatica Spaziale (ITIS), Agenzia Spatiale Italiana (ASI), Matera, Italy
Medicina	32.0	Istituto di Radioastronomia, C.N.R. Bologna, Italy
Noto	32.0	Istituto di Radioastronomia, C.N.R. Bologna, Italy
Ny Ålesund	20.0	Geodetic Institute of the Norwegian Mapping Authority (GI/NMA), Norway
Onsala	20.0	Onsala Space Observatory (OSO), Chalmers Tekniska Högskola (CTH), Sweden
Simeiz	22.0	Crimean Radio Astrophysical Observatory, Simeiz, Ukraine
Wettzell	20.0	Bundesamt für Kartographie und Geodäsie (BKG) - Fundamentalstation Wettzell, Germany
Yebes	13.7	Centro Astronómico de Yebes, Observatorio Astronómico Nacional, Guadalajara, Spain

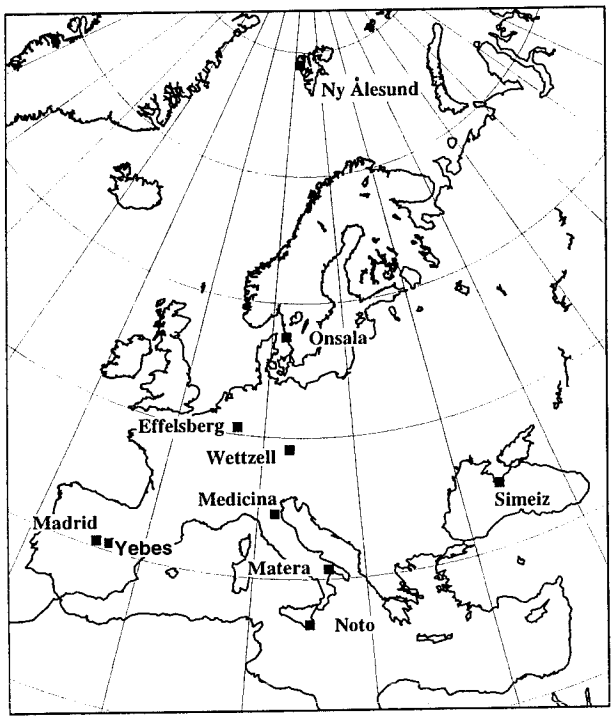

Figure 1: The fixed station European geodetic VLBI network in 1998

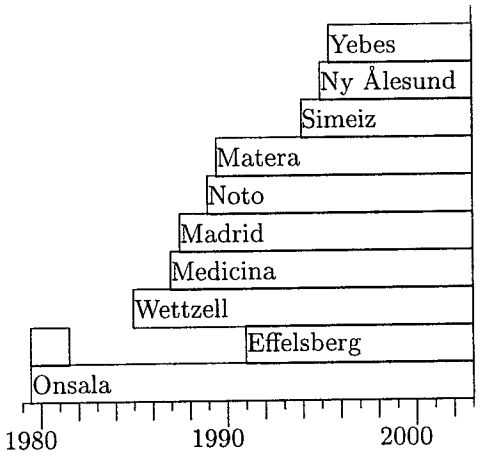

Figure 2: development of European VLBI observatories for high precision geodetic observations

Figure 3 displays the radio telescopes used in the European geodetic VLBI network. Two of the telescopes, the 20 m telescope at Onsala (picture 7) and the 13.7 m telescope at Yebes (picture 10) are covered with radomes to protect the delicate reflector surface because they are used for astronomical mm-VLBI observations, too.

Routine observations in the network started with 3 sessions each in 1990 and 1991. For the following years 6 sessions per year were planned, in 1993 only 4 of them could be observed due to correlator restrictions. The station Effelsberg is highly demanded for astronomy and therefore can only participate once or twice a year in geodetic VLBI sessions. Table 2 lists all 40 sessions observed and analysed so far. The results presented in this paper were obtained using the data of all 40 sessions covering 8 years of observations.

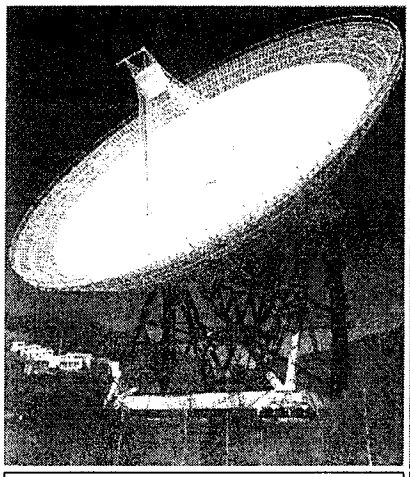

1) Effelsberg (Germany)

2) Madrid (Spain)

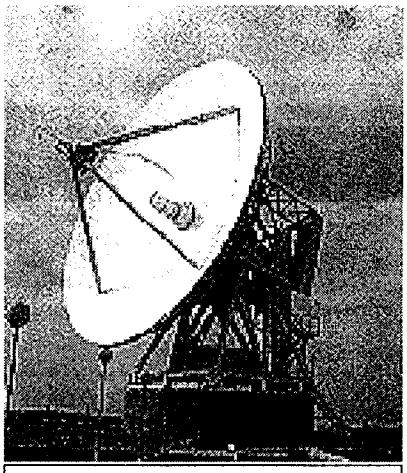

3) Matera (Italy)

4) Medicina (Italy)

5) Noto (Italy)

6) Ny Ålesund (Norway)

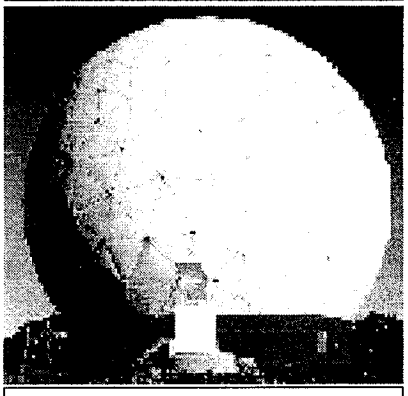

7) Onsala (Sweden)

Figure 3: Pictures 1 to 10 show the radio telescopes used in the European geodetic VLBI network in alphabetic order. The telescopes are of different sizes, the largest is the one at Effelsberg (1) with a diameter of 100 m. The telescope at Madrid (2) has a diameter of 34 m, the two telescopes at Medicina (4) and Noto (5) have diameters of 32 m. Four of the telescopes, namely those at Matera (3), Ny Ålesund (6), Onsala (7) and Wettzell (9) have diameters of 20 m. The smallest is the telescope at Yebes (10) with a diameter of just 13.7 m.

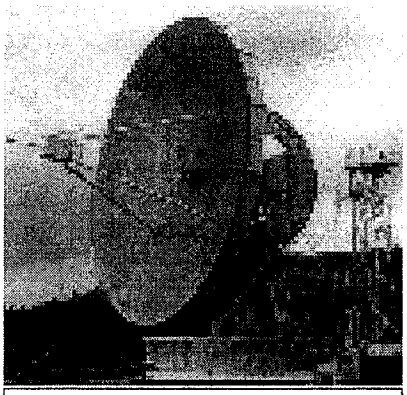

8) Simeiz (Ukraine)

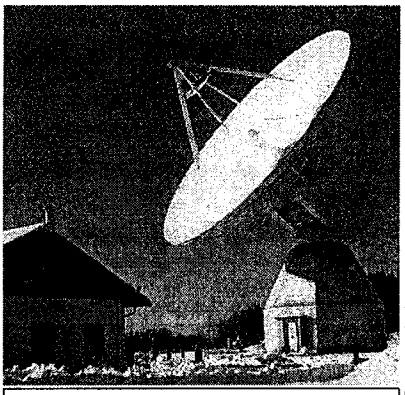

9) Wettzell (Germany)

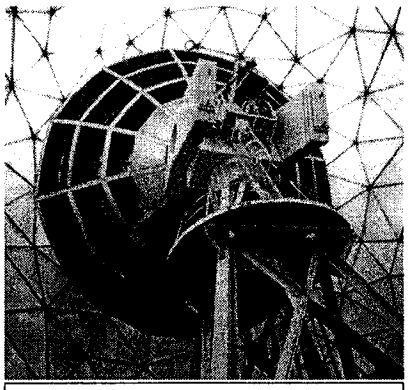

10) Yebes (Spain)

Table 2: European geodetic VLBI sessions from 1990 to 1997 with the date of observation and the participating stations. The abbreviations for the stations are: Wet=Wettzell (Germany), Ons=Onsala (Sweden), Med=Medicina (Italy), Mad=Madrid (Spain), Not=Noto (Italy), Eff=Effelsberg (Germany), Mv2= Mobile VLBI unit, Sim=Simeiz (Ukraine), Nya=Ny Ålesund (Norway), Yeb=Yebes (Spain).

Euro-01	90/01/26	Wet	Ons	Med	Mad	Not						
Euro-02	90/09/05	Wet	Ons	Med	Mad	Not	Mat					
Euro-03	90/12/20	Wet	Ons	Med	Mad	Not	Mat					
Euro-04	91/01/06	Wet	Ons		Mad		Mat					
Euro-05	91/09/08	Wet	Ons	Med	Mad	Not	Mat					
Euro-06	91/12/01	Wet		Med	Mad		Mat	Eff				
Euro-07	92/01/14	Wet	Ons	Med	Mad	Not	Mat					
Euro-08	92/04/08		Ons	Med	Mad	Not	Mat					
Euro-09	92/05/12			Med	Mad		Mat					Mv2
Euro-10	92/07/07		Ons	Med	Mad		Mat					Mv2
Euro-11	92/11/03	Wet	Ons	Med	Mad		Mat					
Euro-12	92/12/01	Wet	Ons	Med	Mad		Mat	Eff				
Euro-13	93/02/16	Wet	Ons	Med	Mad	Not	Mat					
Euro-14	93/04/27	Wet		Med	Mad	Not	Mat					
Euro-15	93/08/18	Wet	Ons	Med	Mad		Mat					
Euro-16	93/12/11	Wet	Ons	Med	Mad		Mat	Eff				
Euro-17	94/02/09	Wet		Med		Not						
Euro-18	94/04/27	Wet	Ons	Med	Mad	Not	Mat	Eff				
Euro-19	94/06/29	Wet	Ons	Med	Mad	Not	Mat					
Euro-20	94/08/31	Wet	Ons	Med	Mad	Not	Mat		Sim			
Euro-21	94/10/26	Wet	Ons	Med		Not	Mat	Eff	Sim	Nya		
Euro-22	94/12/28	Wet	Ons	Med	Mad	Not	Mat			Nya		
Euro-23	95/02/01	Wet	Ons	Med	Mad	Not	Mat		Sim	Nya		
Euro-24	95/04/12	Wet	Ons	Med	Mad	Not	Mat	Eff	Sim	Nya		
Euro-25	95/06/08	Wet	Ons	Med	Mad	Not	Mat		Sim	Nya	Yeb	
Euro-26	95/08/31	Wet	Ons		Mad					Nya		
Euro-27	95/11/09	Wet	Ons	Med	Mad	Not	Mat					
Euro-28	95/12/06	Wet	Ons	Med	Mad	Not	Mat	Eff		Nya		
Euro-29	96/02/07	Wet	Ons	Med	Mad	Not	Mat					
Euro-30	96/04/25	Wet	Ons		Mad				Sim	Nya		
Euro-31	96/06/12	Wet	Ons		Mad	Not	Mat					
Euro-32	96/09/09	Wet	Ons		Mad	Not	Mat					
Euro-33	96/11/03	Wet	Ons	Med	Mad	Not	Mat	Eff		Nya	Yeb	
Euro-34	96/12/05	Wet	Ons	Med	Mad	Not	Mat	Eff		Nya	Yeb	
Euro-35	97/01/29	Wet	Ons	Med			Mat					
Euro-36	97/03/17	Wet	Ons	Med			Mat				Yeb	
Euro-37	97/06/16	Wet	Ons	Med		Not	Mat		Sim	Nya	Yeb	
Euro-38	97/08/25	Wet	Ons	Med		Not	Mat		Sim	Nya		
Euro-39	97/10/30	Wet	Ons	Med	Mad	Not	Mat		Sim	Nya		
Euro-40	97/12/08	Wet	Ons	Med	Mad	Not	Mat	Eff	Sim	Nya		

3 Support of the project by the European Union

Carrying out this multi-national research project requires running costs for coordination, scheduling, shipping of magnetic tapes, data processing etc. by the participating institutions in addition to their regular budgets. Since these costs cannot be covered by any of the institutions the European geodetic VLBI group received grants by the European Union (EU) within the 'Framework Programme for Research and Technical Development' for the years 1993 - 1996. Phase II of the project (1996-2000) is supported by the EU in the 'Training and Mobility of Researchers' (TMR) programme under the title 'Measurement of Vertical Motion in Europe by VLBI'. The grant includes 5 temporary post-doctoral visiting researcher positions in 4 different participating countries. For more details on managing and funding the European geodetic VLBI network see CAMPBELL [1995, 1996, 1997].

4 Geodynamic situation in the network

The European fixed station geodetic VLBI network today extends from the Spitsbergen archipelago in the North to the island of Sicily in the South and from the Iberian Peninsula in the West to the Crimean Peninsula in the East. The northern part of the network, i.e. the Spitsbergen archipelago and Fennoscandia, are characterized by postglacial rebound effects after the last deglaciation. The isostatic rebound response after the vanishing of the ice shield about 10,000 years ago causes vertical and, much smaller, horizontal motions in this area. Maximal vertical uplift in the main uplift area are predicted to be 12 mm/year, maximal tangential deformation is predicted to be 2 mm/year [MITROVICA et al., 1994]. The central part of the network north of the Alpine system is regarded as the essentially 'stable' part of Europe. The southern part of the network, i.e. the Mediterranean region, is dominated by the collision of the African plate with the Eurasian plate. The counterclockwise rotation of the African plate acts with a north-north-westward push against the Eurasian plate, leading to lithosphere shortening of up to 50 mm/year [MUELLER and KAHLE, 1993]. The response of the Mediterranean lithosphere produces complex geotectonic horizontal crustal motions mostly in northerly directions. Vertical movements of the crust are an order of magnitude smaller than horizontal movements [LAMBECK, 1998]. Tectonic models describing the crustal motions in this area are mainly based on the assumptions of mircoplate motion and/or deformation.

In recent years the vertical evolution of the lithosphere has started to become a matter of growing interest. Vertical crustal motion due to isostatic and/or tectonic processes are expected to have an upper limit of 10 to 12 mm/year and are smaller than horizontal motions of tectonic origin. In addition to natural uplift or subsidence there are several man-made causes for vertical changes e.g. due to withdrawal of gas, oil and water, which locally can have larger signals. Loading forces due to ocean tides and atmospheric pressure fields affect the stations in the vertical component as well.

5 Data analysis and results for crustal motion

All 40 sessions from 1990 to 1997 were analyzed with the CALC/SOLVE/GLOBL VLBI data analysis software package [MA et al., 1990]. In our analysis relative clock parameters with respect to a reference clock in each session are estimated every 6 hours. In order to compensate for unmodelled atmospheric refraction effects atmospheric zenith path delays are introduced as unknown parameters every 60 minutes using the NMF 2.0 mapping functions [NIELL, 1996]. Horizontal asymmetries in the atmospheric refraction profile are estimated with 4 horizontal gradient parameters in North and East direction (2 offsets and 2 rates). For our analysis we have chosen an approach which is called 'baseline-solution'. Each session is treated separately in a least squares adjustment and station coordinates are estimated for each station participating in the session. Since VLBI is a relative technique the coordinates of a reference station have to be fixed in the adjustment. In addition, pole coordinates and UT1 have to be fixed to permit the estimation of all station coordinates. In our solution we adopted Earth orientation parameters together with radio source positions from a global VLBI solution by the GSFC VLBI group [MA et al., 1997]. For more details on the different strategies of the analysis of VLBI data see NOTHNAGEL [1993] and NOTHNAGEL AND CAMPBELL [1993].

Solid Earth tides were modeled as functions of frequency and latitude following HAAS [1996] using the harmonic expansion of the tidal potential by TAMURA [1987] and frequency and latitude dependent Love

and Shida numbers by WAHR [1981] together with a Free Core Nutation (FCN) period of 430 sidereal days. Ocean tide loading effects were introduced using a recent ocean tide loading model by SCHERNECK [1996] based on the CSR3.0 ocean tide model by the University of Texas [EANES and BETTADPUR, 1995], expanded by a large number of interpolated ocean tides. The effect of atmospheric loading was not accounted for and thermal deformation of the telescopes was neglected in our analysis.

From the individual least squares adjustments a time series of station coordinates is available which permits the computation of baseline components between individual stations for each epoch. The time series of baseline lengths and baseline components gives insight into the repeatability of the measurements and the quality of the individual sessions. In addition, we can also infer station drift components in horizontal and vertical directions from the series of station coordinates.

The advantage of baseline length results is that they are, to first order, invariant to changes in the Earth orientation parameters (EOP). Thus, any decent EOP series is a sufficient basis if only baseline lengths are considered. The situation is slightly different if station coordinates and, infered from these, transverse and vertical baseline components are to be determined. Here, the particular EOP series introduced will affect the orientation and the evolution of the network resulting in small rotations about the reference point fixed in the solution. The effect itself scales with the extension of the network. Since the European network is rather small compared to intercontinental VLBI networks it is quite safe to adopt Earth orientation parameters from the International Earth Orientation Service (IERS) or from global VLBI analyses.

5.1 Baseline length evolution

The network has a total number of 43 baselines, only the baselines Yebes-Effelsberg and Yebes-Simeiz have not yet been observed. This number of baselines is too large to present all of them in these proceedings. We, therefore, restrict our discussion to baselines from and to Wettzell since the station of Wettzell has a central position in the network. Table 4 lists the baseline length rates and their standard deviations and the weighted root mean square errors (WRMS) of the regression lines.

Table 4: Baselines to Wettzell: baseline length, length rate with standard deviations and the WRMS.

Baseline	length [km]	rate [mm/y]	WRMS [mm]
Wettzell-Effelsberg	447	-0.2 ± 0.5	2.7
Wettzell-Madrid	1655	$+0.7 \pm 0.4$	4.1
Wettzell-Matera	990	-3.7 ± 0.3	3.9
Wettzell-Medicina	522	-2.6 ± 0.2	2.1
Wettzell-Noto	1371	-4.3 ± 0.5	4.5
Wettzell-Ny Ålesund	3283	$+1.0 \pm 1.4$	5.4
Wettzell-Onsala	919	-0.3 ± 0.3	4.0
Wettzell-Simeiz	1684	$+2.2 \pm 4.2$	12.5

In the following subchapters, the individual baselines will be presented and the repeatabilities of the measurements will be discussed. In all plots the individual results of the baseline length measurements with their formal errors are displayed together with a linear regression line. The dashed line represents the predicted baseline length change according to the NUVEL-1A-NNR plate tectonic model [DE METS et al., 1994] which is zero in a Europe fixed frame.

5.1.1 Baselines from Wettzell to the Italian Peninsula and Sicily

The baselines from Wettzell to the Italian stations Medicina, Matera and Noto with baseline lengths of 522 km, 990 km and 1371 km have been measured 31, 33 and 27 times, respectively. The resulting baseline rates with values of -2.6 ± 0.2 mm/year, -3.7 ± 0.3 mm/year and -4.3 ± 0.5 mm/year are strongly significant. The WRMS scatter about the regression lines represents the accuracy of the individual measurements since all sessions are adjusted independently of each other. The WRMS scatter of 2.3 mm, 3.9 mm and 4.5 mm roughly scales with the baseline lengths.

In spite of these excellent repeatabilities there are periodic variations to be recognized in all three baseline plots. In the summer months of 1994 and 1996 the length results seem generally to be longer than what the regression line predicts. The reason for this may be the larger amount of water vapour in the atmosphere in summer and its contribution to atmospheric refraction.

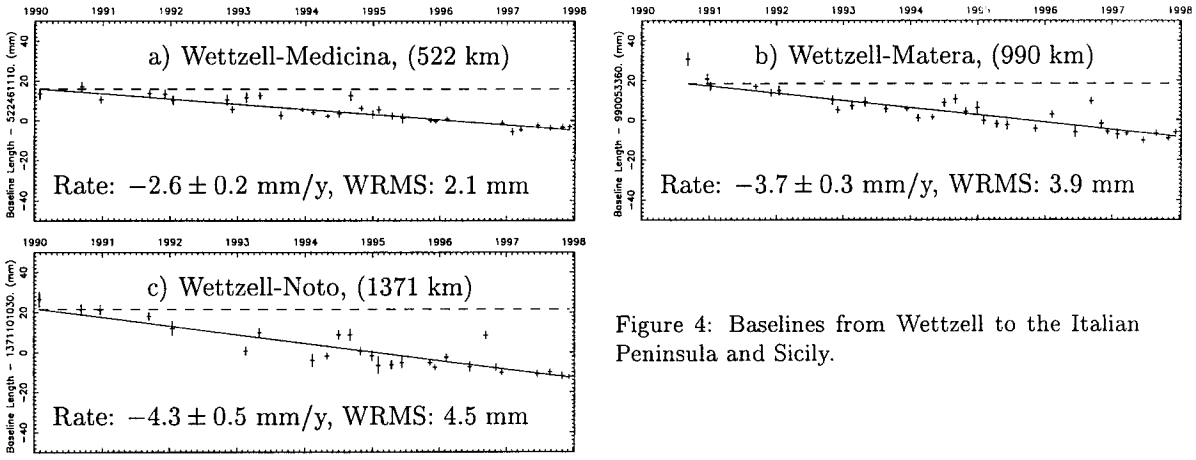

Figure 4: Baselines from Wettzell to the Italian Peninsula and Sicily.

5.1.2 Baselines from Wettzell to the Iberian Peninsula

The baseline from Wettzell to Madrid with a length of 1655 km has been observed 31 times yielding a baseline rate of $+0.7 \pm 0.4$ mm/year with a WRMS of 4.1 mm. The baseline to Yebes with a length of 1575 km has been observed only 5 times so far. The determination of drift rates is, therefore, premature.

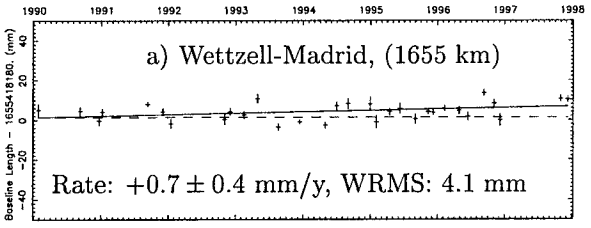

Figure 5: Baselines from Wettzell to Madrid.

5.1.3 Baselines from Wettzell to Fennoscandia and Spitsbergen

The baseline Wettzell to Onsala with 919 km length has been observed 34 times in the European VLBI sessions producing a baseline length rate of -0.3 ± 0.3 mm/year with a WRMS of 4.0 mm. This is equivalent to a measurement accuracy of 4.4 parts per billion. Since the Ny Ålesund site is operational just for a few years now, only 14 sessions are available. The rate of $+1.0 \pm 1.4$ mm/year and its standard deviation are heavily dependent on the short observing time. The WRMS of the individual length determination is 5.4 mm and compares quite well with that of the Onsala-Wettzell baseline considering that, with a length of 3283 km, it is more than three times the length of the latter.

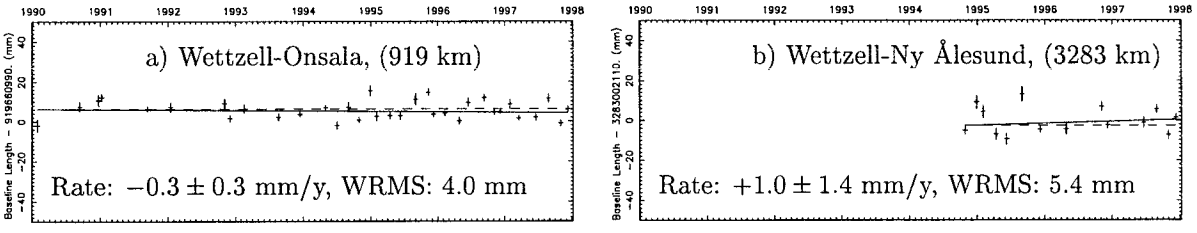

Figure 6: Baselines from Wettzell to Fennoscandia and Spitsbergen

5.1.4 Baseline from Wettzell to the Crimean peninsula and to Effelsberg

The baseline to Simeiz has only been observed 11 times and the baseline length results show uncomparable large scatter. The low quality of this baseline and the station in general is probably mainly due to technical problems at the Simeiz observatory [BAJAKOVA et al., 1996]. If the baseline length rate is computed anyway the length increases by $+2.2 \pm 4.2$ mm/year with a large WRMS of 12.5 mm, which

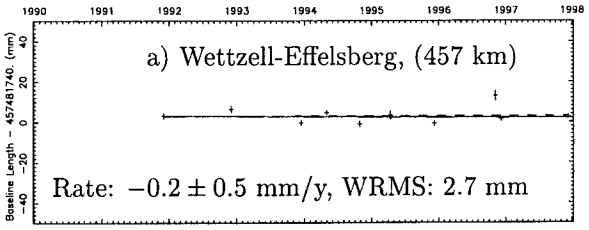

Figure 7: Baseline from Wettzell to Effelsberg.

characterizes the poor quality of the measurements on this baseline numerically. A new Hydrogen Maser which was installed at the end of 1997 rises hopes for a better repeatability in the future.

The intra-German baseline to Effelsberg has been observed 10 times so far but the period covered by the sessions is sufficiently long. The linear regression produces a baseline length rate of -0.2 ± 0.5 mm/year with a WRMS of the individual length results of 2.7 mm. One session in November 1997 seems to have had deficiencies since its baseline length result obviously deviates from the other results deteriorating the WRMS.

5.2 Horizontal and vertical station movements

In addition to the purely baseline oriented results we also produced station related horizontal and vertical drift components. The least squares adjustment of the VLBI data set as described above yields a time series of station coordinates for all stations with respect to a reference station. In order to refer all results to a single reference station we excluded from this analysis three sessions in 1992 which do not include data of Wettzell. From the individual station coordinates a global drift of the European plate was subtracted according to the NUVEL-1A-NNR plate tectonic model [DE METS et al., 1994] producing a European fixed system. After a transformation from cartesian into ellipsoidal coordinates the resulting time series for each station yields the evolution of each station in East and North direction and of ellisoidal height. These time series may be used to determine horizontal and vertical station velocities with respect to the Eurasian plate. The sites of Ny Ålesund, Simeiz and Yebes were left out for their short observational history which produces fairly insignificant and unreliable results.

Fixing the motion of one site to a continental drift model such as NUVEL-1A-NNR and using high accuracy Earth rotation parameters from external sources places a reliable bound on the long term drift of the European continent as represented by the observing sites. Only the Earth rotation parameters have an effect on the determination of the drifts of the stations relative to Wettzell. Since the long term stability is extremely reliable and the short term variations only increase the scatter of the results, the drift vectors determined up to date deserve a high level of confidence. Table 4 displays the horizontal and vertical velocities. Figures 8 and 9 show these results in a graphic representation.

Table 4: Horizontal and vertical velocities with their standard deviations of six stations in the network.

Station	East [mm/y]	North [mm/y]	Height [mm/y]
Effelsberg	$+0.3 \pm 0.6$	-0.5 ± 0.5	$+0.1 \pm 3.2$
Madrid	-0.2 ± 0.4	-0.5 ± 0.3	$+2.3 \pm 1.4$
Matera	$+2.4 \pm 0.3$	$+4.3 \pm 0.3$	$+0.6 \pm 1.1$
Medicina	$+2.1 \pm 0.3$	$+2.4 \pm 0.2$	-4.9 ± 1.2
Noto	-0.4 ± 0.4	$+4.2 \pm 0.5$	-1.4 ± 1.1
Onsala	-1.9 ± 0.4	-0.5 ± 0.3	$+2.6 \pm 1.3$

The solution presented here clearly shows that the southern stations of Medicina, Noto and Matera seem to be heavily affected by the northward thrust of the African continent. The station of Noto on the south-eastern tip of Sicily is probably part of the African plate although its velocity is not large enough to represent the full motion of Africa of about 10 mm/yr. The extension of the Tyrrhenian basin and its interaction with the Calabrian Arc lead to a divergence of the Noto and Matera drift vectors. This motion confirms that these two Italian stations are situated on the Adriatic promontory of the African plate which is penetrating far into the European domain [MUELLER and KAHLE, 1993]. At Medicina the thrust is reduced but still large enough to produce a consistent motion in a north-easterly direction.

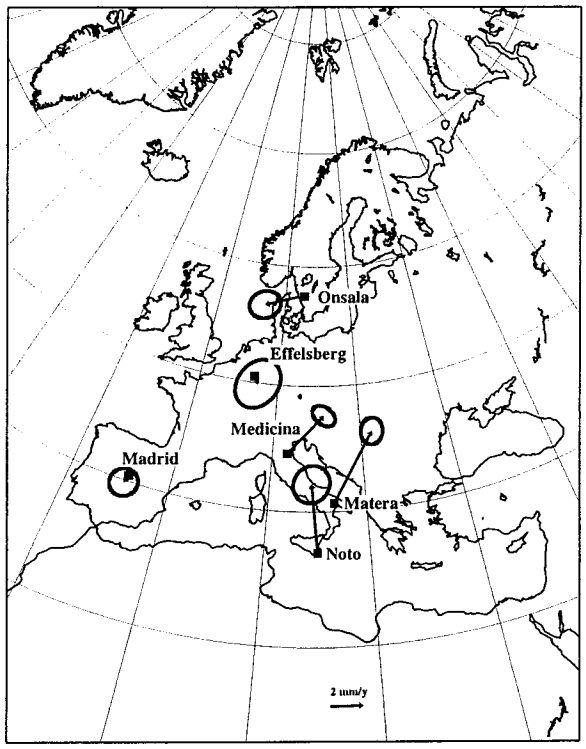

Figure 8: Horizontal site motion

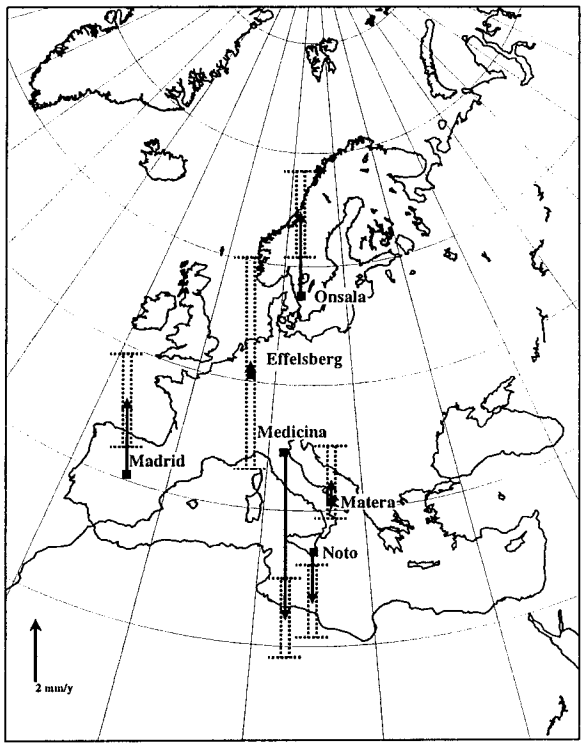

Figure 9: Vertical site motion

The horizontal movements of Onsala and Effelsberg with respect to Wettzell suggest that this part of Europe currently do not encounter any tectonic motion comparable to that of the Mediterranean. A small west-south-west drift of Onsala can be detected. Models for tangential motion due to post-glacial rebound in Fennoscandia predict a westward motion for Onsala of 1.1 mm/year and +0.1 mm/year to the North [MITROVICA et al., 1994].

The predicted uplift of Onsala due to post-glacial rebound is +1.7 mm/year [MITROVICA et al., 1994] which compares reasonable with our result of 2.6 ± 1.3 mm/year. The uplift at Madrid most probably does not have any geotectonic but rather a local explanation. Conventional surveys rise suspicion that the causes for this uplift have to sought locally. The subsidence of Medicina is explained by ground water and gas extration in the Po valley [TOMASI et al., 1997]. In our computations we assumed zero vertical motion at Wettzell. Any real vertical motion at Wettzell which cannot be excluded has still to be added or subtracted from the numbers presented here, though we do not expect them to be any larger than 0.5 mm/year from local surveying [SCHLÜTER, pers. communication]. The predicted subsidence of Wettzell due to post-glacial rebound is 0.1 to 0.4 mm/y [MITROVICA et al., 1994]. Further investigations on this topic are underway.

5.2.1 Station height displacements due to track and wheel replacements

At the stations Medicina, Effelsberg and Madrid, replacements of the tracks and wheels on which the telescopes move were necessary in 1996 and 1997 due to material wear. This lead to an abrupt displacement in the stations vertical positions. Figure 10 shows the evolution of the ellisoidal height for the three stations. The resulting station numerical results are listed in table 5

Table 5: Displacements in station height due to track and wheel replacements

Station	Date of height change	height change [mm]
Effelsberg	1996, October 1	$+16.3 \pm 19.9$
Madrid	1996, July 1	-11.2 ± 15.9
Medicina	1997, April 30	$+15.8 \pm 11.0$

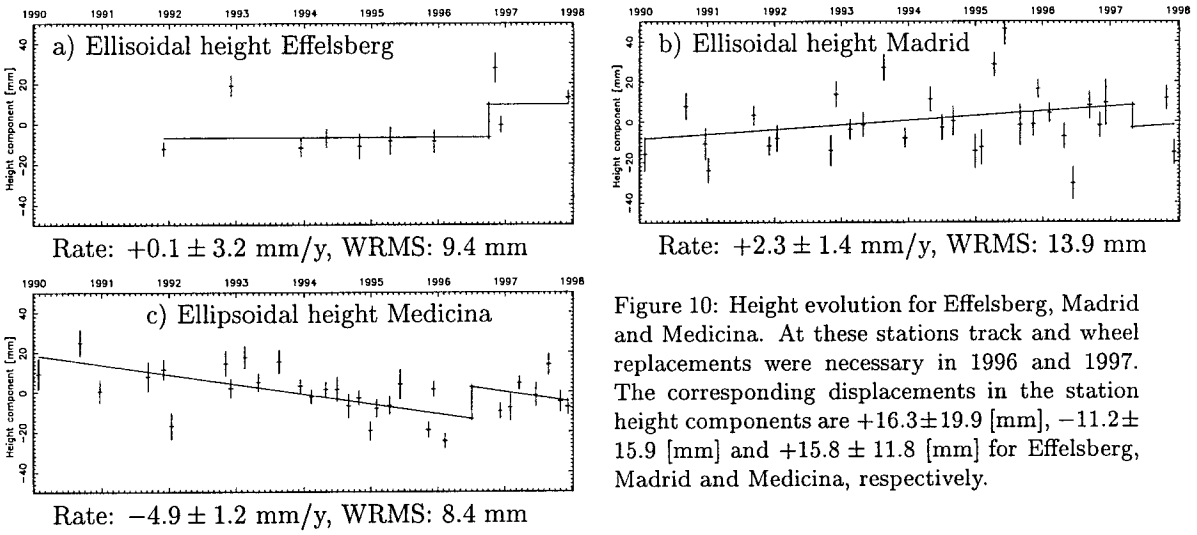

Figure 10: Height evolution for Effelsberg, Madrid and Medicina. At these stations track and wheel replacements were necessary in 1996 and 1997. The corresponding displacements in the station height components are +16.3±19.9 [mm], −11.2± 15.9 [mm] and +15.8 ± 11.8 [mm] for Effelsberg, Madrid and Medicina, respectively.

Since the observation periods after the track repairs are relatively short and the height results a generally more noisy these estimates have large uncertainties and have to be considered very preliminary. Local surveys are underway which will produce more reliable numbers.

6 Conclusions

In recent years the European Geodetic VLBI Network has matured to a reliable high accuracy geodetic and geodynamic observing network. With funding from the EU the first stage of research concentrating on tectonically induced horizontal station motion was completed producing extraordinary results. Geoscientist may use these results to infer upper bounds of present-day tectonics in the areas of interest. In addition, precise station coordinates and reliable time series are available from these measurements. Baseline measurements are possible with an measurement accuracy of 4.4 parts per billon. In this respect the VLBI network may serve as a precise reference for densification of regional and local networks with GPS observations.

At present, the observations in the network and the investigations in the data gathered focus on the height components, again with invaluable support of the EU. First results are very promising but the correlation between the height components and atmospheric refraction presents an obstacle which still has to be overcome. On the other hand, the comparably higher noise in the results may well be compensated for by a longer time series for significant signals to emerge. However, this approach bears the deficit that man-made changes in the heights of the stations may not be separated from natural causes. Therefore, the project continues the endeavour to improve the accuracy of the individual observing sessions by optimizing equipment, observing strategies, refraction models and analysis methods. This includes the application of atmospheric loading effects and corrections due to thermal deformation of the radio telescopes.

For the future we hope to extend and densifiy the European geodetic VLBI network. In particular a further extension to the East and the North is desirable. Existing or planned astronomical VLBI stations in that area like Torun (Poland), Metsähovi (Finland), Svetloe (Russia) and Irbene (Latvia) may be good candidates. These stations would tie the geodetic network more reliably to the stable central European part (Torun) and together with the northern stations allow an improved detection of post-glacial rebound. The astronomical VLBI site Westerbork (The Netherlands) is planned to participate in geodetic VLBI observations in late 1998 and will be an important reference point for the observation of land subsidence and sea level rise in this part of Europe.

Acknowledgements. Rüdiger Haas is supported by the European Union within the TMR programme under contract FMRX-CT960071. We are greatful to the staff members of all observatories participating in the series for their indespensable efforts to ensure successful observations and to the staff at the Bonn correlator for their hard work rescueing even the delay observables from recordings with too many deficits. Those graphs which contain maps were produced with the GMT software package [WESSELS AND SMITH, 1991].

7 References

Bajakova, A., A. Finkelstein, A. Ipatov, D. Ivanov, V. Mardyshkin and T. Pyatunia: *The Geodetic VLBI Observations at CRIMEA Station and Some Results of the Analysis*, Proceedings of the 11th Working Meeting on European VLBI for Geodesy and Astrometry, 200–208, Onsala, Sweden, 1996

Campbell, J.: *Managing Geodetic VLBI in Europe: The European Crustal Motion Network*, Proceedings of the 10th Working Meeting on European VLBI for Geodesy and Astrometry, 79–86, Matera, Italy, 1995

Campbell, J.: *Measurement of Vertical Motion in Europe by VLBI - Further Support of the European Geodetic VLBI network by the European Union*, Proceedings of the 11th Working Meeting on European VLBI for Geodesy and Astrometry, 227–231, Onsala, Sweden, 1996

Campbell, J.: *Measurement of Vertical Motion in Europe by VLBI - Status of the EU-TMR Network*, Proceedings of the 12th Working Meeting on European VLBI for Geodesy and Astrometry, 1–8, Hønefoss, Norway, 1997

De Mets, C.,R. G. Gordon, D. F. Argus and S. Stein: *Effect of recent revision to the geomagnetic reversal time scale on estimates of current plate motions*, Geophys. Res. Lett., Vol. 21, No. 20, 2191–2194, 1994

Eanes, R. J. and S. Bettadpur: *The CSR 3.0 global ocean tide model*, Center for Space Research, Technical Memorandum, CSR-TM-95-06, 1995

Haas, R.: *Untersuchungen zu Erddeformationsmodellen zur Auswertung von geodätischen VLBI-Messungen*, Deutsche Geodätische Kommission, Reihe C: Dissertationen - Heft Nr. 466, 1996, ISSN 0071-9196

Lambeck, K.: *Geophysical Geodesy*, Claredon Press, Oxford, 1988

Ma, C., J. M. Sauber, L. J. Bell, T. A. Clark, D. Gordon and W. E. Himwich: *Measurement of horizontal motions in Alaska using very long baseline interferometry*, J. Geophys. Res., 95, 21991–22011, 1990

Ma, C., et al.: NASA GODDARD SPACE FLIGHT CENTER'S VLBI TERRESTRIAL REFERENCE FRAME SOLUTION NUMBER 1083C, http://lupus.gsfc.nasa.gov/global/glb.html, 1997

Mitrovica, J.X., J. L. Davis, and I. I. Shapiro: *A spectral formalism for computing three-dimensional deformations due to surface loads, 2. Present-day glacial isostatic adjustment*, J. Geophys. Res., 99, 7075–7101, 1994

Mueller, S. and H.-G. Kahle: *Crust-Mantle Evolution, Structure and Dyanmics of the Mediterranean-Alpine Region*, Contrbutions of Space Geodesy to Geodynamics: Crustal Dynamics, Geodynamics Series, Vol. 23, American Geophysical Union, 1993

Niell, A.E.: *Global mapping functions for the atmosphere delay at radio wavelength*, J. Geophys. Res., 101(B2), 3227–3246, 1996

Nothnagel, A.: *IRIS-S batch Solutions at the Geodetic Institute of the University of Bonn*, Proceedings of the 9th Working Meeting on European VLBI for Geodesy and Astrometry, 42–48, Bonn, Germany, 1993

Nothnagel, A. and J. Campbell: *European Baseline Rate Determinations with VLBI*, Proceedings of the 9th Working Meeting on European VLBI for Geodesy and Astrometry, 56–59, Bonn, Germany, 1993

Scherneck, H. G.: *A comprehensive and tentatively complete summary of oceanic effects in space geodetic baseline maesurements*, Proceedings of the 11th Working Meeting on European VLBI for Geodesy and Astrometry, 121–133, Onsala, Sweden, 1996

Seeger, H.: *The EUREF MV III Mobile VLBU Campaign 1989*, in Report on the Symposium of the IAG Subcommission for the European Reference Frame (EUREF) held in Berne 4 - 6 March 1992, Veröffentlichungen der Bayerischen Kommission für die Internationale Erdmessung, Reihe Astronomisch-Geodätische Arbeiten, Heft Nr. 52, 214–215, 1992

Tamura, Y.: *A harmonic development of the tide-generating potential*, Bulletin d'Information Marées Terrestres, Vol. 99, 6813–6855, 1987

Tomasi P., F. Mantovani, M. Negusini, A. Orfei and P. Sarti: *Activities and recent results in Geodynamics*, Proceedings of the 12th Working Meeting on European VLBI for Geodesy and Astrometry, 102–110, Hønefoss, Norway, 1997

Wahr, J. M.: *Body tides on an elliptical, rotating, elastic and oceanless earth*, Geophys. J. R. Astron. Soc., 64, 677–703, 1981

Wessels, P. and W. H. F. Smith: *Free software helps map and display data*, EOS Trans. Amer. Geophys. U., Vol. 55, 293–305, 1991

Very high precision distance measurements of the FGI

Jorma Jokela
Finnish Geodetic Institute
Geodeetinrinne 2, FIN-02430 Masala
e-mail: jorma.jokela@fgi.fi

Abstract

The Finnish Geodetic Institute (FGI) is the National Standards Laboratory of geodetic length. Measurements of standard and calibration baselines are a part of our activities. Recently we have measured four baselines with the Väisälä Interference Comparator, and one more is under construction. In connection with these measurements we have carried out some research to develop the method to make it easier, still improving the reliability and traceability of it. We have used mekometers *Kern ME5000*, too, both in Finland and in a baseline measurement in Lithuania. Results from the latest projects, comparisons between the two methods and some future plans are presented.

1 White light interferometry

Unlike in most interferometric methods, white light is used in the Väisälä Interference Comparator. The measurement principle is presented in numerous publications and not repeated here; an up-to-date presentation by Jokela and Poutanen (1998) is just being printed. The lengths measured with the Väisälä Interference Comparator are traceable to internationally accepted standards through the quartz gauges, which give the scale. The lengths of these 1-m gauges are intercompared regularly, and the latest absolute calibrations were made in 1995. The desired baseline lengths we get from five or six multiplications of the metre, e.g. in Nummela we get 2×2×3×3×4×6×1 m = 864 m.

1.1 Väisälä Baselines in Finland

1.1.1 Nummela Standard Baseline

The baseline of the FGI, considered the most accurate in the world, was measured for the 13th time with the Väisälä Interference Comparator in 1996. The new and the previous (Kääriäinen et al. 1992) results are presented in Table 1 and Figure 1. The construction works in the neighbourhood in the 1970's and 1990's may have caused some small movements, but the long term stability is still remarkably good.

1.1.2 The Baseline of the Laboratory of Geodesy and Cartography of the HUT

The 75-m baseline in the Helsinki University of Technology in Otaniemi was measured with the Väisälä Interference Comparator in February 1998. Two quartz gauges, no. 49 and no. 51, were used. The measurement provided the possibility to study the Väisälä interference method indoors. The circumstances of a proper calibration room proved very stable and the repeatability of the interference observations was up to a few micrometers. Projections from

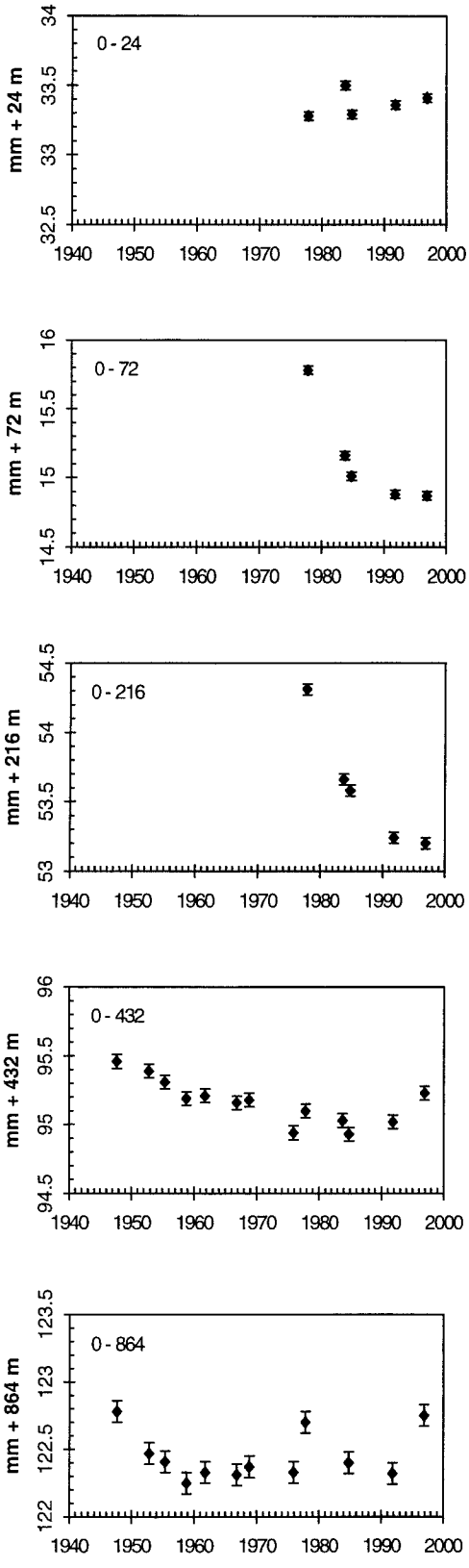

Figure 1 Results of the measurements of the Nummela Standard Baseline in 1947–1996.

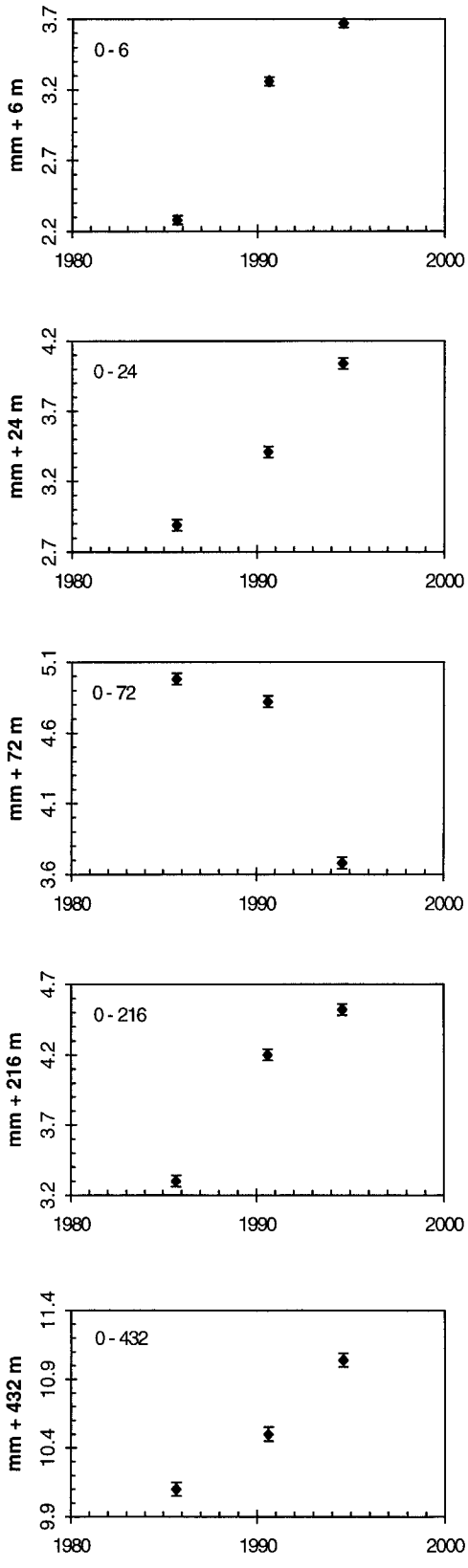

Figure 2 Results of the measurements of the Chang Yang Standard Baseline in 1985–1994.

the mirrors and transferring bars of the comparator to the forced centring devices used in calibration measurements caused troubles, as was to be expected.

The experiments in Otaniemi showed that the traditional theodolite and tape measurements can be replaced by the same kind of transferring method as we use in determining the distance between the mirror surface and transferring bar. The accuracy of the interference observations was ±0.003 mm, after the projection and transfer measurements it was ±0.03 mm. During the 50 years the accuracy has not been improved much using the projection method. By developing the transfer method, a better accuracy is obtainable. This method doesn't use any underground markers, but the observation pillars must be extremely stable.

As it is possible to make measurements with a laser interferometer in Otaniemi, an interesting subject for further studies is the comparison of different interferometric methods.

1.2 Väisälä Baselines in Asia

1.2.1 Chang Yang Standard Baseline

To establish a highly accurate metric scale for geodetic works in China, a 432-m Väisälä baseline was measured near Beijing in 1985. The baseline was remeasured in 1990 and 1994. Unfortunately, as shown in Table 2, bigger than 1 mm movements have occurred (Kääriäinen et al. 1986, Konttinen et al. 1991, Jokela 1996). Figure 2 shows, that the movement of the pillar 0 only could account for most of the differences, but then the pillar 72 is a very problematic one, too. Obvious reasons for the instability are disturbances from activities nearby: ground water pumping under the pillars, new buildings too near the 0-end of the baseline, traffic needed for the neighbouring fruit farms.

1.2.2 Hezhuo, Pixian

"The Chengdu baseline" is the working title of our new project in Sichuan, China. A big part – 768 m – of an existing baseline will be measured with the Väisälä Interference Comparator in October 1998. The extension to the whole baseline length – 1488 m – is planned to be made by mekometer measurements. The transfer method tested in Otaniemi will be developed further.

1.2.3 Taoyuan Standard Baseline

One more Chinese Väisälä baseline is located in Hsinchu, Taiwan (Poutanen 1995). It was measured in 1993. To study the possible movements there, *ME5000* measurements were carried out in 1997 using the same instruments both in Nummela and in Taoyuan. If the stability of a baseline is under suspicion, high precision EDM measurements are recommended for the monitoring, instead of the laborious interference observations.

1.3 Accuracy of the Väisälä Interference Comparator

In the latest projects, influences of many important details have been estimated once again, using methods different from before: new absolute values for the lengths of the quartz gauges, thicknesses of the new mirror coatings, wavelength of light passing the filter at the mirror 1, repeatability of transfer measurements, etc. After all, we didn't conclude in worse (or better) standard errors than in the previous measurements. Better than 0.1 ppm accuracy is quite a normal result, but as the interferometric part of the work is more accurate, better final results should be obtainable. At the Chengdu baseline, in addition to developing transfer methods, functioning of compensator glasses will be one subject of further investigations.

Table 1 Results of the interference measurements of the Nummela Standard Baseline in 1947 – 1996.

Epoch	**0 – 24** mm + 24 m	**0 – 72** mm + 72 m	**0 – 216** mm + 216 m	**0 – 432** mm + 432 m	**0 – 864** mm + 864 m
1947.7	—	—	—	95.46 ±.04	122.78 ±.07
1952.8	—	—	—	95.39 ±.05	122.47 ±.08
1955.4	—	—	—	95.31 ±.05	122.41 ±.09
1958.8	—	—	—	95.19 ±.04	122.25 ±.08
1961.8	—	—	—	95.21 ±.04	122.33 ±.08
1966.8	—	—	—	95.16 ±.04	122.31 ±.06
1968.8	—	—	—	95.18 ±.04	122.37 ±.07
1975.9	—	—	—	94.94 ±.04	122.33 ±.07
1977.8	33.28 ±.02	15.78 ±.02	54.31 ±.02	95.10 ±.05	122.70 ±.08
1983.8	33.50 ±.02	15.16 ±.02	53.66 ±.04	95.03 ±.06	—
1984.8	33.29 ±.03	15.01 ±.03	53.58 ±.05	94.93 ±.06	122.40 ±.09
1991.8	33.36 ±.04	14.88 ±.04	53.24 ±.06	95.02 ±.05	122.32 ±.08
1996.9	33.41 ±.03	14.87 ±.04	53.21 ±.04	95.23 ±.04	122.75 ±.07

Table 2 Results of the interference measurements of the Chang Yang Standard Baseline in 1985 – 1994.

Epoch	**0 – 6** mm + 6 m	**0 – 24** mm + 24 m	**0 – 72** mm + 72 m	**0 – 216** mm + 216 m	**0 – 432** mm + 432 m
1985.7	2.28 ±.03	2.89 ±.04	4.98 ±.04	3.30 ±.04	10.10 ±.05
1990.6	3.26 ±.04	3.41 ±.03	4.82 ±.04	4.20 ±.04	10.50 ±.05
1994.6	3.67 ±.03	4.04 ±.05	3.68 ±.03	4.52 ±.04	11.04 ±.06

2 Mekometer measurements

In May – June 1997, three *Kern ME5000*s were calibrated in Nummela: two from ITRI, Taiwan and one from HUT, Finland. Altogether nine calibrations were carried out. The purpose of these calibrations was not only to determine the instrument corrections, but also to make use of the results immediately at other baselines. Furthermore, we seldom have possibilities for thoroughgoing comparisons between the Väisälä Interference Comparator and other very high precision instruments.

2.1 Calibrations in Nummela

At the Nummela Standard Baseline, close by every underground marker we have an observation pillar to be used in calibration measurements. For the projections between the underground line and the calibration line we make high precision angle measurements when needed. In 1997 we made the projection measurements three times. After these projections we know the distances between the forced centring devices on the observation pillars with about 0.1 mm accuracy.

2.1.1 Measurements for establishing the geodetic length standard in Lithuania

The scale of the Nummela Standard Baseline was transferred to Lithuania by making calibration measurements just before and after the measurements at the new baseline in Kyviškės, east of Vilnius. For this project, the baseline in Nummela was measured in all

combinations twice before and twice after the measurements in Lithuania, altogether 120 distances (Jokela et al. 1998).

2.1.2 Measurements for the maintenance of the Taoyuan Standard Baseline

For the comparisons between the Standard Baselines of Nummela and Taoyuan, two mekometers were used in May 1997, and 90 + 60 measured distances determine the scale factor and the additive constant.

2.2 EDM Calibration Baseline in Kyviškės, Lithuania

The 6-station baseline was constructed in 1996. In June 1997, the 1320-m baseline was measured with the *ME5000* of the HUT. Five measurements in all combinations resulted in 150 distances. The weather didn't favour the measurements: The ground was cold after a cold spring, and when the measurements were started, the weather changed, and the burning sun was heating the air and the soil rapidly. With our psychrometer equipment we didn't obtain representative temperature readings, and the baseline couldn't be measured with better than 0.5 mm accuracy.

However, as the location is excellent and the observation pillars are properly founded, the baseline provides ideal circumstances for further work to improve the length standards in Lithuania. The baseline was recently given an official status by the Lithuanian Metrological Department.

2.3 Accuracy of the Kern Mekometer ME5000

The calibrations of *ME5000*s yielded expected results. Scale corrections for different instruments were –0.20 ppm to +0.36 ppm, variations in single calibrations were –0.35 ppm to +0.43 ppm; the mean doesn't differ significantly from zero. Additive constants were small, too: means +0.02 mm to +0.19 mm, in single calibrations –0.02 mm to +0.22 mm. *Kern* reports the standard deviation of a normal measurement with proper correction for meteorological influences to be 0.2 mm + 0.2 ppm. Our studies confirm that value quite well.

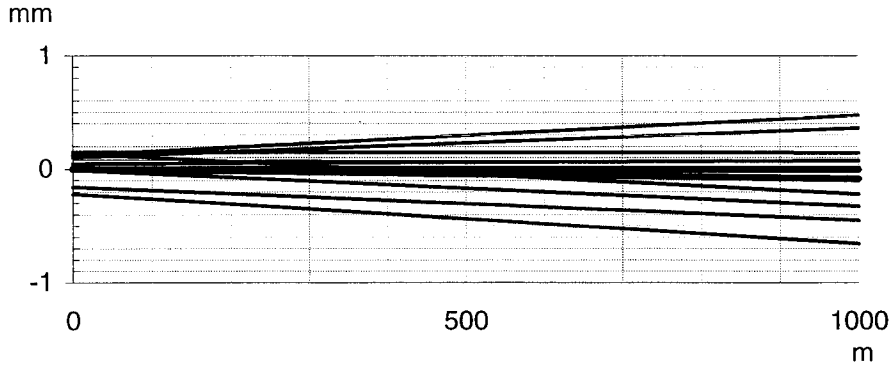

Figure 3 Nine calibrations of three *Kern ME5000* mekometers at the Nummela Standard Baseline; the scale difference between the mekometer measurements (May–June 1997) and the interference measurements (September–December 1996), after the correction for the additive constant. The boldest lines show the mean.

3 Conclusions

The Väisälä Interference Comparator has retained its importance as the most accurate distance measurement method for the distances up to 1 km. The measurements in Nummela and at selected baselines will continue. The full advantage of the Väisälä method has never been taken: formerly because of many technical problems, nowadays because of lack of interest. The *Kern ME5000* was a very nice instrument, too. Most distances in geodesy can nowadays be measured by completely different methods, but should a new high precision EDM instrument be built, the ideas of *Yrjö Väisälä* may be worth of acquaintance.

Co-operating partners

At present, Mr *Jorma Jokela* and Mr *Markku Poutanen* carry out the Väisälä baseline measurements in the FGI. Prof. *Jussi Kääriäinen* is the head of the calibration laboratory.

Our works in China have been carried out according to agreements between the National Bureau of Surveying and Mapping of the People's Republic of China and the FGI. In Chengdu, the Sichuan Bureau of Surveying and Mapping takes care of the actual arrangements.

Due to an agreement between the FGI and the Laboratory of Geodesy and Cartography in the Helsinki University of Technology, the *ME5000* of the HUT was used in the mekometer measurements in Finland and in Lithuania in 1997. The same agreement made possible our interference observations in Otaniemi in 1998.

More mekometer measurements in Nummela in 1997 were carried out by Dr *Chiungwu Lee* and Mr *Ming Wei Chang* from the Center for Measurement Standards in the Industrial Technology Research Institute, Hsinchu, Taiwan.

The works in Lithuania were guided by Dr *Petras Petroškevičius* and Dr *Vytautas Tulevičius* in the Institute of Geodesy in the Vilnius Technical University.

References

Jokela J (1996) Interference measurements of the Chang Yang Standard Baseline in 1994. *Publ. of the FGI*, no. 121.

Jokela J and M Poutanen (1998) The Väisälä baselines in Finland. *Publ. of the FGI* (in print).

Jokela J, P Petroškevičius and V Tulevičius (1998) The Kyviškės Calibration Baseline. Manuscript, to be published as a *Rep. of the FGI.*

Kääriäinen J, R Konttinen, Lu Q and Du Z Y (1986) The Chang Yang Standard Baseline. *Publ. of the FGI*, no. 105.

Kääriäinen J, R Konttinen and M Poutanen (1992) Interference measurements of the Nummela Standard Baseline in 1977, 1983, 1984 and 1991. *Publ. of the FGI*, no. 114.

Konttinen R, J Jokela, and Li Q (1991) The remeasurement of the Chang Yang Standard Baseline. *Publ. of the FGI*, no. 113.

Poutanen M (ed., 1995) Interference measurements of the Taoyuan Standard Baseline. *Publ. of the FGI*, no. 120.

The new satellite laser ranging system of Metsähovi: status report

Matti Paunonen
Finnish Geodetic Institute
Metsähovi Geodetic Observatory
Geodeetinrinne 2
FIN–02430 Masala, Finland
tel +358 9 2564995
fax +358 9 2564995
email: geodeet@csc.fi

Abstract.

The new satellite laser ranging system at Metsähovi started regular operation in January 1998. During the first four months 152 passes with 22428 accepted observations from 10 satellites were obtained. The average precision of the range measurements to the close-Earth satellites was 22 mm and to Lageos 25 mm. This report reviews briefly the instrumental status and performance of the new satellite laser.

Introduction

Satellite range measurements at the Metsähovi Geodetic Observatory were begun in 1978 with a ruby satellite laser. The pulse length of the Q-switched ruby laser was 20 ns, and the ranging precision achieved was about 0.5 m [1]. As a partial upgrade the laser pulse length was shortened to 4.5 ns by an electro-optical shutter in 1985 [2]. In 1993, a 4 ns Nd:YAG was taken into use, which has allowed some 10 cm precision [3]. As a further improvement, construction of a new satellite laser was launched in 1993. A one-metre laser telescope from the Latvian University, Riga, was installed in November 1994. Some development of mode-locked Nd:YAG laser technology to give 50 ps pulses was done earlier. After some basic modifications to the original operation principles of the telescope the preliminary operational status was achieved in August 1997. During the year 1998 both the old (7805) and new systems (7806) have been in regular use. The preliminary evaluation of the ranging data shows a precision of about 25 mm, which is 20 times better than the initial precision 20 years ago, and some five times better than that of the old system.

Equipment

The main specifications of the new satellite laser are given in Table 1. A passively Q-switched and mode-locked Nd:YAG laser with a self-filtering unstable resonator [4,5] was installed in the instrument room near the new telescope upon an iron table. The original model used cavity dumping, which method produces efficiently a single pulse. Unfortunately the Pockels cell was slowly damaged by the high internal power density. Then a different variant, where the laser power is coupled continuously out, was taken into use. This method gives a comb-like pulse train, about 5–10 short pulses separated by the round trip travel time of the resonator (13.436 ns, corresponding twice the 2.014 m optical length of the resonator). From this train an electro-optical shutter passes about half of the trailing pulses, so called semitrain containing 3–5 pulses. The semitrain goes through a double pass amplifier and is finally converted to green (532 nm) by a KTP second harmonic crystal. The pulse length is nominally 50 ps, the pulse energy is limited to 10 mJ, and the pulse rate is 1 Hz.

The laser telescope has a 1-m diameter Cassegrain-Mangin optics, common for the transmitted and received beam. At the Metsähovi scheme an aperture sharing method is used, where the transmit beam is shifted from the optical axis and goes unobstructed between the primary and secondary mirrors. The beam divergence can be changed by moving the negative input lens. The receive path goes outside the transmit 45 degree mirror through the field limiting aperture and an interference filter to the photomultiplier. In this case the effective receiver area is diminished by about 15% from the original model, where two rotating mirrors were used to separate the beams. The tracking is controlled by a PC. The telescope has also visual channel, which is separated from the receiving channel by a dichroic mirror. An image amplifier, a CCD camera and a PC are used to monitor the satellite, when visible, during tracking. The mount accuracy with error modelling is better than 30 arcsec (rms).

In the receiver a fast photomultiplier is used as the detector. Pulse timing is done with a fast constant-fraction timing discriminator. The time interval is measured by an event timer, which gives the delay with 20 ps precision and also the transmit epoch with 400 ns precision. The system time is syncronized with a second tick from the GPS station clock. A third PC is used to control the time interval counter and range gating and to calculate the predicted orbits. The start pulse is formed by channeling a small sample from the transmit beam to the receiving channel. In the scheme employed a common detector is used for start and stop pulses. Although the use of the common detector is a good measure against drifts [6], its use is rare. The system delay was determined by measuring tme intervals to the external calibration prisms at the distances of 320.664 m and 11.236 m. An electronic calibrator is used to monitor the status of the time interval counter. Weather data are taken once during the pass.

Satellite ranging results

The following 10 satellites were observed in January–April of 1998: TOPEX/Poseidon, Ajisai, ERS-2, Fizeau, Stella, Starlette, Lageos-1, Lageos-2, Resurs, and GFO-1. The number of passes and observations with their average rms precisions are given in Table 2. The data preprocessing is more complicated than that with single pulses because of possible multiple levels at the measured ranges, Figure 1. In this plot the time bias is adjusted and the mean observed deviation from the predicted orbit is removed. The levels are combined to the main track in the folding process which adjust the sub-ranges by 2.014 m or its multiples, Figure 2. In this plot the mean offset used is modified by the appearance of the deviations in comparison to that in Figure 2. Then the observations are screened by analytical Kepler (Sterne) orbit fitting or by polynomial fitting to the observed range deviations with respect to the calculated ranges using automatic adaptive median filtering of the deviations, Figure 3. Finally, the field generated normal points, i.e. representative single range measurements over specified averaging times (120 s for Lageos, 15 s for remote sensing satellites and 30 s for the other close-Earth satellites) arc formed and sent to the Eurolas data centre in Germany. The precision of the normal points have usually been in the range of 4-10 mm, Figure 4. Weekly reports from the University of Texas at Austin/Center for Space Research indicate that the possible range bias is stable and may be not more than 20 mm.

Table 1. Specifications of the new Metsähovi satellite laser ranging system

Laser	Nd:YAG oscillator with polarization-coupled self-filtering unstable resonator, passive dye Q-switching and mode-locking, external semitrain gating (3-4 pulses), double-pass amplifier, KTP second harmonic crystal (60% eff.), wavelength 532 nm
Pulse duration	50 ps nominal (not measured)
Laser energy	5 mJ at 532 nm (first pulse), 10 mJ overall maximum
Repetition rate	1 Hz
Beam divergence	0.7 mrad, adjusted by a pair of lenses
Receiving and transmitting optics	1-m diameter Cassegrain-Mangin, focal length 11.6 m, secondary mirror 0.25 m dia., receiving beam angle 15-120 arcsec, transmit beam in off-axis position, beam diameter 30 cm, beam angle variable 5-40 arcsec, static mirrors only
Visual optics	visual channel common with the main optics, dichroic mirror, image amplifier, CCD camera controlled by PC-No.3
Telescope mount	Azimuthal, model TPL-1 by the Latvian University, Observatory, Riga, step motors driven, one step equal to 1 arcsec, speed 7200 steps/s, control by PC-No.1 with hardware and software from Riga, manual offsets, electro-mechanical shutters protecting photomultiplier and image amplifier at the laser firing time
Detector	Hamamatsu R4998 photomultiplier, quantum efficiency 8% Start and stop pulses have common photomultiplier and timing discriminator
Preamplifier	Gain 5 V/V, 1 GHz bandwidth
Interference filter	1 nm bandwidth
Time interval counter	COMTIS 911E from Riga, 20 ps rms, includes epoch registering and range gate, uses PC-No.2, external frequency from a hydrogen maser or BVA crystal oscillator
Timing processor	Ortec 9307 pico-Timing discriminator
Time syncronization	TRAK Systems 8810 GPS Station Clock
Calibration	External corner cubes, distances 320.664 m and 11.236 m Counter calibrated by external electric pulses
Range noise	20 mm (rms) to close-Earth satellites 25 mm (rms) to Lageos (measured range 8612 km) 12 mm (rms) at laser calibration
Weather instruments	Pressure sensor Vaisala PTB200A, accuracy 0.2 hPa Temperature sensor Vaisala HMP35D, accuracy 0.2 K Humidity sensor Vaisala HMP35D, accuracy 3%

Table 2. Satellite observations with the new laser in January–April 1998

Satellite	Passes	Observations	RMS (m)
TOPEX/Poseidon	39	8181	0.033
Stella	32	3053	0.021
ERS-2	28	2588	0.021
Lageos-1	18	5593	0.025
Ajisai	18	2372	0.031
Starlette	6	214	0.022
Resurs	6	210	0.023
Fizeau	3	69	0.016
Lageos-2	1	120	0.023
GFO-1	1	28	0.017
Total	152	22428	

Future work

Tracking of close-Earth satellites and Lageos at nighttime has been nearly satisfactory, but the tracking capability in daylight or tracking of far-orbiting satellites, like GPS-satellites and Etalons at 20000 km height, is still missing. The latter will be remedied by installing an additional 100 mJ, 100 ps Nd:YAG laser parallel to the present one. Daylight tracking needs improvements in the alignment and accuracy of the mount and installation of the existing narrow band (0.3 nm) holographic filter. The receiving efficiency can be improved 3-4 times by introduction of a photon counting mode avalanche photodiode detector.

References

1. Kakkuri, J., O. Ojanen, and M. Paunonen, Ranging precision of the Finnish satellite laser range finder. *Reports of the Finnish Geodetic Institute*, 78:8, Helsinki 1978, 11 p.
2. Paunonen, M., Performance of the second generation satellite laser ranging system at Metsähovi. *Proc. 10th General Meeting of the Nordic Geodetic Commission*, Helsinki, 29.9.- 3.10.1986.
3. Paunonen, M., Status of permanent GPS activity and satellite laser ranging at Metsähovi. *Proc. 12th General Meeting of the Nordic Geodetic Commission*, Ullensvang, Norway, 30.5.- 3.6.1994, pp. 364-371.
4. Gobbi, P.G., S. Morosi, G.C. Reali, and Amin S. Zarkasi, Novel unstable resonator configuration with a self-filtering aperture: experimental characterization of the Nd:YAG loaded cavity. *Applied Optics*, Vol. 24, No. 1, pp. 26-33, 1985.
5. Paunonen, M., Cavity dumping of a mode-locked self-filtering unstable resonator Nd:YAG laser. *Proc. 7th International Workshop on Laser Ranging Instrumentation*, Matera, Italy, Oct. 2-6, 1989, pp. 167-171.
6. Degnan, J.J., Satellite laser ranging: Current status and future prospects. *IEEE Trans. Geoscience and Remote Sensing*, Vol. GE-23, No. 4, pp. 398-413, 1985.

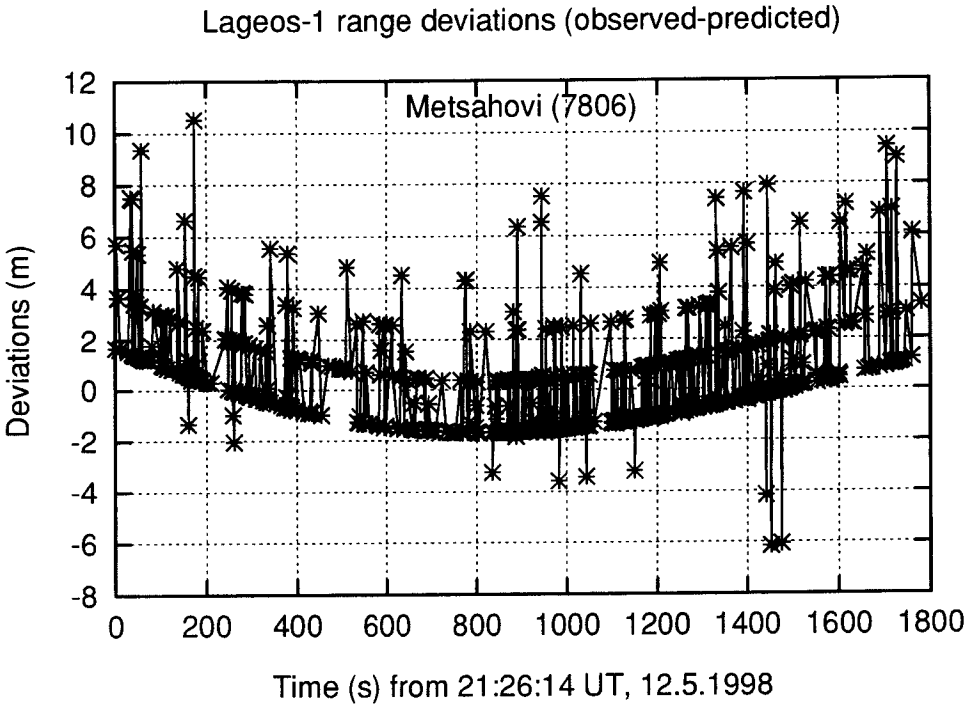

Figure 1: Raw observed range deviations

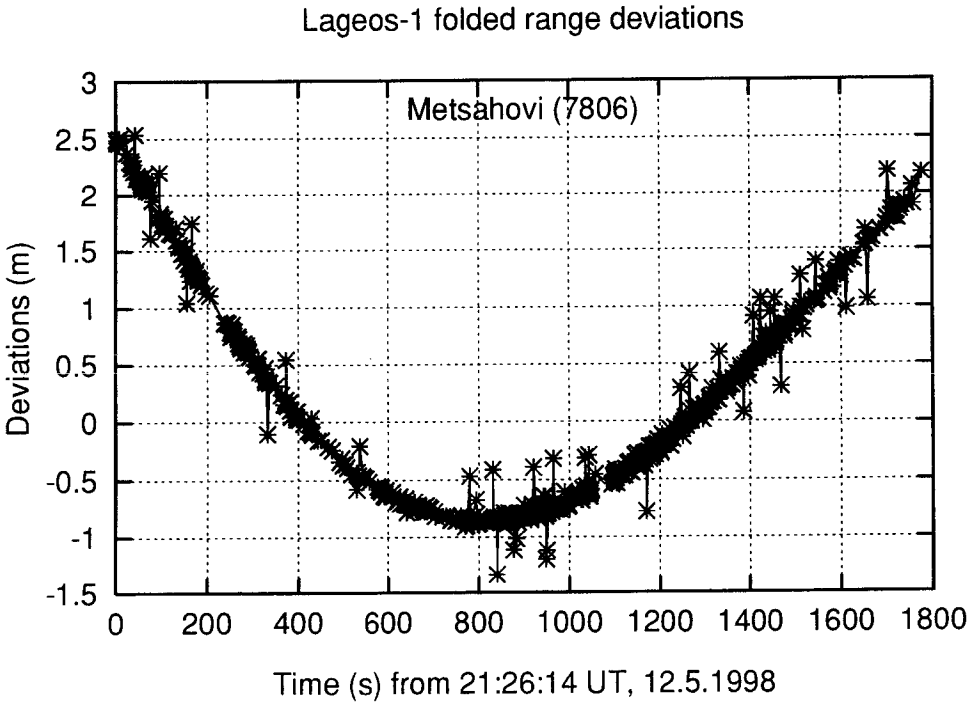

Figure 2: Range deviations after folding

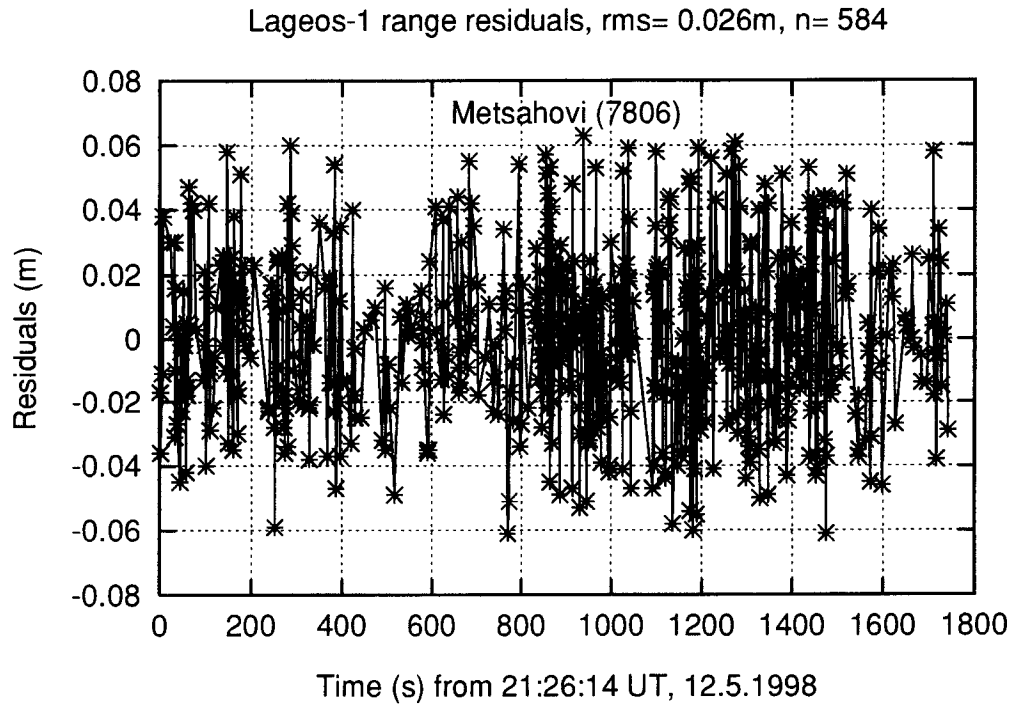

Figure 3: Filtered range residuals

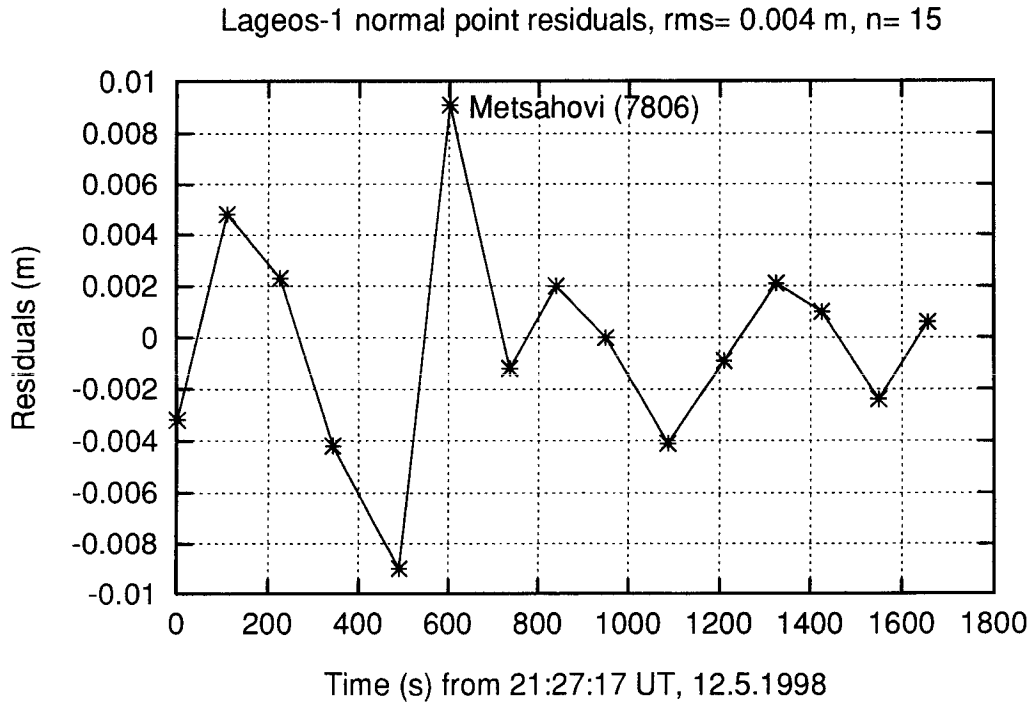

Figure 4: Normal point (120 s) range residuals

GeoDisp, a Windows Program for the Displaying of Geodetic Data.

presented in Gävle
by Jon Olsen, KMS, Denmark

The program was primary designed to be used as a tool for obtaining fast overviews of geodetic data, in order to facilitate the error finding process in the calculation of triangulation networks. Using the computer screen as a coordinate window in which the triangulation points and the observations was drawn, and adding mouse controlled zoom & navigation to the window fulfilled the basic goal. The program was based on the fast and precise coordinate transformation system designed by Knud Poder. Via this system the drawings could be carried out in virtually all geodetic coordinate systems.

The program runs on 32 bits PC's under Windows95 or WindowsNT. Programming language is Borland C++ and the compiler used is Borland C++ version 5.02

A couple of years has passed since the first version of the program was written, and during this time a lot of new ideas and possibilities has been included in the program, it seemed that every new user came up with new suggestions. The program is now quite large - its popup menus contains close to 200 menu items - therefore I will here give just a short resumé of a few of its main functions.

The Coordinate Window.

Via combinations of mouse clicks and drawing of "rubber rectangles" it is easy to change the position and the zoom factor for the coordinate window. The coordinate system used in the window can be changed via a menu selection. Geographic grid is drawn as default. Geodetic coordinates for the mouse cursor appears in the status bar.

Geodetic Data.

The geodetic data to be displayed are read from text files containing coordinate lists and observations written in the format used at KMS. The program will accept different kinds of observations:

Horisontal directions.
Ellipsoidal distances.
GPS coordinate observations.
GPS vectors.
Levelling observations.
Zenith distances.

Residuals for the observations are calculated, and observations having residuals exceeding a userselected errorlevel are drawn in the error color. Such suspicious observations can via mouse clicks be inspected as information on error size, station numbers, fieldbook page appears in the status bar.

The mouse can be used to add points to the internal coordinate list, or to delete points. Also to calculate geodetic distances, azimuths and angles between the points.

Coordinate Systems.

The program used one fixed coordinate system for the storing of point coordinated. Normally this system is determined as the system defined by the first coordinate list read by the program

Background.

As a background for the visualized geodetic data the program can use digitized coastlines and other polygon lines (municipal borders), or topographical maps. Currently we have a full coverage of Denmark in scales from 1:25000 to 1:2 M available on CD-Roms. The Faeroe Island map in 1:100000 and small scale maps of the Nordic countries including Iceland and Greenland (1:2 M) have been digitized. When map of a certain area are to be drawn and different maptypes (mapscales) are available, the program can chose "the best" maptype having a pixelcompression factor close to one. Brightness and contract for the map can be adjusted.

Screen Texts.

Texts can be placed in the window using the fonts, sizes and colors provided by Windows. Such screentexts are stored together with coordinate information, and is redrawn in the same locations when the window is redrawn (zoomed or moved).

Vectors.

Vectors are read by the program either as coordinate lists containing vector components or they are calculates as coordinate differences between two lists of coordinates. The scale for the vectordrawing is adjustable.

Geoids.

The geoid models available for the program can be visualized by the drawing of contours. Point values for these models can be read in the statusbar, or written in the window simply by mouse clicks.

Point selection.

A useful feature is the fast way of selecting an area defined subgroup of points from a coordinate list: when the list is stored internally in the program, each point is either selected or unselected.
The user can select/unselect points on the screen via mouse clicks or by using the mouse to draw polygons. The program can detect which points are inside the last drawn polygon and in this way the selection state can be changed. When the selection is completed, a list of the selected points can be written to a file.

Multi View

The program supports the opening of several coordinate windows, just how many depends on the capacity of the computer. These windows can have different scales, positions, draw system and content. The position of the mouse cursor in the active window is reflected by slave cursors in the other windows. All the windows can be synchronized (positionwise) via a popup menu in the active window.

Printing

When the content of the window is satisfying, a printout can be performed: the drawing process is repeated, this time to the printer. The user can select a mapping scale for the printout or he can let the program scale the print to fill the available paper size. As the printing is performed independent of the screen pixels, large prints can be made in high resolution.

Saving the program parameters.

When the program is closed down, many of the userselected parameters (colors, paths to data, and other preferences) are written to the INI-file and are read at the next startup of the program. It is at the present not possible to save the result of a program session to a file in order to close down the program and then reassume the work on a later occasion. The content of the window can only be saved as a BMP file containing pixel information only. The print can be redirected to a "encapsulated postscript" file, but up until now we have not succeeded in the reading of such a file as a graphic file containing distinct objects.

*** *** ***

The window-class used in GeoDisp has been reused in a group of sibling programmes. Some of these are designed for the maintenance of the digital coastlines and district lines used in GeoDisp, Others may be of more general interest. Three such programmes shall be mentioned here:

PS Trans.

Calculating parameters for polynomie transformations between two coordinate systems. Passpoint coordinates are read into the program as two coordinate lists and the used decides which type of polynomie is to be used (regular or complex), and also decides the degree of the polynomium. The residuals for the passpoints are presented as vectors on the screen, errornous points can be weeded out (unselected) and the transformation recalculated, perhaps including new settings of degree or polynomie type. When the process is completed, the transformation of a file (coordinate list) can be performed, or the transformation parameters can be saved for use in another program.

Affine Trans.

This program is very similar to PS-Trans: working in almost the same way (from the users point of view) It calculates linear transformations between two coordinate systems in two or three dimensions. The transformation type can be selected to be either Affine or "Helmert-type".

Voronoi.

Used for the visualisation of terrain models given as a set of irregular (non-grid) datapoints. The program performs a Delauney triangulation on the data, resulting in a subdivision of the area covered by the datapoints in triangles - each triangle having three of the datapoints as vertexes. Height contours are calculated using linear interpolation inside the triangles.
The set of the triangles are used in another part of the program. Here the model is visualized in a "OpenGL-window" and the user can make a fligh-through the terrain model, navigating via the keyboard (arrow-keys) and inspecting different details of the model. Further OpenGL features are planned to be incorporated for better visualisation: control of the lightning and of surface reflection, texture painting and also better means for controlling he "flight". On my 180 MHZ computer (60 MB ram) the program can manage a set of more than 100000 triangles, although in such large models the flight becomes rather slow. In models of less then 15000 triangles the performance is far more realistic.

*** *** ***

Although the visualisation programmes I have mentioned here can be vastly improved, they have in their present versions already turned to be quite useful in our daily work. As I may be doing some programming along the visualisation line in the future, I am interested in an exchange of ideas - and maybe programmes - with colleagues doing the same kind of work. Please e-mail me : jco@kms.dk

462

STATENS KARTVERK

ROAD MAPPING BY USE OF GPS IN COMBINATION WITH INERTIAL NAVIGATION SYSTEM

PAPER PRESENTED TO

The 13th General Meeting of the Nordic Geodetic Commission

Gevle 25.-29. Mai 1998

by Lars Bockmann

ROAD MAPPING USING GPS AND INERTIAL NEVIGATION SYSTEM

INTRODUCTION

Statens Kartverk has, as a part of the work related to building up a new road database, a demand for an effective and accurate system for determination of the centreline on a road. With this as a background Statens Kartverk, Geodetic Division, entered into a contract with Seatex a/s, Trondheim, with the objective to develop a system for this purpose.

Seatex a/s was also heavily involved in the development of the national SATREF Services for distribution of the GPS corrections signals, one of the areas Statens Kartverk has been focusing on.

Seatex a/s has past experience with Inertial navigation System (INS) through projects for the oil industry in the North Sea.

The project was finalised in spring 1993, and production of a system for the land Mapping Division at Statens Kartverk started immediately after.

Operation of the system was assigned to the Geodetic Division.

MAPPING PRINCIPLE

The system is developed for accurate mapping of the centreline of the road. This is achieved by driving av vehicle (car) equipped with the system along the road, while the position of the vehicle is logged.

The system is based on a combination of differential GPS and INS.

After initialisation of the system INS will give position every second relative to the start position. When driving the system a difference between the GPS coordinates and the INS coordinates will take place due to the different positioning techniques. This can be used to determine the deviation between DGPS and INS position.

This deviation is again used to estimate some of the parameters in an error model for the INS. In periods with reduced accuracy in DGPS or complete loss of DGPS position, the INS data corrected with data from the error model can be used as position measurements.

When GPS falls out in shorter periods (for instance 3-60 seconds) this will still give high accuracy position data, independent of shading of the GPS signals by trees or other topographic reasons.

The system gives the position in real-time. However, all raw data are logged for post processing. By this way the accuracy can be improved by use of filtering and smoothing of

raw data. Besides, post processing is an absolute requirement in areas where DGS corrections signals are not obtainable for various reasons.

DESCRIPTION OF THE SYSTEM

The main units in the system are the inertial platform, the GPS and the actual vehicle. Below a short description of each of the main units.

THE INERTIAL PLATFORM

The inertial platform is delivered by the US company Honeywell, and forms a self-contained system for position determination, when only starting position coordinates and heights are given.

A full understanding of the complete inertial platform requires comprehensive studies. Therefore, only a short description of the main principle of this measurements method will be given in this paper.

The main component is a «mass platform» defines by three orthogonal axis, which are oriented in space by use of special gyros.

RING LASER GYRO

The gyros used in this inertial platform are ring laser gyros. They are mounted directly to the vehicle chassis and therefore follow its movements. This type of arrangements is called a strap-down inertial system.

The advantage with this is that there is not necessary a need for a gimbal system, reducing size, weight and power consumption significantly, and accordingly also costs.

Laser beams are sent in opposite directions from a source in a triangular arrangement, which reflects the laser beam in each of the corner of the triangel. The wavelength of the light is adjusted to the length of the circular path, causing standing waves, i.e. the optical wavelength is equal to a number of full wavelengths.

When the vehicle is stationary, the two laser beams will travel the same distance and the wavelengths are the same.

As soon as the gyros ar exposed to a rotating movement around one of the axis perpendicular to the light plane, one of the laser beams will travel longer optical path than the other, dependent on the direction of the rotation. The two resonant frequencies change to adjust to longer or shorter optical path , and the frequencies change is directly proportional to the angular turning rate. The difference in frequency between the two laser beams will then represent an expression for the velocity of rotation.

In this way, the system is continuously registering the changes in the vehicles direction, with reference to the alignment position at the start of the motion.

Alignment position is determined while the vehicle is standing still and the system is only sensing the earth's rotation.

The position is determined by use of differential GPS. The alignment position and the earth rotation force components in the car system directions are measured, then it is possible to determine the directional axis North, East and up relative to the mass platform. The three orthogonal axes of the mass platform are the directions which the system computer "remembers" and measures the rotation relative to.

ACCELEROMETERS

Attached to each gyro axis is a very sensitive accelerometer. The accelerometer measure the acceleration along each of the axis with high accuracy. The measured accelerations are integrated to determine the velocity along the axes, and a second integration gives the distances relative to previous position.

This can mathematically expresses as follows:

Change in the position per time unit (velocity) is:

$Vx = dx/dt$, $Vy = dy/dt$, $Vz = dz/dt$

and change in velocity per time unit (acceleration) is:

$Ax = d^2x/dt^2$, $Ay = d^2y/dt^2$, $Az = d^2z/dt^2$

When acceleration is measured, we will get:

Velocity calculated from $Vx = \int Axdt$, $Vy = \int Aydt$ $Vz=\int Azdt$

and change position $Dx = \int Vxdt$, $Dy = \int Vydt$ $Dz = \int Vzdt$

Since accelerometers have a non-linear drift, the vehicle (the system) has to be brought to a complete stop after a certain period of time in operation, the length of time is dependant of the accuracy required.

This routine, called the Zero Velocity Updating (ZUPT), takes only 20 seconds. In this particular system the intervals between each ZUPT is set to maximum 10 minutes.

If the vehicle for any reason should come to a stand still, the system automatically tries to carry out a ZUPT.

THE GPS

A Trimble 4000SSE GPS receiver is installed in the vehicle, which determines the vehicles position by use of pseudorange measurements on C/A code, together with doppler smoothing. The accuracy in position by use of pseudorange measurement alone is approximately 100 meters or 30 meters, dependant on whether or not selective availability (SA) is on.

By use of DGPS, with correction signals from SATREF services, this will bring a typical pseudorange accuracy down to 1.5 meter, under the following assumptions:

*	Number of satellites available	>	5
*	H DOP	<	1.5
*	P DOP	<	2.4
*	Distance to SATREF reference station	<	300 km

These assumptions are difficult to fulfil when driving the vehicle, since one have to expect signals from satellites constantly to be shaded because of the topography. Since 1994, when the GPS system was fully developed with 24 satellites, these assumptions has been much easier to meet.

So far, trials seem to indicate that the system generally meets the accuracy mentioned above.

Transmission of DGPS corrections signals can be done from SATREF reference stations via NMT mobile telephone and intelligent modem or via the FM broadcasting system for continuously use, or batch transmission for post processing.

THE VEHICLE

The system was first installed in a Ford Transit van. The vehicle has 200 volts power supply installed. This is achieved by use of three large batteries and a DC/AC converter. The batteries are charged from the vehicles power generator or an external generator. The batteries has the capacity to provide the system with sufficient power for several hours without running the vehicles generator.

The GPS antenna is mounted at car roof level. These positions are determined relative to system origo. The main computer in the system, installed in the vehicle, is a MS-DOS compatible PC, with a Intel Pentium processor and a 1.2 GB harddisk.

During data collections the files will grow at a rate of some 5MB per hour.

In addition to controlling the system from a PC keyboard, a separate operator console is available, which also contains status indicators, function keys and certain "themes" to be registered in the road database.

After a test period, the system was modified and moved to a Chevrolet Astro van. This van has all the accommodations necessary to make the system as safe and user-friendly as possible, for the operators, to work with. In 1997 we again changed car and the system is now installed in a Toyota land-cruiser.

THE INTEGRATED SYSTEM

Separately, the GPS and the INS are insufficient systems. The INS requires frequent stops and a high number of known reference points, while the GPS is dependant on free sight to a minimum of four satellites.

The INS has an error development, which gives a short time accuracy, but the error increases nonlinearly over time.

The DGPS has lower short time accuracy but is only time-dependant of the change in satellite constellations and the atmospheric conditions.

When these two technologies are integrated, one get a system, which partly solves the weaknesses related to each of the two technologies.

The quality of the observations are practically independent of the vehicles speed, and the system works properly for speeds above 100 km/hr. When it comes to following the center line of the road, it is of course more convenient running at a lower speed.

The system can output position in real-time, but while establishing the road database all data are stored for post processing with DGPS.

CALCULATIONS

Calculation can, in addition to being done in real-time, be done by post processing. Normally, the mobile telephone link between the vehicle and the SATREF reference station, will give a number of interruptions, so that one will have to carry out a complete calculation.

One will then have to do a transmission of a continuous DGPS file in advance.

The software for post-processing is used to improve the measurements and to extract the data which shall be incorporated in the database.

The heights will be converted from ellipsoid heights to orthometric heights, by use of the national geoid SKREF96.

Transformation software is also installed into the system, so that final coordinates optionally can be given in either national local systems or WGS84 (EUREF 89).

The road database is established in EUREF 89, and the data will finally be delivered on diskettes in SOSI format. A national SOSI-named format is developed for use in national geographical information systems. The data are finally put into the database by use of a special Norwegian program ‚FYSAK. This program is also checking the data for different types of errors , and connect the roads together by constructing so-called nude points.

FURTHER DEVELOPMENT OF THE SYSTEM

There is a plan for further development for the processing algorithm for complete processing of C/A-code L1 and P-code L1 and L2.

The existing mobile telephone system as well as the RDS-FM has well known areas where it is not working, particularly when leaving the main roads. However, as mentioned earlier, the transmission of DGPS corrections in real-time is not a necessity for establishing a road database.
Statens kartverk is right now involved in an international development project, with the objective to construct a new communication system particularly adapted to this purpose.

PRODUCTIONS

The vehicle has since 1993 been in data production for a total of 600 days. So far the system is meeting all requirements that was set.

All together, more than 30 000 roads have been established or updated all around the country by use of the system.

The control in the field has been done by placing the vehicle on exactly surveyed reference points, and compared these coordinates with the coordinates given by the system.

With a very few exceptions the difference in coordinate values is less than 1- 2 meters, which is in accordance with the specifications for the road database.
Field operation of the system is done by two persons. The driver has, in addition to driving the vehicle, also the responsibility for operating the system and data processing. The driver sits beside the map reader, who keeps track of the road working plan and performs also practical duties such as route planning, keys for toll roads, and various information and communication tasks.

Status indicators will tell when the vehicle has to be stopped for ZUPT, or when it has been too long since last accepted GPS position.

If other, more serious system failure should occur, a red warning light will illuminate, and we have to call for technical support.

The manning of the vehicle has been functioning satisfactory.

Finally, it should be mentioned that the Geodetic Division has great expectations to the system, and will actively try to find other applications for it.

A TEST TRACK FOR REAL TIME MEASUREMENTS.
FOR WHAT AND FOR WHOM ?

By Jean-Marie BECKER

Professor- Royal Institute of Technology - Department of Built Environment, Information Technology for Land, Buildings and Infrastructure: KTH/BMG - Box 88, S-801 02 Gävle, Sweden
telefon +46 26 633728, telefax +46 26 610676, E-Mail : jean-marie.becker@ lm.se

ABSTRACT

The technological evolution of the survey instruments allows today to make real time kinematic measurements for various applications as example for positioning and guidance of construction machines. However it exist few technical means to test, study, compare, evaluate, check and calibrate this new surveying systems for determination of their technical performances as example: prestation, accuracy, repeatability, etc. In the following report the author examine the different needs, present and analyse the actual solutions and finally propose the construction in Sweden of a modern test track for real time kinematic measurements.

The 13th General Meeting of the Nordic Geodetic Commission,
GÄVLE- Sweden, 25-29 May 1998
FIG-XXI International Congress, Brighton UK , 19-25 July 1998

INTRODUCTION

For a few decades, the knowledge of how the measurement systems work is reserved to a few people, for instance instrument manufacturers, electrotechnicians and software developers. Previously, the measurement operator controlled his/her measurement systems (equipment + technics of measurement); he/she could detect errors and make corrections. With today's technologies (electronic + computers), his/her possibilities to influence are limited. He/she is demanded larger reliance on the system's own control functions. The operator's knowledge and understanding of what is happening is decreasing more and more. The technical revolution affects the human being who becomes a slave of his/her own technology. The operator is reduced to a so called push-button-robot which handles a black box. Several other actors manage this "simplified" form of technics of measurement, among others professional groups without knowledge of measurement (e.g. machine operators) and these take over the role of the measurement technicians and one relies on the technics' own reliability.

These establishments are reason enough to feel a certain insecurity and concern in view of the future, particularly considering the fact that real time measurements then will be the basis for accurate positioning for real time control of, for instance, construction machines, cars and trains during their moves.

This development within the technics of measurement also makes new requirements on measurement data for positioning, navigation and steering. The new requirements may be in the form of high accuracy in 3-D, results in digital form and in real time, non-stop measurements and a particularly high reliability. In order to evaluate future measurement systems and measurement methods, a robust test set-up is required.

WHO IS INTERESTED IN KINEMATIC REAL TIME MEASUREMENT?

Among the interested parties in Sweden, the following are principally noted:

⇒ the users of this kind of measurement system, i.e. authorities (The Swedish Road Authority "VV", The National Land Survey of Sweden "NLS", The Swedish National Rail Administration "BV", The National Swedish Administration of Shipping and Navigation "SFV"), military authorities, municipal responsible for measurements, private measurement companies and contracting companies (e.g. NCC, Skanska);
⇒ instrument manufacturers (e.g. Geotronics AB, Spectra-Physics, Arnex AB, etc);
⇒ research institutions ("FMV", the Swedish Defence Material Administration, "FOA", the Research Institute of the Swedish National Defence); and
⇒ institutes of technology (e.g. "KTH", the Royal Institute of Technology, "HGS", the University of Gävle-Sandviken, "Mitthögskolan", Mid Sweden University.)

In addition, several foreign instrument manufacturers, institutes of technology and researchers have reported their interest.

WHY ARE TESTS AND EXAMINATIONS NEEDED?

When the use of results in real time from kinematics measurements is increasing at a hurried pace around the world, needs to try, test, calibrate and evaluate these measurement systems arise. Practical research projects about different technics of measurement, systems and equipment are needed, among other things for the following reasons:
⇒ ascertain the opportunities and limitations at different applications;
⇒ better understand which factors influence the quality and the reliability of the measurement results;
⇒ develop different technics of measurement for positioning, for instance for real time and/or kinematics measurement;
⇒ enable the development of adequate correction models;
⇒ offer researchers and students from institutes of technology the opportunity to test, examine and carry on research; and
⇒ constitute means of assistance for all interested parties/users/manufacturers.

WHICH RESEARCH PROJECTS OUGHT TO BE FEASIBLE?

The projects which primarily are of interest are comparisons between different instruments and methods and may generally be classified as follows:

⇒ ***Performance***; which, for instance, may relate to showing how quickly an instrument displays the position horizontally and vertically for a movable object and/or of a movable measurement instrument (sensor) at various travel of speed, the sensitiveness to different types of obstacles which may influence measurements and the time interval required to reproduce reliable measurement results. This is valid for different types of measurement instruments (classical instruments and others, such as GPS);
⇒ ***Accuracy*** ; as one or different types of instruments may accomplish in relation to the production requirements which are made at different applications. This may, for instance, concern indication of height to control various earth-moving machinery's (e.g. asphalt surfacing machines, road planers, excavators). The effect of different factors on the measurement accuracy can be examined and instructions to obtain the required accuracy can be elaborated;
⇒ ***Reliability***; or with which confidence is the same position for a point obtained, seen over time. Of great interest are analyses of operation reliability and repeatability of the results under different working conditions (sun, rain, dust, vibrations, chilliness, instrument positions and other external factors);
⇒ ***Evaluation*** of equipment in order to examine possibilities and limitations. To build up a knowledge bank which may be used at, for instance consultations in connection with purchase as well as recommendations of use of the measurement equipment for different applications;
⇒ ***Integration and combination*** of several measurement equipment units which are necessary to guarantee that the position determination may take place irrespective of external disturbances and without any interruption; and
⇒ *Special studies* of various kinds for, e.g. specific needs, improvements and further development.

Example of interesting questions:

In connection with the choice of suitable measurement equipment for positioning construction machines, for instance asphalt surfacing machines, one must be able to guarantee a high level of accuracy as well as a continuous operation reliability, irrespective of the environment and the working conditions. Then the following questions have to be answered:
⇒What available measurement equipment for kinematic measurements in real time is suitable for this type of application? At what travel speed? How may we confirm this?
⇒ What measurement equipment guarantees the sufficient horizontal and vertical accuracy? Is it GPS, total station , laser or something else?
⇒ Can this equipment alone guarantee this accuracy for the entire construction project?
⇒ If yes, what methods and precautions have to be used/followed?
⇒ If no, when, how and with what other measurement equipment do we have to combine in order to meet made requirement specifications?
⇒ How should the information from these measurement systems be synchronised in order to eliminate errors due to, for instance, time delays?
⇒ If GPS will be used, what smallest elevation angle should then be allowed? Where on the construction machine should the movable receiver be attached? How should it be fastened? Is there a risk of multiple-way errors (reflection from the machine) etc.? and
⇒ What geodetic support (type of net, configuration, quality, point distance, positioning, type of mark etc.) is needed in order to guarantee the quality and optimise the performance in the most suitable way?

There is, at every application of kinematics real time measurements, a number of similar questions which are specific for these projects and which have to be answered before one decides which measurement equipment should be used and possibly purchased.

WHICH ARE THE REQUIREMENTS AND EXPECTATIONS ?

The projects which were reported earlier and which would be suitable to perform on a test track make the following requirements on the test track:

◊ Several systems should be able to be tested simultaneously. This should take place with the testing objects positioned on the wagons and/or the observation pillars;
◊ Each wagon should be able to transport a test object (GPS, reflector, etc.) having a maximum weight of 25 kg;
◊ The position of the test objects in plane and height along the track should be known with the highest accuracy, i.e. some mm accuracy in 3-D and preferably in real time;
◊ One should be able to perform tests at different speed (from 0 m/s to at least 5 m/s);
◊ It should be possible to partly simulate certain real situations (specific for individual applications) at the track in order to study, for instance, influence of trees, houses together with different mounting surfaces (e.g. on the machine); and
◊ The mechanical performance of the track should be of highest quality and stand the stress from the external environment.

WHAT PRACTICAL TESTING OPPORTUNITIES EXIST TODAY?

We have tried to obtain all available information about existing test set-ups through our national and international contacts. This has been realised through inquires at instrument manufacturers, control authorities (Swedac, Afnor) and professional colleagues (within FIG, IAG, universities).

From specialist literature, we have found out which set-ups around the world are used to perform similar tests and examinations, i.e. kinematics measurements in real time. To our surprise, all tests accounted for are performed at so called miniature test tracks of an extremely small size (less than 10 m in circumference) which hardly may be regarded to reflect the practical application environment. Here follows some examples:

⇒ one of the world's largest instrument manufacturer uses a bicycle wheel which spins;
⇒ another one together with some universities have toy train tracks of around 5 m in circumference or special constructed mechanical circular devise as below fig.1 from ETH-Zurich (Vogel-Mäschler) or fig.2

Abbildung 2.1: Die Kreisformtestapparatur von Vogel/Mächler

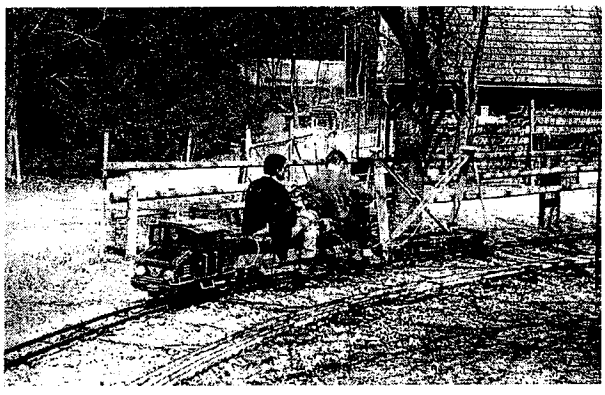

⇒ others test on straight rail sections of about 10 m length

In addition, tests are reported being made along well-known sections/routes which are followed by wagons or car; this is, however, done with a low accuracy (dm).

Furthermore, we have been at LCPC (the test station of the French Road Authority) in Nantes, France to study their test set-up and make some GPS tests.. This test track is formed like a smaller trotter-track with a circumference of about 180 meters and which is located in a horizontal plane. The track consists of a railway rail which is mounted on a concrete bed about 1 m above the ground. A motor-driven robot *SESSYL* (about 450 kg) is moved along this rail with various pre-determined speed (from 0,1 to 20 km/h). At the top of the robot, there is a fastening device for the test objects. Vertical and horizontal movements can be achieved by means of a so called "hood-device" (se fig.3 below). Around the track, there are several measurement pillars which are used as points of reference. The test track operates since several years and is particularly used to test measurement equipment for the applications of the French Road Authority.

Figure no:3

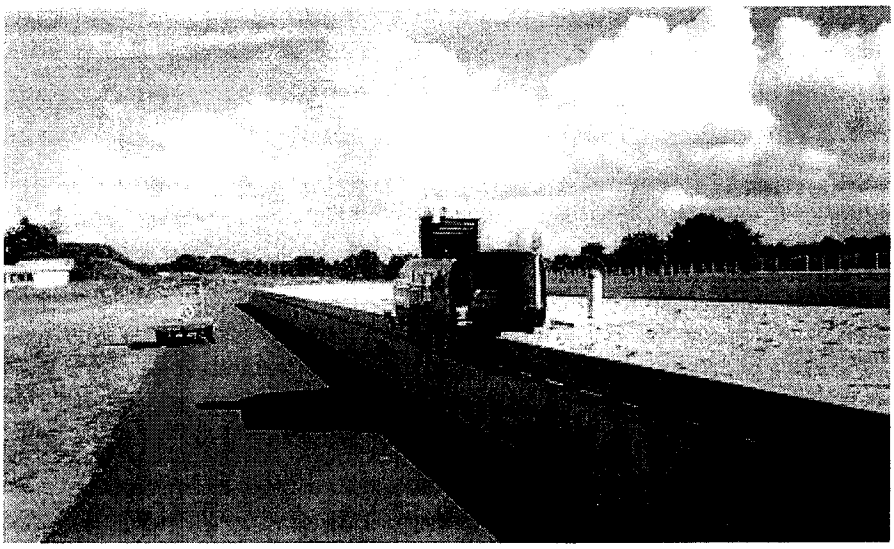

HOW DO THESE TEST SET-UPS MEET OUR EXPECTATIONS ?

The evaluation of existing test set-ups shows that the only one which reasonably reflects conditions prevailing under real working conditions is the one in France at LCPC. This track is built by a so called "End User" (the French Road Authority) which uses the test track to evaluate the measurement equipment it uses in its operation. The French test track has, however, some substantial technical deficiencies and lacks certain test possibilities. As examples, the following points may be mentioned:

⇒ the track is built in a horizontal plane. The reality at building sites is different;
⇒ the height of the test object above the reference surface (rail) is too large (about 1 m) which implies instability at the curves and reduced accuracy. This is particularly obvious at higher speed which reduces the accuracy substantially;
⇒ the achieved accuracy is not at the millimetre level (between 0,5 and 1,0 cm)
⇒ the test robot is very heavy (about 450 kg) and difficult to handle. A lifting device is required for lifting on and off the track
⇒ it is only possible to test one instrument at a time, which reduces the chances for good comparisons between different instruments, brands or systems. This has also been the main criticism which different constructors have expressed when their test results were worse than expected or compared to others. One claims that the test conditions were different.
⇒ it is difficult to test both stationary and movable measurement equipment simultaneously according to the above-mentioned.
⇒ the cost for performing each test series in France (about one week's tests) is high. In addition, there is the difficulty in disposing the French test track whenever you want to.

WITH WHICH TECHNICAL SOLUTION MAY WE MEET OUR NEEDS?

In Sweden or in the Nordic countries, there is no test opportunity whatsoever and nobody (not even Swedac) has assumed any direct responsibility to meet the society's need for a test track. To solve this deficiency, a project group has been formed by various interested parties. (KTH/BMG, NLS, VV, BV and HGS). The project group proposes that a test track for kinematics real time measurements is built in Sweden. A suitable location would be around Gävle and as a suggestion in connection with the existing test field at the Geodetic Observatory in Mårtsbo.

Proposal for realisation

The test track should be of the type closed loop with a circumference of about 150 m and be situated on pillars with a distance of 3 m having a height above the ground, varying between 1,0 and 4,0 m depending on the topography of the terrain. The track will consist of plane and leaning sections. One of the long sides is plane while the other one has a roughly 10 % upward slope over about 20 m, followed by a 10 m plane section and then a fall over about 15 m. The two horizontal curves are given the radius of 5 m or 10 m alternatively In order to solve this, two stainless pipes (60,3 mm x 3,6 mm) are suggested on top of each other.

The track should be situated outdoors and its geometric shape is depicted in fig.4 below with a plan overview and a longitudinal cross section at a projected location in Mårtsbo or Kungsbäck. The construction should stand the specific stress of the external environment. It may be a question of large temperature differences, precipitation, acidification in the air with the ensuing corrosion etc.

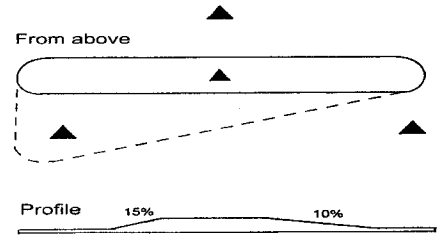

On the track, a "*locomotive*" with wagons (maximum five) will be able to be driven with an adjustable speed from 0 m/s to 5 m/s. The upper pipe carries the locomotive and the wagons while the lower pipe is used to control the wagons vertically. Two conductor rails of 24 V voltage are placed between the pipes for current feeding the locomotive.

Alternatively, the locomotive should be able to be driven by batteries of 24 V. The locomotive and the wagons are equipped with support wheels and driving wheels with urethane surfacing so as to avoid wear of the stainless track.

The test objects will be placed on the wagons by means of centring devices. The location of the train on the track has a guaranteed position stability along the upper surface (reference surface in 3-D) of the upper pipe. The lowest pipe counter-checks horizontal swings. In order to control the position of the train on the track, inductive transmitters are placed along the track with a separation so that always one of the wagons or the locomotive affects a

transmitter. All transmitters are connected to a PLC-control system which is programmed via an ordinary PC. Alteration of a pre-determined speed may take place at fixed positions along the track. The possibility of remote controlling, will be examined at a later stage.

A number of observation *pillars* (at least four, with automatic centring and known co-ordinates) will be built on and around the test track for mounting of various instruments. The pillars are used to calibrate the position of the test track on different test occasions as well as to on these place various instrument which are to be tested, e.g. motorised total station.

The possibility to drive around the test track with vehicles to accurate determine their position and give control information has been treated and will be provided for.

Calibration of the test track:

On the test track, several well-defined points of reference should be fixed, whose positions are controlled before and after each test occasion. These controls should enable calculation of corrections concerning each individual test run because of, for instance, prevailing temperature. Furthermore, there is a possibility, during test runs, to continuously measure in, from the observation pillars, a multiple-grade reflector which is positioned on one of the wagons and thereby to follow the train's position in relation to the transmitters' registrations.

HOW MUCH DOES SUCH A TEST SET-UP COST? HOW SHOULD THIS PROJECT BE FINANCED?

The project group has calculated the cost for all phases from construction start to finished test track ready-to-run to about 200 000 USD. The yearly expense for maintenance and operation will be covered by a contribution from interested parties. The proposed test track would be paid for after about some twenty-five test periods.

Because of the national character of the project with many interested parties, the project group has been in contact with and asked all (VV, BV, FMV, FOA, NLS, HGS, KTH, SFV) about contributions in the form of cash grants, man-power or purchase and delivery of material. Furthermore, contact has been established with some other contributors, such as, for instance the KKK Foundation. Unfortunately, some of the interested parties cannot, for various reasons, invest in this type of set-up but have already reported their interest to use the test track and pay for this.
Manufacturers as example Spectra-Precision will lend their equipment free of charge during and after the construction period.

All decisions concerning the test track should be made jointly in a "Co-operation group" which consists of the financiers of the test track and some representative from the "User Club". The responsibility for the operation of the test set-up rests on KTH/BMG or "NLS".

CONCLUDING WORDS

The role of the test track in Sweden should be given and obvious. Not least considering the various fields of use which have been reported. There ought to be a row of interested parties who need a test track. A test operation in a more down-to-earth environment gives a lot more than tests in laboratories only!

For the moment, about one third of the financing is still missing in order to realise the project and we would gratefully look forward to new contributions and tips.
If we want a test track for real time measurement, it is required that more interested parties contribute actively in the financing thereof. It would be a shame if we were not able to scrape together the remaining part of the capital needed.

REFERENCES

Becker J-M , 1997 Vill Vi i Sverige ha en testbana för realtidsmätningar? För Vad och Vem? Lantmäteritidskrift 1997:2- Sweden

Becker J-M , 1997 Computer Integrated Road Construction. The new Role of the Surveyor, 64th FIG PC Meeting & Int.Symposium, May 11-17, 1997, Singapore

Böckem B & Christ H & Dönicke R, November 1996 . Der ETH-Kreisformtest als wirksame Untersuchungsmethode fur geodätische Messysteme, ETH-Bericht 262

Guilloteau Sylvain, 1995 GPS Simulation and kinematic test measurements, Mémoire, ESGT 28 juin 1995- Evry Cedex France

Lidberg M, 1996 Report from test measurements in Nantes at LCPC (internal report NLS)

Peyret F,. 1997 La localisation en temps-réel des machines de travaux publics, une nouvelle branche de la topographie, Revue XYZ- N*70 , 1er trimestre 1997, pp 26-33

Peyret F & Becker J-M, 1997 Dossier: "Le guidage des engins de chantier ...etc" Revue Géomètre , n*5 , Mai 1997, pp.35-50. France, ISSN:00167967

Peyret F & Bétaille D. & Hintzy G, 1997 High Precision application of GPS in the Field of Real-Time Positioning Equipment , LCPC , ISARC 14, June 8-11, 1997, Pittsburg, USA

Elections

Chairman: Juhani Kakkuri

Establishing and confirmation of NKG Working Groups

As President of NKG, Juhani Kakkuri opened the meeting and announced that the Working Groups on Height Determination, Geodynamics, Satellite Geodesy and Geoid Determination had asked for a continuation. The Working Group on Permanent Geodetic Stations had asked to be merged into the Working Group on Satellite Geodesy. A proposal had come up to establish a new Working Group with the specific tasks to focus on geodetic applications of remote sensing as well as geodetic issues in the application of remote sensing.

The meeting agreed to continue four of the old Working Groups, to merge the Working Group on Permanent Geodetic Stations into the Working Group on Satellite Geodesy and to establish the new Working Group Remote Sensing.

The following chairpersons for the Working Groups were elected:

Height Determination:	Jean-Marie Becker, Sweden
Geodynamics:	Martin Vermeer, Finland until a new chairperson is proposed by the first meeting of the Working Group
Satellite Geodesy:	Markku Poutanen, Finland
Geoid Determination:	Dag Solheim, Norway
Remote Sensing:	Per Knudsen, Denmark

Appointment of Members to the NKG Presidium

As members of the new Presidium the following representatives were announced:

Denmark:	Niels Andersen, Sigvard Stampe Villadsen
Finland:	Jussi Kääriäinen, Martin Vermeer
Norway:	Björn Engen, Björn Geirr Harsson
Sweden:	Bo Jonsson, Lars Sjöberg

No proposals from Iceland came up for consideration

The Presidium elected Björn Engen as chairman and Bo Jonsson as secretary for the next four years period.

Resolutions

Chairman: Björn Geirr Harsson

To the Resolution Committee at the 13th General Meeting, Gävle, Sweden 1998, the following members were appointed:

Björn Geirr Harsson, Norway, chairman
Sigvard Stampe Villadsen, Denmark
Martin Vermeer, Finland
Martin Ekman, Sweden

Björn Geirr Harsson read all the resolutions and then one by one the resolutions were discussed by the NKG General Assembly. The accepted resolutions follow below.

Resolutions adopted at the 13th General Meeting of the Nordic Geodetic Commission in Gävle 25 -29 May 1998

No. 1 Gävle 29 May 1998

The Nordic Geodetic Commission

recognizing the need of the political decision makers for scientific support and guidance on their way to sustainable development,

recognizing the fundamental role of a detailed monitoring of the Earth system for acquiring the knowledge required for such a support,

recommends that geodesy contributes to the establishment of a Global Geophysical Observing System and that the International Association of Geodesy (IAG) and the International Union of Geodesy and Geophysics (IUGG) support the implementation of such a system, which would be a crucial contribution of the Earth sciences community to the achievement of the objectives set down in the Agenda 21.

No. 2 Gävle 29 May 1998

The Nordic Geodetic Commission

recognizing the sensitive role of the Arctic in climate change, both as a region where significant changes can be expected and where impacts can be detected at an early stage,

recognizing the importance of sea level as an indicator of climate change,

recommends that the Arctic tide gauges are co-located with continuous GPS and absolute gravity in order to separate sea level changes and vertical crustal movements.

No. 3 Gävle 29 May 1998

The Nordic Geodetic Commission

recognizing the international initiative to support the Russian Global Navigation Satellite System GLONASS, the International GLONASS experiment (IGEX 98),

noting the importance of the increased satellite availability, better geometry, and increased accuracy, especially at high latitudes, obtained by combined use of GLONASS and GPS,

recommends that IGS-EUREF permanent sites operated by the NKG are co-located with GLONASS receiving systems in support of the IGEX 98 pilot project.

No. 4 Gävle 29 May 1998

The Nordic Geodetic Commission

recognizing the general increasing use of geographic information by coordinates,

emphasizing that the EUREF Commission has recommended a geodetic datum for Europe and that there is a need for map coordinates in a common map projection for the Nordic countries,

recommends EUREF 89 as geodetic datum and the principles of UTM as a common Nordic map projection.

No. 5 Gävle 29 May 1998

The Nordic Geodetic Commission

recognizing the need for gravity data from the Baltic Sea to improve the Nordic geoid,

noting the use of the best possible geoid model for unification of geodetic vertical networks of countries around the Baltic Sea,

recommends that a coordinated project be carried out to survey the Baltic Sea region by ship and/or airborne gravimetry.

No. 6 Gävle 29 May 1998

The Nordic Geodetic Commission

recognizing the considerable investments and the different priority changes regarding the completion of the ongoing precise levellings in the Nordic countries,

noting the difficulties caused to some of the countries,

recommends that all the countries strengthen their efforts to complete the measurements in the national levelling networks at the latest in the year 2003.

No. 7 Gävle 29 May 1998

The Nordic Geodetic Commission

recognizing the long time needed to realize a final adjustment and establish a new height system for the national levelling networks and for the common Nordic bloc,

noting the enormous volume of field data to be correctly handled in preparation for adjustment,

recommends that preparation of data for the adjustment starts immediately, as well as consideration of a height system.

No. 8 Gävle 29 May 1998

The Nordic Geodetic Commission

observing the successful establishment and operation of a permanent GPS monitoring network in the general area of the Fennoscandian shield, including the Baltic countries and Russian Carelia,

congratulates all those having cooperated to achieve this success and

considers this an illustration of the importance of continued free availability of the data concerned for scientific use.

No. 9 Gävle 29 May 1998

The Nordic Geodetic Commission and its members

present at the 13th general meeting of the Commission in Gävle express their sincere thanks to Lantmäteriverket and to the local organizing committee for the excellent arrangement and warm atmosphere during the meeting and at the social events.

Statement

The Geodetic Commission of Estonia, Latvia and Lithuania submitted to the Nordic Geodetic Commission an application for inclusion in the work of the Nordic Geodetic Commission as an observer or as a corresponding member.

The statement below was proposed and accepted by acclamation

Statement adopted at the 13th General Meeting of the Nordic Geodetic Commission in Gävle 25 -29 May 1998

No. 1 Gävle 29 May 1998

The Nordic Geodetic Commission

recognizing that co-operation projects in the field of geodesy carried out in the Baltic Sea Region in the past years have indicated the need for intensifying the exchange of information as well as co-operation between the Geodetic Commission of Estonia, Latvia and Lithuania and the Nordic Geodetic Commission.

welcoming the application from the Geodetic Commission of Estonia, Latvia and Lithuania for inclusion in the work of NKG.

invites representatives of the Geodetic Commission of Estonia, Latvia and Lithuania to take part in General Meetings, Autumn Schools and Working Group Meetings.

looks forward to be continuously informed about the work of the Geodetic Commission of Estonia, Latvia and Lithuania.

Closing ceremony

Chairman: Juhani Kakkuri

The chairman opened the closing session by expressing his satisfaction with the 13th General Meeting of NKG. He noted that the success of the meeting has come from the professional quality of the presented papers and the vitality of the discussions, but first of all from the warm and easy relations, which have developed among the participants during the meeting.

On behalf of the Finnish group Juhani Kakkuri invited NKG to the next General Meeting in Finland in 2002. The invitation was accepted with acclamation.

The chairman expressed his thanks to all those, who have made this meeting possible. Many have been involved, but special thanks to the members of the Organizing Committee for their excellent work.

Finally the chairman thanked all the participants for their contribution to the meeting and wished them a safety trip back home.

There was no other business and the chairman concluded that the 13th General Meeting of NKG had come to an end.